ASSESSING MICROPLASTIC ABUNDANCE AND DISTRIBUTION IN RIVERS: A MECHANISTIC MODELING APPROACH

by

Zeynep Akdoğan

B.Sc. in Environmental Engineering, Istanbul University, 2008

M.S. in Environmental Technology, Boğaziçi University, 2014

Submitted to the Institute of Environmental Sciences in partial fulfillment of the requirements for the degree of

Doctor of Philosophy

in

Environmental Sciences

Boğaziçi University

2023

ASSESSING MICROPLASTIC ABUNDANCE AND DISTRIBUTION IN RIVERS: A MECHANISTIC MODELING APPROACH

APPROVED BY:

Assoc. Prof. Dr. Başak Güven Thesis Advisor	. . . . .
Prof. Dr. Nadim Copty	. . . . .
Prof. Dr. Burak Demirel	. . . . .
Prof. Dr. Güleda Engin	. . . . .
Prof. Dr. Melike Gürel	. . . . .

DATE OF APPROVAL: 08/12/2023

ACKNOWLEDGEMENTS

I would like to express my sincere gratitude to Assoc. Prof. Dr. Başak Güven for her guidance and constant support throughout my PhD. I am grateful to her for sharing her knowledge and experience whenever I need and encouraging me to be a researcher. Besides my supervisor, I would like to thank the committee members Prof. Dr. Nadim Copty, Prof. Dr. Burak Demirel, Prof. Dr. Güleda Engin and Prof. Dr. Melike Gürel for their valuable contributions on the coming this dissertation to existence. I would also like to express my appreciation to the former committee member Prof. Dr. Işıl Balcıoğlu for her valuable remarks at the beginning of my thesis.

Special thanks to Prof. Dr. Ahmet E. Kıdeyş for providing me access to his research laboratory and his valuable contributions on experimental work of this thesis.

I highly appreciate Gülşah Can Kayadelen and Ertan Keş, for their help with the visual identification and extraction of microplastics. Thanks to Burcu Selen Çağlayan from Boğaziçi University Advanced Technologies Research & Development Center for her efforts in Raman analysis.

I would like to express my gratitude to all the members of the Institute of Environmental Sciences. Many thanks to Filiz Ayılmaz for her support with laboratory equipment. I am thankful to my friends Başak Kılıç, Binnur Aylin Alagöz, Berivan Ülger, Zeynep Demiray, Elif Bal, and Buse Yetişti for their friendship and pleasant days we had at the institute.

I am very lucky to have a companion like Suat Vardar. I am grateful to him for making everything easier with his endless support and help whenever I needed. I would also like to thank my dear friends Ayşe Seval Palteki, Nazmiye Cemre Birben, and Nazlı Hande Wood for their valuable friendship and support in all aspects.

Last but not least, I would like to express my deepest gratitude to my family. This dissertation could not be possible without them. I am thankful to them for their never-ending love and support throughout my life.

This dissertation was supported by Boğaziçi University Research Fund (grant number 14507).

ABSTRACT

ASSESSING MICROPLASTIC ABUNDANCE AND DISTRIBUTION IN RIVERS: A MECHANISTIC MODELING APPROACH

Rivers are major transport pathways for microplastics to reach the oceans. Microplastics have numerous different shapes; however, theoretical models generally assume microplastics as spherical particles. This study aims to investigate (i) spatiotemporal distribution and the potential sources of microplastics in an industrially polluted river, (ii) the relationship of microplastic abundance with river's morphological and hydrodynamic characteristics, and (iii) vertical transport of microplastics and the effect of particle and flow characteristics on settling and resuspension. To achieve these aims, water and sediment samples were collected from six sites of the Ergene River in May 2019 and Sep 2020. A mechanistic model was developed using the data of microplastics, and river hydrodynamics and morphology. According to the results, the Ergene River had excessive levels of microplastics compared to many other rivers. Microplastic concentrations in water correlated positively with depth but negatively with channel width. Fibers were the most abundant shape of microplastics suggesting that effluents from textile industries were the foremost contributor of microplastics in the river. The model results revealed that the residence time of microplastics in water was directly related to the flow characteristics, while initial concentration of particles in water dominates the other parameters in settling and resuspension fluxes of microplastics. According to the scenario analysis, settling and resuspension fluxes increased with increasing sphericity and size of the particles, as well as higher bed shear stress. The model results were sensitive to changes in shape factor developed for this model, therefore this parameter should be improved in future studies.

ÖZET

NEHİRLERDE MİKROPLASTİK BOLLUĞUNUN VE DAĞILIMININ BELİRLENMESİ: MEKANİSTİK MODELLEME YAKLAŞIMI

Nehirler, mikroplastiklerin okyanuslara erişmesi için ana ulaşım yollarıdır. Mikroplastiklerin çok sayıda farklı şekli vardır; ancak teorik modeller genellikle mikroplastiklerin küresel parçacıklar olduğunu varsaymıştır. Bu çalışma, (i) endüstriyel olarak kirlenmiş bir nehirdeki mikroplastiklerin mekân-zamansal dağılımını ve potansiyel kaynaklarını, (ii) mikroplastik bolluğunun nehrin morfolojik ve hidrodinamik özellikleriyle ilişkisini ve (iii) mikroplastiklerin dikey taşınımı ve hem parçacık hem de akış özelliklerinin çökelme ve yeniden süspansiyon üzerindeki etkisini araştırmayı amaçlamaktadır. Bu amaçla, Mayıs 2019 ve Eylül 2020'de Ergene Nehri'nin altı noktasından su ve sediman örnekleri toplanmıştır. Mikroplastik, nehir hidrodinamiği ve morfolojisi verileri kullanılarak mekanistik bir model geliştirilmiştir. Sonuçlara göre Ergene Nehri'nde diğer birçok nehire kıyasla yüksek düzeyde mikroplastik bulunmuştur. Sudaki mikroplastik konsantrasyonları derinlikle pozitif, kanal genişliğiyle negatif korelasyon göstermiştir. Mikroplastik şekilleri içinde en çok lifler bulunmuştur; bu da tekstil endüstrilerinden kaynaklanan atıkların nehirdeki mikroplastik kirliliğine sebep olan en önemli faktör olduğunu göstermektedir. Model sonuçları, mikroplastiklerin suda tutulma süresinin akış özellikleri ile doğrudan ilişkili olduğunu, sudaki parçacıkların başlangıç konsantrasyonunun ise mikroplastiklerin çökelme ve yeniden süspansiyon akıları üzerinde diğer parametrelere göre baskın olduğunu ortaya çıkarmıştır. Senaryo analizine göre, parçacıkların küreselliği ve boyutunun yanı sıra, yatak kayma geriliminin artışı da çökelme ve yeniden süspansiyon akılarını arttırmıştır. Model sonuçlarının, bu model için geliştirilen şekil faktörüne duyarlı olduğu bulunmuştur, dolayısıyla gelecekteki çalışmalarda bu parametrenin iyileştirilmesi gerekmektedir.

TABLE OF CONTENTS

ACKNOWLEDGEMENTS iii

ABSTRACT iv

ÖZET v

TABLE OF CONTENTS vi

LIST OF FIGURES ix

LIST OF TABLES xiv

LIST OF SYMBOLS/ABBREVIATIONS xvii

1. INTRODUCTION 1

2. LITERATURE REVIEW 4

2.1. Microplastics in the Environment 4

2.1.1. Sources 4

2.1.2. Fate and Transport in the Aquatic Environments 6

2.1.2.1. Marine environment 6

2.1.2.2. Estuaries 8

2.1.2.3. Rivers 8

2.1.3. Uptake and Effects 9

2.1.4. Microplastic Pollution in Rivers 11

2.2. Analysis of Microplastics 12

2.2.1. Sampling from the Aquatic Environments 12

2.2.1.1. Water sampling 12

2.2.1.2. Sediment sampling 13

2.2.2. Extraction of Microplastics 14

2.2.2.1. Extraction from the water samples 14

2.2.2.2. Extraction from the sediment samples. 14

2.2.2.3. Removal of organic matter 15

2.2.3. Visual Analysis 15

2.2.4. Polymer Characterization 16
2.3. Mathematical Modeling of Microplastic Transport 18
2.3.1. Mathematical Models 18
2.3.2. Applications in Rivers 20
3. MATERIALS AND METHODS 23
3.1. Study Area and Sample Collection 24
3.2. Detection and Analysis of Microplastics 26
3.2.1. Extraction from Samples 26
3.2.2. Identification and Characterization 27
3.2.3. Quality Assurance and Control 28
3.2.4. Statistical Analyses 28
3.3. Modeling the Transport of Microplastics 29
3.3.1. Settling and Resuspension 29
3.3.2. Turbulence Modeling: Boundary Layer Theory 32
3.3.3. Mechanistic Model: Mass-Balance Approach 35
3.3.4. Data Acquisition and Model Calibration 37
3.3.5. Scenario Analysis 38
3.3.5.1. Particle shape 39
3.3.5.2. Particle size 39
3.3.5.3. Bed shear stress 39
3.3.6. Uncertainty and Sensitivity Analysis 40
4. RESULTS AND DISCUSSION 42
4.1. Microplastic Abundance and Distribution in the Ergene River 42
4.1.1. Microplastic Abundance in Water and Sediment 42
4.1.2. Microplastic Abundance and River Characteristics 45
4.1.3. Shape, Size, Color, and Type of Microplastics 46
4.2. Modeling Vertical Transport of Microplastics in Turbulent Flow 55
4.2.1. Monte-Carlo Simulation Results 55

4.2.2. Model Calibration and Validation 66
4.2.3. Scenario Analysis 69
4.2.4. Uncertainty and Sensitivity Analysis 74
5. CONCLUSIONS AND RECOMMENDATIONS 83
REFERENCES 86
APPENDIX A: MICROPLASTIC ABUNDANCE DATA IN THE WATER AND SEDIMENT SAMPLES 113
APPENDIX B: DATA ON SHAPE, SIZE, COLOR, AND POLYMER DISTRIBUTION OF MICROPLASTICS 115
APPENDIX C: SETTLING VELOCITIES OF MICROPLASTICS WITH DIFFERENT TYPE AND SHAPE 128
APPENDIX D: MODELING MICROPLASTIC TRANSPORT IN GOLDSIM SOFTWARE 131
APPENDIX E: SCENARIO ANALYSIS 137
APPENDIX F: SENSITIVITY ANALYSIS 146

LIST OF FIGURES

Figure 2.1. Sources, sinks, and transport pathways of microplastics between terrestrial and aquatic environments.. 6

Figure 3.1. Methodology scheme. 23

Figure 3.2. Map of the study area: (a) Ergene River Basin and location of the OIZs and WWTPs within the study site. (b) Sampling sites. 25

Figure 3.3. Vertical velocity profile. 33

Figure 3.4. Schematic representation of the mass balance for microplastics in reach i. 35

Figure 4.1. Microscopic images of microplastics: (a) fibers, (b) hard fragments and fibers, (c) soft fragments and fibers, (d) pellets and fibers, (e) foams, and (f) rubber. 46

Figure 4.2. Percentage distribution of microplastics by shape in (a) water samples and (b) sediment samples. 47

Figure 4.3. Percentage distribution of microplastics by size in (a) water samples and (b) sediment samples. 50

Figure 4.4. Microplastic color distribution: (a) water samples and (b) sediment samples. 53

Figure 4.5. Microplastic types in the river samples: (a) Polymer distribution in water, (b) Polymer distribution in sediment. 54

Figure 4.6. Probable variation of microplastic concentration in water under turbulent flow conditions in (a) Site 1, (b) Site 2, (c) Site 3, (d) Site 4, and (e) Site 5 in 2019. 57

Figure 4.7. Probable variation of microplastic concentration in water under turbulent flow conditions in (a) Site 1, (b) Site 2, (c) Site 3, (d) Site 4, and (e) Site 5 in 2020. 58

Figure 4.8. Probable variation of microplastic concentration in sediment under turbulent flow conditions in (a) Site 1, (b) Site 2, (c) Site 3, (d) Site 4, and (e) Site 5 in 2019.....61

Figure 4.9. Probable variation of microplastic concentration in sediment under turbulent flow conditions in (a) Site 1, (b) Site 2, (c) Site 3, (d) Site 4, and (e) Site 5 in 2020.....62

Figure 4.10. Change in microplastics settling flux in the sampling sites in 2019.....63

Figure 4.11. Change in microplastics settling flux in the sampling sites in 2020.....64

Figure 4.12. Change in microplastics resuspension flux in the sampling sites in 2019.....64

Figure 4.13. Change in microplastics resuspension flux in the sampling sites in 2020.....65

Figure 4.14. Results of model calibration: Regression analysis of predicted and measured results of mean velocity of the river ($\bar{u}$). 67

Figure 4.15. Results of model validation: Regression analysis of predicted and measured results of settling velocity of microplastics (ωs).....69

Figure 4.16. Changes in settling flux of different shaped microplastics with time.....70

Figure 4.17. Changes in resuspension flux of different shaped microplastics with time.....70

Figure 4.18. Changes in settling flux of different sized microplastics with time. 71

Figure 4.19. Changes in resuspension flux of different sized microplastics with time.....72

Figure 4.20. Changes in settling flux of microplastics with time under different bed shear stresses. 72

Figure 4.21. Changes in resuspension flux of microplastics with time under different bed shear stresses. 73

Figure 4.22. Sensitivity of microplastic concentration on *d*. 75

Figure 4.23. Sensitivity of microplastic concentration on S. 76

Figure 4.24. Sensitivity of microplastic concentration on $D84$. 77

Figure 4.25. Sensitivity of microplastic concentration on μ. 78

Figure 4.26. Sensitivity of microplastic concentration on $\tau cr*$. 79

Figure 4.27. Sensitivity of microplastic concentration on φ. 79

Figure 4.28. Sensitivity of microplastic concentration on a. 80

Figure 4.29. Sensitivity of microplastic concentration on ρ_p. 80

Figure 4.30. Sensitivity of microplastic concentration on ρ_w. 80

Figure 4.31. Sensitivity of microplastic concentration on C_0. 82

Figure B.1. Raman spectrum of PET particle in the water sample from Site 3. 124

Figure B.2. Raman spectrum of PS particle in the water sample from Site 1 124

Figure B.3. Raman spectrum of PA particle in the water sample from Site 3 124

Figure B.4. Raman spectrum of poly(ethylene-co-vinylacetate) particle in the water sample from Site 2 125

Figure B.5. Raman spectrum of PP particle in the water sample from Site 5 125

Figure B.6. Raman spectrum of PI particle in the water sample from Site 5 125

Figure B.7. Raman spectrum of carboxyl-terminated polyester with epoxy coating found in the water sample from Site 3 126

Figure B.8. Raman spectrum of a composite polymer (PSU/PA) found in the sediment sample from Site 1 126

Figure B.9. Raman spectrum of a plastic colorant (Mortoperm blue) found in the water sample from Site 3 126

Figure B.10. Raman spectrum of modal particle in the water sample from Site 6 127

Figure B.11. Raman spectrum of quartz (SiO_2) particle in the sediment sample from Site 5 127

Figure D.1. Model layout in GoldSim 131

Figure D.2. Probable variation of microplastic concentration in water under turbulent flow conditions in (a) Site 1, (b) Site 2, (c) Site 3, (d) Site 4, and (e) Site 5 in 2019 (with mean C_0) 133

Figure D.3. Probable variation of microplastic concentration in water under turbulent flow conditions in (a) Site 1, (b) Site 2, (c) Site 3, (d) Site 4, and (e) Site 5 in 2020 (with mean C_0) 134

Figure D.4. Probable variation of microplastic concentration in sediment under turbulent flow conditions in (a) Site 1, (b) Site 2, (c) Site 3, (d) Site 4, and (e) Site 5 in 2019 (with mean C_0) 135

Figure D.5. Probable variation of microplastic concentration in sediment under turbulent flow conditions in (a) Site 1, (b) Site 2, (c) Site 3, (d) Site 4, and (e) Site 5 in 2020 (with mean C_0) 136

Figure E.1. Probable variation of concentration of near-spherical particles in water within Site 2 137

Figure E.2. Probable variation of concentration of near-spherical particles in sediment within Site 2. 137

Figure E.3. Probable variation of concentration of fragments in water within Site 2 138

Figure E.4. Probable variation of concentration of fragments in sediment within Site 2 138

Figure E.5. Probable variation of concentration of fibers in water within Site 2.....139

Figure E.6. Probable variation of concentration of fibers in sediment within Site 2 139

Figure E.7. Probable variation of concentration of 50 μm-particles in water within Site 2 140

Figure E.8. Probable variation of concentration of 50 μm-particles in sediment within Site 2.....140

Figure E.9. Probable variation of concentration of 500 μm-particles in water within Site 2 141

Figure E.10. Probable variation of concentration of 500 μm-particles in sediment within Site 2...141

Figure E.11. Probable variation of concentration of 5000 μm-particles in water within Site 2 142

Figure E.12. Probable variation of concentration of 5000 μm-particles in sediment within Site 2.142

Figure E.13. Probable variation of microplastic concentration in water under 0.15 N m^{-2} bed shear stress.....143

Figure E.14. Probable variation of microplastic concentration in sediment under 0.15 N m^{-2} bed shear stress 143

Figure E.15. Probable variation of microplastic concentration in water under 0.50 N m^{-2} bed shear stress.....144

Figure E.16. Probable variation of microplastic concentration in sediment under 0.50 N m^{-2} bed shear stress 144

Figure E.17. Probable variation of microplastic concentration in water under 0.90 N m^{-2} bed shear stress.....145

Figure E.18. Probable variation of microplastic concentration in sediment under 0.90 N m^{-2} bed shear stress 145

LIST OF TABLES

Table 2.1. Factors driving microplastic fate and transport. 9

Table 2.2. Comparison of most commonly used microplastic characterization methods. 18

Table 3.1. Sampling sites in the Ergene River. 26

Table 3.2. Meteorological data and on-site measured parameters of the Ergene River. 26

Table 3.3. Pearson correlation scale. 29

Table 3.4. Data requirements for the model. 38

Table 4.1. Microplastic concentrations in water and sediment samples. 43

Table 4.2. Comparison of microplastic concentrations in this study with other rivers. 44

Table 4.3. Pearson Correlation coefficients (r) between river hydrodynamical variables and microplastic abundance. 45

Table 4.4. Results of model calibration. Comparison of predicted and measured results of mean velocity of the river. 66

Table 4.5. Results of model validation: Comparison of predicted settling velocities of microplastics with literature. 68

Table 4.6. Correlation matrix of stochastic parameters and model results. 74

Table 4.7. Sensitivity ranking of the parameters. 82

Table A.1. The calculation of microplastic concentrations in the water samples 113

Table A.2. The calculation of microplastic concentrations in the sediment samples 114

Table B.1. Microplastic shape distribution in the water samples in May 2019 115

Table B.2. Microplastic shape distribution in the water samples in September 2020 115

Table B.3. Microplastic shape distribution in the sediment samples in May 2019.....116

Table B.4. Microplastic shape distribution in the sediment samples in September 2020.....116

Table B.5. Microplastic size distribution in the water samples in May 2019 117

Table B.6. Microplastic size distribution in the water samples in September 2020 117

Table B.7. Microplastic size distribution in the sediment samples in May 2019 118

Table B.8. Microplastic size distribution in the sediment samples in September 2020.....118

Table B.9. Microplastic color distribution in the water samples in May 2019 119

Table B.10. Microplastic color distribution in the water samples in September 2020 120

Table B.11. Microplastic color distribution in the sediment samples in May 2019.....121

Table B.12. Microplastic color distribution in the sediment samples in September 2020.....122

Table B.13. Polymer distribution in the water and sediment samples 123

Table C.1. Calculation of the settling velocity of near-spherical polymers 128

Table C.2. Calculation of the settling velocity of fragment polymers 129

Table C.3. Calculation of the settling velocity of fiber polymers 130

Table F.1. Model response (microplastic concentration in water) to changes in input parameters .146

Table F.2. Input Variation (IV), Output Variation (OV), and Ratio of Variation (ROV) for the model results for water 147

Table F.3. Model response (microplastic concentration in sediment) to changes in input parameters 149

Table F.4. Input Variation (IV), Output Variation (OV), and Ratio of Variation (ROV) for the model results for sediment 150

LIST OF SYMBOLS/ABBREVIATIONS

Symbol	Explanation	Unit
a	Particle size	m
b	Intermediate axis length	m
c	Shortest axis length	m
d	River depth	m
A_1	Cross-sectional area	m^2
C	Microplastic concentration	items m^{-3}
D_*	Dimensionless particle diameter	unitless
D_{84}	Diameter of 84% of sediment particles	m
D_n	Nominal diameter	m
f_{nb}	Fraction of non-buoyant particles	unitless
g	Gravitational acceleration	m s^{-2}
J_r	Resuspension flux	items m^{-2} s^{-1}
J_s	Settling flux	items m^{-2} s^{-1}
k	Nikuradse sand roughness	m
κ	von Karman's constant	unitless
l	Prandtl's mixing length	m
Re	Reynolds number	unitless
S	Surface slope	unitless
T_s	Sample temperature	^oC
T_w	Weather temperature	^oC
u	River velocity	m s^{-1}
u^*	Shear velocity	m s^{-1}
v'	Vertical velocity fluctuation	m s^{-1}
v_b	Burial velocity	m s^{-1}
v_r	Resuspension velocity	m s^{-1}
v_s	Settling velocity under turbulent conditions	m s^{-1}
V	Control volume	m^3
z	Distance from the bottom of river	m
μ	Kinematic viscosity	m^2 s^{-1}
ρ_p	Particle density	kg m^{-3}

ρ_w	Water density	kg m^{-3}
τ_0	Bed shear stress	N m^{-2}
τ_{cr}	Critical shear stress	N m^{-2}
τ_{cr} *	Dimensionless critical shear stress	unitless
φ	Shape factor	unitless
ω_*	Dimensionless settling velocity	unitless
ω_s	Settling velocity	m s^{-1}
∀	Particle volume	m^3
Fe	Iron	
H_2O_2	Hydrogen Peroxide	
H_2SO_4	Sulfuric Acid	
KOH	Potassium Hydroxide	
NaBr	Sodium Bromide	
NaCl	Sodium Chloride	
NaI	Sodium Iodide	
$ZnBr_2$	Zinc Bromide	
$ZnCl_2$	Zinc Chloride	

Abbreviation	**Explanation**
ADCP	Acoustic Doppler Current Profiler
ANOVA	Analysis of Variance
ATR	Attenuated Total Reflection
CSTR	Continuously Stirred Tank Reactors
DO	Dissolved Oxygen
DSC	Differential Scanning Calorimetry
FTIR	Fourier Transform Infrared
IV	Input Variation
NEWS	Nutrient Export from Watersheds
OIZ	Organized Industrial Zone
OV	Output Variation
PA	Polyamide
PAHs	Polycyclic Aromatic Hydrocarbons
PBDEs	Polybrominated Diphenyl Ethers
PCBs	Polychlorinated Biphenyls
PE	Polyethylene

PET	Polyethylene Terephthalate
PI	Polyisoprene
POM	Polyoxymethylene
POPs	Persistent Organic Pollutants
PP	Polypropylene
PS	Polystyrene
PSU	Polysulfone
PVC	Polyvinyl Chloride
Py-GC/MS	Pyrolysis-Gas Chromatography/Mass Spectrometry
R	Replicate
RMSE	Root Mean Square Error
ROV	Ratio of Variation
S	Site
SD	Standard Deviation
SEM	Scanning Electron Microscopy
SPSS	Statistical Package for Social Sciences
TGA	Thermogravimetry
TRWP	Tire and Road Wear Particles
UV	Ultraviolet
WWTP	Wastewater Treatment Plant

1. INTRODUCTION

Beginning in the 1950s, plastic production has increased dramatically over the last decades in line with expanding population and increasing consumption. Mass production of plastics almost reached 370 million tones globally in 2020 (PlasticsEurope, 2021), however, more than half of this production is leaking and littering the environment (UNEP, 2021). Therefore, approximately 60-80% of anthropogenic litter in the environment is plastic (Derraik, 2002). Microplastic pollution has become a global concern, particularly in the last decade, due to its rapid increase and the potential hazards it poses to the environment. The plastic materials are mostly nondegradable or have very slow degradation rates, resulting in accumulation in various environmental compartments, in the form of microplastics -tiny plastic particles smaller than 5 mm in size. Microplastics may originate from primary or secondary sources. Primary sources mainly include cosmetic and medical products that constitute plastic pellets (Guerranti et al., 2019), whilst secondary microplastics are derived from the fragmentation of larger plastic items as a result of physical, chemical and biological processes (Cole et al., 2011). The majority of microplastics in the environment is originated from secondary sources (An et al., 2020).

Since oceans are accepted as ultimate sinks for microplastics, scientific research has generally focused on the occurrence, abundance and transport of microplastics in marine environments. However, approximately 80% of plastics in the marine environment originated from land-based sources where rivers act as the major transport pathways (Andrady, 2011; Bowmer & Kershaw, 2010). For example, González-Fernández et al. (2021) estimated that 307- 925 million macro floating litter items are released annually from European rivers into the ocean of which 84% was plastics. Özgüler et al. (2022) calculated the total microplastics load from only ten small/large volume local rivers to Mersin Bay (the north-eastern Mediterranean) as high as 2,216 billion items per year. Major sources of riverine microplastics can be listed as wastewater treatment plants (WWTPs) (Browne et al., 2011; Vermaire et al., 2017), textile industry (Deng et al., 2020), cosmetics and medical products, fishing activities and anthropogenic litter (Guerranti et al., 2019; Daniel et al., 2020; Bashir et al., 2021), followed by agricultural plastics and tire and road wear particles (TRWP) (Nizzetto et al., 2016b; Unice et al., 2019a). Macro and micro-plastics may be introduced to rivers by the effluents of WWTPs, surface runoff, wind dispersal and atmospheric deposition (Dris et al., 2016; Napper & Thompson, 2016).

Microplastics have been reported in many global rivers, such as the Danube, Austria (Lechner et al., 2014); Seine, France (Gasperi et al., 2014); Rhine, Germany (Klein et al., 2015; Mani et al., 2015); Thames, UK (Horton et al., 2017a); Ottawa, Canada (Vermaire et al., 2017); Saigon, Vietnam (Lahens et al., 2018); Nakdong, South Korea (Eo et al., 2019); Ganges, India (Napper et al., 2021; Singh et al., 2021); and others such as, Maozhou, Manas and Fenghua in China (Wang et al., 2021a; Wu et al., 2020; Xu et al., 2021). Most of these studies were conducted with great volumes of river samples collected via manta trawls or plankton nets, typically with 100 μm or 330 μm pore sizes, due to relatively low concentrations of microplastics in the studied compartment. Recent studies have started to collect bulk samples (Eo et al., 2019; Wang et al., 2017; Wang et al., 2021a), which may provide a more straightforward investigation of smaller microplastics as tiny as 10 μm (Wu et al., 2020). However, knowledge of the occurrence of smaller spectrum of microplastics in aquatic environments is still limited, yet, research indicates that the adverse effects of microplastics increase with the decreased size of the plastic particles (Browne et al., 2008; Chen et al., 2017; Ma et al., 2016).

Some of the microplastics in the riverine environment may get deposited onto the bottom sediments. Therefore, besides being transport routes, rivers can also be hotspots due to the accumulation of microplastics in these environments. In this context, understanding how microplastics move vertically and horizontally in rivers is a requirement to assess the potential hotspots and the risks associated with microplastic abundance. Although fate and transport of microplastics has been subject of research in recent years, there is still limited investigation on riverine transport of microplastics, especially in terms of modeling. Microplastic transport in rivers is mainly governed by the particle properties, such as density, size and shape, and hydrodynamical conditions of rivers. Scientific research has also indicated the effect of interaction of microplastics with other particles and biota on vertical transport in the aquatic environments (Kooi et al., 2017; Shen et al., 2023). To date, discharge of microplastics to rivers via surface runoff, erosion, advective transport, as well as biofouling, aggregation, deposition and resuspension of microplastics along the rivers have been investigated developing process-based models (Besseling et al., 2017; Bondelind et al., 2020; Nizzetto et al., 2016a). However, these models have generally assumed microplastics as spherical and did not consider different flow regimes of rivers. In the literature, experimental studies have been carried out to understand the significance of particle shape on settling and rising velocities of microplastics (Francalanci et al., 2021; Kowalski et al., 2016; Waldschläger & Schüttrumpf, 2019a), yet the effect of different flow regimes is poorly understood. Recently, a few experimental studies have investigated transport of microplastics in turbulent environments (Shen et al., 2023; Stride et al., 2023); however, to the best of my knowledge, there is no process-based dynamic modeling approach applied to real systems in the literature that attempts to determine the transport of

different shaped particles under turbulent flow. This may be attributed to wide range of microplastic characteristics and hydrodynamical conditions of rivers, which makes investigation of transport processes complicated.

Ergene River is one of the most polluted rivers in Turkey, receiving significant amount of industrial waste due to lack of inspection and inadequate treatment. Nevertheless, the Ergene River Basin is still an important agricultural area, where significant portion of rice, sunflower and wheat production of Turkey is carried out (Tokatlı & Varol, 2021). The use of river's water for irrigation of agricultural lands in the basin has become a potential public health issue, which makes the study site a hotspot for microplastic research. This study aims to (i) investigate the occurrence of microplastics in an industrially polluted river, (ii) determine the distribution of microplastics larger than 45 μm in size in two compartments, including water surface and sediment and (iii) develop a mechanistic model to investigate vertical transport of microplastics and understand the effect of particle and flow characteristics on settling and resuspension mechanisms within each sampling site, using mass-balance and hydrodynamic equations. For this purpose, the Ergene River's upstream tributaries, Çorlu and Ergene, were chosen as the study site, mainly because of the heavy industrialization located in this area. This research is the first study on the occurrence, identification and transport of microplastics in the Ergene River.

The thesis consists of five sections. The theoretical background related to microplastic research in the aquatic environments, analysis methods and modeling approaches in rivers are described in Section 2. Section 3 includes the applied methods for (i) sample collection and on-site measurements, (ii) the detection and analysis of microplastics in the water and sediment samples, and (iii) mechanistic modeling approach developed in this thesis. In Section 4, results of the abundance and characteristics of microplastics in the Ergene River, and the model developed to investigate vertical transport of microplastics are described and discussed in detail. The major outcomes of the thesis and recommendation for future work are presented in Section 5.

2. LITERATURE REVIEW

2.1. Microplastics in the Environment

This section was published in 'Environmental Pollution' journal, titled as 'Microplastics in the environment: A critical review of current understanding and identification of future research needs' (Akdogan & Guven, 2019).

2.1.1. Sources

Microplastics originate from primary and secondary sources. Primary microplastics include polyethylene (PE), polypropylene (PP), and polystyrene (PS) particles in cosmetic and medical products (Horton et al., 2017b), while secondary microplastics originate from physical, chemical, and biological processes resulting in fragmentation of plastic debris (Ryan et al., 2009; Thompson, 2006). Exposure to ultraviolet (UV) radiation catalyzes the photooxidation of plastic, causing it to become brittle and fragment into microplastics. While the heat and sunlight, and the well aerated conditions are ideal for generating microplastics through iterative fragmentation processes, the cold and anoxic conditions of aquatic environments and sediments can cause very slow degradation of plastic particles for centuries (Harshvardhan & Jha, 2013; Zhang, 2017). Different sources of microplastics cause them to occur in diverse shapes such as pellets, fibers, and fragments in environmental samples (Klein et al., 2015).

Primary microplastics are most likely entering the aquatic environment through household sewage discharge or spillage of plastic resin powders or pellets used for airblasting (Gregory, 1978, 1996). Another significant source of primary microplastics is the application of sewage sludge containing synthetic fibers or microplastics from personal care or household products to land (Horton et al., 2017b). Fibers are the most commonly reported form (Browne et al., 2011), most likely due to the continual abrasion of clothes and upholstery made from synthetic textiles, and washing machine effluent release (Napper & Thompson, 2016). Although synthetic fibers primarily made of polyester, acrylic, and polyamide, are secondary microplastics, they are released to the environment along with primary microplastics (Horton et al., 2017b). It has been estimated that 1900 fibers per item may come out during washing, and be released to aquatic and terrestrial environments through wastewater effluents and sewage sludge applications (Browne et al., 2011). In this context, textile mills could also be a point-source release to the environment; which has not been investigated. Areas in proximity

to plastics industry are predicted to be hotspots; concentrations of approximately 100 000 plastic particles per m^3 of seawater have been reported in a Swedish harbor area adjacent to a polyethylene (PE) production plant (Noren & Naustvoll, 2010).

Secondary sources of microplastics are considered as a great contributor of microplastic pollution given the large amount of macroplastic wastes entering the environment (Duis & Coors, 2016). Secondary microplastics, originate from anthropogenic activities, such as littering and are released during municipal solid waste collection and disposal processes (Horton et al., 2017b). Most of the plastic litter arrives to the oceans or disposed on the land. Geyer et al. (2017) estimated that approximately 6300 million tons of plastic waste were generated between the years 1950 and 2015, 4977 million tons of which accumulated in landfills and the natural environment. These large plastic items and their degraded products may be introduced to aquatic environments by wind dispersal, soil erosion or surface runoff. Likewise, light macro- and microplastics can be transported across the land by wind, while denser polymers are more likely to be buried deeper in soil layers (Horton et al., 2017b). There is evidence that low temperatures, low oxygen levels and coverage with water, sediment, or soil reduce exposure to UV radiation, hampering plastic fragmentation. Hence, photo-oxidative fragmentation is extremely slow for macro and microplastics buried in the soil; thus, soils have been considered as a sink of microplastics (Duis & Coors, 2016).

Surface runoff from agricultural lands and urban areas is another significant source of microplastic load to surface waters. Recent studies suggest that agriculture is one of the main anthropogenic activities that contribute to microplastic pollution in soil. It is estimated that between 125 and 850 tons of microplastics per million inhabitants are added annually to European agricultural soils through the application of sewage sludge (Nizzetto et al., 2016b). The use of agricultural plastics, such as plastic mulches to increase the crop yield is also a significant source of microplastics in soil (Rodríguez-Seijo & Pereira, 2019). Additionally, there is evidence to suggest that tires and road markings may also cause microplastic pollution, stormwater runoff acting as a prominent transport pathway for carrying tire and road wear particles (TRWP) to surface waters (Horton et al., 2017a; Kole et al., 2017; Unice et al., 2019a). Moreover, recent studies have demonstrated that large amounts of fibers have been transported via atmospheric fallout. Microplastics have been measured in atmospheric fallout in Paris (Dris et al., 2016) and in China (Cai et al., 2017), with greater concentrations in urban areas. Dris et al. (2016) estimated that between three to ten tons of synthetic fibers were deposited on Paris agglomeration (area around 2500 km^2) by atmospheric fallout every year. Possible sources of airborne microplastics include, synthetic fibers from clothes and houses, artificial turf, landfills and waste incineration (Dris et al., 2016). These particles in the atmosphere

can be transported by wind to the aquatic environment or deposited on the terrestrial environment. Consequently, spatial distribution of microplastics between different environmental compartments are shaped by physical processes, such as wind, tides, surface runoff and flooding that change by climatic forces (Zhang, 2017). Sources, sinks, and pathways of microplastic transport between terrestrial, freshwater, and marine environments are illustrated in Figure 2.1.

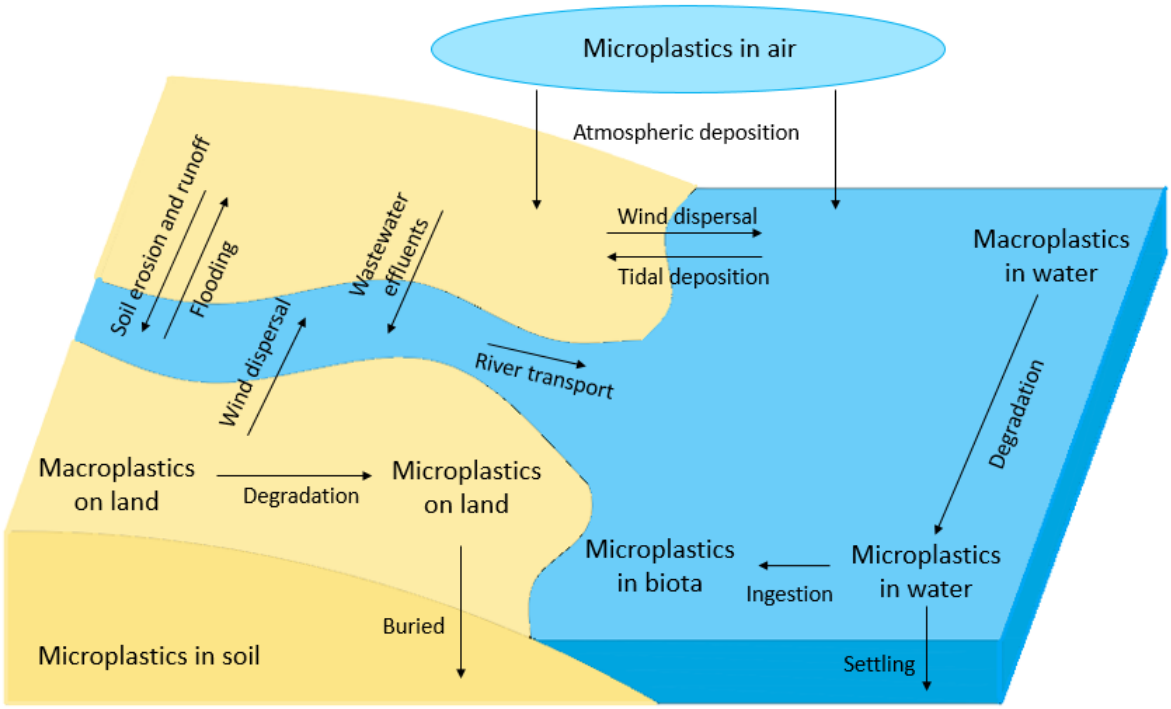

Figure 2.1. Sources, sinks, and transport pathways of microplastics between terrestrial and aquatic environments (Modified and adapted from Critchell & Lambrechts, 2016 and Horton et al., 2017b).

2.1.2. Fate and Transport in the Aquatic Environments

2.1.2.1. Marine environment. Fate and transport of microplastics in the marine environment have generally been investigated using mathematical models that are based on principles of fluid mechanics and hydrodynamics (Chubarenko & Stepanova, 2017; Critchell & Lambrechts, 2016; Iwasaki et al., 2017). Water currents, wind and tides are the main components of microplastic transport in the marine environment, which lead to prolonged sinking process of micro particles and migrations in sea coastal zone (Bagaev et al., 2017). Buoyant polymer particles, such as PE and PP tend to be transported on sea surface, whereas denser polymers, such as Polyvinyl chloride (PVC) may still be transported by underlying currents (Engler, 2012; Wang et al., 2016). Bagaev et al. (2017) indicate that after reaching bottom, microfibers are captured for a certain time period by higher turbulence in the benthic boundary layer and/or resuspended by bottom currents. Numerical models

have been developed to investigate the transport of macro and/or microplastics by surface currents and wind waves in the North Atlantic subtropical gyre (Law et al., 2010), world's oceans (Lebreton et al., 2012), eastern North and South Pacific Oceans (Law et al., 2014), Baltic Sea (Bagaev et al., 2017; Chubarenko & Stepanova, 2017) and Sea of Japan (Iwasaki et al., 2017). The model developed by Law et al. (2010) reveals that plastic pollution can quickly migrate from the US eastern seaboard to North Atlantic subtropical gyre in less than 60 days. One other advection-diffusion model developed by Critchell and Lambrechts (2016) demonstrates the relative importance of physical processes, such as beaching, settling, re-floating, degradation and wind drift governing macro- and microplastic accumulation and reveals that the topography of the source location has by far the largest influence on the fate of the microplastics.

Particle density and size distribution are dynamically changing parameters, which needs to be described explicitly to develop a comprehensive fate and transport modeling framework (Enders et al., 2015; Zhang, 2017). Several studies in the literature investigated microplastic distribution in water column, have shown high dispersal of small microplastics over surface mixed layer, and dependence on the size, density and shape of microplastic (Enders et al., 2015; Kooi et al., 2016; Kowalski et al., 2016). Indeed, most of the synthetic polymers, such as PE and PP are buoyant (Wang et al., 2016); however, aggregation with organic and inorganic particles or fouling with microbial organisms can increase the size and density of microplastics, which accelerate settling of microplastic particles onto deep sediments. Although PE and PP have densities less than that of freshwater, they have been regularly identified in deep sediments (Claessens et al., 2011; Corcoran et al., 2015; Vianello et al., 2013). Given the high concentrations of suspended sediments, particulate organic matter, and detrital particles in the aquatic environment, aggregation, biofouling and subsequent sedimentation might dominate the fate and transport of microplastics in aquatic environments (Besseling et al., 2017; Kooi et al., 2017; Long et al., 2017). Kooi et al. (2017) developed a theoretical model based on settling, biofilm growth, and ocean depth profiles for light, water density, temperature, salinity, and viscosity to simulate the effect of biofouling on the fate of microplastics, and predicted size-dependent vertical transport of microplastics in the ocean. According to their outcomes, after initial settling, buoyant microplastics never settle a fixed water level, but keep moving up and down in the water column. The density of seawater generally increases with depth, so that oscillations of micro particles in water column can be explained by dynamics based on the density differences between seawater and the plastic particle. Microplastic sinking and bioavailability may also differ among species (Katija et al., 2017; Long et al., 2015; Long et al., 2017). For example, Long et al. (2015) found that diatom aggregates sunk faster than cryptophyte aggregates, which is explained by the frustule made of biogenic silica that is denser than the organic matter. Fractal and porous particles impact the sinking

rate of aggregates (Li & Yuan, 2002; Xiao et al., 2012), in which water can flow through easily, increasing the settling velocity (Li & Yuan, 2002; Long et al., 2015). Kowalski et al. (2016) also revealed that weathering and biofouling may alter the sinking behavior of microplastics considerably, yet the particle shape strongly affects the sinking velocity, as well. Since deep sediments are considered as an ultimate sink for marine microplastics (Woodall et al., 2014), similar studies addressing vertical transport of microplastics are encountered in the literature (Bagaev et al., 2017; Enders et al., 2015; Katija et al., 2017; Näkki et al., 2017). Näkki et al. (2017) found that bioturbation, which covers all the actions of benthic fauna changing the sediment structure, transports microplastic particles deeper within marine sediments. Katija et al. (2017) also revealed that giant larvaceans *Bathochordaeus stygius* can contribute to the vertical transport of microplastics by packaging microplastic particles into their fecal pellets.

2.1.2.2. Estuaries. Marine microplastics predominantly originate from coastal regions. They may remain nearshore for a long time or reach the oceans depending on the intensity and direction of surface currents and wind waves. Yonkos et al. (2014) investigated the impact of urban development and storm events on microplastic quantities in four estuarine tributaries within the Chesapeake Bay, USA, and found that the greatest microplastic concentrations occurred shortly after major rainfall events. Liubartseva et al. (2016) developed the Markov chain model to simulate the macroplastic abundance at the sea surface and fluxes onto the coastline, and to identify source - receptor relationships among the subregions of the Adriatic Basin, between the years 2009-2015. According to the model outcomes, the coastline was the main sink of floating plastic debris. One other study implemented by Kaiser et al. (2017) examined how biofouling changes the sinking behavior of microplastics in estuarine and marine waters. After six weeks of incubation, the results revealed that despite the higher density of marine water, sinking velocity of PS particles incubated in ocean water increased more rapidly for particles sinking in the estuarine water. This was attributed to biofouling to be the major control over the sinking of microplastics.

2.1.2.3. Rivers. Microplastic research in freshwaters has gained increased attention over the last years, yet there is still limited knowledge on the fate and transport mechanisms of microplastics in rivers. Similar to marine environment, density and particle size affect retention of microplastics in river sediments, but they are not solely the dominant factors determining the distribution of these micro particles in rivers (Besseling et al., 2017; Nizzetto et al., 2016a). Particle properties and flow characteristics are the main factors influencing the fate and transport of microplastics in rivers. Nizzetto et al. (2016a) upgraded a mathematical model of catchment hydrology, soil erosion and sediment budgets for theoretical assessment of microplastic transport in river catchments. The authors

revealed that microplastics that have densities higher than water could be retained in the sediment; however, high flow periods could remobilize this pool, meaning sediments in low flow river segments are likely hotspots for deposition of microplastics. Besseling et al. (2017) implemented scenario studies on the fate and transport of nano- and microplastics in rivers by constructing a model that accounts for advective transport, homo- and heteroaggregation, sedimentation-resuspension, polymer degradation, presence of biofilm and burial. According to the model outcomes, particle size affects retention and positioning of the accumulation hotspots in the sediment along the river, yet aggregation and further sedimentation act as major processes controlling the fate and retention of microplastics along the river, due to excess mass of suspended solids that form heteroaggregates with microplastics, which overwhelm the modeled effects of polymer density and biofilm formation. Physical, chemical, and biological factors likely to affect the fate and transport of microplastics in the aquatic environment are given in Table 2.1.

Table 2.1. Factors driving microplastic fate and transport (Modified and adapted from Harrison et al. (2018)).

Governing Issues	**Effective Factors**
Surface chemistry and structure	Polymer type
	Adsorbed and leaching chemicals
	Age/weathering
	Particle size
Biological interactions	Pioneer colonizers
	Successional stage
	Competition
	Ingestion
Local environmental conditions	Temperature
	Oxygen
	Nutrients
	Light
	Salinity
	Pressure
	Presence of other pollutants
Movement and transport between habitats	Buoyancy
	Flocculation
	Particle spiraling
	Flooding
	Currents
Biogeography	Geographic location

2.1.3. Uptake and Effects

Microplastic uptake by organisms represents a growing concern due to toxicological risks associated with these micro particles. Small dimensions of microplastics increase their

bioavailabilities to aquatic organisms. To date, ingestion has been considered as the fundamental pathway for marine and freshwater species to uptake microplastics (e.g. Nelms et al., 2018; Reichert et al., 2018; Tosetto et al., 2016). Many of the studies have proved the ingestion of microplastics by detecting different type of polymer particles in the intestines and stomachs of various organisms, such as zooplanktons (Desforges et al., 2015; Jeong et al., 2017; Sun et al., 2017), shellfish (Gandara E Silva et al., 2016; Li et al., 2016; Tosetto et al., 2016), corals (Hall et al., 2015; Reichert et al., 2018), fish (Hermsen et al., 2017; Jabeen et al., 2017; McNeish et al., 2018), marine mammals (Fossi et al., 2016; Nelms et al., 2018), and earthworms (Hodson et al., 2017; Huerta Lwanga et al., 2017). For example, Hurley et al. (2017) investigated the ingestion of microplastics by Tubifex worms from bottom sediments in a major urban waterbody fed by the Irwell River, Manchester, UK and estimated the mean concentration of ingested microplastics as 129 ± 65.4 particles per gram tissue. Most of these studies have shown that the majority of ingested particles consist of fibers, which are generally in the range of 66-71% of the total count and followed by fragments and pellets (Bellas et al., 2016; Güven et al., 2017; Silva-Cavalcanti et al., 2017).

Ingestion may occur directly due to misidentification or indiscriminate consumption of microplastics for feeding (Ory et al., 2017), or indirectly as a result of trophic transfer along the food web (Nelms et al., 2018). Microplastics have also been found in different organs besides the digestive tract, which are not involved in the process of ingestion. In addition to stomach and hepatopancreas, Brennecke et al. (2015) observed microplastics also in the gills of the fiddler crab. A study by Watts et al. (2014) also indicated that the shore crab (*Carcinus maenas*) can uptake microplastics through the inspiration across the gills. Moreover, Kolandhasamy et al. (2018) investigated the adherence of microplastics to soft tissues of mussels as a novel way for organisms to uptake microplastics beyond ingestion. The authors found that adherence of microplastics to specific organs; such as adductor, foot and visceral tissue contributed about 50% of the microplastic uptake in mussels.

Adverse effects of microplastics on aquatic organisms have also been investigated performing both lab-based and field-based experiments. According to a study carried out on the blue mussel *Mytilus edulis*, after exposure to microplastics under laboratory conditions, it was observed that smaller microplastics tend to accumulate in the tissues more than larger particles, and can translocate from the gut to the circulatory system within three days and persisted for over 48 days (Browne et al., 2008). Additionally, impact of microplastics alone or in combination with toxic chemicals including heavy metals, polychlorinated biphenyls (PCBs), polycyclic aromatic hydrocarbons (PAHs) and polybrominated diphenyl ethers (PBDEs) have been examined performing exposure experiments for microalgae (*Tetraselmis chuff*), Norway lobsters (*Nephrops norvegicus*), common gobies

(*Pomatoschistos microps*), and amphipods (*Allorchestes compressa*); respectively (Chua et al., 2014; Davarpanah & Guilhermino, 2015; Devriese et al., 2017; Oliveira et al., 2013). According to de Sá, Luís, and Guilhermino (2015), microplastic particles and their adsorptive capacity may lead to growth delay, decrease in reproductivity, and mortality increase of organisms. The authors investigated the predatory performance of goby fish (*Pomatoschistus microps*) in the presence of microplastics combined with prey (*Artemia nauplii*) in two estuaries located in NW Iberian coast, USA under different environmental conditions. A significant reduction in predatory performance (65%) of fish from one estuary was observed, while the fish from other estuary were not affected significantly, suggesting that developmental conditions may influence the prey selection capability of fish.

2.1.4. Microplastic Pollution in Rivers

Rivers act as a major transport pathway for plastic debris. It has been estimated that between 70 and 80% of marine plastics are transported to the seas through the conduits provided by rivers (Bowmer & Kershaw, 2010). For example, annual microplastic load from the Ebro River, Spain to the Mediterranean Sea was estimated at over 2 billion pieces (Simon-Sánchez et al., 2019). Considering the origin and risk posed by microplastics, the studies investigating the occurrence and abundance in freshwaters have increased, many of which have focused on rivers. The level of microplastic pollution in riverine waters was first reported in California, in 2011 (Moore et al., 2011). Microplastics were also found in many rivers, such as the Danube, Austria (Lechner et al., 2014); Rhine, Germany (Klein et al., 2015; Mani et al., 2015); 29 Great Lakes tributaries, US (Baldwin et al., 2016); Ombrone, Italy (Guerranti et al., 2017); Thames, UK (Horton et al., 2017a); Shanghai Rivers, China (Peng et al., 2018); Nakdong, South Korea (Eo et al., 2019); and others such as, Maozhou, Manas and Fenghua in China (Wang et al., 2021a; Wu et al., 2020; Xu et al., 2021). The influence of municipal and industrial effluents on microplastic concentration in surface water and sediment have been investigated for a variety of rivers, such as St. Lawrence (Castaneda et al., 2014) and Ottawa, Canada (Vermaire et al., 2017), Seine in Paris (Dris et al., 2015), the Rhine-Main area in Germany (Klein et al., 2015), Raritan in New Jersey (Estahbanati & Fahrenfeld, 2016), and Saigon in Vietnam (Lahens et al., 2018). Dris et al. (2015) carried out the first study in the Seine River to investigate microplastic pollution in urban compartments including wastewater, atmospheric fallout and rivers. Vermaire et al. (2017) examined microplastic abundance in surface waters and sediments of the Ottawa River, Canada, and revealed that microplastic concentrations were significantly higher downstream of the wastewater treatment plant compared with the upstream of the effluent output. Horton et al. (2017a) investigated the abundance and sources of microplastics in sediments of the Thames River. The authors found significantly higher number of plastic particles at downstream of a

storm drain outfall receiving urban runoff that contains fragments derived from road marking paints. Nel et al. (2018) assessed the microplastic pollution dynamics in an urban river sediment experiencing temporal differences in river flow and found that microplastic amount in winter was approximately 25 times higher than in summer, likely due to the increased sedimentation associated with reduced river flows during the winter season.

A global model of macro and microplastic discharge from rivers into oceans based on waste management, population density and hydrological information was developed by Lebreton et al. (2017). The authors estimated that between 1.15 and 2.41 million tonnes of plastic waste enters the ocean every year from rivers, over 74% of emissions occurring between May and October. The study also reveal that the top 20 polluting rivers are mostly located in Asia and accounted for 67% of the global annual discharge. One other modeling approach was developed using an existing global model for nutrients, the Global NEWS (Nutrient Export from WaterSheds) to analyze the composition and quantity of point-source microplastic fluxes from European rivers to the seas and to explore future trends up to the year 2050 (Siegfried et al., 2017). The model results indicated that about two-thirds of the microplastics modeled flow into the Mediterranean and Black Sea, and most of these particles were synthetic polymers from TRWP (42%) and plastic-based textiles abraded during laundry (29%).

Research indicates that there is a need for the investigation of microplastic transport processes between terrestrial and freshwater systems. A study by Unice et al. (2019a) investigated the transport of TRWP in the Seine Watershed (France) by developing a comprehensive watershed-scale modeling methodology. The authors studied both terrestrial transport to soil, air, and roadways, as well as freshwater transport processes including heteroaggregation, degradation and sedimentation. The model estimated that the per capita mass release of TRWP in the Seine Watershed was 1.8 kg per inhabitant in a year, 18% of which were transported to the freshwater, whereas 2% were exported to the estuary. The model also confirmed the significance of particle size and density on estuarial transport of TRWP (Unice et al., 2019b).

2.2. Analysis of Microplastics

2.2.1. Sampling from the Aquatic Environments

2.2.1.1. Water sampling. Microplastic research generally requires the large volume of water samples due to relatively low concentrations of these particles in the aqueous samples. The scientific research indicates that a standardized method for microplastic sampling and analysis is not available in

literature, yet sampling methods for the marine and freshwater environments are similar to each other (Lechner et al., 2014; Mani et al., 2015; Vermaire et al., 2017). The water quality and hydrodynamic conditions of the study site plays a significant role in selection of the sampling method. Surface water and water column samples are usually collected via plankton nets and sieves filtering great volume of water up to hundreds of liters (Klein et al., 2018; Prata et al., 2019). Neuston nets and Manta trawls, typically with a mesh size of 330 μm, are dropped horizontally to the water surface to collect microplastic samples, especially in seas, lakes, dams and large rivers with high flow rates. For low flow rivers, plankton nets with the mesh sizes ranging from 50 to 100 μm are generally used. The volume of water filtered is measured via flowmeter attached on the plankton net. Following sampling, the inside of the plankton net is rinsed with pure water to wash down microplastics into the collector of the plankton net. Finally, the sample in the collector is transferred to a glass bottle and preserved at +4^{o}C until the lab analysis.

To date, plankton nets are the most used instruments for microplastic sampling in the aquatic environments, including freshwaters. However, plankton nets with smaller mesh sizes are prone to clogging, which limits the quantification and identification of small-sized microplastics. In addition, the lack of standardized use of plankton nets and different mesh sizes hamper the comparability of the quantitative data on microplastic concentrations in freshwater samples. To overcome these problems, filter cascades have been developed, which provide size fractionation during the sampling and reduce the matrix burden onto smaller mesh sizes (Löder & Gerdts, 2015).

An alternative to plankton nets is on-site filtration or sieving using buckets, but this method is less preferred as it is time consuming and demanding (Prata et al., 2019). Another method for collecting sample from the water column is direct filtration of the water with submersible pumps (Klein et al., 2018). It is also common to collect water samples in glass bottles and process in the lab (Dubaish & Liebezeit 2013; Leslie et al., 2017), which is advantageous in sampling and analyzing small-sized microplastics. The volume of the sample collected varies depending on the water quality and pollution.

2.2.1.2. Sediment sampling. Similar to water sampling, there is no standardized method for sediment sampling in microplastic research, yet use of grab samplers (Van Veen and Ekman grab samplers) provides relatively comparable results due to being frequently used sampling instrument. Microplastic concentrations in sediments varies with depth. Particularly, the top layer of sediments between 1-5 cm contains more microplastics than in deeper sediments (Prata et al., 2019). New methods, such as application of sediment corers allows the investigation of microplastic depth profiles

(Uddin et al., 2021). Microplastics concentrations in sediments are reported considering the amount of sediment (dry or wet), which can be expressed as weight (g, kg) or volume (mL, L).

The collected samples are transferred to glass bottles and preserved at -20^{o}C in freezer before the analysis.

2.2.2. Extraction of Microplastics

2.2.2.1. Extraction from the water samples. The most frequent method for extraction of microplastics from water samples is filtering or sieving. Aqueous samples collected in the glass bottles are usually filtered through a filter paper or plankton mesh in the lab. The pore size of the filter paper or mesh size of the sieve can vary depending on the size range of the particles that will be investigated (Prata et al., 2019). However, smaller pore or mesh sizes are prone to clogging in a short time by organic matter, which can require the removal of the organic matter by the method given in Section 2.2.2.3.

2.2.2.2. Extraction from the sediment samples. A common method for the extraction of microplastics from sediment samples is density separation developed by Thompson et. al (2004). The method is based on mixing sediment with a salt saturated solution to increase the density, float plastic particles, and finally filter the supernatant. Sodium chloride (NaCl), sodium bromide (NaBr), sodium iodide (NaI), zinc chloride ($ZnCl_2$) and zinc bromide ($ZnBr_2$) are some of the salts used in extraction of microplastics from sediments (Klein et al., 2018; Prata et al., 2019). The application of NaCl solution (1.2 g cm^{-3}) is more extensive than other salts due to being cost-effective and ecofriendly. However, it is insufficient to extract high density polymers, such as polyoxymethylene (POM), polyvinyl chloride (PVC) and polyethylene terephthalate (PET). Likewise, scientific research revealed that NaBr (1.4 g cm^{-3}) had low recovery rates for extraction of higher density polymers (Quinn et al., 2016). Although, NaI (1.6 g cm^{-3}) and $ZnBr_2$ (1.7 g cm^{-3}) are effective for separation of dense polymers, they are too expensive for application in large volume samples (Corcoran et al., 2009; Klein et al., 2018). Moreover, $ZnBr_2$ is hazardous to the environment. As an alternative to NaCl, $ZnCl_2$ (1.7 g cm^{-3}) is frequently used in recent studies due to the capability of extraction of heavier particles and lower costs compared to NaI and $ZnBr_2$ (Horton et al., 2017a; Imhof et al., 2012). However, $ZnCl_2$ is also hazardous, which can be overcome by recycling the solution (Klein et al., 2018).

Elutriation column developed by Claessens et al. (2013) is an alternative to density separation, which separates particles according to their terminal falling velocities depending on the density, size

and shape of the particles. The method allows recovery of dense microplastics effectively, yet the sand recovery yield is also high (Kedzierski et al., 2016). According to Kedzierski et al. (2016), the method can be improved with a pre-size fractionation of the sample.

Digestion of sediment and following filtration is another method for extraction of microplastics from sediment samples. This method has started to be used, especially in recent studies (e.g. Gao et al., 2023) due to probable low recovery of microplastics in density separation method. Digestion methods are explained in detail in Section 2.2.2.3.

2.2.2.3. Removal of organic matter. The accurate analysis of microplastics in environmental samples is one of the most challenging problems during the detection and identification period, since environmental samples consist of a complex mixture of organic matter, such as plant and animal residues as well as cells and tissues of organisms, with a high content of inorganic matter (Dumichen et al., 2017). For this reason, sample preparation including organic digestion plays a significant role in analyzing microplastics accurately.

Organic matter can be removed before or after filtration by adding chemicals, such as hydrogen peroxide (H_2O_2), potassium hydroxide (KOH) or sulfuric acid (H_2SO_4) depending on the amount of organic matter, or by Fenton reaction to enhance oxidative potential of H_2O_2 using iron (Fe^{2+}) salt as a catalyst (Ameta et al., 2018). However, strong acids can damage microplastics by changing the structure of the polymer, which results in loss of microplastics during analysis (Enders et al., 2017). The research revealed that H_2O_2 and KOH are less damaging to microplastics; however, the contact time should not exceed 7 days (Nuelle et al., 2014). Rapid degradation of the organic matter can be achieved by heating the sample under controlled conditions (~50-55^{o}C), as previous studies have indicated that some polymers are damaged above 60^{o}C (Thiele et al., 2019).

2.2.3. Visual Analysis

Following filtration, the samples are examined under a stereomicroscope for visual identification of microplastics. Microplastic particles are transferred to filter papers, previously checked for airborne contamination, and photographed to count and categorize microplastics according to their physical properties, such as color and shape. The size of each particle is also determined using a photo processing software. This method has been applied almost in all microplastic studies so far. Visual analysis has many advantages including low cost, simple operation and little chemical hazard, yet it is time-consuming and cannot provide data on the chemical composition of microplastics (Lavers et

al., 2016; von Moos et al., 2012). Another method for visual analysis is scanning electron microscopy (SEM), which provides morphological identification of microplastics, generating high-resolution images of the surface structure (Mariano et al., 2021). SEM can be used to identify the smaller microplastics as tiny as 1 nm (Shim et al., 2017). However, SEM images cannot be used to determine color and chemical composition of microplastics (Eriksen et al., 2013).

2.2.4. Polymer Characterization

Plastics are complex structures with big molecules, produced by polymerization of the same or different monomers (Chen et al., 2022). Many different spectroscopic approaches are available for chemical characterization of microplastics. The majority of these methods require sample pre-treatment, whereas there are several methods that allow direct analysis of the samples. However, the factors, such as degradation, aging and the presence of plastic additives and other contaminants can complicate the chemical characterization and lead to misinterpretation about the microplastic sample. For this reason, sample processing and visual analysis of particles before characterization is important to lessen the practical problems with spectroscopic analysis (Prata et al., 2019).

Fourier Transform Infrared (FTIR) and Raman spectroscopy are the most commonly used methods in characterization of microplastics. These are vibrational spectroscopy techniques that are based on producing a spectrum resulting from the interaction of light with molecules. FTIR provides an infrared spectrum due to the changes of material dipole moment (Prata et al. 2019). In other words, when a molecule interacts with infrared radiation in FTIR, it selectively absorbs radiation of specific wavelengths, thereby its vibrational energy level transfers from ground state to excited state (Mariano et al., 2021). FTIR can provide information of chemical compositions using diverse techniques: transmission, specular reflectance/reflection-adsorption and attenuated total reflection (ATR) (Huang et al., 2023; Mariano et al., 2021). Transmission and reflectance modes can be applied thick (>5 μm) and opaque samples (Shim et al., 2017), but irregular surfaces of particles can interfere with analysis with reflectance mode due to refractive error (Harrison et al., 2012; Mariano et al., 2021). ATR-FTIR provides information with high accuracy on large (>500 μm) and irregular particles (Huang et al., 2023; Prata et al. 2019), but small microplastics require micro-FTIR, which can identify particles as small as 20 μm. The advantages of FTIR spectroscopy include being non-destructive to samples, relatively simple pre-treatment procedure and less susceptibility to fluorescence interference. However, microplastics smaller than 20 μm cannot be detected. Furthermore, FTIR spectroscopy is susceptible to the presence of other substances and degradation of microplastics (Huang et al., 2023).

Raman produce a fingerprint spectrum resulting from the polarizability of chemical bonds (Prata et al., 2019). When a monochromatic light interacts with the sample molecule, the molecule is excited to a higher vibrational level and a photonic scattering occurs, which results in shift in energy levels of the scattered photon due to the excitation energy. In other words, Raman spectrum is produced by the inelastic scattering between the photons of an incident radiation and the molecules (Ribeiro-Claro et al., 2017). Raman spectroscopy has many advantages, including the characterization of microplastics < 20 μm, possibility of non-destructive analysis, small sample amounts and reduced sample preparation. Moreover, thickness of particles is not a problem for characterization. However, plastic additives and chemicals adsorbed on the surface of microplastics can generate a different Raman spectrum, which can overlap with the Raman spectra of polymers and hinder the identification of microplastics. Also, fluorescence interference is a significant problem, which overlays the Raman bands and thereby limits obtaining high-quality spectra. This problem can be overcome by shifting the laser wavelength to the near-infrared spectral region or increasing exposure time before recording the spectra (Ribeiro-Claro et al., 2017). FTIR and Raman spectroscopy can be used together to obtain reliable results. In such cases, FTIR spectroscopy is recommended for detection of microplastics between 50 and 500 μm size range, whilst Raman spectroscopy is recommended for microplastics in the 1-50 μm size range (Fortin et al., 2019; Käppler et al., 2016).

An alternative to vibrational spectroscopic methods is thermal analysis, based on the identification of polymer according to its thermal stability and degradation products. Thermal analysis methods include thermogravimetry (TGA), differential scanning calorimetry (DSC), pyrolysis-gas chromatography-mass spectrometry (Py-GC/MS) and combinations of these techniques (Mariano et al., 2021). Py-GC/MS is the most commonly used thermal analysis method, which allows characterization of polymers, additives present in the sample and other chemicals adsorbed to microplastics, such as persistent organic pollutants (POPs) (Ribeiro-Claro et al., 2017). The method is also ideal for identifying trace concentrations of microplastics in environmental samples. However, Py-GC/MS is a destructive technique, which hamper the probable analysis of microplastics by other further methods.

The advantages and limitations of most commonly used characterization methods are given in Table 2.2.

Table 2.2. Comparison of most commonly used microplastic characterization methods (Huang et al., 2023; Mariano et al., 2021; Tagg et al., 2015).

Analysis Method	Advantages	Limitations
ATR-FTIR	• Non-destructive • Low cost • Short analysis time	• Water interference • Complex spectrum • Convenient for large particles (>500 μm)
Micro-FTIR	• Non-destructive • Low to medium cost • Identification of small particles (down to 20 μm) • Mapping is possible	• Water interference • Complex spectrum • Medium to long analysis time • Low lateral resolution (~20 μm)
Raman	• Non-destructive • Identification of small microplastics and nanoplastics (< 1 μm) • Mapping is possible • Low water interference • High lateral resolution (~1 μm)	• High cost • Fluorescence interference • Long analysis time
Py-GC/MS	• Characterization of trace concentrations of microplastics and additives	• Destructive • Complex data

2.3. Mathematical Modeling of Microplastic Transport

2.3.1. Mathematical Models

A mathematical model can be defined as an idealized formulation that represents the complex relationships and processes in the environment using a set of equations, algorithms and logical statements (Chapra, 1997). Mathematical models typically represent a simplified version of reality and are best used to describe physical systems that tend to behave in a highly repeatable manner. Real systems are complex and involve numerous uncertainties. Since mathematical models are generally based on available data, assumptions and approximations, they cannot represent all the uncertainties, so can have limitations. Modeling approaches can be classified depending on the mathematical approach used, model certainty, system and type of variables as follows;

(i) deterministic vs. stochastic, depending on model certainty or uncertainty;
(ii) empirical vs. mechanistic, depending on how the processes are described;
(iii) dynamic vs. static, depending on changing variables in time domain.

Deterministic models often use algebraic or differential equations to represent the relationship between system's variables (Zeidan, 2017). In a deterministic model, there is a predetermined relationship between the input and output variables, which means that the future state of the system is completely determined by its current state and inputs supplied. Deterministic models use fixed input and output variables without considering errors and uncertainties, therefore given the same initial conditions and inputs, the model will always produce the same output. Stochastic models incorporate randomness and uncertainty to predict system's behavior. Unlike deterministic models, stochastic models consider random variations, fluctuations, and associated uncertainties and use probability distributions to estimate the model outcomes. Rather than an exact outcome, stochastic models give the output as an interval or a distribution. Monte-Carlo simulations are a commonly used method to estimate probability distributions, which was also adopted in the development of the model presented in this study. This modeling approach is particularly useful, when the system is affected by the random events or processes, as well as when the available data is limited or uncertain.

Mathematical models can also be classified as empirical or mechanistic depending on how the model describe the processes. Empirical models (or statistical models) are based on inductive or data-based approach, in which the model indicates the relationship between variables using experimental data and statistical analyses (Chapra, 1997). Regression analysis is often used to assess the reliability of predictions. Empirical models provide insights for investigating cause and effect relationship. Some of the empirical models are defined as 'black box' models due to presenting solely the relationship between input and output variables and not representing any specific mechanisms involved in the model (Zeidan, 2017). On the other hand, mechanistic models, also known as process-based models, simulate complex systems by explicitly representing the underlying physical, chemical, or biological processes involved. This kind of models aid to understand the effect of environmental changes, develop management strategies and decision support systems.

Another classification of mathematical models depends on the variation of variables in time. A static model describes the structure of the system, in which the results are obtained by a single computation of all equations while a dynamic model describes the behavior of the system over time. Unlike static models, in dynamic models, the results are obtained by repetitive computation of all equations over time (Zeidan, 2017). In this context, system dynamics models are useful tools in

representing the relationships among various variables, processes and model components to understand system's behavior and predict its future state. The structure of a system's dynamic is based on stocks and flows, feedback processes, time delays and other sources of dynamic complexity (Sterman, 2001). Stocks represent the accumulation, while flows represent the rate of inflow and outflow within the system. Feedback loops are the key mechanism that involves the causal relationships and interactions between different components of the model. System dynamics models are versatile in that they aid to understand the changes in the system's behavior under different conditions and explore the long-term consequences of processes, random events or decisions of stakeholders.

2.3.2. Applications in Rivers

Mathematical models can be used to determine the transport processes and potential hotspots of microplastics, as well as other processes, such as interaction with chemicals, natural particles and biota. Many modeling approaches are available in literature to investigate fate and transport of microplastics in river systems. Different modeling methods have been developed to investigate microplastics, such as hydrodynamic, statistical, mass-balance, process-based, and hybrid models that involves the combination of such models (Uzun et al., 2022). For example, mass-balance models were developed to understand the contribution of rivers on microplastic pollution in seas and oceans. These models were global-scale and simulated microplastic discharge from rivers to oceans considering potential sources, hydrological conditions and anthropogenic factors, such as population and waste management, as well as predicted future microplastic loads (Lebreton et al., 2017; Siegfried et al., 2017).

There are many process-based and hydrodynamic models developed in literature to understand the effect of particle properties and river hydrodynamics, as well as environmental processes, such as aggregation and biofilm formation, on transport of microplastics. For example, Besseling et al. (2017) developed a process-based, hydrodynamic model considering homo- and hetero-aggregation, biofilm, sedimentation, degradation, resuspension, and burial as the key processes of the fate and transport of microplastics in rivers. The authors used NanoDUFLOW, a spatiotemporally resolved hydrological model, to simulate the concentration of spherical particles with different sizes along the river. Moreover, transport of microplastics from terrestrial environments to rivers was modeled in various studies. For example, Unice et al. (2019a) investigated transport of TRWPs from land-based sources to the freshwater systems and considered settling, hetero-aggregation, and degradation of these particles in receiving waters using mass-balance and hydrodynamic equations. Likewise, Bondelind

et al. (2020) developed a hydrodynamic model using MIKE 3 FM software to investigate transport of TRWPs by stormwater runoff and understand the effect of particle size and density on fate of these plastics in freshwaters. Another study by Whitehead et al. (2021) used INKA, a process-based dynamic model, to investigate inputs, loads, and concentrations of microplastics along the Thames River under changing effluent discharges and land applications of sludge. However, most of these models have focused on only spherical or near-spherical microplastics. Therefore, other shaped particles, such as fragments and fibers will possibly not modeled successfully by such models. In addition, different flow regimes and river morphology are other significant factors in transport behavior of microplastics, which are mostly overlooked in developed models.

In addition to the models given above, experimental studies have also been carried out and compared to the theoretical models in order to understand transport of microplastics in rivers. For example, Cook et al. (2020) investigated longitudinal dispersion of buoyant microplastics (PE) in laboratory flume conditions and found that both the microplastics and dye (Rhodamine) displayed fundamental dispersion theory in uniform open channel flow. Longitudinal dispersion coefficients obtained from the experiments agreed well with Elder (1959) and Chikwendu (1986) models. More specifically, Waldschläger and Schüttrumpf (2019a) investigated the effect of particle properties including density, size, and shape on settling and rising velocities of microplastics by laboratory experiments. The authors implemented statistical analysis, developed new formulas to calculate settling and rising velocities of microplastics, and compared their test results with the results of theoretical calculations. Another experimental study by Waldschläger and Schüttrumpf (2019b) determined the critical shear stresses of microplastics with different densities, sizes, and shapes on different sediment beds to examine the erosion behavior of microplastics. Congruent to the results of their statistical model, the authors developed an equation to calculate critical shear stresses of different microplastics considering different sediment-microplastic combinations.

The effect of flow characteristics on particle settling has been subject of research over the last years (Nghiem et al., 2022; Odum et al., 2023). For example, Jacobs et al. (2016) conducted a set of experiments in a grid turbulence facility to determine the settling velocities of natural, synthetic, and industrial particles under various turbulent flows. According to their results, particle settling velocity either remained unchanged or increased relative to stagnant flow. The authors also found that the largest particles were mostly unaffected, while the smallest ones were more influenced by the flow conditions. In recent years, scientific research has started to focus transport of microplastics in turbulent flow, so the number of both experimental studies and developed models related to the subject has started to increase. For example, a study by Shamskhany and Karimpour (2022) developed

a hydrodynamic model to simulate entrainment and vertical mixing of microplastics with different sizes and densities under turbulent flow. The authors used a hybrid Eulerian-Lagrangian computational model and revealed that the movement of large particles can be dominated by gravitational settling or rising, whereas transport of small microplastics was mainly governed by the turbulent flow. Similarly, Xing et al. (2022) conducted a set of laboratory experiments in a circulating water tank, as well as performed three Markov models, including a continuous time random walk model, Bernoulli model, and spatial Markov model to test whether these models faithfully capture transport of PE particles in an open channel flow. Another study modeled the mixing and longitudinal dispersion of buoyant microplastics (PE) and dyes (Nile red and Rhodamine) in vegetated and turbulent flows (Stride et al., 2023). To achieve this, the authors conducted an experimental study in laboratory flume conditions and also developed a hydrodynamic model based on advection-dispersion equations. According to the results, both the PE particles and dyes had the same behavior regardless of the complexity of flow characteristics. Another experimental study was conducted by Born et al. (2023) to investigate vertical concentration profiles of microplastics in turbulent flow and test the Rouse's formula applicability for buoyant and sinking microplastics. The results revealed that the concentration profile shapes of settling microplastics were similar to those of natural sediments and running reversed for buoyant particles. In addition, the Rouse's formula applicability was confirmed for approximately uniform flows. Most of these studies considered microplastics as pure particles with spherical or near-spherical shape, so more extensive experimental tests and modeling approaches focusing various particle properties, hydraulic parameters, and environmental processes are required to fill these research gaps.

3. MATERIALS AND METHODS

The abundance and distribution of microplastics in water and sediment samples collected from six sites of the Ergene River were determined via laboratory analyses. The modeling methodology in this thesis combines microplastic abundance and characteristics data and river variables utilizing a mechanistic model developed using hydrodynamic and mass-balance equations. The scheme of the research methodology is given below.

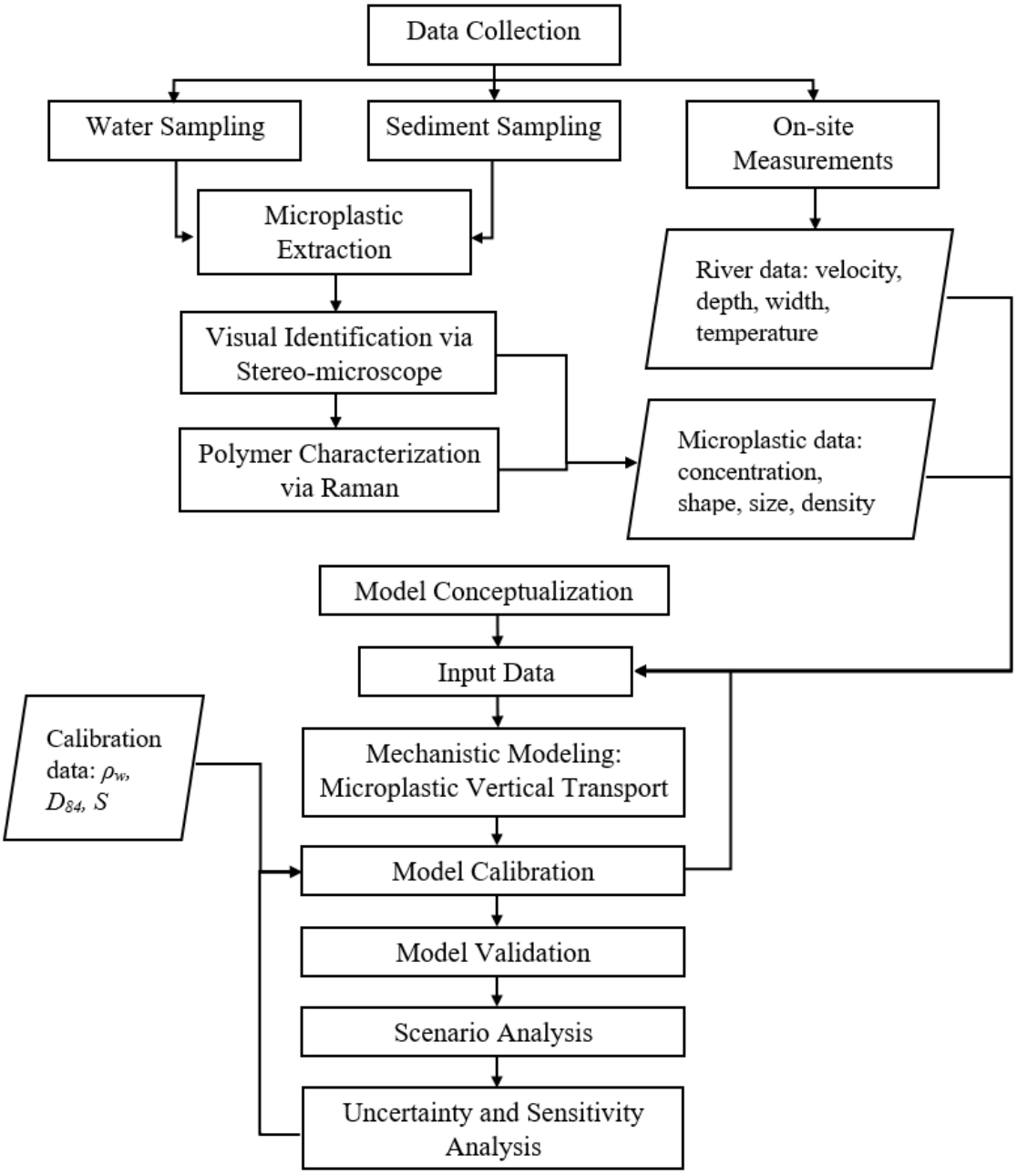

Figure 3.1. Methodology scheme.

Section 3.1 and 3.2, which involve sampling and identification of microplastics in the Ergene River, were published in 'Environmental Research' journal, titled as 'Microplastic distribution in the surface water and sediment of the Ergene River' (Akdogan et al., 2023).

3.1. Study Area and Sample Collection

The Ergene River Catchment is located in the northwestern region (Thrace) of Turkey with a 17323 km^2 drainage area. The river rises from the Istranca Mountains in the northeastern part of the basin and flows for 283 km through the northwest-southwest direction, with a maximum depth of 6.8 m, before reaching the Aegean Sea. Significant amount of waste originating from industry and unplanned urbanization threaten the water resources feeding the Ergene River. Çorlu and Ergene tributaries are approximately in 60 km length and join the main stream from the eastern side of the river. There are numerous Organized Industrial Zones (OIZs) within the basin, being especially intensive in the sub-basins of the Çorlu and Ergene tributaries (Figure 3.2a), which makes the area one of the most prone regions to contamination.

River samples were collected from the surface water and sediment in May 2019 and Sep 2020. Although the second sampling was planned to be done in the same year, it was postponed and performed in the year 2020 due to the Covid-19 pandemic. The sampling was performed once in six stations including the Çorlu and Ergene tributaries and on the mainstream, where the tributaries met (Figure 3.2b). These stations were particularly selected because of the heavy industrialization located in this area. Water sampling was carried out using stainless-steel buckets and collecting samples into glass bottles. 15 liters of surface water samples (0-15 cm depth) were collected in duplicates from each sampling site and preserved at +4^{o}C prior to analysis. Sediment samples were collected using a Van Veen grab sampler, which were then transferred to aluminum foil containers and covered tightly. Three replicates were collected for sediment samples and preserved at -20^{o}C in the freezer before extraction. Additionally, the parameters including velocity (m s^{-1}), depth (m) and channel width (m) of the river were measured using Acoustic Doppler Current Profiler (ADCP) instrument. After measuring the river's hydrodynamical and morphological parameters, four consistent measurements with an error rate of less than 5% were considered for each location. In addition, water quality parameters including sample temperature (T_s) and dissolved oxygen (DO), as well as weather temperature (T_w) were measured on-site.

Map of the study area is shown in Figure 3.2.

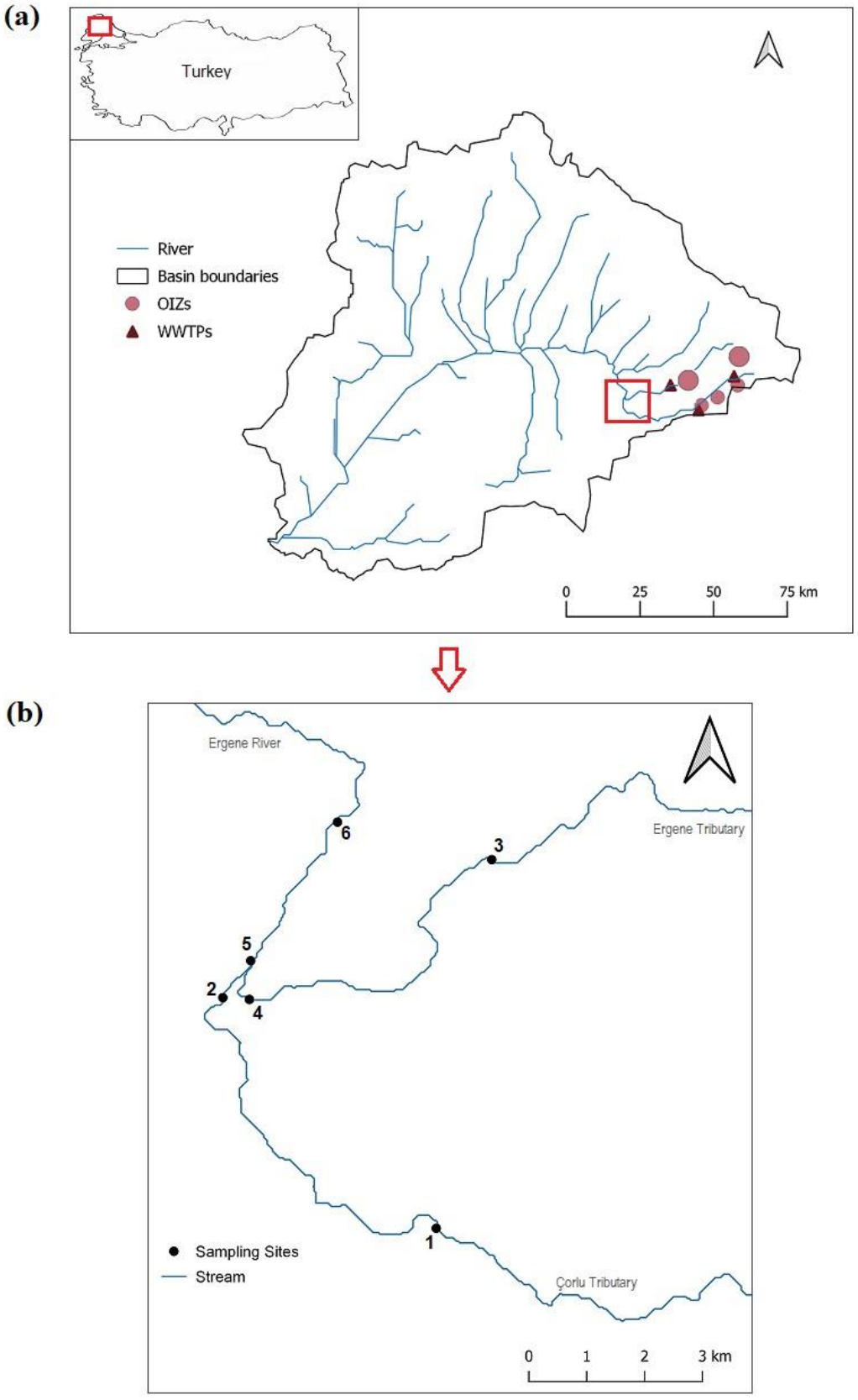

Figure 3.2. Map of the study area: (a) Ergene River Basin and location of the OIZs and WWTPs within the study site. (b) Sampling sites.

The coordinates of the sampling sites are given in Table 3.1.

Table 3.1. Sampling sites in the Ergene River.

Site	Location	Coordinates	
S1	Çorlu Tributary	41.162833 N	27.492725 E
S2	Çorlu Tributary	41.196444 N	27.470667 E
S3	Ergene Tributary	41.215876 N	27.526184 E
S4	Ergene Tributary	41.134454 N	27.476339 E
S5	Ergene River	41.202172 N	27.476447 E
S6	Ergene River	41.223676 N	27.494495 E

Meteorological data during the sampling periods, and on-site measurements are given in Table 3.2. Meteorological data were obtained from Turkish State Meteorological Service. Hydrodynamical and morphological parameters of the stream were not measured at Site 6 due to inconvenience of the field.

Table 3.2. Meteorological data and on-site measured parameters of the Ergene River.

	Site	Time	T_w (°C)	Wind (km h^{-1})	Wind Direction (from)	T_s (°C)	DO (mg L^{-1})	River Velocity (m s^{-1})	River Depth (m)	Channel Width (m)
May 20, 2019	S1	12:45	27	20	Southwest	25.0	1.37	0.421	0.418	9.9
	S2	11:48	26	6	South	24.4	2.34	0.424	0.550	10.2
	S3	19:10	22	13	South	24.3	2.16	0.542	0.594	5.7
	S4	16:21	25	22	South	24.1	0.88	0.361	0.559	8.5
	S5	15:00	25	17	Southwest	24.2	0.22	0.475	0.401	21.1
	S6	17:40	22	11	South	24.0	1.42	-	-	-
Sep 30, 2020	S1	18:10	21	15	Northwest	22.4	0.23	0.725	0.526	8.6
	S2	15:40	22	22	Northwest	21.6	0.10	0.748	0.334	12.0
	S3	11:38	19	20	Northwest	21.1	0.16	0.383	0.586	4.9
	S4	16:30	21	17	West	22.1	0.11	0.258	0.415	10.7
	S5	14:30	22	15	Northwest	22.2	0.15	0.438	0.484	18.6
	S6	13:40	21	13	West	22.6	0.16	-	-	-

3.2. Detection and Analysis of Microplastics

3.2.1. Extraction from Samples

The organic matter in the water samples was removed prior to microscopic observation by a modified version of the wet peroxide oxidation method developed by Masura et al. (2015). Firstly, the supernatant of water samples was filtered through a plankton mesh with a 45 µm pore size, previously checked for airborne contamination. On the other hand, organic matter that had settled at the bottom of the bottle was transferred to a beaker and digested adding 35% hydrogen peroxide

(H_2O_2) solution. Depending on the amount of organic matter, H_2O_2 was added gradually at certain time intervals and the covered beakers were kept at 50°C in water bath until the organic matter disappeared. In case of any organic matter remained in the sample, the process was repeated so as not to exceed seven days (Nuelle et al., 2014). Finally, the digested aliquot was filtered through a 45 μm plankton mesh. For sediment samples, microplastics were extracted from each sediment replicate through the density separation method developed by Thompson et al. (2004). After homogenization, a 50 mL aliquot of each sediment replicate was weighed and stirred for 1.5 min in a glass beaker with 500 mL of concentrated NaCl solution (1.2 kg L^{-1}), which subsequently was allowed to settle for one hour. The supernatant liquid including extracted particles from the sediment was filtered through a 45 μm plankton mesh. This procedure was repeated two times for three replicates of sediment samples.

3.2.2. Identification and Characterization

Microplastic particles were visually identified under a stereo-microscope (Olympus SZX 16, 30x) and transferred to a clean cellulose filter paper (Whatman filter paper with 4-7 μm pore size), previously checked for airborne contamination. After photographing microplastics, ImageJ software was used to count the plastic particles and determine the length of each particle individually. Microplastics identified were categorized according to their colors and shapes as fiber, hard fragment, soft fragment, pellet, foam, rubber and others. The differentiation between hard and soft plastics is significant due to their distinct properties, applications and recycling capabilities. Such differentiation could provide additional information on the sources of microplastics. Hard and soft fragments were distinguished visually or by applying slight pressure with the tip of the forceps. After visual inspection, particles were preserved in closed Petri dishes until polymer characterization.

Extracted particles were analyzed by Raman Spectroscopy (Renishaw Invia) to identify polymer types using 532 nm or 785 nm laser, laser power varying from 0.5 mW to 10 mW, with a 20x objective. Integration time and scan accumulations varied depending on the samples. The background interference was checked in each spectrum and as needed, background subtraction was applied to increase the spectrum quality. Spectra were recorded between 100 - 3200 cm^{-1} Raman shift and then corrected using Spectragryph Software (Menges, 2020). Finally, Wiley KnowItAll ID Expert Software was used to match the spectra with the reference polymer spectra found in the library. The spectra that have a match above 60% with the reference spectra were considered.

3.2.3. Quality Assurance and Control

All laboratory work was carried out in a fume hood to prevent airborne contamination. The interior of the fume hood was cleaned with deionized water and ethyl alcohol before use. All laboratory glassware and equipment used were rinsed with tap water thoroughly followed by a final rinse using ethyl alcohol and deionized water. Laboratory glassware and sample containers were covered with aluminum foil. Possible sources of microplastic contamination were prevented by wearing nitrile gloves, cotton clothes and a lab coat during the study. Before filtration, plankton meshes were checked for probable airborne contamination under a stereo-microscope and cleaned by removing particles via forceps in case any airborne particle was detected. Control samples were produced to determine probable contamination. For this purpose, with each sample being examined, a 500 mL glass beaker filled with deionized water was placed in the fume hood, which was examined and analyzed under the stereo-microscope after going through the same processes. In case of any microplastics exist in the control samples, the number of particles detected in the blanks were subtracted from the number of particles in the river samples.

3.2.4. Statistical Analyses

Statistical analyses were conducted with SPSS 16 defining statistical significance as $p < 0.05$. The microplastic concentration dataset was transformed into the logarithmic form since the Kolmogorov-Smirnov normality test revealed that microplastic concentrations in water and sediment samples were not normally distributed ($p < 0.05$), nevertheless normality test of the transformed data met the value of $p > 0.05$. The differences in microplastic concentrations between the spring (May 2019) and fall (September 2020) seasons were examined both for water and sediment samples by running an independent t-test. Moreover, one-way analysis of variance (ANOVA) with Tukey's post hoc analysis was used to understand whether there is a significant spatial distribution between sampling stations. Finally, Pearson correlation tests were conducted to observe the relationship between environmental variables including river velocity, river depth and channel width together with microplastic abundance in the river. The strength of correlation was determined using five scales from 'very weak' to 'very strong', given in Table 3.3.

Table 3.3. Pearson correlation scale.

Pearson's *r*	Strength of Correlation
0 to ±0.2	Very weak
±0.2 to ±0.4	Weak
±0.4 to ±0.6	Moderate
±0.6 to ±0.8	Strong
±0.8 to ±1	Very strong

3.3. Modeling the Transport of Microplastics

3.3.1. Settling and Resuspension

Microplastic transport was investigated for the purpose of understanding the effect of particle and flow characteristics on the transport of these particles. Vertical transport was modeled based on microplastic density and size, to simulate settling and resuspension at the water-sediment interface. Since microplastics can have numerous different shapes, a modification of Stokes' equation (Equation 3.1) originated to calculate settling velocity of non-spherical particles (Dietrich, 1982) and adapted to microplastics (Kooi et al., 2017; Kowalski et al., 2016), was also used in this study to simulate vertical transport of microplastics:

$$\omega_s = \left(\frac{\rho_p - \rho_w}{\rho_w} g \mu \omega_*\right)^{1/3} \tag{3.1}$$

where ω_s is the settling velocity (m s^{-1}), ρ_p is the density of plastic particle (kg m^{-3}), ρ_w is the density of the river water (kg m^{-3}), g is the gravitational acceleration (m s^{-2}), μ is the kinematic viscosity of the river water (m^2 s^{-1}) and ω_* is the dimensionless settling velocity. The dimensionless settling velocity ω_* is defined as (Dietrich, 1982):

$$\omega_* = 1.71 \times 10^{-4} {D_*}^2 \text{ for } D_* < 0.05 \tag{3.2}$$

$$log\omega_* = -3.76715 + 1.92944 logD_* - 0.09815(logD_*)^2 - 0.00575(logD_*)^3 + 0.00056(logD_*)^4$$

$$\text{for } 0.05 \leq D_* \leq 5 \times 10^9 \tag{3.3}$$

where D_* is the dimensionless particle diameter, calculated as below (Dietrich, 1982):

$$D_* = \frac{(\rho_p - \rho_w) g {D_n}^3}{\rho_w \mu^2} \quad (3.4)$$

where D_n is the nominal diameter (m), which is the equivalent diameter of a spherical particle equal in volume and calculated as below:

$$D_n = \left(\frac{6\forall}{\pi}\right)^{1/3} \quad (3.5)$$

where $\forall$ is the particle volume (m^3). Depending on Equation 3.5 and the geometric shapes of the particles, the nominal diameter of fibers (cylinder) and fragments (irregularly-shaped) were calculated by the following two equations, respectively.

$$D_{n,fiber} = \left(\frac{3}{2} abc\right)^{1/3} \quad (3.6)$$

$$D_{n,fragment} = (abc)^{1/3} \quad (3.7)$$

where *a* is the longest, *b* is the intermediate and *c* is the shortest axes of the particle, respectively. In this study, microplastics between 45-5000 μm size range were investigated and the size of each particle was determined measuring the longest axis (*a*) during visual analysis (given in detail in Section 3.2.2). Due to the limitations in measuring all axes of the particles (e.g. lack of three-dimensional images), a shape factor (φ) was defined to calculate D_n. For spherical particles, φ is equal to 1, but decreases with increasing flatness and irregular shape of the particle. To determine the minimum value of φ, a 5000 μm length-particle was considered, assuming the minimum value of *b* and *c* was 1 μm. Thus, the relationship between φ and D_n can be given as:

$$D_n = \varphi a \qquad \text{for } 0.004 \leq \varphi \leq 1 \quad (3.8)$$

The approximate ratio of the shortest axis (*c*) to the longest axis (*a*) was determined by examining the microscopic images of the fibers and assumed as 0.1 for the thickest fibers. The particles that have higher ratio than this (c/a >0.1) were assumed as fragments (or irregularly-shaped particles). Likewise, the fragments that have the c/a values higher than 0.8, were assumed as near-spherical particles. According to these assumptions, the range of φ was determined for fibers, fragments and near-spherical particles by below:

$0.004 \leq \varphi < 0.25$ for fibers (3.9)

$0.25 \leq \varphi < 0.9$ for fragments

$0.9 \leq \varphi < 1$ for near-spheres.

Most rivers are naturally turbulent environments due to excessive flow rates, currents and rough river bed in flow channel, which leads to fluctuations both in horizontal and vertical velocities (given in detail in Section 3.3.2). In this case, the settling velocity of particles under turbulent conditions, v_s, can be defined as below:

$$v_s = \omega_s + v' \tag{3.10}$$

where v' is the vertical velocity fluctuation (m s^{-1}). These fluctuations lead river water to move in circular eddies exerting a shear stress at the bottom. In this case, the particles deposited onto sediment begin to be resuspended. On the other hand, a portion of the deposited particles buried in deep layers and may remain permanently in the sediment. In this study, a dynamic equilibrium was assumed between settling, resuspension and burial in the sediment-water interface. Under steady-state, mass balance for particles in the sediment-water interface can be written as (Chapra, 1997):

$$0 = v_s C_1 - v_r C_2 - v_b C_2 \tag{3.11}$$

where C_1 is the concentration of microplastics in water (items m^{-3}), C_2 is the concentration of microplastics in water-sediment interface (items m^{-3}), v_r is the resuspension velocity of microplastics (m s^{-1}) and v_b is the burial velocity of microplastics (m s^{-1}). If resuspension dominates burial ($v_r >> v_b$), microplastic concentration in water will approach the initial concentration, as each particle that settles immediately will become resuspended (Chapra, 1997). In this case, burial velocity becomes equal to zero, which results in the maximum resuspension flux:

$$v_{r_{max}} C_2 = v_s C_1 \tag{3.12}$$

Resuspension occurs once bed shear stress exceeds the critical shear stress. The mathematical relationship between resuspension and maximum resuspension can be defined as (Besseling et al., 2017):

$$v_r = v_{r\,max}\left(\frac{\tau_0}{\tau_{cr}} - 1\right) \qquad \text{for } \tau_0 > \tau_{cr} \tag{3.13}$$

where τ_0 is the bed shear stress (N m^{-2}) and τ_{cr} is the critical shear stress (N m^{-2}), calculated as below (Mao et al., 2008):

$$\tau_{cr} = \tau_{cr}{}^{*}(\rho_p - \rho_w)gD_n \tag{3.14}$$

where $\tau_{cr}{}^{*}$ is the dimensionless critical shear stress.

Substituting Equation 3.12 into 3.13, resuspension velocity of microplastics was calculated as:

$$v_r = \frac{v_s C_1}{C_2}\left(\frac{\tau_0}{\tau_{cr}} - 1\right) \tag{3.15}$$

Burial velocity can be written as below substituting Equation 3.15 into 3.11:

$$v_b = \frac{v_s C_1}{C_2}\left(2 - \frac{\tau_0}{\tau_{cr}}\right) \tag{3.16}$$

3.3.2. Turbulence Modeling: Boundary Layer Theory

Apart from the particle characteristics, microplastic movement is affected by hydraulic and hydrodynamic characteristics of the river including river morphology and flow (Guven & Howard, 2006). The flow pattern of a stream is governed by the ratio of inertial forces to the viscous forces, which is represented by the Reynolds number (*Re*). Depending on the strength of viscosity relative to inertia, the flow may be laminar (*Re* < 500), turbulent (*Re* > 2000), or transitional (500 < *Re* < 2000) (Richards, 1982). In natural systems, laminar flow is generally encountered in low-flow and shallow streams, such as canals, in which water flows in definite smooth paths or streamlines (Chow, 1959). However, flow in most rivers is naturally turbulent, in which water molecules move in irregular paths due to excessive flow rates, curves or rough surfaces in the flow channel. Unlike laminar flow, turbulent flow has horizontal and vertical fluctuating velocity components. Vertical velocity fluctuation leads the lower mass to move towards the upper mass or vice versa and exchanges momentum of the river flow completely.

Flow in river channel is also retarded by resistance of the riverbed and the banks, which causes velocity to increase as the logarithm of height (Chow, 1959) and vertical velocity profile to occur (Richards, 1982). Vertical velocity profile is shown in Figure 3.3.

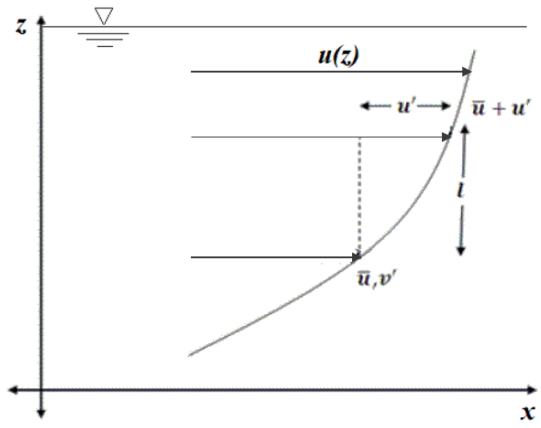

Figure 3.3. Vertical velocity profile.

Boundary layer theory is a commonly used method to understand vertical velocity profile in open channels. The theory is an approximate method, which includes an assumption of steady flow and uniform channel. The relationship between river velocity and height can be given as:

$$u(z) = u^* \frac{1}{\kappa} ln\left(\frac{z}{z_0}\right) \tag{3.17}$$

where $u(z)$ is the river velocity profile, u^* is the shear velocity (m s^{-1}), κ is von Karman's universal constant, z is the distance from the bottom of river (m) and z_0 is the height where velocity is zero (m) and is determined by the boundary roughness projection height (k):

$$z_0 = {}^{k}/_{30} \tag{3.18}$$

where k is referred to as the 'Nikuradse sand roughness', which can be defined as (Richards, 1982; Millar, 1999):

$$k = 3.5D_{84} \tag{3.19}$$

where D_{84} is the diameter of 84% of sediment particles (m).

Turbulence is thought to be generated in high shear zones, which, in a river, would be found near the riverbed. According to Chow (1959), the shear velocity can be defined as:

$$u^* = \sqrt{\tau_0 / \rho_w} \tag{3.20}$$

where τ_0 is the bed shear stress (N m^{-2}). The shear stress at any point in turbulent flow is given as:

$$\tau_0 = \rho_w g z S \tag{3.21}$$

where *S* is the surface slope.

According to Prandtl's mixing theory, velocity fluctuations in turbulent environments can be approximated as:

$$|u'| \approx |v'| \approx l \frac{du}{dz} \tag{3.22}$$

where $|u'|$ and $|v'|$ are the absolute values of the instantaneous horizontal and vertical turbulent velocity fluctuations in time *dt*, respectively, *l* is a characteristic length known as the mixing length (m) and du/dz is the velocity gradient. The mixing length is experimentally defined as:

$$l = \kappa z \tag{3.23}$$

River velocity fluctuation leads the lower mass to move towards the upper mass and exchanges momentum of river flow completely. Velocity fluctuations of both directions were taken into consideration by below equations:

$$u = \bar{u} + u' \approx \bar{u} + l \frac{du}{dz} \tag{3.24}$$

$$v_s = \omega_s + v' \approx \omega_s + l \frac{du}{dz} \tag{3.25}$$

where $\bar{u}$ is the mean velocity of the river (m s^{-1}).

3.3.3. Mechanistic Model: Mass-Balance Approach

Vertical transport of microplastics under turbulent flow was identified mechanistically, using a mass-balance approach for each sampling site. For this purpose, control volumes of water column and sediment were considered. In addition, settling and resuspension mechanisms occurring in the water-sediment interface was modeled to understand the dynamic behavior within the compartments. Schematic representation of the mass balance for microplastics in the study sites are given in Figure 3.4.

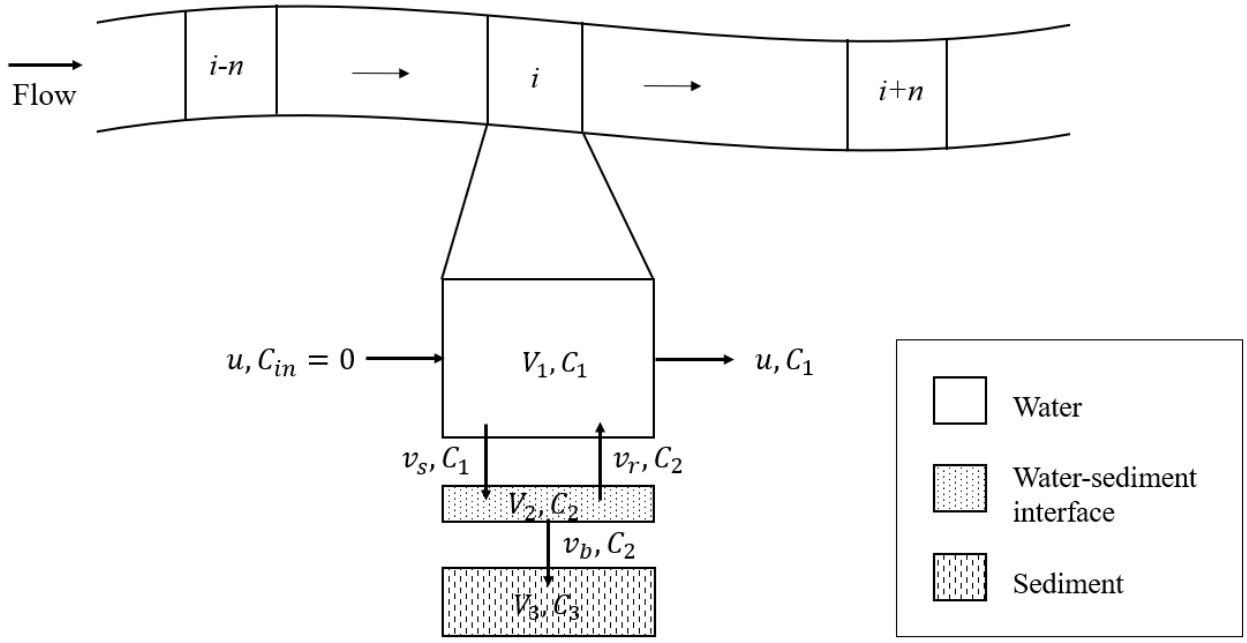

Figure 3.4. Schematic representation of the mass balance for microplastics in reach *i*.

In river modeling, an infinite number of reservoirs (tanks-in-series) is typically considered as an approximation of river systems (Guven & Howard, 2006). In this approach, the river reach is divided into conceptual reservoirs, which allows users to set the values of parameters and variables in the location of interest, based on user information (Keupers & Willems, 2017). Series of reservoirs is a widely used method in modeling river systems (Beck & Finney, 1987; Keupers & Willems, 2017; Whitehead et al., 1979), which are generally modeled as Continuously Stirred Tank Reactors (CSTR) to utilize mass-balance equations. In this model, each water column was considered as a CSTR, in which river hydraulics and morphology were assumed to be homogeneous.

Mass-balances for microplastic in the water, water-sediment interface and deep sediment can be written as below. Equations 3.26, 3.27 and 3.28 give rate of change of microplastic concentration in water, water-sediment interface and sediment, respectively.

$$\frac{dC_1}{dt} = -\frac{uA_1}{V_1}C_1 - f_{nb}\frac{v_s}{d}C_1 + \frac{v_r}{d}C_2 \quad (3.26)$$

$$\frac{dC_2}{dt} = \frac{v_s}{d}C_1 - \frac{v_r}{d}C_2 - \frac{v_b}{d}C_2 \quad (3.27)$$

$$\frac{dC_3}{dt} = \frac{v_b}{d}C_2 \quad (3.28)$$

where V_1 is the control volume of water (m^3), A_1 is the cross-sectional area of the control volume (m^2), f_{nb} is the fraction of non-buoyant particles, C_1 is the concentration of suspended microplastics in water (items m^{-3}), C_2 is the concentration of microplastics in sediment-water interface (items m^{-3}) and C_3 is the concentration of microplastics in sediment (items m^{-3}).

A mechanistic model based on 'stock and flow' approach was constructed to investigate the vertical transport of microplastics within the sampling sites. Since microplastic characteristics, such as density, size and shape are variable and river velocity fluctuates with turbulent flow, a stochastic model was developed. The probable change of microplastic abundance in water, water-sediment interface and sediment, as well as variation of settling and resuspension flux of microplastics with time at sampling locations were simulated by Monte-Carlo analysis, using GoldSim (version 14.0) software (GoldSim Technology Group, 2021). GoldSim was chosen as the modeling environment, particularly due to its convenience in dynamic modeling of environmental systems and ability in quantitively representing the stochastic data mentioned above. Equations given above (Equation 3.1-3.28) were utilized in GoldSim, assuming the control volumes were stocks, and microplastic settling, resuspension and burial were flow. This was performed for each sampling site separately. The model was run for 60 s with 500 realizations selecting four random values from the strata of each element's probability distribution. Following assumptions were made for the model conceptualization:

Initial and boundary conditions:

- Initial concentrations of microplastics in water column is equal to the measured concentration of microplastics in the water sample collected from the relevant site.

- Initial concentrations of microplastics in sediment is zero.
- There is a dynamic equilibrium between settling, resuspension and burial in water-sediment interface.
- No microplastics were released from any other source.
- Only non-buoyant particles are modeled.
- Hydraulic and morphological characteristics of the channel are homogeneous.

It should be noted that microplastics were assumed as pure particles, neglecting processes, such as aggregation with other chemicals and biofilm formation on plastic particles. In this respect, the settling and resuspension of only non-buoyant particles were modeled. To achieve this, fraction of non-buoyant microplastics (f_{nb}) was determined according to the polymer types and densities identified by Raman analyses.

3.3.4. Data Acquisition and Model Calibration

The required data for model development was basically obtained from three different sources: (i) on-site measurements including river's hydrodynamical and morphological parameters, such as river velocity, water viscosity and depth, (ii) the results of microplastic analysis including initial concentration, particle size, type and shape, and (iii) literature (e.g. κ, D_{84} and $\tau_{cr}{}^{*}$). Model parameters were defined as stochastic variables due to the uncertainties that may be associated with particle characteristics and the random behavior of microplastic transport occurring in natural environments. Since the characteristics of microplastics, such as density, size and shape vary widely even within a single sample, these parameters were entered to the model as stochastic data ranging between certain values. In addition, z value (the distance from the bottom of river to a given height) was assumed as stochastic due to the variation of river velocity with depth because of turbulence and resultant velocity fluctuations. The other input parameters were entered to the model as deterministic data.

Model calibration was conducted using the ρ_w, D_{84}, and S. The approximate slope values of the sampling sites were first determined via Geographical Information Systems (GIS). After collecting the required data, model calibration was performed by minor changes on the values of ρ_w, D_{84}, and S, comparing the measured river mean velocity with the predicted mean velocity ($\bar{u}$). Regression analysis was implemented by calculating coefficient of determination (R^2) and root mean square error (RMSE) to evaluate model fit.

Data requirements for the development of Monte-Carlo model are given in Table 3.4.

Table 3.4. Data requirements for the model.

Parameters	**Value**					**Source**
Deterministic	**S1**	**S2**	**S3**	**S4**	**S5**	
ρ_w (kg m^{-3})	997[ab]	997[a] 998[b]	997[a] 998[b]	997[ab]	997[a] 998[b]	T_s measurements / Calibrated
μ (m^2 s^{-1})	8.9×10^{-7} [a] 9.5×10^{-7} [b]	9.1×10^{-7} [a] 9.7×10^{-7} [b]	9.1×10^{-7} [a] 9.8×10^{-7} [b]	9.1×10^{-7} [a] 9.5×10^{-7} [b]	9.1×10^{-7} [a] 9.5×10^{-7} [b]	T_s measurements
κ	0.4	0.4	0.4	0.4	0.4	Chow (1959)
d (m)	0.418[a] 0.526[b]	0.550[a] 0.334[b]	0.594[a] 0.586[b]	0.559[a] 0.415[b]	0.401[a] 0.484[b]	On-site measurements
D_{84} (mm)	0.1[a] 5.5×10^{-3} [b]	0.25[a] 9×10^{-4} [b]	0.1[a] 1[b]	1[a] 1[b]	0.05[a] 0.3[b]	Millar (1999)
S	1.6×10^{-4} [a] 2.1×10^{-4} [b]	1.4×10^{-4} [a] 2.8×10^{-4} [b]	1.7×10^{-4} [a] 1.4×10^{-4} [b]	1.4×10^{-4} [a] 10^{-4} [b]	1.8×10^{-4} [a] 1.7×10^{-4} [b]	QGIS / Calibrated
$\tau_{cr}{}^*$	0.056	0.056	0.056	0.056	0.056	Shields (1936)
f_{nb}	0.7	0.7	0.7	0.7	0.7	Raman analysis
Stochastic	**S1**	**S2**	**S3**	**S4**	**S5**	
ρ_p (kg m^{-3})	1050-1400	1050-1400	1050-1400	1050-1400	1050-1400	Raman analysis and Polymer database[c]
a (μm)	45-5000	45-5000	45-5000	45-5000	45-5000	Microscopic analysis and ImageJ
φ	0.004-1	0.004-1	0.004-1	0.004-1	0.004-1	Estimate
C_0 (items m^{-3})	900-2300[a] 2990-3980[b]	2920-10280[a] 3670-4250[b]	4250-10630[a] 15980-19040[b]	1740-4910[a] 2510-2900[b]	1990-4650[a] 3310-6060[b]	Lab and microscopic analysis
z (m)	0-0.418[a] 0-0.526[b]	0-0.550[a] 0-0.334[b]	0-0.594[a] 0-0.586[b]	0-0.559[a] 0-0.415[b]	0-0.401[a] 0-0.484[b]	On-site measurements (d)

[a] Measured/calibration data for May 20, 2019
[b] Measured/calibration data for Sep 30, 2020
[c] Retrieved from http://www.polymerdatabase.com (Oct 1, 2021)

3.3.5. Scenario Analysis

Scenario analyses were performed to understand the effect of particle properties including shape and size, as well as differences in river hydraulics on settling and resuspension of microplastics. To achieve this, considering different scenarios, the changes in settling flux (J_s, items m^{-2} s^{-1}) and

resuspension flux (J_r, items m^{-2} s^{-1}) of microplastics were simulated. J_s and J_r can be defined as the following:

$$J_s = v_s C_1 \tag{3.29}$$

$$J_r = v_r C_2 \tag{3.30}$$

Considering particle shape, particle size and bed shear stress, nine different scenarios were generated. These are given in detail below.

3.3.5.1. Particle shape. Three scenarios were considered to determine the effect of particle shape on settling and resuspension of microplastics:

- Scenario 1: All the particles in the control volume are fibers.
- Scenario 2: All the particles in the control volume are fragments.
- Scenario 3: All the particles in the control volume are near spherical.

3.3.5.2. Particle size. Three different particle sizes were considered to understand the model response to the changes in microplastic size:

- Scenario 1: All the particles in the control volume are 50 μm.
- Scenario 2: All the particles in the control volume are 500 μm.
- Scenario 3: All the particles in the control volume are 5000 μm.

3.3.5.3. Bed shear stress. The variations in river hydraulics, such as river depth and slope can change bed shear stress and hence flow patterns. Although bed shear stress is a variable depending on the river morphological parameters, it was assumed as a deterministic input parameter in scenario analyses to evaluate the effect of different flow characteristics on settling and resuspension of microplastics more directly and clearly. Similar to the above, three scenarios were considered as:

- Scenario 1: $\tau_0 = 0.15$ N m^{-2}
- Scenario 2: $\tau_0 = 0.50$ N m^{-2}
- Scenario 3: $\tau_0 = 0.90$ N m^{-2}

3.3.6. Uncertainty and Sensitivity Analysis

Uncertainty and sensitivity analyses were performed to assess the robustness of the model outputs. Uncertainty analysis can be described as the process of determining the range of model outputs depending on the uncertainty of the inputs, whereas parameter sensitivity analysis is performed to understand the sensitivity of model outputs to changes in the inputs. Uncertainty analysis aids to identify the effect of the lack of knowledge or conceptual errors of the model (Mountford et al., 2017), while sensitivity analysis can be conducted for several purposes including (Hamby, 1994; Mulligan & Wainwright, 2004):

- better understanding which parameters are highly correlated with the model output and require additional research to mitigate the possible errors;
- determining which parameters are insignificant and do not require an additional research to strengthen the model;
- calibration/validation of the model; and
- targeting model parameterization for optimal data collection.

Multi-variate analysis was conducted in GoldSim to determine the effect of stochastic data including particle size (a), microplastic density (ρ_p), shape factor (φ) and distance from the bottom of river (z) on the uncertainty of the model outputs. For this purpose, a correlation matrix was generated in GoldSim, which indicates the degree to which all selected variables are correlated to each other. Moreover, statistical analysis was conducted by calculating coefficient of determination, correlation coefficients, standardized regression coefficients, partial correlation coefficients, and importance measures.

Sensitivity analysis was carried out in GoldSim using 'Sensitivity Analysis' tool of the software. One-at-a-time parameter sensitivity analysis was performed, which is based on changing one parameter at a time, while holding the others fixed. This method aids to understand the influence of the input parameters on the model outcomes by assessing the model output variations due to the changes in input parameters. In this study, the effect of variations in d, S, D_{84}, μ, τ_{cr}*, φ, a, ρ_p, ρ_w and C_0 on microplastic concentrations in water and sediment were evaluated. The variation in input and output was calculated by the following equations (Dubus et al., 2003):

$$Input\ Variation = \frac{I - I_{BC}}{I_{BC}} \times 100 \tag{3.31}$$

$$Output\ Variation = \frac{O - O_{BC}}{O_{BC}} \times 100 \tag{3.32}$$

where I is the value of the input parameter, I_{BC} is the value of the input parameter for the base-case scenario, O is the value of the output variable and O_{BC} is the value of the output variable for the base-case scenario.

Sensitivity ranking of the parameters was implemented by calculating ratio of variation (*ROV*) for each input parameter:

$$ROV = \frac{Output\ Variation}{Input\ Variation} \tag{3.33}$$

4. RESULTS AND DISCUSSION

4.1. Microplastic Abundance and Distribution in the Ergene River

The results given in this section was published in 'Environmental Research' journal, titled as 'Microplastic distribution in the surface water and sediment of the Ergene River' (Akdogan et al., 2023).

4.1.1. Microplastic Abundance in Water and Sediment

A total of 643 and 1031 microplastic particles were extracted from the water samples collected in May and September, respectively. On the other hand, a total of 118 and 320 particles were extracted from the sediment samples, respectively. Water samples had average concentrations of 4.65 ± 2.06 and 6.90 ± 5.16 items L^{-1} (mean ± standard deviation, n = 12), and sediment samples' average concentrations were 97.90 ± 71.72 and 277.76 ± 207.21 items kg^{-1} (n = 18) for the May 2019 and September 2020 periods, respectively. Both water and sediment samples collected at the end of the dry season (September) include higher concentrations of microplastic in total than the samples collected in the wet season (May). Several studies in the literature also reported higher microplastic abundance in rivers during dry seasons (Nel et al., 2018; Wicaksono et al., 2021; Wu et al., 2020), which was generally associated with decreased river flux that is limiting the dilution of microplastic concentration in rivers (Wu et al., 2020; Yan et al., 2019). In this study, the temporal variation of microplastic abundance was more dramatic for sediment samples than those for water samples. A statistically significant difference in the number of microplastics between the two periods was found for sediment ($F = 14.63$, $df = 20.19$, $t = -2.44$, $p = 0.02 < 0.05$), whilst statistical analysis did not indicate a significant temporal difference for riverine water ($F = 4.03$, $df = 22$, $t = -1.19$, $p = 0.25 > 0.05$). These outcomes can be attributed to variation in waste management, change in microplastic characteristics, such as polymer density and particle size, and associated settling and accumulation of these particles in sediment during the dry season. On the other hand, the sampling was done in the wet and at the end of the dry seasons, and no major differences were observed in river morphology and flow rates between two periods (Table 3.2), which could explain the relatively less temporal variation of microplastic abundance in water samples. A significant increase in flow rates was observed only at Site 1 and Site 2 in Sep 2020, probably due to heavy rainfall event the day before the sampling day. However, this did not cause a meaningful seasonal difference in microplastic concentrations within these sites. Moreover, particular sampling sites (2 and 4) had an inverse manner

compared to the other sites, where microplastic abundance was higher in May than those in September (Table 4.1). These variations can be as a result of differences in meteorological conditions between two sampling periods. Wind speed on the day of sampling in September (mean = 17 km h^{-1}) was slightly higher than in May (mean = 14.83 km h^{-1}), whilst the wind directions were totally different (Table 3.2). A recent study by Leads et al. (2023) indicated that wind direction had a great effect on microplastic abundance and temporal variability.

Microplastic abundance data of all sites are given in Table 4.1. A significant spatial variation was found for water samples, particularly between Site 3 (upstream of the Ergene River tributary) and the other sampling sites in September ($F = 4.37$, $df = 23$, $p = 0.009 < 0.05$). These results are expected, considering a variety of environmental factors in the study area, especially due to different land uses (e.g. industries, agriculture, and farmland) and associated wastewater effluents (Baldwin et al., 2016; Kapp & Yeatman, 2018). Several studies indicated the relationship between increased microplastic concentrations and industrial areas (Alam et al., 2019; Cordova et al., 2022; Wong et al., 2020). Site 3 had the highest amount of microplastics in both seasons, probably depending upon the surrounding land use (residential area) and proximity to WWTPs and OIZs, in which textile industries heavily exist. Besides, both seasons had similar trends in the microplastic distribution along the river, exhibiting an increase in the abundance of microplastics along the Çorlu Tributary from Site 1 to Site 2, while the number of particles suddenly decreased from Site 3 to Site 4 along the Ergene River Tributary. Microplastic levels continued to decline at Site 5, the downstream of the junction, where the Çorlu Tributary meets the mainstream and the river reaches its maximum width amongst the sampling sites, but then increased again at Site 6. On the other hand, sediment samples did not illustrate a statistically significant spatial distribution ($F = 1.40$, $df = 35$, $p = 0.25 > 0.05$).

Table 4.1. Microplastic concentrations in water and sediment samples.

Site	**Water Mean ± SD* (items L^{-1})**		**Sediment Mean ± SD* (items kg^{-1})**	
	May 20, 2019	**Sep 30, 2020**	**May 20, 2019**	**Sep 30, 2020**
S1	1.60 ± 0.99	3.49 ± 0.71	57.18 ± 14.48	448.92 ± 66.66
S2	6.60 ± 5.20	3.96 ± 0.41	57.99 ± 48.06	107.17 ± 40.04
S3	7.44 ± 4.51	17.51 ± 2.16	62.76 ± 46.08	125.73 ± 92.64
S4	3.32 ± 2.24	2.70 ± 0.27	45.02 ± 18.57	276.80 ± 400.44
S5	3.32 ± 1.88	4.69 ± 1.95	250.64 ± 137.32	67.17 ± 22.89
S6	5.60 ± 2.11	9.04 ± 5.68	113.81 ± 40.66	640.76 ± 444.63
* Standard Deviation				

Microplastic abundance data obtained from this study were compared with some of the other studies conducted in different rivers of the world (Table 4.2).

Table 4.2. Comparison of microplastic concentrations in this study with other rivers.

Rivers	Mesh Size (µm)	Mean ± SD		Reference
		Water (items L^{-1})	Sediment (items kg^{-1})	
Ergene River, Turkey	45	4.65 ± 2.06 to 6.90 ± 5.16	97.90 ± 71.72 to 277.76 ± 207.21	This study
Mersin Rivers, Turkey	26	0.29 ± 0.06	-	Özgüler et al. (2022)
Seine River, France	80	0.11 ± 0.09	-	Dris et al. (2018)
Pearl River, China	50	8.9 to 19.86	-	Yan et al. (2019)
Qiantang River, China	45	1.18 ± 0.27	-	Zhao et al. (2020)
Yangtze River, China	50	2.52 ± 0.91	-	Wang et al. (2017)
Ciwalengke River, Indonesia	1.2	5.85 ± 3.28	303 ± 159	Alam et al. (2019)
Nakdong River, South Korea	20	0.29 ± 0.08 to 4.76 ± 5.24	1970 ± 62	Eo et al. (2019)
Antua River, Portugal	55	0.31	318.67	Rodrigues et al. (2018)
Ottawa River, Canada	100	1.35×10^{-3}	220	Vermaire et al. (2017)
Shanghai rivers, China	1	-	802 ± 594	Peng et al. (2018)
Pearl River, China	20	-	1669	Lin et al. (2018)
Rhine River, Germany	63	-	861	Klein et al. (2015)

Compared to many other rivers, the Ergene River had excessive levels of microplastics. Average concentrations in the surface water were much higher than those in other rivers including eight rivers of Mersin, Turkey (Özgüler et al., 2022); European rivers (Dris et al., 2018; Rodrigues et al., 2018) and Ottawa River, Canada (Vermaire et al., 2017), but considerably lower than the concentrations in the Pearl River, China (Yan et al., 2019). Compared to other east Asian rivers, such as Qiantang (Zhao et al., 2020), Yangtze (Wang et al., 2017) and Nakdong (Eo et al., 2019), the abundance of microplastics were higher in the Ergene River (Table 4.2). However, it should be noted that the differences in sampling and analysis methods hinder the comparability of the results with the literature data. For example, microplastic levels for both water and sediment in this study were comparable to the Ciwalengke River, Indonesia (Alam et al., 2019), which receives industrial wastewater discharge similar to the Ergene River. Yet, unlike this study, the authors performed the analysis with a 1.2 µm plankton mesh, which hampered the exact comparison of the results. Microplastic levels in the sediment samples of this study were comparatively lower than other rivers including Nakdong (Eo et al., 2019), Pearl (Lin et al., 2018), Rhine (Klein et al., 2015) and Shanghai rivers (Peng et al., 2018), but comparable to the Antua (Rodrigues et al., 2018) and Ottawa Rivers

(Vermaire et al., 2017). According to these results, river hydrodynamics can have an effect on relatively low concentrations of microplastics in river sediments due to resuspension of the particles.

4.1.2. Microplastic Abundance and River Characteristics

Currently, there is little knowledge on the relationship of microplastic abundance with river morphology and hydrodynamics. In this study, Pearson correlation tests were conducted to determine if there was a relationship between microplastic levels and the river's hydrodynamical variables including river velocity, river depth and channel width. The test results are given in Table 4.3.

Table 4.3. Pearson Correlation coefficients (r) between river hydrodynamical variables and microplastic abundance.

Hydrodynamical Parameters	**Pearson's *r***
Water	**items L^{-1}**
River velocity (m s^{-1})	0.17
River depth (m)	0.51*
Channel width (m)	-0.45*
Sediment	**items kg^{-1}**
River velocity (m s^{-1})	0.21
River depth (m)	-0.19
Channel width (m)	0.13
* indicates significance with $p < 0.05$.	

For water samples, results showed a moderately positive correlation between the number of microplastics and river depth. This can be explained by the different flow regimes in the river and associated dispersion of microplastics. Bed shear stress is higher in deep water, which generally results in elevated levels of turbulence that can increase the transport of sediment particles (Besseling et al., 2017; Richards, 1982). Indeed, once bed shear stress exceeds the critical shear stress, sediment particles begin to be resuspended (Waldschläger & Schüttrumpf, 2019). He et al. (2021) also indicated the lower deposition of microplastics onto sediment in the Brisbane River mouth (Australia) could be due to the higher bed shear stress and dispersion of particles in that location, where water depth was much higher than in river upstream. Moreover, dispersion of particles increases with expanding channel width, which may cause dilution of microplastic concentrations. On the other hand, a moderately negative correlation was defined between the microplastic abundance and channel width, as a result of Pearson correlation tests. Coherently, it was expected to find a relationship between river morphological variables and sediment microplastic levels; yet, no significant correlations between these variables and sediment microplastic levels were observed. This may be due to the fact

that ANOVA test did not define a statistically significant spatial distribution for the sediment samples. Likewise, statistical analyses implemented by Nel et al. (2018) did not find a significant relationship of sediment microplastic concentrations with river depth and channel width.

Previous studies demonstrated a considerable relationship between microplastic abundance and river velocity (Kapp & Yeatman, 2018; Nel et al., 2018). However, in this study, statistical analyses did not exhibit a meaningful correlation between river velocity and microplastic abundance, either for water or sediment (Table 4.3). This may be because no significant spatiotemporal changes were observed in the flow rates of six different sampling locations. Hence, the longer-term continuous sampling and measurements are required to monitor remarkable changes in river flow and exactly understand whether river velocity influences microplastic levels in the Ergene River.

4.1.3. Shape, Size, Color, and Type of Microplastics

Particle density, shape and size distribution are dynamically changing parameters that strongly affect the sinking velocity, thereby the fate of microplastics (Enders et al., 2015; Kooi et al., 2016; Kowalski et al., 2016). Here, microplastic particles extracted were categorized according to their shapes as fiber, hard fragment, soft fragment, pellet, foam and other (rubber, film, etc.), which are shown in Figure 4.1.

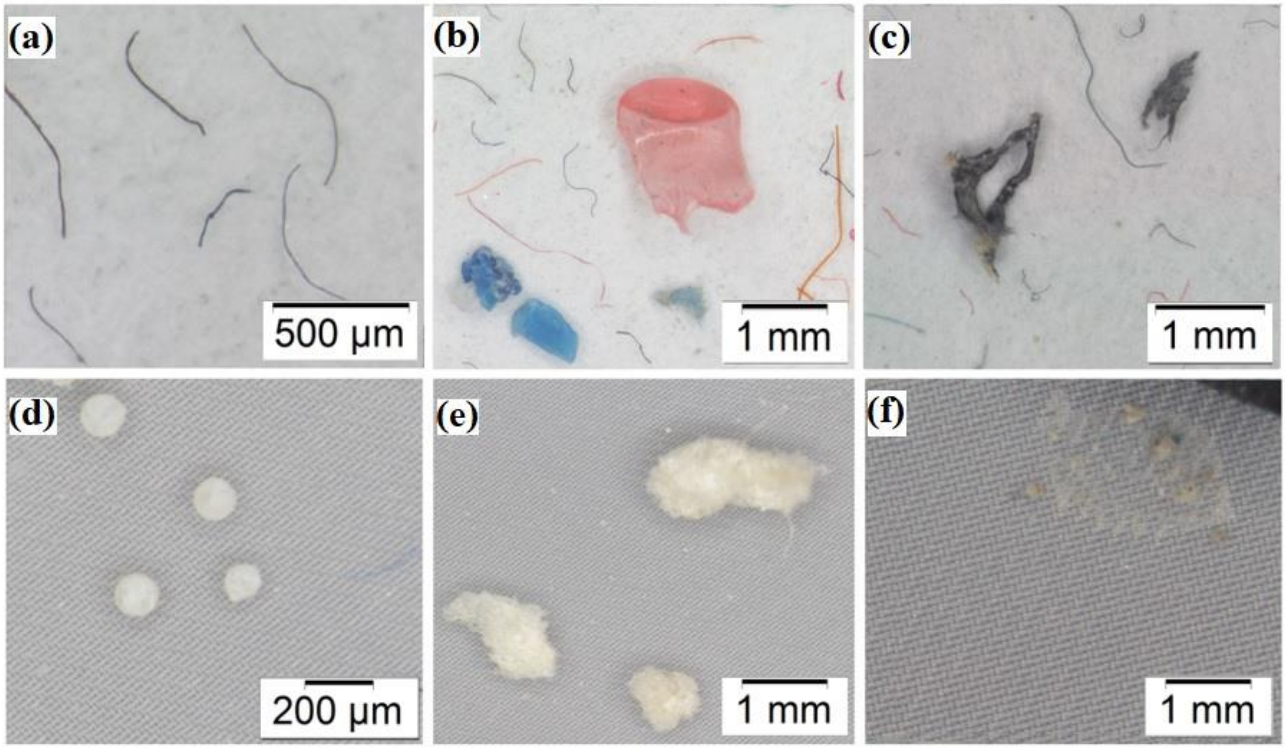

Figure 4.1. Microscopic images of microplastics: (a) fibers, (b) hard fragments and fibers, (c) soft fragments and fibers, (d) pellets and fibers, (e) foams, and (f) rubber.

Different sources of microplastics cause them to occur in various shapes in the environment (Klein et al., 2015). In total, fibers (88%) were dominant in water samples, followed by soft fragments (4%), hard fragments (4%), pellets (2%), foams (1%), rubbers (<1%) and other (<1%). Plastic particles that could not precisely be identified were categorized as 'Other'. Although fibers were dominating shape also in the sediment samples (70%), hard fragments had a considerable proportion (23%) in sediment. Furthermore, a small number of soft fragments (5%), pellets (2%) and rubbers (<1%) were detected in the sediment samples. The spatiotemporal distribution of microplastic shapes in water and sediment is given in detail in Figure 4.2.

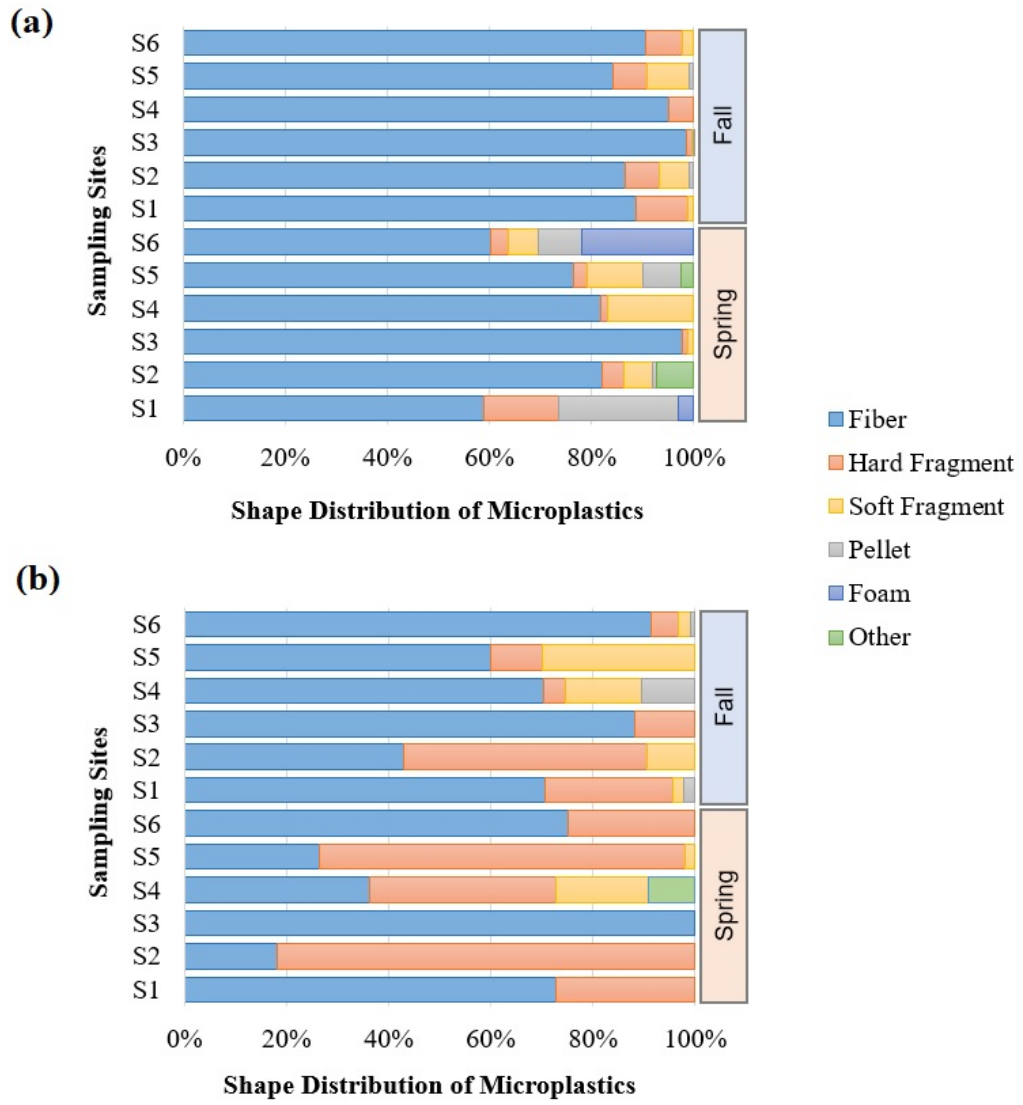

Figure 4.2. Percentage distribution of microplastics by shape in (a) water samples and (b) sediment samples.

To date, fibers have generally been the dominantly found microplastic shape in aquatic environments (Browne et al., 2011), most likely due to the continual abrasion of synthetic textiles

and laundry wastewater release (Napper & Thompson, 2016), as well as atmospheric fallout (Dris et al., 2016). Textile industries have also been reported as a significant point source of synthetic fibers (Cordova et al., 2022; Deng et al., 2020). From this viewpoint, fiber levels detected in water and sediment samples were not surprising, as, in our study area, textile industries and spinning mills were intensively active, especially within the Çorlu District and the north-eastern part of the Ergene sub-basin (upstream of Site 3). Besides domestic sewage, the river has been receiving a considerable amount of industrial wastewater from these regions for many years. As discussed in Section 4.1, notably higher amounts of microplastics were detected in water samples of Site 3, the closest location to the aforementioned industrial zones, in which the number of fibers was also extremely higher, compared to the samples of the other sites. Indeed, almost no other shape of microplastics than fiber was detected in the water and sediment samples from Site 3. The proportion of fibers was found higher both in the samples in the fall than those in the spring. This can be attributed to the differences in meteorological conditions, such as higher wind speed and altered wind direction on the day of sampling in September, discussed in Section 4.1. Indeed, Bullard et al. (2021) suggested that microplastic enrichment by wind was higher for fibers than pellet shaped particles, which could explain the increased number of fibers in the samples collected in the fall. Also, in this study, the second sampling (30 Sep 2020) was carried out during the Covid-19 pandemic. Recent studies identified disposable face masks as a potential source of synthetic fibers in the environment (Fadare & Okoffo, 2020; Shen et al., 2021). Thus, an increase in fiber levels may be due to changing habits such as frequent cleaning and laundry and the use of single-use face masks during the Covid-19 pandemic.

Fibers were generally followed by hard or soft fragments in all samples, yet their abundance and predominance changed from site to site. Fragments detected in the samples revealed the degradation of plastic debris originated from secondary sources that mostly include anthropogenic activities, such as littering. Waste from various industries, such as plastic, machinery and automotive can be a potential source of hard fragments in the study area. Previous studies suggested that agricultural activities were also a substantial source of microplastics due to the use of plastic products, such as nylon mulch in crop growth (Nizzetto et al., 2016b; Rodríguez-Seijo & Pereira, 2019). While the surrounding of Sites 1 and 3 mostly include industrial and residential areas, downstream of the river (Site 2 and from Site 4 to 6) is surrounded by farms and cultivated lands. Thus, some of the soft fragments (nylon particles and polyethylene greenhouse coverings) observed in these sites can be attributed to agricultural activities in the neighboring area. On the other hand, relatively low numbers of foam and rubber were detected in the samples. Foams were observed only in the water samples of two sites (Sites 1 and 6), whilst only one rubber was observed in all samples, which was detected in

the sediment sample of Site 4. A small number of pellets were detected both in water and sediment samples. The existence of pellets is an indicator of primary source microplastics originating from cosmetic and medical products (Patel et al., 2009; Zitko & Hanlon, 1991). Primary microplastics most likely enter the aquatic environment through domestic wastewater discharge or spillage of plastic pellets used in industries (Gregory, 1996). Ergene River receives both domestic sewage and wastewater from Çorlu and Ergene OIZs near the study area, where several plastic and cosmetic industries, probably using plastic pellets in production, are located. However, a predominance of fibers and fragments suggests that microplastic pollution in the Ergene River and Çorlu Stream mostly originates from secondary source microplastics as a result of the abrasion of textiles and fragmentation of larger plastic items.

Here, microplastics were also categorized according to their sizes. Spatiotemporal distribution of particle sizes is given in detail in Figure 4.3.

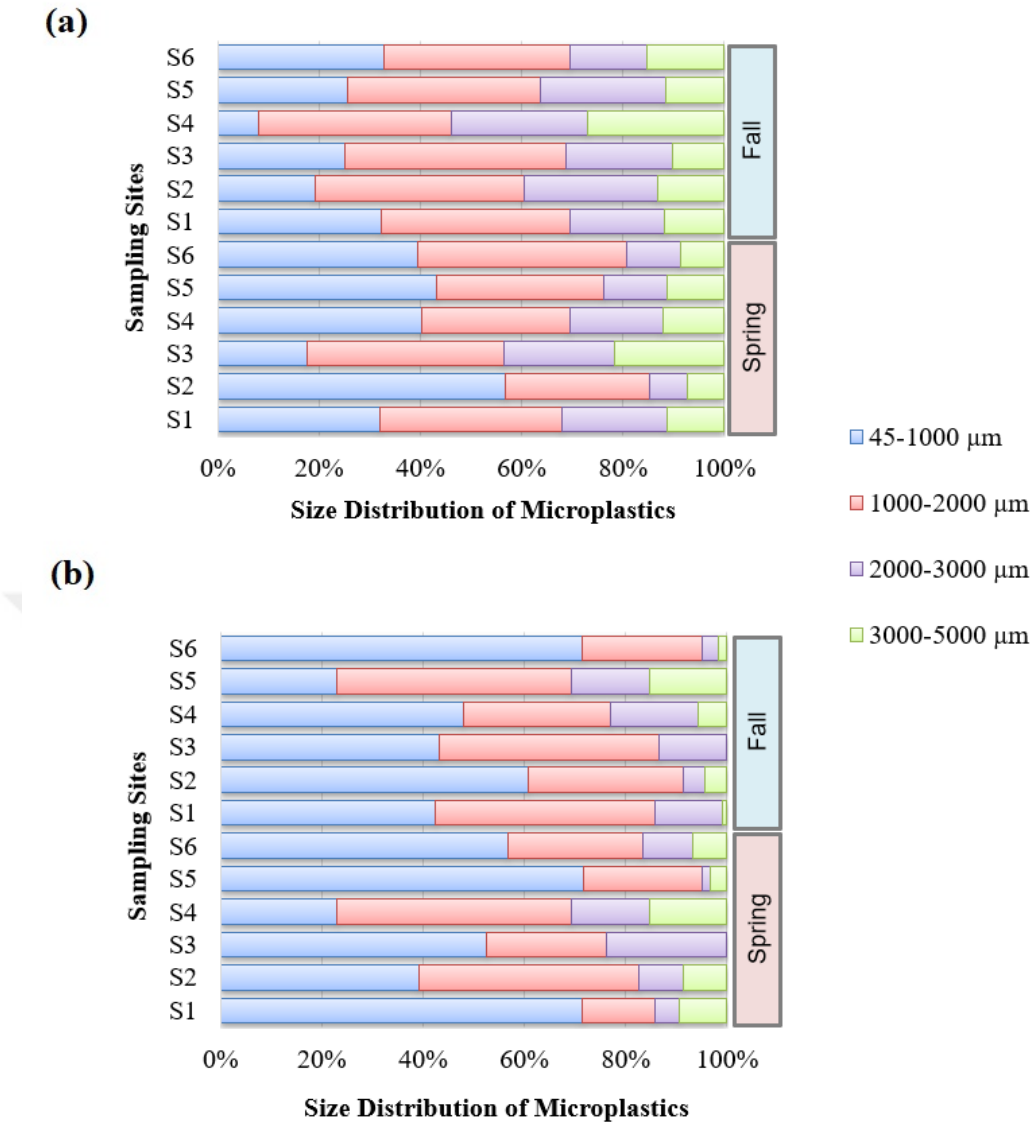

Figure 4.3. Percentage distribution of microplastics by size in (a) water samples and (b) sediment samples.

A slight increase in the proportion of larger particles (>1000 µm) was observed in the water samples collected in the fall, whilst no significant temporal variation was observed in the sediment samples. This may be due to the temporal variations in the characteristics of plastic materials and environmental factors, such as flow regime, sunlight, temperature and dissolved oxygen levels, which govern the fragmentation processes of microplastics. Being different from previous studies (Wang et al., 2017; Wang et al., 2021a; Wu et al., 2020), a higher abundance of medium-sized microplastics ranging between 1000 to 2000 µm (38%) was observed in the water samples, which was followed by small-sized microplastics between 45-1000 µm (31%) and larger particles between 2000-3000 µm (18%) and 3000-5000 µm (13%), respectively. A similar outcome was observed in the Netravathi River, India, where the authors attributed their results to the shorter residence time of plastics and associated lower degradation, due to high flow rates (Amrutha & Warrier, 2020). In our study area,

the mean flow rate of the river ranged from 0.258 to 0.748 m s^{-1} (Table 3.2). Therefore, the predominance of medium-sized particles in water may depend on other factors such as the source or characteristics of the plastic materials. Heat, sunlight and well-aerated conditions are ideal for the fragmentation of plastics (Harshvardhan & Jha, 2013). However, the Ergene River has very low dissolved oxygen values and dark color because of heavy industrial pollution for many years. In field measurements, it was observed that dissolved oxygen levels may decrease up to 0.1 mg L^{-1} (Table 3.2). This may slow down the fragmentation process and thus, influence the size of the particles, both due to decreased light penetration and the presence of anoxic conditions. Moreover, as previously mentioned, effluents of WWTPs can be considered the major sources of microplastics along the upstream of sampling sites. Although characteristics of microplastics in WWTPs may vary by location, recent studies indicated that the average particle size increased from influent (1111 μm - 1135 μm) to effluent (1221 μm - 1309 μm) of WWTPs, probably due to more effective removal of smaller particles in the biological treatment step (Akarsu et al., 2020; Vardar et al., 2021). Therefore, it becomes quite likely that particle size distribution in the river would depend on the properties of microplastics in WWTPs' effluents. However, though WWTPs located near our study area have similar treatment technologies to the above-mentioned plants, it is not possible to obtain a precise outcome with the data produced in this study. To understand these complex factors, future work should undertake a more intensive sampling scheme to determine the characteristics of microplastics in wastewater effluents and monitor the source-to-sink variation of particle sizes along the Ergene River. On the other hand, the majority of the microplastics in sediment samples were surprisingly smaller than those detected in water samples. In total, the dominant size range was found to be between 45-1000 μm (55%), followed by 1000-2000 μm (32%), 2000-3000 μm (9%) and 3000-5000 μm (4%). These results for sediment samples are congruent with the previous studies (Li et al., 2020; Wu et al., 2020). However, here, the difference between the two compartments suggests higher fragmentation of microplastics in sediments than those on water surfaces. This may be because of the higher residence time of the microplastics deposited and buried deeper in the sediments allowing for fragmentation. Additionally, smaller-sized microplastics are more convenient both for homo- and hetero-aggregation than those with larger sizes, due to their lessened stabilities and adsorption on the surface of large suspended solids (Besseling et al., 2017; Li et al., 2019; Song et al., 2019). It is known that aggregation can increase the size and density of microplastics, which can accelerate the deposition of particles onto sediments (Ballent et al., 2016). Research also revealed that deposition as a result of aggregation can cause a decrease in the fraction of small-sized microplastics (<1000 μm) in the surface water (Cózar et al., 2011; Yan et al., 2021). Therefore, aggregation of small microplastics with each other or suspended solids may cause small-sized particles to be dominant in the sediment samples of the Ergene River.

The colors of microplastics can offer information on potential sources and weathering process of particles (Wicaksono et al., 2021). Identification of microplastic color is also important for understanding their bioavailability, since aquatic organisms may accidentally ingest colored microplastics during feeding, due to their resemblance to their prey. Previous studies suggested that light-colored microplastics, such as white, transparent and blue could easily be misidentified and ingested by fish (Ory et al., 2017; Romeo et al., 2015). In this study, different colors of particles were observed in the overall samples, yet they were not equally distributed. Most of the particles were black (49%) and blue (25%) in the water samples, followed by red (14%), white (5%), brown (2%), transparent (1%), green (1%), orange (1%), purple (1%), pink (<1%), grey (<1%) and yellow (<1%). Likewise, dominant particle colors detected in the sediment samples were black (39%), blue (18%), transparent (15%) and red (14%). Besides, white (5%), green (3%), brown (2%), pink (1%), purple (1%), grey (1%) and yellow (1%) particles were also observed in the sediment samples. As mentioned above, the proportion of fibers was quite high in both seasons, which may affect the color diversity in the samples to some extent causing some colors to be similar and dominant (Wang et al., 2021a). Therefore, color cannot solely be sufficient to identify potential sources of microplastics. Considering the industrial activities in the study area, it is quite likely that the main sources of colored fibers are textiles and waste from spinning mills. Other colored microplastics can be originated from plastic production factories, paints and packaging waste. White and transparent microplastics are generally associated with plastic bags and food packaging materials. Besides, microplastic colors are faded by environmental factors, which results in the occurrence of light-colored particles. In this study, the distribution of microplastic colors is similar both in water and sediment samples, yet a higher proportion of transparent particles in sediment samples is most likely due to a higher abundance of transparent hard fragments in sediment, as well as higher residence time and weathering process. The distribution of microplastic colors is shown in Figure 4.4 for the water and sediment samples.

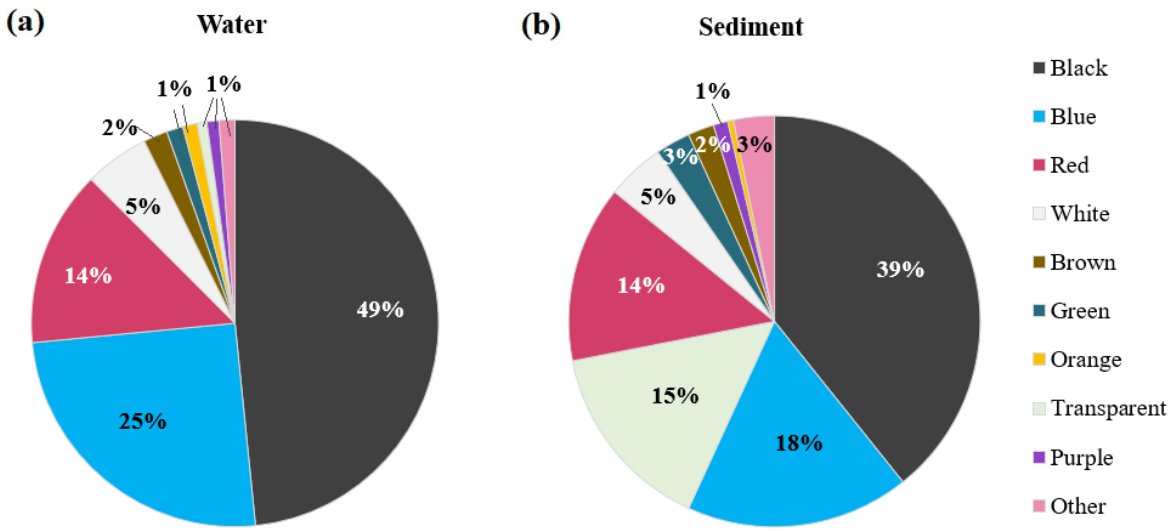

Figure 4.4. Microplastic color distribution: (a) water samples and (b) sediment samples.

Polymer types were detected by analyzing 200 randomly selected particles with Raman Spectroscopy. 150 particles were successfully analyzed, whilst the remaining 50 particles could not be identified due to no match or below 60% similarity with the reference spectra. Amongst 150 particles, 134 of them were identified as microplastic (89%), whereas 16 particles were non-plastic (11%) including nine silicon dioxide (SiO_2) particles, six natural fibers (cotton and modal fibers), and one plastic additive (mortoperm blue). The majority of the particles that could not be identified by Raman were fiber. Although it was suspected that some of these may be non-plastic fibers, such as cotton, viscose and wool fibers, further analysis is needed before a definite conclusion. Previous research indicated that dyed fibers including cotton, viscose, acrylic and wool can have different peaks according to their colors and can be detected more clearly at different Raman laser wavelengths varying from 514 nm to 830 nm (Buzzini & Massonnet, 2015; Prego Meleiro & García-Ruiz, 2016; Thomas et al., 2005; Was-Gubala & Machnowski, 2014). Hence, future work should also focus on the relevant particles considering these factors to obtain a precise outcome about the type of these non-identified particles.

The results of the Raman analysis are given in Figure 4.5.

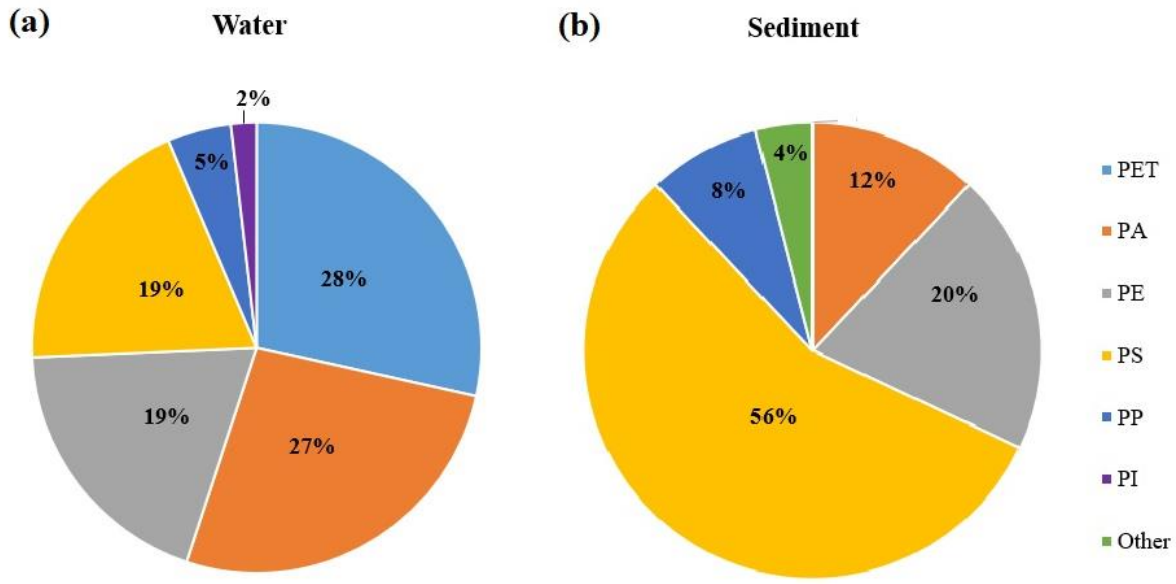

Figure 4.5. Microplastic types in the river samples: (a) Polymer distribution in water, (b) Polymer distribution in sediment.

According to the results, many of the plastic particles in water were polyethylene terephthalate (PET, 28%) and polyamide (PA, 27%), which were followed by polyethylene (PE, 19%), polystyrene (PS, 19%), polypropylene (PP, 5%), and polyisoprene (PI, 2%). In sediment samples, PS (56%) was predominant, followed by PE (20%), PA (12%), PP (8%), and other (4%) including one polysulfone/polyamide (PSU/PA) composite polymer. Examples of plastic and non-plastic spectra with the reference spectra are given in Figure B.1-B.11. PS, PA, PET and PE were the four most abundant polymers within the samples in total. PS is a hard and resistant thermoplastic resin, with a variety of applications from foam products used in disposable food containers to rigid materials in the electronics and automotive industries. The number of foam particles was relatively low, but many of the hard fragments found were identified as PS, which may have originated from the waste of machinery and automotive industries located in the neighboring area or degradation of plastic litter. PET is an aliphatic polyester that is used in the production of everyday items including clothes, carpets and other home textile products and water bottles, and it dominates synthetic fiber production for around 60% by volume (Radzi et al., 2021). PA (or nylon) is usually used in manufacturing items that require strength and flexibility, such as textile products, seatbelts, airbags, fishlines and parts of machines. After PET, PA is one of the most used polymers in the production of synthetic fibers (Dalla Fontana et al., 2020). Therefore, it can be concluded that the majority of PET and PA, particularly in shape of fiber, originated from the textile industries or discharges from WWTPs from the upstream river. It is likely that other PA particles came from the wastewaters of various industries manufacturing part of machines or automobile. PE is also a versatile polymer, mainly used for packaging and shopping bags, and can also be used in water pipes, housewares, insulating materials,

agricultural mulches, etc. In our study area, the industries producing such materials can be sources of PE particles, yet, plastic mulches used in agricultural lands around the downstream of the Çorlu and Ergene tributaries can be another source of detected PE, as discussed previously. These sources derive secondary microplastics, which are assumed to constitute the majority of microplastics in the environment. PS and PE particles are also used in cosmetic and medical products in pellet form as primary microplastics (An et al., 2020). It is worthwhile to note that, some of the polymers mentioned above could originate from the degradation of anthropogenic litters, so it becomes necessary to implement a more comprehensive investigation to assess the exact contribution of each source to microplastic contamination in the river.

Amongst these polymers, PET has the highest density (1.38 g cm^{-3}), followed by PA (1.01-1.08 g cm^{-3}), PS (1.05 g cm^{-3}) and PE (0.88-0.96 g cm^{-3}). According to our results, despite the higher densities of PET and PA than water, these polymers were identified in the water samples compared to other low-density plastics, such as PE. This can be attributed to river's hydrodynamical conditions, which may cause resuspension of denser polymers by turbulence. In addition, the occurrence of excessive levels of textile fibers in the water samples, which generally constitute PET and PA, results in these polymers being the most abundant types in water samples. PET is the most used material in manufacturing synthetic fibers, accounting for around 60% by volume (Radzi et al., 2021). Therefore, predominance of PET and PA in the production of plastic items in the study area and associated higher release of these particle types to the river, as well as river hydrodynamics can results in higher levels of these polymers in the surface water. On the contrary, no PET particles were found in the sediment samples, despite having the highest density amongst the extracted polymers. This can be attributed to the fact that NaCl solution (1.20 g cm^{-3}) is insufficient for extraction of high-density polymers, such as POM (1.41 g cm^{-3}), PVC (1.38 g cm^{-3}) and PET (1.38 g cm^{-3}). Therefore, these polymers can be lost during the density separation method for extracting microplastics from the sediment samples.

4.2. Modeling Vertical Transport of Microplastics in Turbulent Flow

4.2.1. Monte-Carlo Simulation Results

A mechanistic model was developed and Monte-Carlo analyses were conducted in GoldSim (version 14.0) to simulate the probable variation of microplastic concentrations in water and sediment with time for each sampling site. These simulations were performed to indicate the time required for microplastics to leave the water compartment and the probable maximum concentrations of

microplastics in sediment. For this purpose, the initial conditions for microplastic concentrations in the water column were assumed as the concentrations in the grab samples collected from the surface water of six sampling sites. As given in Section 3.1, water samples were collected in duplicates, therefore initial concentrations were entered to the model considering the range of microplastic concentrations in water for each each sampling site. The model layout is given in Appendix D (Figure D.1). The model results for the water column are given in Figures 4.6 and 4.7 for the years 2019 and 2020, respectively.

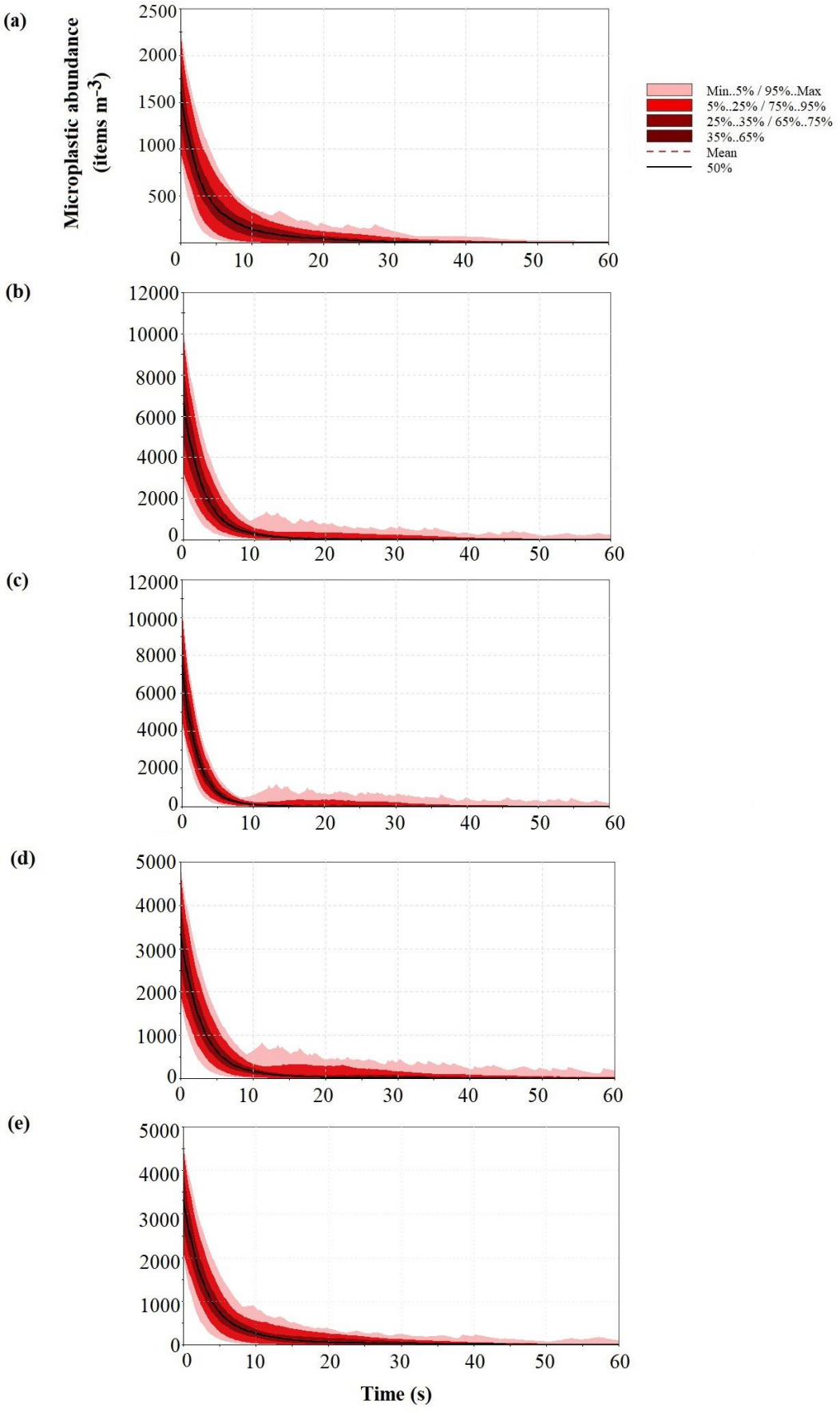

Figure 4.6. Probable variation of microplastic concentration in water under turbulent flow conditions in (a) Site 1, (b) Site 2, (c) Site 3, (d) Site 4, and (e) Site 5 in 2019.

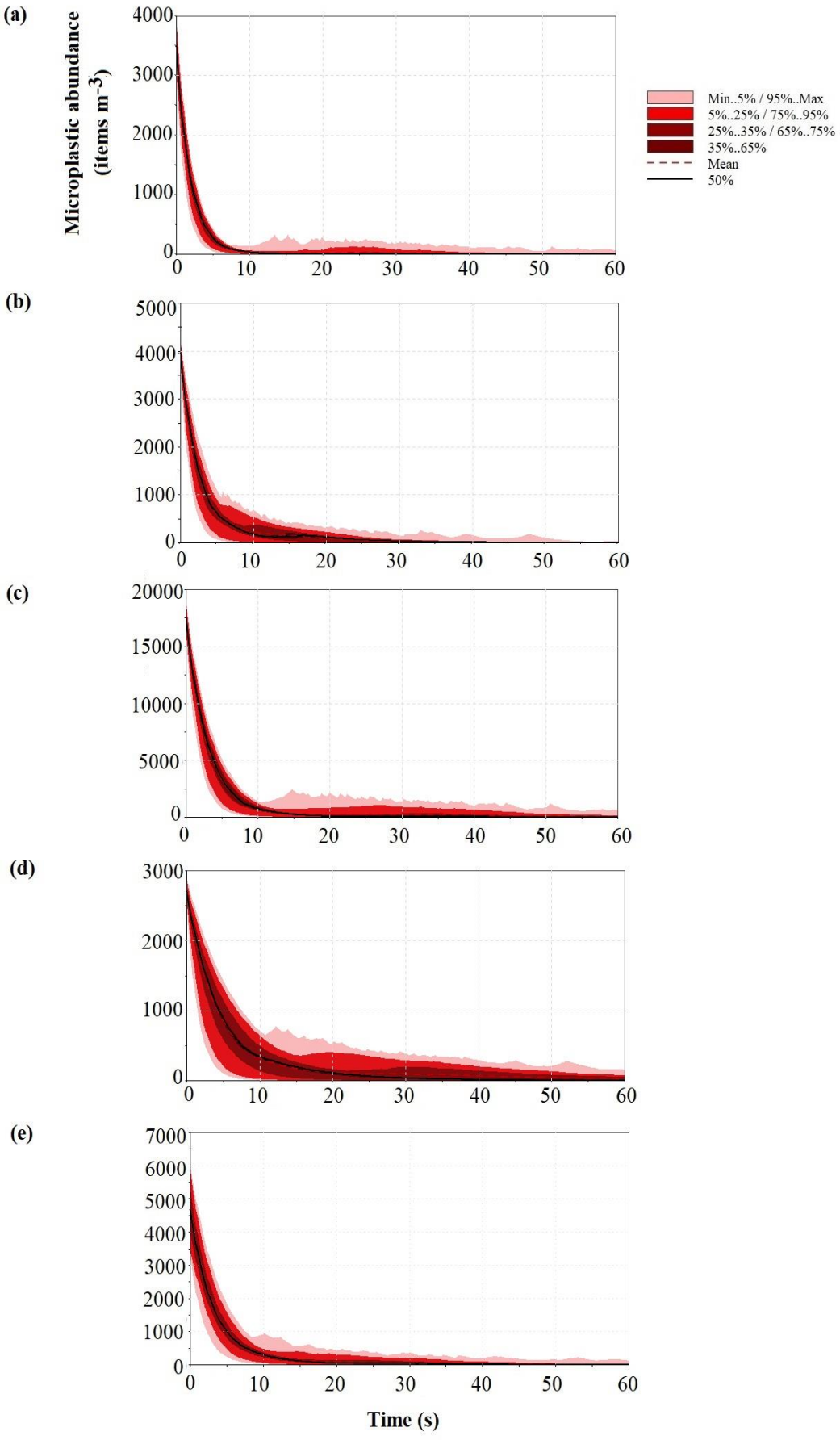

Figure 4.7. Probable variation of microplastic concentration in water under turbulent flow conditions in (a) Site 1, (b) Site 2, (c) Site 3, (d) Site 4, and (e) Site 5 in 2020.

The model outcomes illustrated a Gaussian distribution between minimum and maximum values of microplastic concentrations. This distribution had a wide range, particularly in sampling sites with shallow water accompanied by low flow velocities (e.g. Figure 4.7d), as at these locations, particle settling is mainly governed by a number of other microplastic characteristics, such as shape, size and density, rather than the flow characteristics. On the contrary, Gaussian distribution showed a narrow range for the sampling sites with deeper water and higher flow rates (e.g. Figure 4.7a). Deep waters can prolong the settling time of microplastics, as well as increase bed shear stress, which often results in elevated levels of turbulence (Besseling et al., 2017; Richards, 1982). This can cause flow of microplastics to the downstream more quickly and increase the settling velocities of the remaining particles due to rise in the vertical velocity component (v'). Previous research also revealed that turbulent conditions increase microplastic settling due to the particles being dragged to the downward side of eddies (Jacobs et al., 2016; Nielsen, 1993).

Flow conditions and particle settling have high impact on the residence time of microplastics in the water column. Water bodies with high flow rates and small volume have short residence times, which are referred to as fast flushers (Chapra, 1997). According to the model outcomes here, residence time of microplastics in the water column varied by site. It is worthwhile to note that the value of input parameters related to the particle characteristics (ranges of density, size and shape factor) in the model developed in this study were assumed as the same (e.g. the values of ω_s were almost equal in all sites), but initial concentrations of microplastics and site characteristics varied by location. In this respect, it can be concluded that the variation in residence times by site was directly related to the differences in flow characteristics and river hydrogeometry. Flow conditions affect particle settling, directly due to the fluctuations in vertical flow velocity. As discussed earlier, higher vertical velocities can cause rapid deposition of microplastics onto the sediment bed causing shorter residence times in the water column. For example, although Site 5 had a higher initial concentration than Site 4 in 2020, the particles left the water column earlier than that in Site 4, probably due to the effect of higher flow rate (0.430 m s^{-1}) in Site 5 (Figure 4.7e). In contrast, Site 4 had the lowest flow rate (0.259 m s^{-1}) among the sampling sites in 2020. Comparing mean values of microplastic abundance in Figure 4.7, microplastics resided more in the water column in Site 4, despite its lowest initial concentration (Figure 4.7d). This relationship can also be explained by the transfer function ($\beta = C/C_{in}$), which is a commonly used approach in mechanistic models (Chapra, 1997). Transfer function represents the assimilative capacity of lakes or river reaches. Similar to residence time, transfer function is directly affected by flow, settling velocity and the control volume of the system. If β<<1, then the reservoir (or control volume) has great assimilative capacity to reduce the level of contaminants. Conversely, if $\beta \rightarrow 1$, then assimilative capacity is minimal, so the concentration of

contaminants will approach their initial values. In this study, a comparison of β values of Site 4 and 5 for t = 30 s, indicated that Site 5 had smaller transfer function (β = 0.012) than Site 4 (β = 0.033), revealing a higher assimilative capacity for Site 5 causing lower residence times of microplastics in this location. These findings were also confirmed by examining the seasonal changes in microplastic transport. The mean values of the simulation results indicated longer residence time of particles in Site 1, in 2019 (Figure 4.6a, β = 0.015, t = 30 s) than those in 2020 (Figure 4.7a, β = 0.004, t = 30 s), which can be attributed to seasonal changes in flow rate and river morphology, given in detail in previous chapter (Table 3.2). However, it should also be noted that high river flow can lead to elevated levels of turbulence, hence increased resuspension, which can cause fluctuation of microplastic levels in water, reducing the assimilative capacity of river, and therefore, extend the residence time of microplastics in the water column.

The model results for sediment are given in Figures 4.8 and 4.9 for the years 2019 and 2020, respectively.

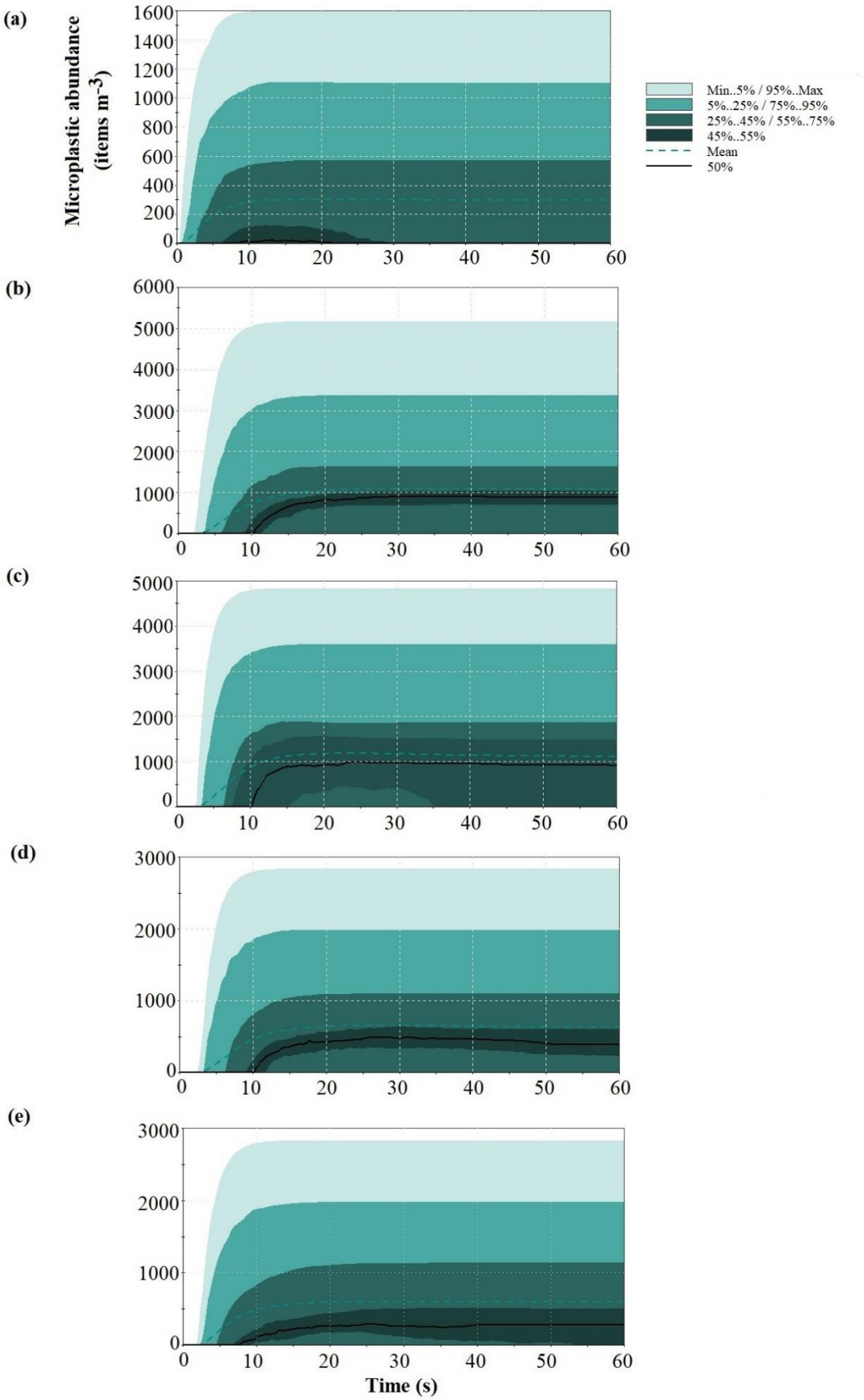

Figure 4.8. Probable variation of microplastic concentration in sediment under turbulent flow conditions in (a) Site 1, (b) Site 2, (c) Site 3, (d) Site 4, and (e) Site 5 in 2019.

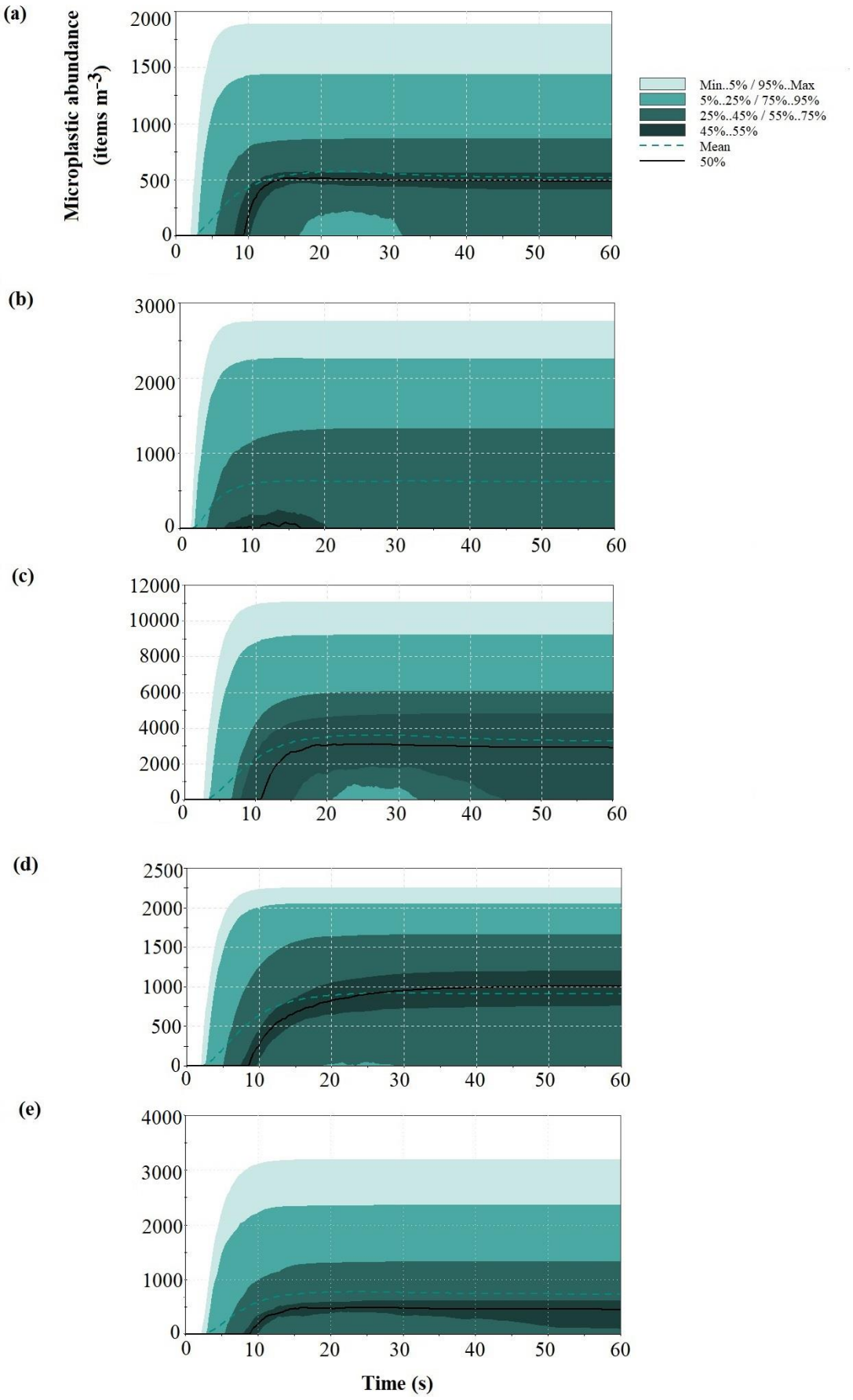

Figure 4.9. Probable variation of microplastic concentration in sediment under turbulent flow conditions in (a) Site 1, (b) Site 2, (c) Site 3, (d) Site 4, and (e) Site 5 in 2020.

According to Figures 4.8 and 4.9, microplastic levels increased by settling and burial and finally reaching to an equilibrium due to resuspension of the particles. Expectedly, sediments in the sampling sites with higher initial concentrations in water column reached to greater microplastic concentrations. Moreover, Monte-Carlo simulation results exhibited a higher variance compared to the water column, most likely due to the fact that sediment microplastic levels are directly related to the vertical velocity fluctuations and particle properties. In addition, unlike the water compartment, it was assumed that there was not a horizontal movement of microplastics in the sediment, which probably resulted in a greater variance in the Gaussian distribution. Uncertainty analysis given in the further section (Section 4.2.4) also revealed higher correlations between sediment microplastic concentrations and stochastic parameters, including river morphological parameters and particle characteristics. According to the correlation matrix given in Table 4.6, most of the stochastic parameters, including particle size, polymer density, and distance from the riverbed to a given height (z) had greater impact on the uncertainties of model outcomes for sediments. Similar to the water column, these variances and uncertainties and their differences between sampling sites depend on many complex factors, such as flow conditions, river geomorphological characteristics, and particle properties, which directly affect the settling time of microplastics onto the sediment. The effects of these parameters were investigated by sensitivity analysis and discusses in detail, in Section 4.2.4.

The change of mean values of settling and resuspension fluxes for each site were also simulated, given in Figures 4.10, 4.11, 4.12, and 4.13 for the years 2019 and 2020, respectively.

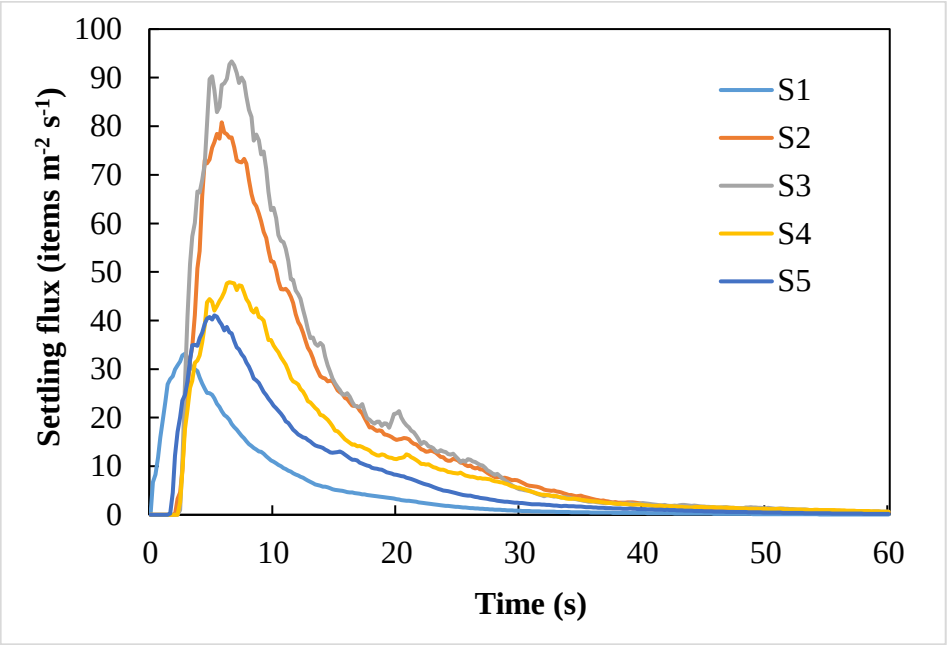

Figure 4.10. Change in microplastics settling flux in the sampling sites in 2019.

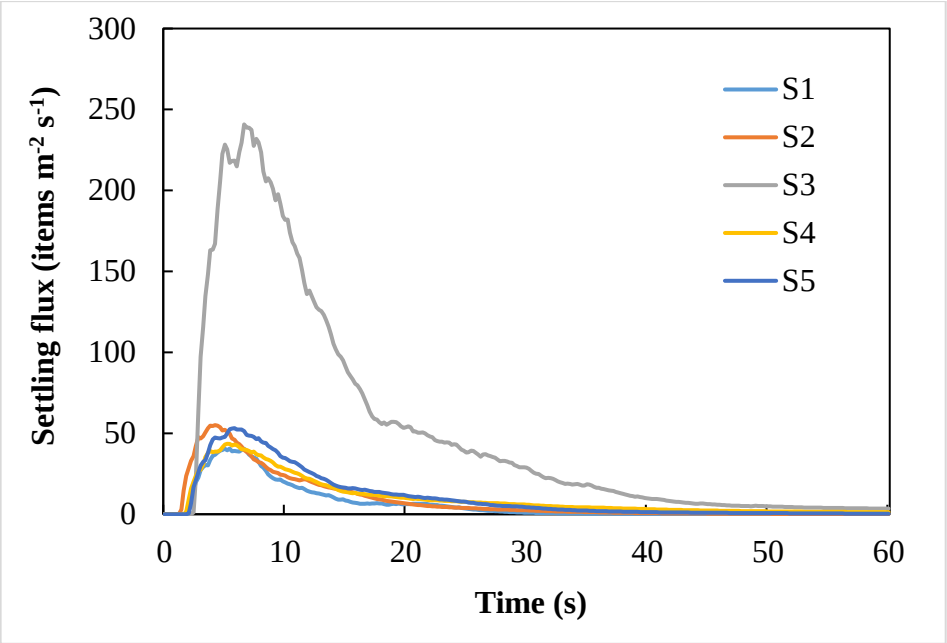

Figure 4.11. Change in microplastics settling flux in the sampling sites in 2020.

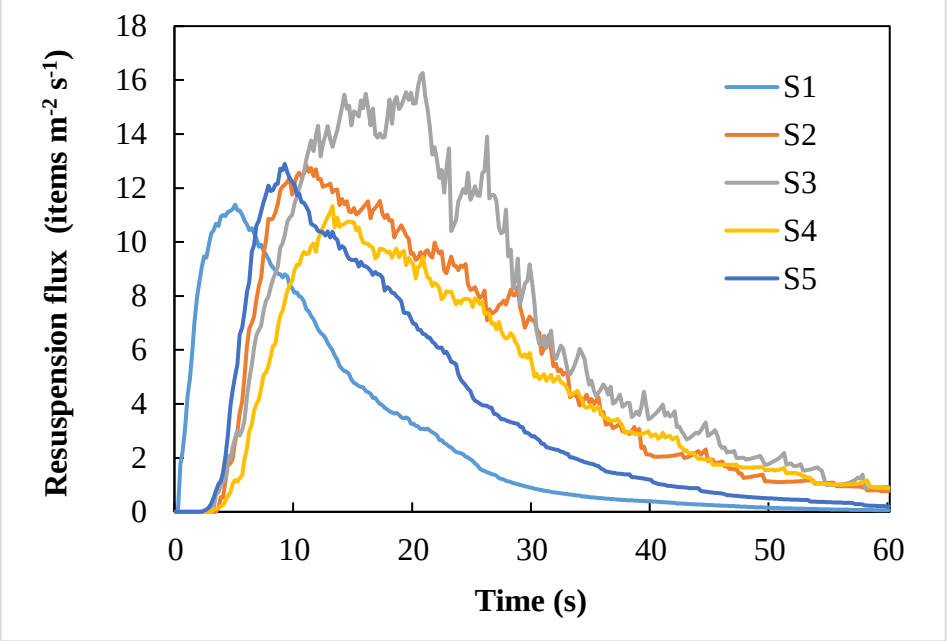

Figure 4.12. Change in microplastics resuspension flux in the sampling sites in 2019.

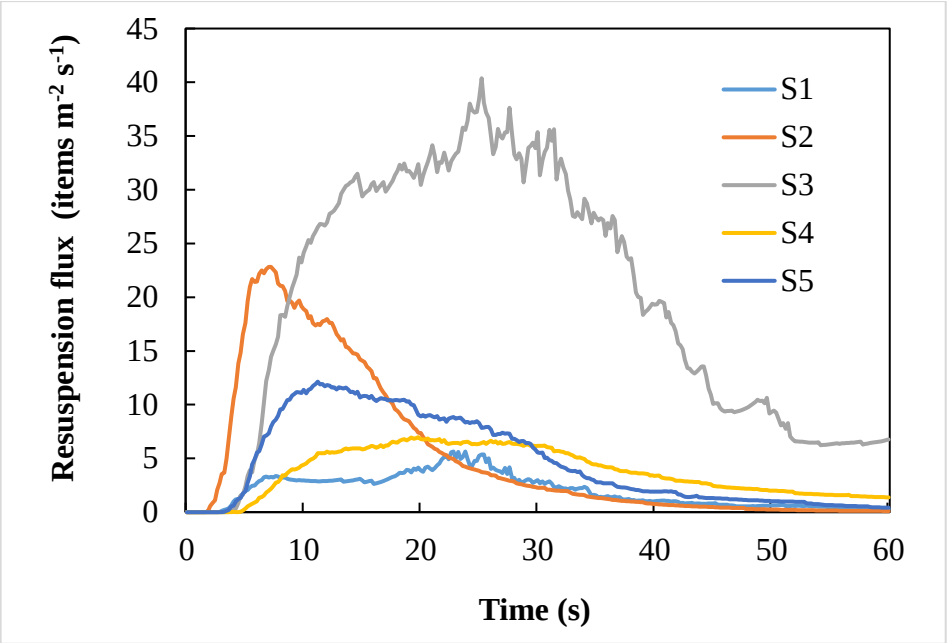

Figure 4.13. Change in microplastics resuspension flux in the sampling sites in 2020.

According to the results, Site 3 had the highest settling flux, followed by the sites 2, 4, 5, and 1 in 2019. Likewise, in 2020, the highest settling flux was found in Site 3, followed by Site 2, 5, 4, and 1. The values of resuspension flux in each site (Figures 4.12 and 4.13) were congruent with the results of the settling fluxes. These outcomes revealed that the settling and resuspension fluxes had a direct relationship with the microplastic initial concentrations, which means that initial concentrations dominated the other parameters including settling velocity. Since initial concentrations of microplastics in sediment were assumed as zero, resuspension flux of the particles in this model was directly related to the settling of microplastics. Yet, settling and resuspension also depend on particle characteristics and river hydrodynamics, which will be further investigated in Scenario Analysis.

Settling and subsequent resuspension of microplastics were delayed at some of the sampling sites, such as Site 3, due to increasing river depths and the associated longer particle settling times at these locations (Table 3.2). This also caused fluctuations in resuspension flux values as higher water depth can increase bed shear stress and affecting vertical velocities in both directions (Figures 4.12 and 4.13). Nevertheless, higher turbulence also accelerates the horizontal movement of microplastics in water. This can cause microplastics to flow downstream more quickly, as well as the rapid settling and resuspension of these particles. Therefore, turbulent conditions can both increase and decrease microplastic concentrations in the water and sediment, affecting the transfer function of the river. Accordingly, the influence of these hydrodynamical conditions on resuspension can extend or reduce the residence time of microplastics in both compartments; yet, water depth or turbulent conditions are not the only critical parameters in particle resuspension. High concentrations of microplastics can

trigger continuous precipitation and resuspension between water and sediment, resulting in fluctuation in microplastic flux values. For example, Site 3 had the highest microplastic concentration (Table 4.1) and water depth (0.586 m), but a low flow rate (0.378 m s^{-1}) in 2020 (Table 3.2 and Table 4.4); so, the fluctuation in settling and resuspension flux in this location was greater than the other sampling sites. Compared to Site 2 (2020) with lower microplastic concentrations and river depth (0.384 m) but higher flow rate (0.745 m s^{-1}), settling and resuspension occurred more slowly in Site 3 and left the control volume later (Figure 4.13).

4.2.2. Model Calibration and Validation

Model calibration was carried out by trial and error, the one of the most used methods in model calibration, in which the accuracy of the outcome highly depends on the number of parameters adjusted in calibration (Hosseiny, 2022). In other words, a large number of calibration parameters can increase the level of uncertainty and reduce the reliability of the outcomes. In this study, model calibration was implemented by changing the values of input parameters including ρ_w, D_{84}, and S. Values for these parameters were adjusted individually by trial and error to improve the model fit by comparing predicted mean velocity of the river ($\bar{u}$) with the measured data. The values of measured and predicted $\bar{u}$ are given in Table 4.4.

Table 4.4. Results of model calibration. Comparison of predicted and measured results of mean velocity of the river.

Date	Site	Measured $\bar{u}$	Predicted $\bar{u}$
May 20, 2019	S1	0.421	0.428
	S2	0.424	0.426
	S3	0.542	0.544
	S4	0.361	0.366
	S5	0.475	0.473
Sep 30, 2020	S1	0.725	0.724
	S2	0.748	0.745
	S3	0.383	0.378
	S4	0.258	0.259
	S5	0.438	0.430

Linear regression analysis was conducted considering the results given in Table 4.4, which are shown in Figure 4.14.

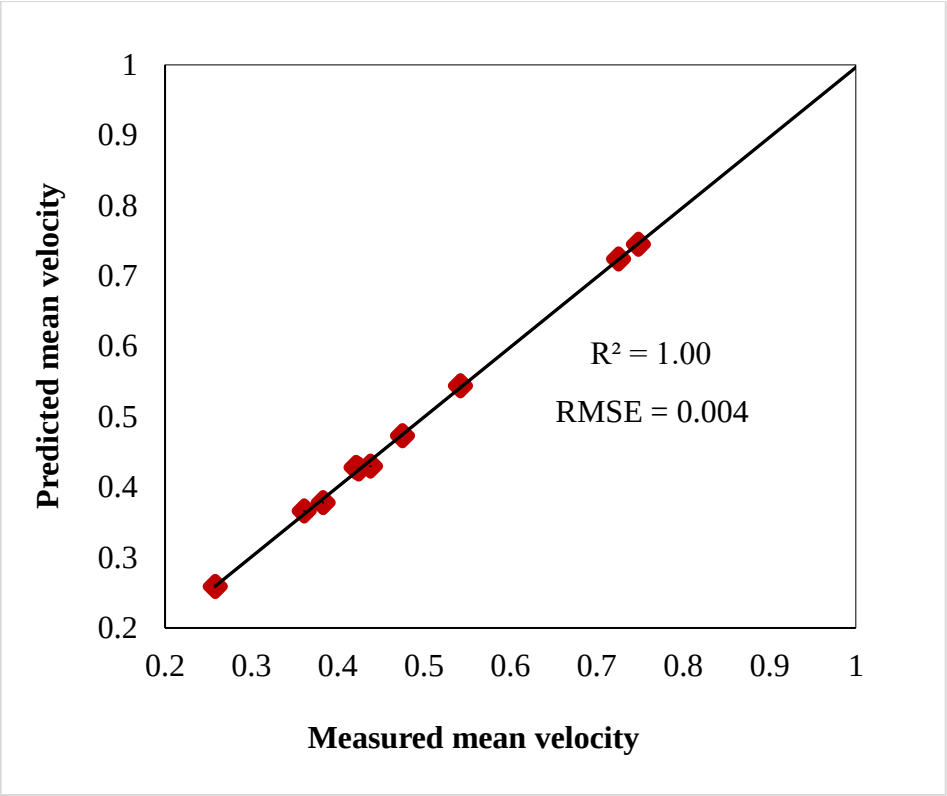

Figure 4.14. Results of model calibration: Regression analysis of predicted and measured results of mean velocity of the river ($\bar{u}$).

Settling velocities of microplastics were calculated for three different shape classes of microplastics including near-spherical, fragments and fibers (in Appendix C from Table C.1 to C.3). These shapes were particularly selected due to their abundancy within the samples of this study and available data in the literature. Settling velocities were calculated assigning the mean values of shape factor calculated for each shape class of particles (Equation 3.9). Considering the available data from the literature, such as polymer type, particle size and shape, settling velocities of three predominant polymers found in this study, PS, PET and PA, were calculated for specific particle sizes. The predicted results were compared to the results of two experimental studies (Wang et al., 2021b; Nguyen et al., 2022) and one theoretical study (Goral et al., 2023), given in detail in Table 4.5.

Table 4.5. Results of model validation: Comparison of predicted settling velocities of microplastics with literature.

Particle Shape	Polymer Type	Size (μm)	Settling Velocity (m s^{-1})		Reference
			Model	Literature	
Near-sphere	PS	371	0.003	0.003	Wang et al. (2021b)
		1167	0.015	0.013	
Near-sphere	PET	69	0.0009	0.009	
		1927	0.110	0.090	
Near-sphere	PA	1895	0.054	0.042	
		3565	0.099	0.078	
Fragment	PS	697	0.004	0.008	
		1131	0.008	0.014	
Fragment	PET	138	0.001	0.007	
		2858	0.100	0.120	
Fragment	PA	265	0.002	0.003	
		3234	0.060	0.065	
Fiber	PET	1100	0.003	0.0003	Nguyen et al. (2022)
		2250	0.007	0.0003	
		4250	0.020	0.0004	
Fiber	PA	5000	0.011	0.011	Goral et al. (2023)
		5000	0.011	0.017	

The comparison given in Table 4.5 revealed that the settling velocities of near-spherical particles and fragments are closer to fibers'. In particular, predicted and experimentally measured settling velocities of fibers (Nguyen et al., 2022) did not fit well, while a stronger correlation was found between the results of this study and calculations by Goral et al. (2023). This can be attributed to the fibers' cylindrical morphology and their wide size range and aspect ratio (*a/c*). Moreover, settling velocity equations in the literature were developed for lower aspect ratio particles, so they can fail to predict fibers' dynamics in the water column (Nguyen et al., 2022). Also, fiber settling direction is generally neglected in traditional settling equations. However, the angle between the vertical direction and the fiber main axis is crucial to determine the exact settling velocity of these particles as it alters the drag force exerting on settling fibers. Nguyen et al. (2022) found that fibers settle slower at the horizontal direction and become fastest, when they shift to the vertical direction.

Linear regression analysis was conducted to validate the model considering the results given in Table 4.5. The results of the regression analysis are demonstrated in Figure 4.15. The analysis results indicated that R^2 value was 0.92 and RMSE was 0.011.

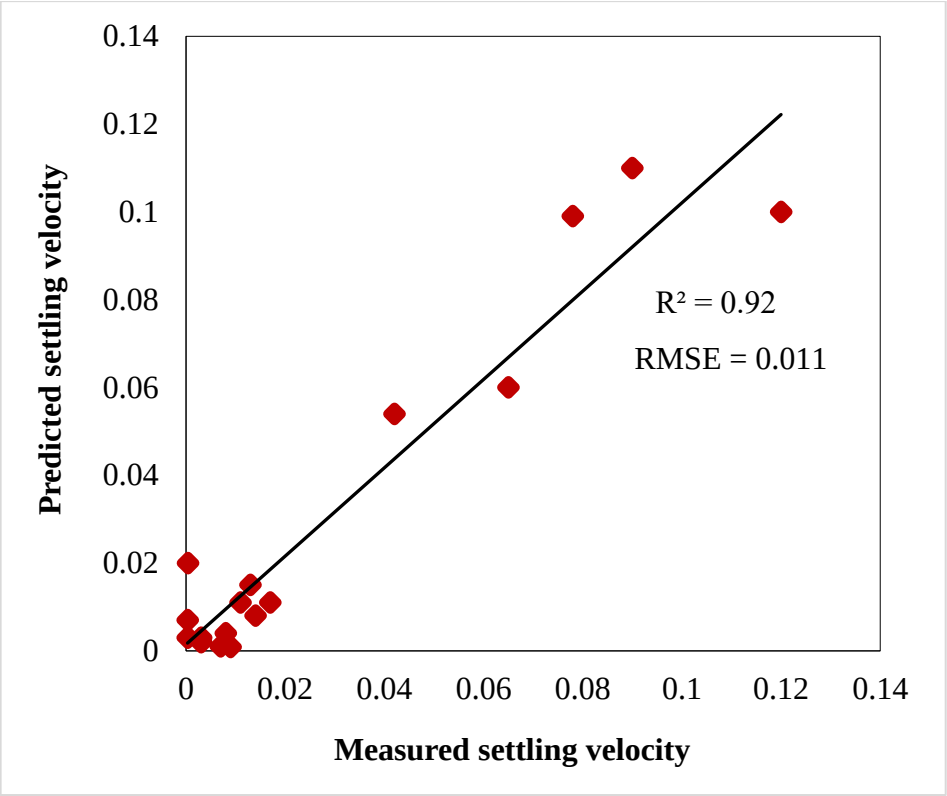

Figure 4.15. Results of model validation: Regression analysis of predicted and measured results of settling velocity of microplastics (ω_s).

4.2.3. Scenario Analysis

Scenario analyses were carried out to understand the effect of particle properties including shape and size, as well as differences in river hydraulics on settling and resuspension fluxes of the particles. For this purpose, nine scenarios in total were made by changing stochastic data including shape factor (φ) and particle size (a) with deterministic values within Site 2 for 2020. To investigate the effect of flow, previously calculated bed shear stress (τ_0) was also changed by giving deterministic values.

First three scenarios were generated to understand the effect of particle shape. It was assumed that all particles were fibers, fragments or near-spheres. To achieve this, mean values of shape factors calculated for each type of particles (Equation 3.9), were assigned. The graphs given from Figures 4.16 to 4.21 indicate the mean values of settling and resuspension fluxes. The changes in settling and resuspension flux of different shaped microplastics with time are given in Figure 4.16 and 4.17.

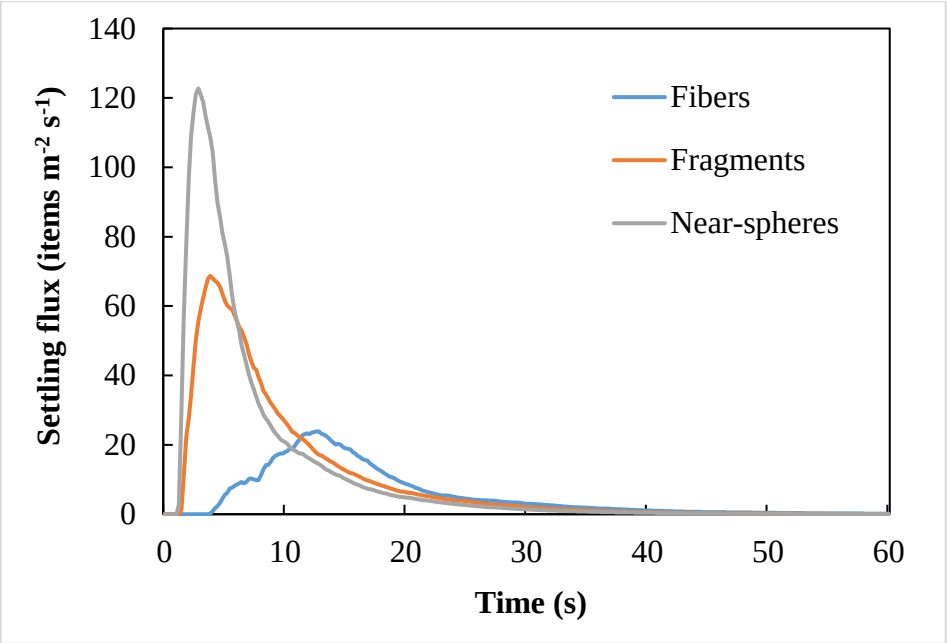

Figure 4.16. Changes in settling flux of different shaped microplastics with time.

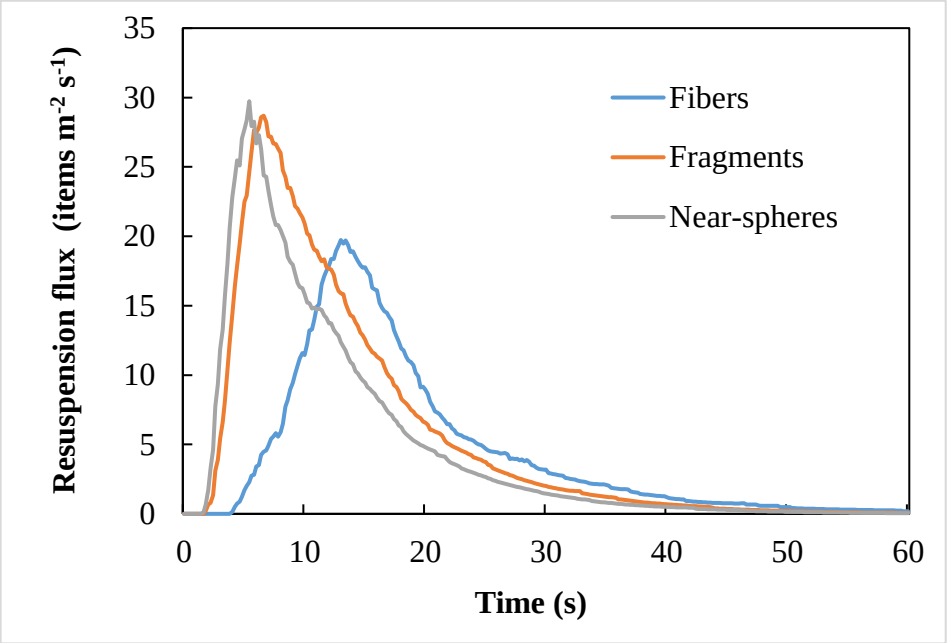

Figure 4.17. Changes in resuspension flux of different shaped microplastics with time.

According to Figure 4.16, since all the dense particles settled rapidly, settling flux reached its maximum value at a certain time, but then decreased gradually as some of the particles resuspended and started to leave the control volume with the outflowing river. Similarly, resuspension of the particles occurred following settling reached its peak flux after some time and decreased gradually until all the particles in water left the control volume (Figure 4.17). The results revealed that near-spherical particles had the highest settling and resuspension flux, followed by fragments and fibers. However, the influence of particle shape on settling was higher compared to resuspension. These

results are in line with literature indicating that as the flatness and irregularity of particles increase, the settling velocity of microplastics decrease (Waldschläger & Schüttrumpf, 2019a; Wang et al., 2021b). According to Figure 4.17, the resuspension of fibers was delayed due to lower settling velocity and associated longer settling time compared to the other shaped particles.

Second of all, the effect of different sized particles on settling and resuspension behavior of microplastics was investigated generating three different scenarios. All the particles in the water column were assumed to be 50 µm, 500 µm and 5000 µm, respectively. Graphs showing the changes in settling and resuspension flux of microplastics with different sizes are given in Figures 4.18 and 4.19, respectively.

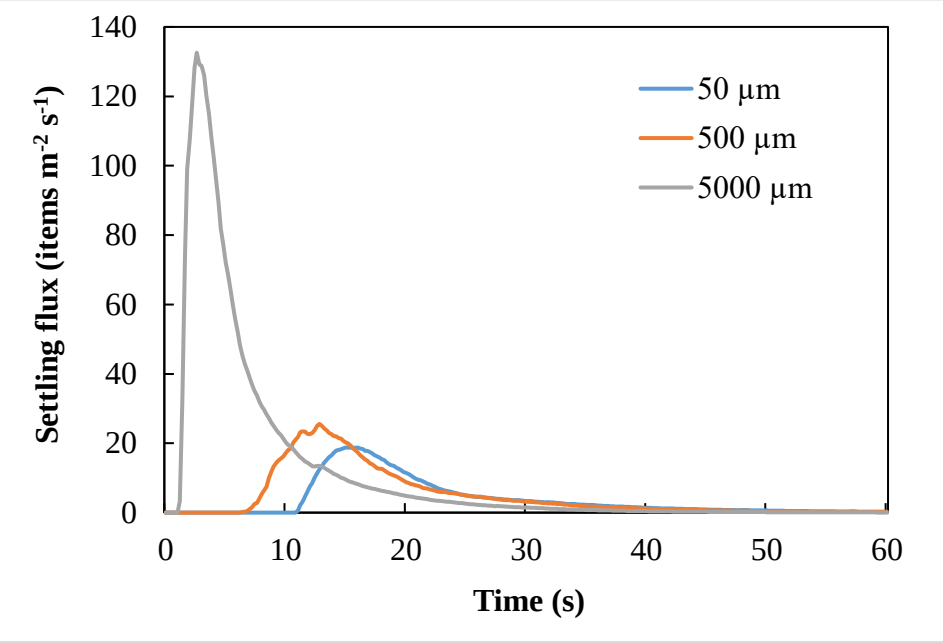

Figure 4.18. Changes in settling flux of different sized microplastics with time.

Like the scenario results of different shapes, following the rapid increase in settling flux, some of the particles resuspended and left the control volume with the flow, which caused a gradual decrease in the settling flux. Although resuspension had a similar pattern, it was less affected by the differences in particle sizes. As the particle size increased, the settling flux of microplastics increased; however, this difference was clearer for the 5000 µm-sized particles than 500 µm and 50 µm ones. This can be attributed to the lower settling velocities of smaller particles and probable loss due to river flow during that time. Therefore, the settling flux of microplastics below a certain size may converge at a certain value with the effect of flow. In addition, settling and subsequent resuspension of small microplastics were delayed due to their longer settling time than those of the larger particles'.

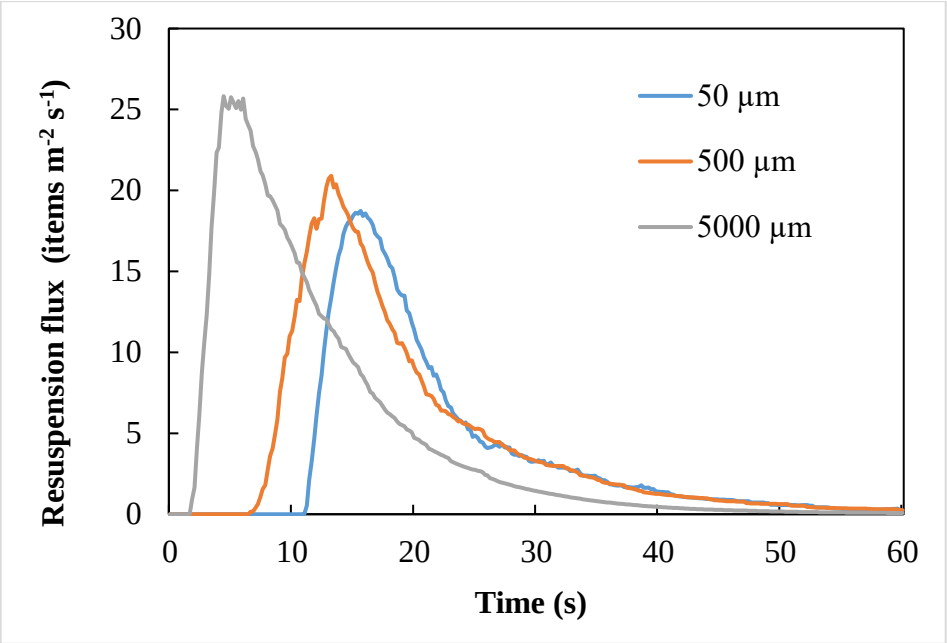

Figure 4.19. Changes in resuspension flux of different sized microplastics with time.

Thirdly, the effect of river hydraulics and associated flow characteristics on vertical transport of microplastics were investigated by assigning deterministic values to the bed shear stress considering three different scenarios. Bed shear stress was assumed to be 0.15 N m^{-2}, 0.50 N m^{-2}, and 0.90 N m^{-2}, respectively. The changes in settling and resuspension fluxes of microplastics with time under different bed shear stresses are given in Figures 4.20 and 4.21, respectively.

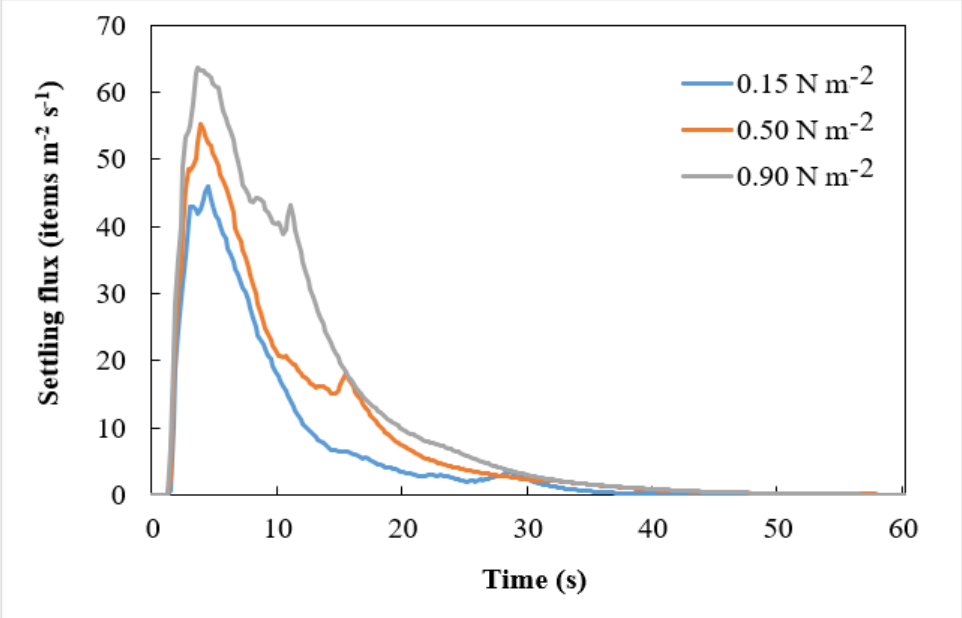

Figure 4.20. Changes in settling flux of microplastics with time under different bed shear stresses.

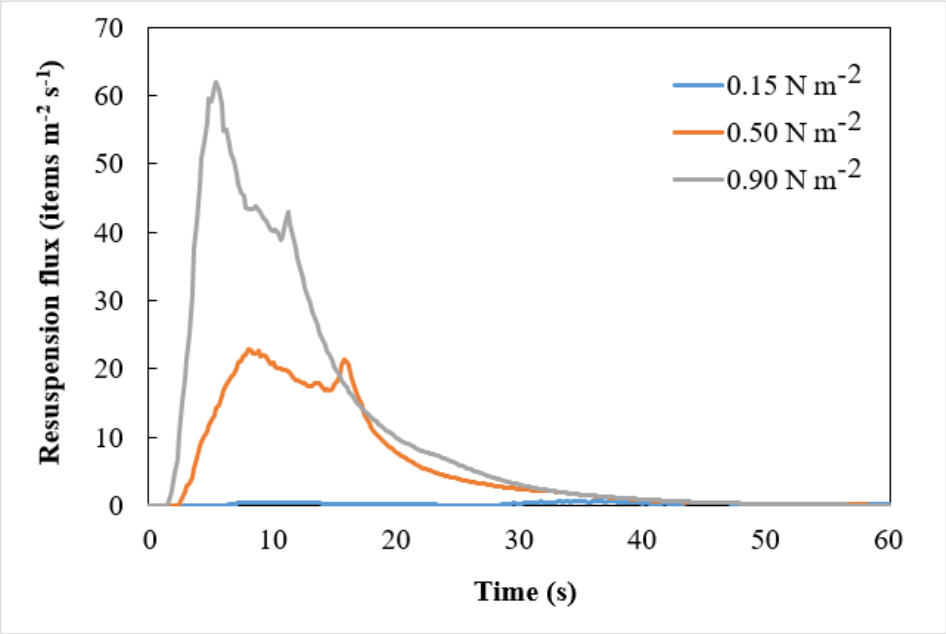

Figure 4.21. Changes in resuspension flux of microplastics with time under different bed shear stresses.

According to the graphs, as bed shear stress increases, the settling and resuspension fluxes also increase. A previous study by Jacobs et al. (2016) also indicated that majority of the microplastic particles settled more rapidly in turbulent conditions. This can be explained by the particles interacting with the eddies and being dragged to the downward side of vortices (Nielsen, 1993; Jacobs et al., 2016). However, on the contrary of previous scenarios related to the particle shape and size, resuspension flux was more affected by the changes in bed shear stress. These results were expected since bed shear stress has a critical significance in resuspension of particles in the riverine environments. As discussed in Section 4.1.2, once bed shear stress exceeds the critical shear stress, sediment particles begin to resuspend and can move towards downstream. Another study by He et al. (2021) revealed that the lower deposition of microplastics onto sediments occurred in the locations with the greater bed shear stress, due to higher resuspension and dispersion of the particles in those areas. According to the model outcomes in this study, settling and resuspension fluxes approach each other under high bed shear stress (0.90 N m^{-2}), which means that the deposition of microplastics is very low, even almost zero, since each particle that settled becomes immediately resuspended. On the other hand, despite the continuing settling onto the sediment, resuspension of microplastics was equal to zero, when bed shear stress was very low (0.15 N m^{-2}).

In addition to settling and resuspension fluxes, the variation of microplastic concentrations in both water and sediment were also simulated in scenario analysis and provided in Appendix E from Figure E.1 to Figure E.18.

4.2.4. Uncertainty and Sensitivity Analysis

Uncertainty analysis was conducted to understand the effect of stochastic (or uncertain) parameters on model results using GoldSim's Multivariate Analysis tool. A correlation matrix of stochastic input parameters and model results, including microplastic concentration in water (C_1) and sediment (C_3) were generated, which is given in Table 4.6.

Table 4.6. Correlation matrix of stochastic parameters and model results (Highlighted cells represent model outcomes for water and sediment).

	C_1	C_3	z	a	ρ_p	φ	C_0
C_1	1.00	-0.86	0.30	-0.45	-0.30	-0.50	0.14
C_3	-0.86	1.00	-0.41	0.47	0.33	0.45	0.13
z	0.30	-0.41	1.00	-0.03	-0.03	0.02	0.00
a	-0.45	0.47	-0.03	1.00	-0.01	-0.03	0.03
ρ_p	-0.30	0.33	-0.03	-0.01	1.00	-0.04	0.02
φ	-0.50	0.45	0.02	-0.03	-0.04	1.00	-0.06
C_0	0.14	0.13	0.00	0.03	0.02	-0.06	1.00

The strength of correlation between stochastic parameters and model results was determined using five scales given in previous chapter (Table 3.3). According to the results, the correlations between stochastic parameters were very weak (0 to ±0.2). The distance from the bottom of river to a given height (z) is related with the river depth and affects turbulence levels and resuspension in the river; thus, there was a moderate negative relationship between z and the concentration in sediment (±0.4 to ±0.6), whereas a weak positive relationship was found for water. Likewise, a moderate correlation between microplastic concentrations in both environments and particle characteristics, including particle size (a) and shape factor (φ), was found. Compared to particle size and shape, a weaker correlation was found between particle density (ρ_p) and model results. As expected, a negative correlation was observed between particle characteristics (size, density, shape factor) and microplastic levels in water, while this was positive for those in the sediment. On the other hand, the correlations between initial concentrations in the water column and model outcomes were very weak. Additionally, a strong negative correlation was found between microplastic concentrations in water and sediment.

Uncertainty analysis indicated that the model results for water were mostly affected by φ amongst the stochastic parameters, followed by a, ρ_p, z and C_0. On the other hand, the uncertainties of sediment microplastic levels were mostly affected by a, followed by φ, z, ρ_p and C_0. However, more significant correlations were found between stochastic parameters and microplastic levels in

sediment, particularly for z, a and ρ_p, which can be attributed to the fact that uncertainties of these parameters have a higher influence on the model outcomes for sediment, increasing variances (or uncertainties) in the predicted results for sediment. The fact that the model results for water were less affected by the relevant stochastic parameters can be due to the effect of river velocity ($\bar{u} + u'$) on microplastic transport in this environment. While settling velocity ($\omega_s + v'$) is affected by several stochastic parameters, such as particle characteristics and z, the river velocity is only affected by the uncertainties in z. However, according to the uncertainty analysis, z had a higher impact on the model results for sediment because of its relationship with bed shear stress, which plays an important role in particle resuspension. These findings mean that the lack of knowledge and errors regarding shape factor and particle size will affect the model results more than the other stochastic parameters. Evidently, it becomes important to assign accurate values to the parameters that have significant correlation with the model results.

In addition, the sensitivity of the model to input parameters was determined by one-at-a-time parameter sensitivity analysis. This method is based on changing one parameter at a time, while holding the others fixed. The model responses to change in input parameters including d, S, D_{84}, μ, $\tau_{cr}{}^*$, φ, a, $(\rho_p - \rho_w)$ and C_0 were investigated. The value of each parameter was changed from -50% to +50% by 10% increments of its calibration value. Only ρ_p and ρ_w were changed in the range of ±10% and ±0.4%, respectively, to assign reasonable values corresponding to real data. The percentage variations of microplastic concentrations in water and sediment were simulated and discussed below. The results of sensitivity analyses on the above parameters are shown from Figures 4.22 to 4.31.

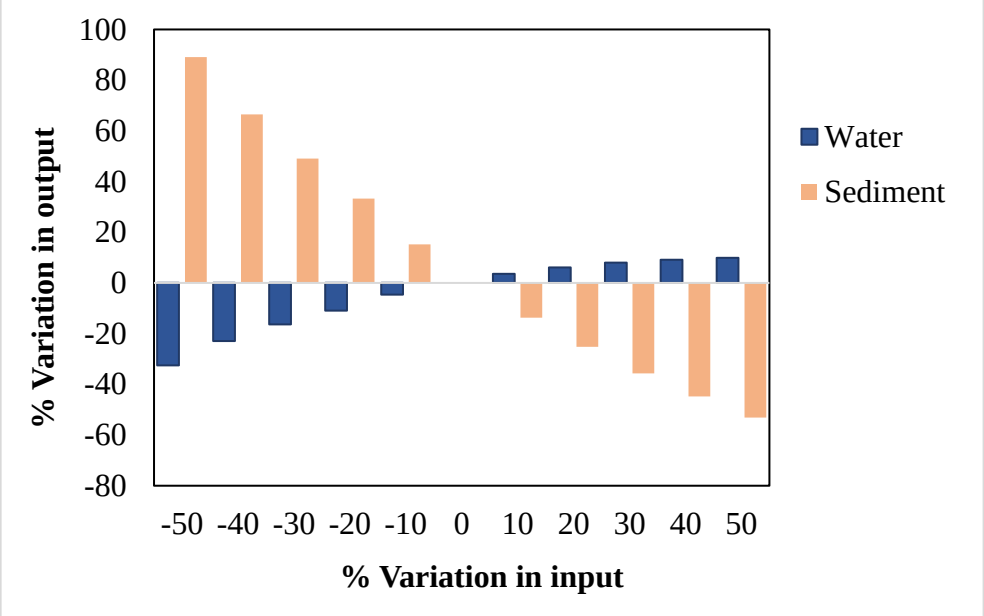

Figure 4.22. Sensitivity of microplastic concentration on d.

The results of sensitivity analysis on depth (*d*) suggested a positive relationship between microplastic concentrations in water and *d* (Figure 4.22). This result is consistent with the result of Pearson correlation test investigating the relationship between river depth (*d*) and microplastic abundance in water. As discussed in Section 4.2, microplastic concentrations are higher in deeper waters by the influence of increased bed shear stress and elevated levels of turbulence that increase the resuspension of particles back to the water column. This also leads to lower deposition of microplastics onto the sediments. The results of sensitivity analysis also confirmed that microplastic concentrations in sediment had an inverse relationship with *d*, yet they were more sensitive to changes in *d* compared to water. This was an expected outcome as according to the model developed here, microplastic concentration in water depended on both river flow and vertical transport of the particles, while there were no mechanisms other than settling and resuspension in for the sediment compartment.

As slope (*S*) increases, river velocity increases, so the particles in water move towards the downstream of river by advective flow, hence deposition onto the sediment in that location decreases. According to Figure 4.23, microplastic concentrations both in water and sediment increased with decreasing *S*, but concentrations in water was not very sensitive to the increasing *S*, whereas microplastic concentration in sediment exhibited more sensitivity to increasing values of *S*. This can be attributed to the fact that higher *S* increases not only velocity, but also bed shear stress (Equation 3.21), which results in remobilization of sediment particles and lower concentrations of microplastics in those environments.

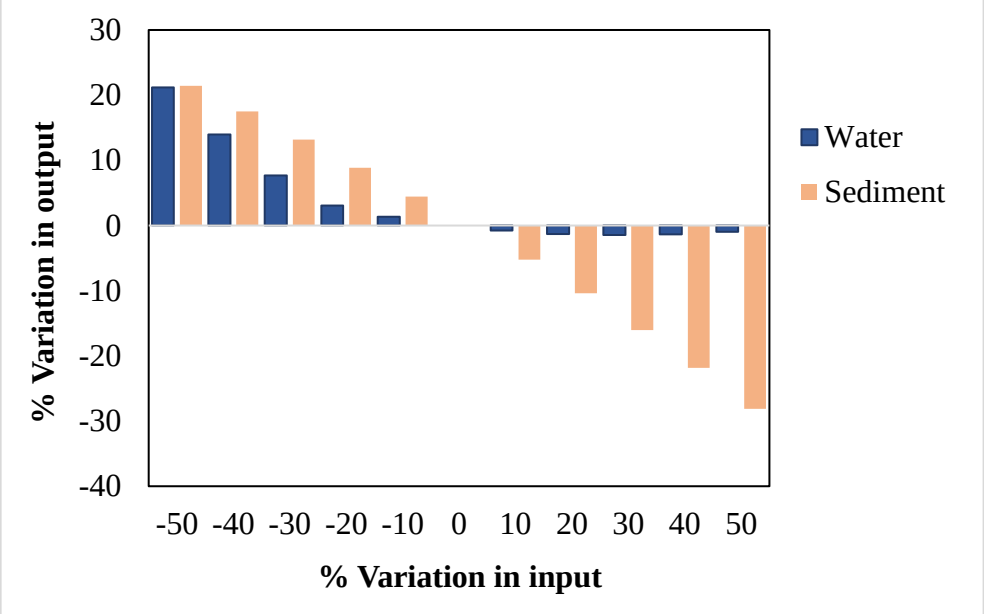

Figure 4.23. Sensitivity of microplastic concentration on *S*.

S was also used as calibration data in this study. According to the parameter sensitivity analysis, *S* is a significant parameter, and it is essential to assign accurate values to *S* to increase the reliability of the model. In this respect, model calibration was performed by making minor changes to the *S* values determined from GIS for each site to provide the best approximations for these values.

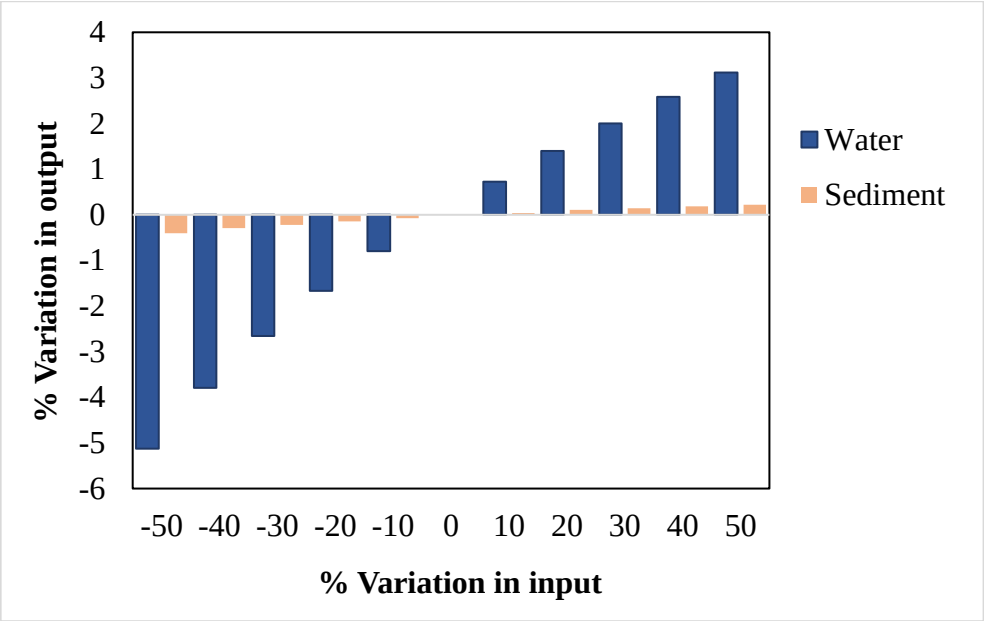

Figure 4.24. Sensitivity of microplastic concentration on D_{84}.

The results of sensitivity analysis on D_{84} indicated that the model was not very sensitive to the changes in D_{84}, yet there was a clearer positive linear relationship between microplastic concentrations in water and D_{84}, while sediment microplastic concentrations were not affected (Figure 4.24). D_{84} is another calibration data of the model developed here, but does not have a significant effect on the model outcomes.

The results obtained from sensitivity analysis on viscosity (μ) suggested that microplastic concentrations in water was slightly sensitive to the changes in μ and they increased with increasing μ (Figure 4.25). In contrast, model for the sediment compartment was quite sensitive to the changes in μ, having an inverse relationship. It is known that μ directly affects the drag force on a particle. Moreover, this relationship can mathematically be explained by Dietrich's (1982) equation given in Equation 3.1, which reveals that the higher the viscosity, the lower the settling velocity and accumulation of particles in the sediment.

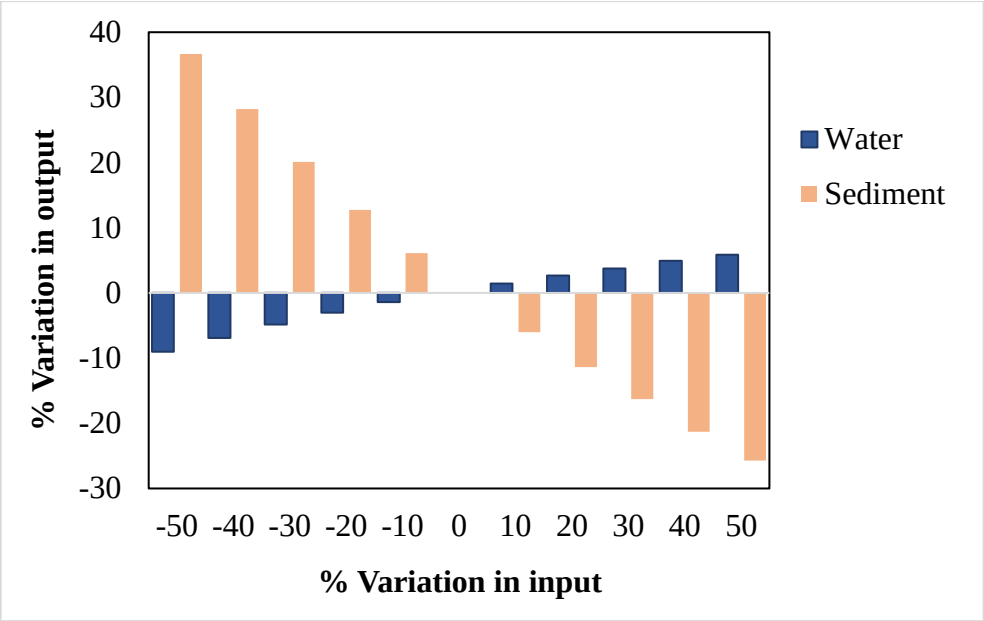

Figure 4.25. Sensitivity of microplastic concentration on μ.

Dimensionless critical shear stress ($\tau_{cr}{}^{*}$) is a parameter that directly affects the critical shear stress. Equation 3.14 represents this relationship mathematically. The critical shear stress is significant in vertical transport of particles, since once bed shear stress exceeds critical shear stress, the particles within the sediment compartment begin to be resuspended (Kumar et al., 2021; Waldschläger & Schüttrumpf, 2019). Congruently, Figure 4.26 indicated that higher values of $\tau_{cr}{}^{*}$ caused an increase in microplastic concentrations in the sediment; and therefore, decreased in the water column. This can be explained by the microplastics remaining in the sediment compartment due to lower resuspension.

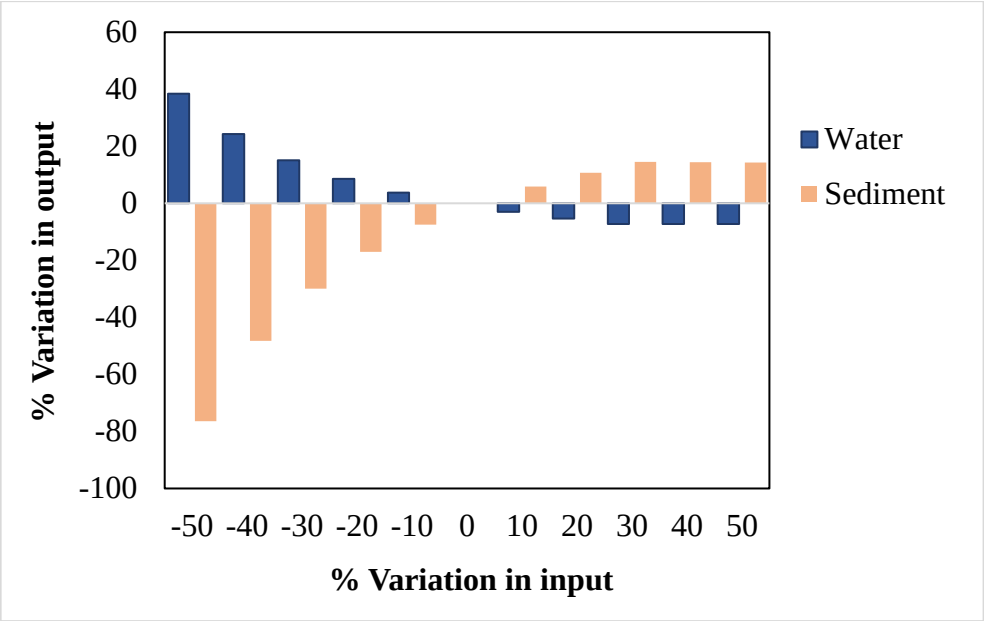

Figure 4.26. Sensitivity of microplastic concentration on $\tau_{cr}{}^{*}$.

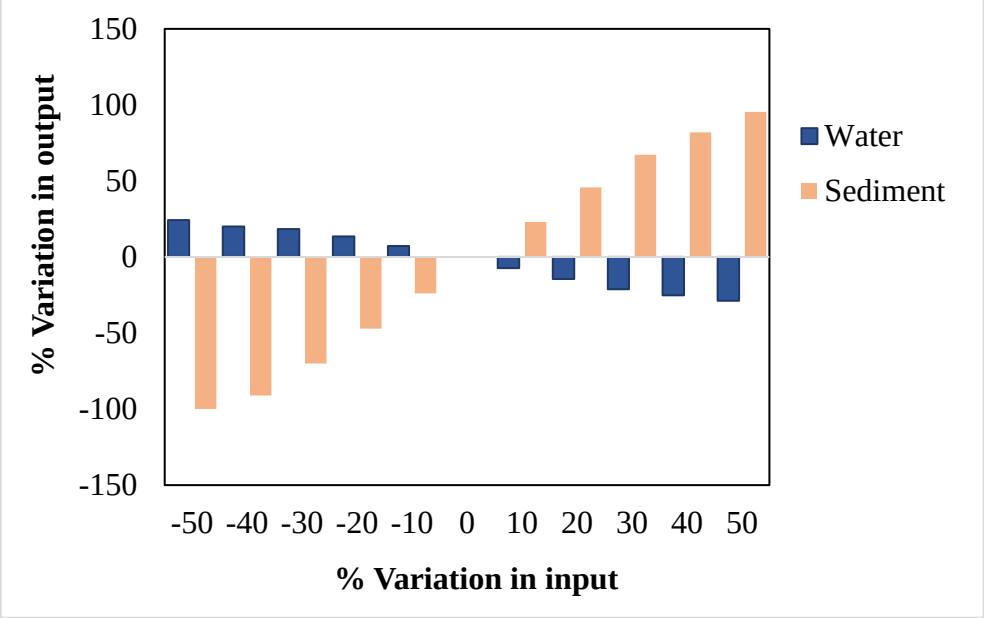

Figure 4.27. Sensitivity of microplastic concentration on φ.

Figure 4.27 demonstrates the sensitivity of the model to the changes in shape factor (φ). Here, higher values of φ represent higher sphericity of microplastics. Scenario analyses in this study as well as previous research have indicated that spherical particles have greater settling velocities than irregular-shaped ones (Wang et al., 2021b). In this respect, an increase in microplastic concentrations in the sediment with increasing φ and consequently inverse linear relationship with concentrations in water could be expected. However, φ directly affects microplastic levels in the sediment due to being effective on settling behavior of microplastics. Therefore, concentrations in sediment are more sensitive to the changes in φ compared to the model outcomes in the water.

Similar to particle shape, particle size (a) also governs the settling of microplastics. The model response to the changes in a is shown in Figure 4.28.

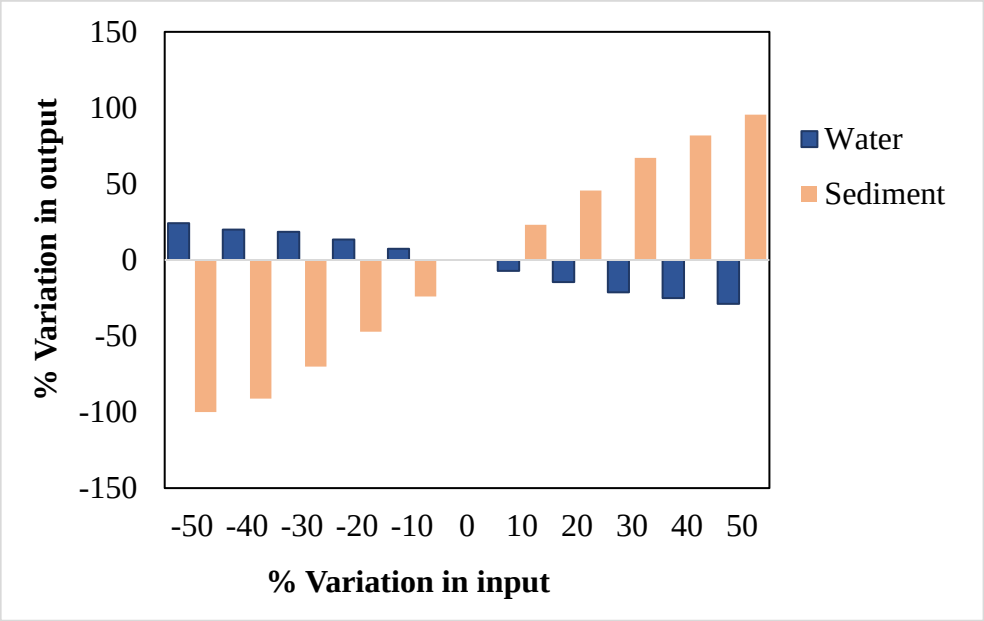

Figure 4.28. Sensitivity of microplastic concentration on a.

The results of sensitivity analysis on a revealed that a had the same influence as φ on the model results, probably due to the equal weights of both a and φ in calculation of nominal diameter (D_n), represented in Equation 3.8 in this study.

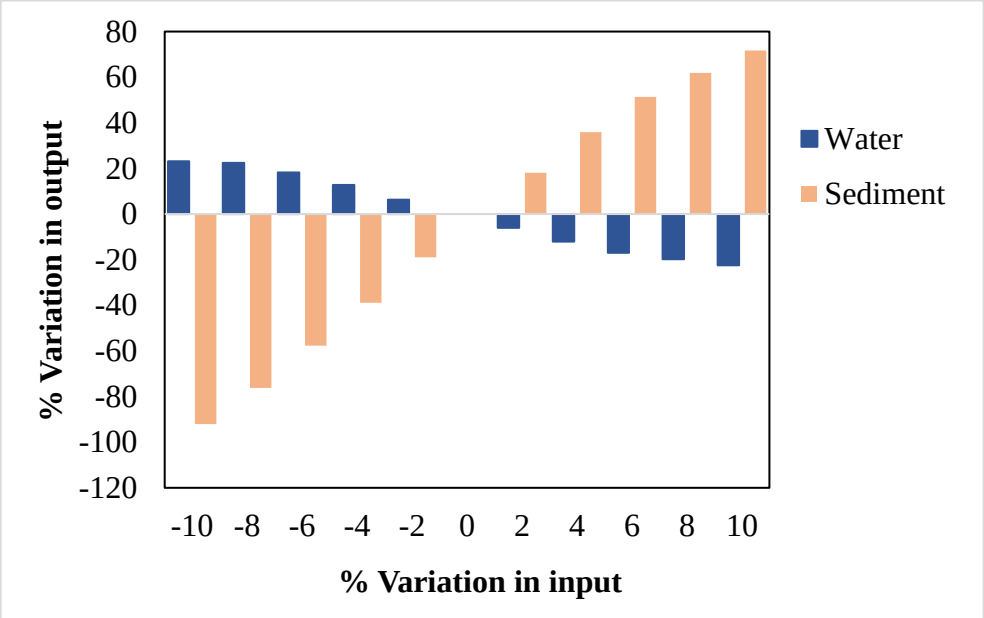

Figure 4.29. Sensitivity of microplastic concentration on ρ_p.

Figure 4.29 demonstrates the variations in the model outcomes with the changes in particle density (ρ_p). According to the figure, microplastic concentrations in water decreased with increasing ρ_p, whilst there was a positive linear relationship between sediment microplastic levels and ρ_p. Although the values of ρ_p were changed from -10% to +10% by 2% increments, the sensitivity of microplastic concentrations both in water and sediment to the changes in ρ_p can clearly be seen in the relevant graph. These outcomes are not surprising since polymer density and particle size are commonly accepted as primary controls on the settling behavior of microplastics (Elagami et al., 2022). In addition to particle characteristics, ambient conditions are also critical in fate and transport of these particles. In aquatic environments, both polymer and water density directly affect the gravitational force on a particle. Moreover, the density of freshwater can reach up to 1026 kg m^{-3}, especially in estuarine environments (Millero, 1984). From this viewpoint, apart from river's morphological parameters discussed above, the influence of variations in water density (ρ_w) on model outcomes was also investigated, changing the values of ρ_w in the range of ±0.4% by 0.1% increments of its calibration value (Figure 4.30). In contrast to ρ_p, there was a positive linear relationship between ρ_w and microplastic concentrations in water, as expected. Nevertheless, the results revealed a negative linear relationship between ρ_w and sediment microplastic levels.

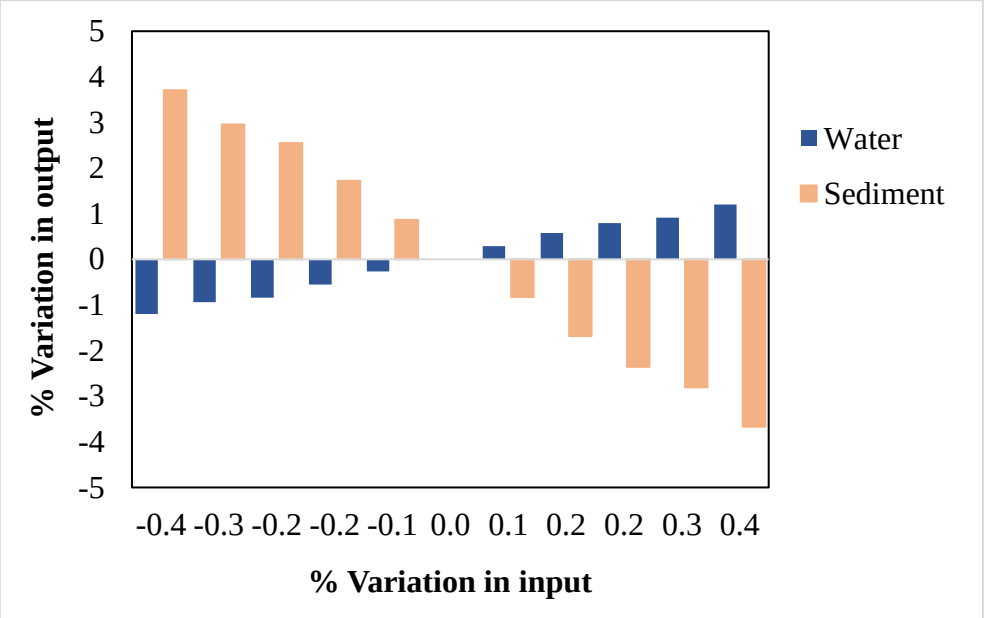

Figure 4.30. Sensitivity of microplastic concentration on ρ_w.

The influence of initial concentration of microplastics in the water column (C_0) on model outcomes are shown in Figure 4.31. C_0 affected microplastic concentrations significantly, and presumably, their high values resulted in higher levels of microplastics in both water and sediment.

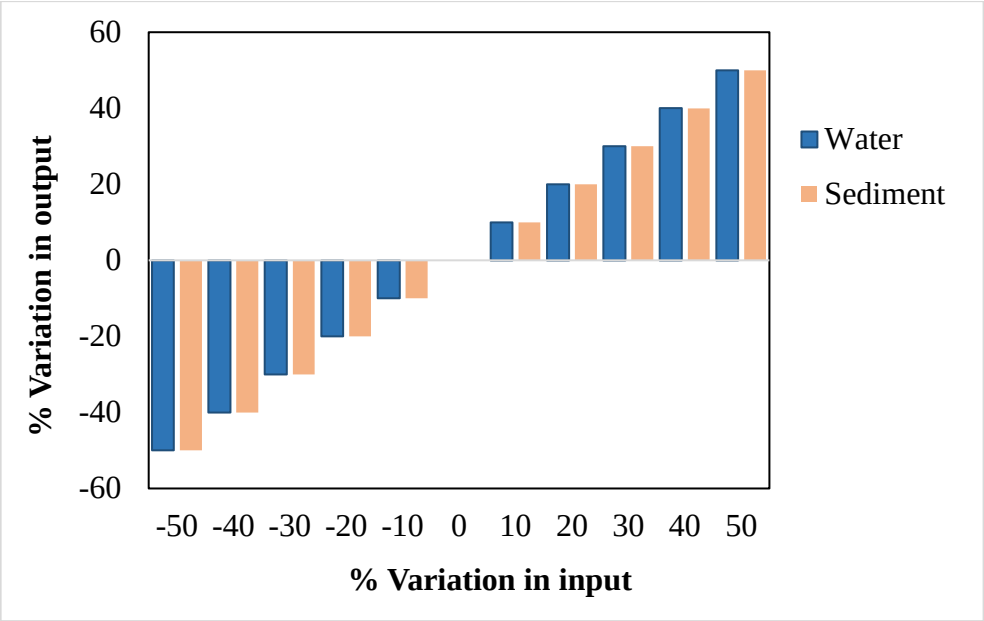

Figure 4.31. Sensitivity of microplastic concentration on C_0.

The sensitivity ranking of the parameters was determined by calculating the ratio of variation (ROV), given in Equation 3.33, for each parameter. The calculations of sensitivity analysis are given in Appendix F from Table F.1 to Table F.4. The sensitivity ranking of the model parameters is given in Table 4.7 in the order of importance.

Table 4.7. Sensitivity ranking of the parameters.

Sensitivity ranking	**Microplastic concentration**	
	Water	**Sediment**
1	$\rho_p - \rho_w$	$\rho_p - \rho_w$
2	C_0	φ and a
3	φ and a	d
4	d	C_0
5	${\tau_{cr}}^*$	${\tau_{cr}}^*$
6	S	μ
7	μ	S
8	D_{84}	D_{84}

According to Table 4.7, the microplastic concentrations both in water and sediment was most sensitive to the changes in $(\rho_p - \rho_w)$. As given in Stokes' equation (Equation 3.1), the gravitational force on a particle is directly affected by both ρ_w and ρ_p. Moreover, the other parameters related to particle characteristics, including φ and a were more significant for microplastic levels in sediment than in water. On the other hand, model results both in water and sediment were less influenced by changes in D_{84}. This importance ranking of input parameters, can aid to assign accurate values during model calibration.

5. CONCLUSIONS AND RECOMMENDATIONS

This study investigates the spatiotemporal distribution of microplastics in surface water and sediment of an industrially polluted river (i.e. the Ergene River, Turkey). According to the results, water samples had an overall average concentration of 4.65 ± 2.06 and 6.90 ± 5.16 items L^{-1} (mean ± standard deviation, n = 12) for the May 2019 and September 2020 periods, respectively, while those were 97.90 ± 71.72 and 277.76 ± 207.21 items kg^{-1} (n = 18) for sediment samples, respectively. Statistical analyses suggested a moderately positive correlation between microplastic levels in water and stream depth, whilst a moderately negative correlation was found between microplastic abundance and channel width. Fibers were found to be the dominant shape both in water (88%) and sediment samples (70%). In total, medium-sized microplastics ranging between 1000 to 2000 μm (38%) were found as the most abundant particles in surface water, whilst the dominant size range was 45-1000 μm (55%) in sediment. The majority of the particles were black, which constituted 49% and 39% of all microplastics detected in water and sediment, respectively. According to the Raman analysis, most of the particles were PET (28%) and PA (27%) in water samples, while PS (56%) were dominating the sediment samples.

Rivers are both transport pathways and sinks of microplastics. This study focuses on the upstream of the Ergene River, an area of intensive industrialization, being close to the potential sources of microplastics (e.g. OIZs and WWTPs). Compared with the microplastic levels in other rivers (e.g. Yangtze, China and Mersin rivers, Turkey), Ergene River has excessive levels of microplastics, especially the upstream being a significant source of microplastic pollution. Domestic sewage and effluents of various industries, especially textile, are the main contributors of microplastics in the study area. Agricultural plastics, anthropogenic litters and other industrial effluents, such as plastic, machinery and automotive are also sources of microplastics, particularly in the form of fragments. Evidently, more comprehensive and holistic research should be adopted to determine the exact contribution of each source to the total amount of microplastics in the study site. Future work should undertake a more intensive sampling scheme to determine the characteristics of microplastics from both point and non-point sources. In this context, accurate and effective management strategies, such as improved treatment technologies and waste management strategies can be developed for mitigation of microplastics in the Ergene River. It should be noted that in this thesis, no significant spatiotemporal changes were observed in the flow rates of six different sampling locations. Thus, longer-term sampling and on-site measurements are required to monitor differences in flow conditions and exactly understand the influence of flow rate on microplastic concentrations

in rivers. Further research should also investigate the source-to-sink variation of microplastics to precisely understand microplastic levels along the Ergene River and riverine loading to the sea.

The model results revealed that the residence time of microplastics in the water column was directly related to the flow characteristics and river hydraulics, rather than microplastic concentration. On the other hand, the settling and resuspension fluxes had a direct relationship with microplastic initial concentrations, which means that initial concentrations dominate the settling velocity of microplastics. The model fitted well with previous studies in prediction of settling velocities of near-spherical particles and fragments, whilst a weak relationship was found with the results of experimental studies and this study for fibers. According to the scenario analysis, settling and resuspension fluxes of microplastics increased with increasing sphericity and size of the particles. In addition, higher bed shear stress resulted in increased settling and resuspension fluxes of the particles. The model results for water and sediment were most sensitive to the changes in difference between ρ_p and ρ_w, whilst D_{84} was the least significant parameter affecting model results both for water and sediment.

In conclusion, these results suggest that the mechanistic model developed here is successful in

(i) simulating probable distribution of fragments and near-spherical microplastics in the water column and sediment and
(ii) understanding the settling and resuspension mechanisms of microplastics in turbulent flow conditions.

It is worth noting that in this study, an approximation was developed to determine settling velocities of different shaped microplastics by defining a shape factor. Although such an approximation is inevitable for theoretical models due to lack of data, the model developed in this study was found to be statistically sensitive to φ. Therefore, experimental work should be implemented to improve φ and obtain more accurate results in future studies. Also, the model can be improved by considering the processes, such as biofilm, homo- and hetero-aggregation, and degradation of plastic particles.

According to these results, the areas that merits further investigation can be summarized as the following:

(i) Undertaking a more intensive sampling scheme to determine the characteristics of microplastics from both point and non-point sources to determine the exact contribution of each source.

(ii) Implementing the longer-term continuous sampling and on-site measurements to monitor remarkable changes in river flow and exactly understand the effect of different flow conditions on microplastic concentrations in rivers.

(iii) Monitoring source-to-sink variation of microplastics along the Ergene River to understand riverine loading to the sea.

(iv) Implementing experimental work or more advanced methodologies to improve φ developed for the modeling approach here.

(v) Considering the processes, such as biofilm formation, homo- and hetero-aggregation, and degradation of plastic particles to improve the modeling approach developed here.

According to the results here, it is likely that microplastic abundance is correlated with proximity to particular industry, wastewater discharges and land use practices within a watershed. The literature review undertaken in this thesis addressed that one of the most understudied areas of microplastics is watershed-based research practices. Although presence of microplastics in water, land and air has been demonstrated, these environments are commonly considered independently, but in reality, are closely linked. Studying the particle behaviors and transport mechanisms of microplastics between these environmental compartments can aid in understanding how and where microplastics will accumulate. The occurrence of microplastics in rivers has received attention over the last years, but there is a lack of research linking the sources, such as surface runoff, and sinks. This is necessary to assess the risks associated with microplastic concentrations. So, it would be very useful for future researchers to focus on the sources, sinks and transport of these emerging pollutants on watershed scale. Indeed, field studies in combination with integrated watershed modeling and risk mapping would provide valuable insights for understanding the issues governing microplastic accumulation in soil and water. Consequently, future studies should focus on filling these research gaps and developing novel modeling approaches to assess microplastic occurrence, fate and transport in the environment.

REFERENCES

Akarsu, C., Kumbur, H., Gökdağ, K., Kıdeyş,, A.E., & Sanchez-Vidal, A. (2020). Microplastics composition and load from three wastewater treatment plants discharging into Mersin Bay, north eastern Mediterranean Sea. *Marine Pollution Bulletin*, *150*, 110776 https://doi.org/10.1016/J.MARPOLBUL.2019.110776

Akdogan, Z., & Guven, B. (2019). Microplastics in the environment: A critical review of current understanding and identification of future research needs. *Environmental Pollution*, *254*, 113011. https://doi.org/10.1016/j.envpol.2019.113011

Akdogan, Z., Guven, B., & Kideys, A.E. (2023). Microplastic distribution in the surface water and sediment of the Ergene River. *Environmental Research*, *234*, 116500. https://doi.org/10.1016/j.envres.2023.116500

Alam, F.C., Sembiring, E., Muntalif, B.S., & Suendo, V. (2019). Microplastic distribution in surface water and sediment river around slum and industrial area (case study: Ciwalengke River, Majalaya district, Indonesia). *Chemosphere*, *224*, 637–645. https://doi.org/10.1016/J.CHEMOSPHERE.2019.02.188

Ameta, R., Chohadia, A.K., Jain, A., & Punjabi, P.B. (2018). Fenton and photo-fenton processes. In S. C, Ameta, & R, Ameta (Eds.). *Advanced oxidation processes for waste water treatment: Emerging green chemical technology* (1st ed., pp. 49–87). Retrieved from https://doi.org/10.1016/B978-0-12-810499-6.00003-6

Amrutha, K., & Warrier, A.K. (2020). The first report on the source-to-sink characterization of microplastic pollution from a riverine environment in tropical India. *Science of the Total Environment*, *739*, 140377. https://doi.org/10.1016/j.scitotenv.2020.140377

An, L., Liu, Q., Deng, Y., Wu, W., Gao, Y., & Ling, W. (2020). Sources of microplastic in the environment. In D, He, & Y, Luo (Eds.). *Microplastics in terrestrial environments: the handbook of environmental chemistry* (1st ed., pp. 143-159). Cham, Switzerland: Springer. https://doi.org/10.1007/698_2020_449

Andrady, A.L. (2011). Microplastics in the marine environment. *Marine Pollution Bulletin, 62*(8), 1596–1605. https://doi.org/10.1016/j.marpolbul.2011.05.030

Bagaev, A., Mizyuk, A., Khatmullina, L., Isachenko, I., & Chubarenko, I. (2017). Anthropogenic fibres in the Baltic Sea water column: Field data, laboratory and numerical testing of their motion. *Science of the Total Environment, 599,* 560-571. https://doi.org/10.1016/j.scitotenv.2017.04.185

Baldwin, A.K., Corsi, S.R., & Mason, S.A. (2016). Plastic debris in 29 great lakes tributaries: relations to watershed attributes and hydrology. *Environmental Science & Technology, 50*(19), 10377-10385. https://doi.org/10.1021/acs.est.6b02917

Ballent, A., Corcoran, P.L., Madden, O., Helm, P.A. & Longstaffe, F.J. (2016). Sources and sinks of microplastics in Canadian Lake Ontario nearshore, tributary and beach sediments. *Marine Pollution Bulletin, 110*(1), 383–395. https://doi.org/10.1016/j.marpolbul.2016.06.037

Bashir, S.M., Kimiko, S., Mak, C.W., Fang, J.K.H., & Gonçalves, D. (2021). Personal care and cosmetic products a potential source of environmental contamination by microplastics in a densely populated Asian city. *Frontiers in Marine Science, 8,* 683482 https://doi.org/10.3389/fmars.2021.683482

Beck, M. B., & Finney, B. A. (1987). Operational water quality management: problem context and evaluation of a model for river quality. *Water Resources Research, 23*(11), 2030–2042. https://doi.org/10.1029/WR023i011p02030

Bellas, J., Martínez-Armental, J., Martínez-Cámara, A., Besada, V., & Martínez- Gómez, C. (2016). Ingestion of microplastics by demersal fish from the Spanish Atlantic and Mediterranean coasts. *Marine Pollution Bulletin, 109*(1), 55-60. https://doi.org/10.1016/j.marpolbul.2016.06.026

Besseling, E., Quik, J.T.K., Sun, M., & Koelmans, A.A. (2017). Fate of nano- and microplastic in freshwater systems: A modeling study. *Environmental Pollution, 220,* 540–548. https://doi.org/10.1016/j.envpol.2016.10.001

Bondelind, M., Sokolova, E., Nguyen, A., Karlsson, D., Karlsson, A., & Björklund, K. (2020). Hydrodynamic modelling of traffic-related microplastics discharged with stormwater into the Göta River in Sweden. *Environmental Science and Pollution Research, 27,* 24218–24230.

https://doi.org/10.1007/s11356-020-08637-z

Born, M.P., Brü, C., Schaefer, D., Hillebrand, G., & Schü, H. (2023). Determination of microplastics' vertical concentration transport (rouse) profiles in flumes. *Environmental Science & Technology*, *57*(14), 5569–5579. https://doi.org/10.1021/acs.est.2c06885

Bowmer, T., & Kershaw, P. (2010). *Proceedings of the GESAMP international workshop on micro-plastic particles as a vector in transporting persistent, bio-accumulating and toxic substances in the oceans*. Paris, France: UNESCO-IOC

Brennecke, D., Ferreira, E.C., Costa, T.M.M., Appel, D., da Gama, B.A.P., & Lenz, M. (2015). Ingested microplastics (>100mm) are translocated to organs of the tropical fiddler crab *Uca rapax*. *Marine Pollution Bulletin*, *96*(1-2), 491-495. https://doi.org/10.1016/10.1016/j.marpolbul.2015.05.001

Browne, M.A., Dissanayake, A., Galloway, T.S., Lowe, D.M., & Thompson, R.C. (2008). Ingested microscopic plastic translocates to the circulatory system of the mussel, *Mytilus edulis* (L.). *Environmental Science & Technology*, *42*(13), 5026-5031. https://doi.org/10.1021/es800249a

Browne, M.A., Crump, P., Niven, S.J., Teuten, E., Tonkin, A., Galloway, T., & Thompson, R. (2011). Accumulation of microplastic on shorelines worldwide: Sources and sinks. *Environmental Science & Technology*, *45*(21), 9175-9179. https://doi.org/10.1021/es201811s

Bullard, J.E., Ockelford, A., O'Brien, P., & McKenna Neuman, C. (2021). Preferential transport of microplastics by wind. *Atmospheric Environment*, *245*, 118038. https://doi.org/10.1016/j.atmosenv.2020.118038

Buzzini, P., & Massonnet, G. (2015). The analysis of colored acrylic, cotton, and wool textile fibers using micro-Raman spectroscopy. Part 2: comparison with the traditional methods of fiber examination. *Journal of Forensic Sciences*, *60*(3), 712–720. https://doi.org/10.1111/1556-4029.12654

Cai, L., Wang, J., Peng, J., & Chen, Q. (2017). Characteristic of microplastics in the atmospheric fallout from Dongguan city, China: preliminary research and first evidence. *Environmental Science and Pollution Research*, *32*, 24928-24935. https://doi.org/10.1007/s11356-017-0116-x

Castaneda, R.A., Avlijas, S., Simard, M.A., & Ricciardi, A. (2014). Microplastic pollution in St. Lawrence river sediments. *Canadian Journal of Fisheries and Aquatic Sciences*, *71*(12), 1767-1771. https://doi.org/10.1139/cjfas-2014-0281

Chapra, S. C. (1997). *Surface water-quality modeling*. Illinois, USA: Waveland Press

Chen, J., Wu, J., Sherrell, P.C., Chen, J., Wang, H., Zhang, W.X., & Yang, J. (2022). How to build a microplastics-free environment: strategies for microplastics degradation and plastics recycling. *Advanced Science*, *9*(6), 2103764. https://doi.org/10.1002/advs.202103764

Chen, Q., Gundlach, M., Yang, S., Jiang, J., Velki, M., Yin, D., & Hollert, H. (2017). Quantitative investigation of the mechanisms of microplastics and nanoplastics toward zebrafish larvae locomotor activity. *Science of the Total Environment*, *584*-585, 1022–1031. https://doi.org/10.1016/j.scitotenv.2017.01.156

Chikwendu, S.C. (1986). Application of a slow-zone model to contaminant dispersion in laminar shear flows. *International Journal of Engineering Science*, *24*(6), 1031–1044. https://doi.org/10.1016/0020-7225(86)90034-0

Chow, V.T. (1959). *Open-channel hydraulics*. New York, USA: McGraw-Hill

Chua, E.M., Shimeta, J., Nugegoda, D., Morrison, P.D., & Clarke, B.O. (2014). Assimilation of polybrominated diphenyl ethers from microplastics by the marine amphipod, *Allorchestes compressa*. *Environmental Science & Technology*, *48*(14), 8127-8134. https://doi.org/10.1021/es405717z

Chubarenko, I., & Stepanova, N. (2017). Microplastics in sea coastal zone: lessons learned from the Baltic amber. *Environmental Pollution*, *224*, 243-254. https://doi.org/10.1016/j.envpol.2017.01.085

Claessens, M., Meester, S.D., Landuyt, L. V., Clerck, K.D., & Janssen, C.R. (2011). Occurrence and distribution of microplastics in marine sediments along the Belgian coast. *Marine Pollution Bulletin*, *62*(10), 2199-2204. https://doi.org/10.1016/j.marpolbul.2011.06.030

Claessens, M., Van Cauwenberghe, L., Vandegehuchte, M.B., & Janssen, C.R. (2013). New techniques for the detection of microplastics in sediments and field collected organisms. *Marine Pollution Bulletin*, *70*(1–2), 227–233. https://doi.org/10.1016/J.MARPOLBUL.2013.03.009

Cole, M., Lindeque, P., Halsband, C., & Galloway, T.S. (2011). Microplastics as contaminants in the marine environment: a review. *Marine Pollution Bulletin, 62*(12), 2588–2597. https://doi.org/10.1016/j.marpolbul.2011.09.025

Cook, S., Chan, H.L., Abolfathi, S., Bending, G.D., Schäfer, H., & Pearson, J.M. (2020). Longitudinal dispersion of microplastics in aquatic flows using fluorometric techniques. *Water Research, 170*, 115337. https://doi.org/10.1016/J.WATRES.2019.115337

Corcoran, P.L., Biesinger, M.C., & Grifi, M. (2009). Plastics and beaches: A degrading relationship. *Marine Pollution Bulletin, 58*(1), 80–84. https://doi.org/10.1016/J.MARPOLBUL.2008.08.022

Corcoran, P.L., Norris, T., Ceccanese, T., Walzak, M.J., Helm, P.A., & Marvin, C.H. (2015). Hidden plastics of Lake Ontario, Canada and their potential preservation in the sediment record. *Environmental Pollution, 204*, 17-25. https://doi.org/10.1016/j.envpol.2015.04.009

Cordova, M.R., Nurhati, I.S., Shiomoto, A., Hatanaka, K., Saville, R., & Riani, E. (2022). Spatiotemporal macro debris and microplastic variations linked to domestic waste and textile industry in the supercritical Citarum River, Indonesia. *Marine Pollution Bulletin, 175*, 113338. https://doi.org/10.1016/J.MARPOLBUL.2022.113338

Cózar, A., Echevarría, F., Ignacio González-Gordillo, J., Irigoien, X., Úbeda, B., Hernández-León, S., Palma, Á.T., Navarro, S., García-De-Lomas, J., Ruiz, A., Fernández-De-Puelles, M.L., & Duarte, C.M. (2011). Plastic debris in the open ocean. *PNAS, 111*(28), 10239–10244. https://doi.org/10.1073/pnas.1314705111

Critchell, K., & Lambrechts, J. (2016). Modelling accumulation of marine plastics in the coastal zone; what are the dominant physical processes? *Estuarine, Coastal and Shelf Science, 171*, 111-122. https://doi.org/10.1016/j.ecss.2016.01.036

Dalla Fontana, G., Mossotti, R., & Montarsolo, A. (2020). Assessment of microplastics release from polyester fabrics: the impact of different washing conditions. *Environmental Pollution, 264*, 113960. https://doi.org/10.1016/J.ENVPOL.2020.113960

Daniel, D.B., Thomas, S.N., & Thomson, K.T. (2020). Assessment of fishing-related plastic de- bris along the beaches in Kerala Coast, India. *Marine Pollution Bulletin, 150*, 110696

https://doi.org/10.1016/j.marpolbul.2019.110696

Davarpanah, E., & Guilhermino, L. (2015). Single and combined effects of microplastics and copper on the population growth of the marine microalgae *Tetraselmis chuii*. *Estuarine, Coastal and Shelf Science, 167*(Part A), 269-275. https://doi.org/10.1016/j.ecss.2015.07.023

de Sá, L.C., Luís, L.G., & Guilhermino, L. (2015). Effects of microplastics on juveniles of the common goby (Pomatoschistus microps): confusion with prey, reduction of the predatory performance and efficiency, and possible influence of developmental conditions. *Environmental Pollution, 196*, 359-362. https://doi.org/10.1016/j.envpol.2014.10.026

Deng, H., Wei, R., Luo, W., Hu, L., Li, B., Di, Y., & Shi, H. (2020). Microplastic pollution in water and sediment in a textile industrial area. *Environmental Pollution, 258*, 113658. https://doi.org/10.1016/J.ENVPOL.2019.113658

Derraik, J.G.B. (2002). The pollution of the marine environment by plastic debris: a review. *Marine Pollution Bulletin*, *44*(9), 842–852. https://doi.org/10.1016/S0025-326X(02)00220-5

Desforges, J.P.W., Galbraith, M., & Ross, P.S. (2015). Ingestion of microplastics by zooplankton in the Northeast Pacific Ocean. *Archives of Environmental Contamination and Toxicology*, *69*, 320-330. https://doi.org/10.1007/s00244-015-0172-5

Devriese, L.I., De Witte, B., Vethaak, A.D., Hostens, K., & Leslie, H.A. (2017). Bioaccumulation of PCBs from microplastics in Norway lobster (*Nephrops norvegicus*): an experimental study. *Chemosphere, 186*, 10-16. https://doi.org/10.1016/j.chemosphere.2017.07.121

Dietrich, W.E. (1982). Settling velocity of natural particles. *Water Resources Research*, *18*(6), 1615−1626. https://doi.org/10.1029/WR018i006p01615

Dris, R., Gasperi, J., Rocher, V., & Tassin, B. (2018). Synthetic and non-synthetic anthropogenic fibers in a river under the impact of Paris megacity: sampling methodological aspects and flux estimations. *Science of the Total Environment, 618*, 157–164. https://doi.org/10.1016/j.scitotenv.2017.11.009

Dris, R., Gasperi, J., Rocher, V., Saad, M., Renault, N. & Tassin, B. (2015). Microplastic

contamination in an urban area: a case study in Greater Paris. *Environmental Chemistry*, *12*, 592-599. https://doi.org/10.1071/EN14167

Dris, R., Gasperi, J., Saad, M., Mirande, C. & Tassin, B. (2016). Synthetic fibers in atmospheric fallout: a source of microplastics in the environment? *Marine Pollution Bulletin*, *104*(1-2), 290-293. https://doi.org/10.1016/j.marpolbul.2016.01.006

Dubaish, F., & Liebezeit, G. (2013). Suspended microplastics and black carbon particles in the jade system, southern North Sea. *Water, Air, & Soil Pollution, 224*, 1352. https://doi.org/10.1007/s11270-012-1352-9

Dubus, I.G., Brown, C.D., & Beulke, S. (2003). Sensitivity analyses for four pesticide leaching models. *Pest Management Science, 59*(9), 962-982. https://doi.org/10.1002/ps.723

Duis, K., & Coors, A. (2016). Microplastics in the aquatic and terrestrial environment: sources (with a specific focus on personal care products), fate and effects. *Environmental Sciences Europe*, *28*, 2. https://doi.org/10.1186/s12302-015-0069-y

Dumichen, E., Eisentraut, P., Bannick, C.G., Barthel, A.K., Senz, R., & Braun, U. (2017). Fast identification of microplastics in complex environmental samples by a thermal degradation method. *Chemosphere*, *174*, 572-584. https://doi.org/10.1016/j.chemosphere.2017.02.010

Elagami, H., Ahmadi, P., Fleckenstein, J.H., Frei, S., Obst, M., Agarwal, S., & Gilfedder, B.S. (2022). Measurement of microplastic settling velocities and implications for residence times in thermally stratified lakes. *Limnology and Oceanography*, *67*(4), 934–945. https://doi.org/10.1002/lno.12046

Elder, J.W. (1959). The dispersion of marked fluid in turbulent shear flow. *Journal of Fluid Mechanics, 5*(4), 544–560. https://doi.org/10.1017/S0022112059000374

Enders, K., Lenz, R., Beer, S., & Stedmon, C.A. (2017). Extraction of microplastic from biota: recommended acidic digestion destroys common plastic polymers. *ICES Journal of Marine Science*, *74*(1), 326–331. https://doi.org/10.1093/icesjms/fsw173

Enders, K., Lenz, R., Stedmon, C.A., & Nielsen, T.G. (2015). Abundance, size and polymer composition of marine microplastics ≥10 mm in the Atlantic Ocean and their modelled vertical

distribution. *Marine Pollution Bulletin*, *100*(1), 70-81. https://doi.org/10.1016/j.marpolbul.2015.09.027

Engler, R.E. (2012). The complex interaction between marine debris and toxic chemicals in the ocean. *Environmental Science & Technology, 46*(22), 12302-12315. https://doi.org/10.1021/es3027105

Eo, S., Hong, S.H., Song, Y.K., Lee, J., Lee, J., & Shim, W.J. (2018). Abundance, composition, and distribution of microplastics larger than 20 mm in sand beaches of South Korea. *Environmental Pollution*, *238*, 894-902. https://doi.org/10.1016/j.envpol.2018.03.096

Eriksen, M., Mason, S., Wilson, S., Box, C., Zellers, A., Edwards, W., Farley, H., & Amato, S. (2013). Microplastic pollution in the surface waters of the Laurentian Great Lakes. *Marine Pollution Bulletin*, *77*(1-2), 177–182. https://doi.org/10.1016/j.marpolbul.2013.10.007

Estahbanati, S., & Fahrenfeld, N.L. (2016). Influence of wastewater treatment plant discharges on microplastic concentrations in surface water. *Chemosphere*, *162*, 277–284. https://doi.org/10.1016/j.chemosphere.2016.07.083

Fadare, O.O., & Okoffo, E.D. (2020). Covid-19 face masks: a potential source of microplastics fibers in the environment. *Science of the Total Environment*, *737*, 140279 https://doi.org/10.1016/j.scitotenv.2020.140279

Fortin, S., Song, B., & Burbage, C. (2019). Quantifying and identifying microplastics in the effluent of advanced wastewater treatment systems using Raman microspectroscopy. *Marine Pollution Bulletin*, *149*, 110579. https://doi.org/10.1016/J.MARPOLBUL.2019.110579

Fossi, M.C., Marsili, L., Baini, M., Giannetti, M., Coppola, D., Guerranti, C., Caliani, I., Minutoli, R., Lauriano, G., Finoia, M.G., Rubegni, F., Panigada, S., Bérubé, M., Urbán Ramírez, J., & Panti, C. (2016). Fin whales and microplastics: The Mediterranean Sea and the Sea of Cortez scenarios. *Environmental Pollution*, *209*, 68-78. https://doi.org/10.1016/j.envpol.2015.11.022

Francalanci, S., Paris, E., & Solari, L. (2021). On the prediction of settling velocity for plastic particles of different shapes. *Environmental Pollution*, *290*, 118068. https://doi.org/10.1016/j.envpol.2021.118068

Gandara E Silva, P.P., Nobre, C.R., Resaffe, P., Pereira, C.D.S., & Gusmão, F. (2016). Leachate from microplastics impairs larval development in brown mussels. *Water Research, 106,* 364-370. https://doi.org/10.1016/j.watres.2016.10.016

Gao, S., Wu, Q., Peng, M., Zeng, J., Jiang, T., Ruan, Y., Xu, L., & Guo, K. (2023). Rapid urbanization affects microplastic communities in lake sediments: A case study of Lake Aha in southwest China. *Journal of Environmental Management*, *338*, 117824. https://doi.org/10.1016/J.JENVMAN.2023.117824

Gasperi, J., Dris, R., Bonin, T., Rocher, V., & Tassin, B. (2014). Assessment of floating plastic debris in surface water along the Seine River. *Environmental Pollution, 195,* 163–166. https://doi.org/10.1016/j.envpol.2014.09.001.

Geyer, R., Jambeck, J.R., & Law, K.L. (2017). Production, use, and fate of all plastics ever made. *Science Advances*, *3*(7), e170078. https://doi.org/10.1126/sciadv.170078

GoldSim Technology Group, 2021. GoldSim User's Guide, Version 14.0. WA.

González-Fernández, D., Cózar, A., Hanke, G., Viejo, J., Morales-Caselles, C., Bakiu, R., Barceló, D., Bessa, F., Bruge, A., Cabrera, M., Castro-Jiménez, J., Constant, M., Crosti, R., Galletti, Y., Kideys, A.E., Machitadze, N., de Brito, J.P., Pogojeva, M., Ratola, N., Rigueira, J., Rojo-Nieto, E., Savenko, O., Schöneich-Argent, R.I., Siedlewicz, G., Suaria, G., & Tourgeli, M. (2021). Floating macro-litter leaked from Europe to the ocean. *Nature Sustainability, 4,* 474–483. https://doi.org/10.1038/s41893-021-00722-6

Goral, K.D., Guler, H.G., Larsen, B.E., Carstensen, S., Christensen, E.D., Kerpen, N.B., Schlurmann, T., & Fuhrman, D.R. (2023). Settling velocity of microplastic particles having regular and irregular shapes. *Environmental Research*, *228*, 115783. https://doi.org/10.1016/j.envres.2023.115783

Gregory, M.R. (1978). Accumulation and distribution of virgin plastic granules on New Zealand beaches. *New Zealand Journal of Marine and Freshwater Research*, *12*(4), 399-414. https://doi.org/10.1080/00288330.1978.9515768

Gregory, M.R. (1996). Plastic ‘scrubbers’ in hand cleansers: a further (and minor) source for marine pollution identified. *Marine Pollution Bulletin*, *32*(12), 867-871. https://doi.org/10.1016/S0025-326X(96)00047-1

Guerranti, C., Cannas, S., Scopetani, C., Fastelli, P., Cincinelli, A., & Renzi, M. (2017). Plastic litter in aquatic environments of maremma regional park (Tyrrhenian sea, Italy): contribution by the Ombrone River and levels in marine sediments. *Marine Pollution Bulletin*, *117*(1-2), 366-370. https://doi.org/10.1016/j.marpolbul.2017.02.021

Guerranti, C., Martellini, T., Perra, G., Scopetani, C., & Cincinelli, A. (2019). Microplastics in cosmetics: environmental issues and needs for global bans. *Environmental Toxicology and Pharmacology*, *68*, 75–79. https://doi.org/10.1016/J.ETAP.2019.03.007

Guven, B., & Howard, A. (2006). Modelling the growth and movement of cyanobacteria in river systems. *Science of the Total Environment*, *368*(2-3), 898-908. https://doi.org/10.1016/j.scitotenv.2006.03.035

Güven, O., Gökdağ, K., Jovanović, B., & Kıdeyş, A.E. (2017). Microplastic litter composition of the Turkish territorial waters of the Mediterranean Sea, and its occurrence in the gastrointestinal tract of fish. *Environmental Pollution*, *223*, 286-294. https://doi.org/10.1016/j.envpol.2017.01.025

Hall, N.M., Berry, K.L.E., Rintoul, L., & Hoogenboom, M.O. (2015). Microplastic ingestion by scleractinian corals. *Marine Biology*, *162*, 725-732. https://doi.org/10.1007/s00227-015-2619-7

Hamby, D. M. (1994). A review of techniques for parameter sensitivity analysis of environmental models. *Environmental Monitoring and Assessment*, *32*, 135-154. https://doi.org/10.1007/BF00547132

Harrison, J.P., Hoellein, T.J., Sapp, M., Tagg, A. S., Ju-Nam, Y., & Ojeda, J.J. (2018). Microplastic-associated biofilms: a comparison of freshwater and marine environments. In M, Wagner, & S, Lambert (Eds.). *Freshwater microplastics* (1st ed., pp. 181-201). Cham, Switzerland: Springer

Harrison, J.P., Ojeda, J.J., & Romero-González, M.E. (2012). The applicability of reflectance micro-Fourier-transform infrared spectroscopy for the detection of synthetic microplastics in marine sediments. *Science of The Total Environment*, *416*, 455–463.

https://doi.org/10.1016/J.SCITOTENV.2011.11.078

Harshvardhan, K., & Jha, B. (2013). Biodegradation of low-density polyethylene by marine bacteria from pelagic waters, Arabian Sea, India. *Marine Pollution Bulletin*, *77*(1-2), 100-106. https://doi.org/10.1016/j.marpolbul.2013.10.025

He, B., Smith, M., Egodawatta, P., Ayoko, G.A., Rintoul, L., & Goonetilleke, A. (2021). Dispersal and transport of microplastics in river sediments. *Environmental Pollution*, *279*, 116884. https://doi.org/10.1016/J.ENVPOL.2021.116884

Hermsen, E., Pompe, R., Besseling, E., & Koelmans, A.A. (2017). Detection of low numbers of microplastics in North Sea fish using strict quality assurance criteria. *Marine Pollution Bulletin*, *122*(1-2), 253-258. https://doi.org/10.1016/j.marpolbul.2017.06.051

Hodson, M.E., Duffus-Hodson, C.A., Clark, A., Prendergast-Miller, M.T., & Thorpe, K.L. (2017). Plastic bag derived-microplastics as a vector for metal exposure in terrestrial invertebrates. *Environmental Science & Technology*, *51*(8), 4714-4721. https://doi.org/10.1021/acs.est.7b00635

Horton, A.A., Svendsen, C., Williams, R.J., Spurgeon, D.J., & Lahive, E. (2017a). Large microplastic particles in sediments of tributaries of the River Thames, UK - abundance, sources and methods for effective quantification. *Marine Pollution Bulletin*, *114*(1), 218-226. https://doi.org/10.1016/j.marpolbul.2016.09.004

Horton, A.A., Walton, A., Spurgeon, D.J., Lahive, E., & Svendsen, C. (2017b). Microplastics in freshwater and terrestrial environments: evaluating the current understanding to identify the knowledge gaps and future research priorities. *Science of the Total Environment*, *586*, 127-141. https://doi.org/10.1016/j.scitotenv.2017.01.190

Hosseiny, H. (2022). Implementation of heuristic search algorithms in the calibration of a river hydraulic model. *Environmental Modelling & Software*, *157*, 105537. https://doi.org/10.1016/J.ENVSOFT.2022.105537

Huang, Z., Hu, B., & Wang, H. (2023). Analytical methods for microplastics in the environment: a review. *Environmental Chemistry Letters*, *21*, 383–401. https://doi.org/10.1007/s10311-022-01525-7

Huerta Lwanga, E., Gertsen, H., Gooren, H., Peters, P., Salánki, T., van der Ploeg, M., Besseling, E., Koelmans, A. A., & Geissen, V. (2017). Incorporation of microplastics from litter into burrows of *Lumbricus terrestris*. *Environmental Pollution*, *220*(Part A), 523-531. https://doi.org/10.1016/j.envpol.2016.09.096

Hurley, R.R., Woodward, J.C., & Rothwell, J.J. (2017). Ingestion of microplastics by freshwater Tubifex worms. *Environmental Science & Technology*, *51*(21), 12844-12851. https://doi.org/10.1021/acs.est.7b03567

Imhof, H. K., Schmid, J., Niessner, R., Ivleva, N. P., & Laforsch, C. (2012). A novel, highly efficient method for the separation and quantification of plastic particles in sediments of aquatic environments. *Limnology and Oceanography: Methods, 10*(7), 524–537. https://doi.org/10.4319/lom.2012.10.524

Iwasaki, S., Isobe, A., Kako, S., Uchida, K., & Tokai, T. (2017). Fate of microplastics and mesoplastics carried by surface currents and wind waves: A numerical model approach in the Sea of Japan. *Marine Pollution Bulletin, 121*(1-2), 85-96. https://doi.org/10.1016/j.marpolbul.2017.05.057

Jabeen, K., Su, L., Li, J., Yang, D., Tong, C., Mu, J., & Shi, H. (2017). Microplastics and mesoplastics in fish from coastal and fresh waters of China. *Environmental Pollution, 221*, 141-149. https://doi.org/10.1016/j.envpol.2016.11.055

Jacobs, C.N., Merchant, W., Jendrassak, M., Limpasuvan, V., Gurka, R., & Hackett, E.E. (2016). Flow scales of influence on the settling velocities of particles with varying characteristics. *PLoS ONE*, *11*(8), 1–20. https://doi.org/10.1371/journal.pone.0159645

Jeong, C.B., Kang, H.M., Lee, M.C., Kim, D.H., Han, J., Hwang, D.S., Souissi, S., Lee, S.J., Shin, K.H., Park, H.G., & Lee, J.S. (2017). Adverse effects of microplastics and oxidative stress-induced MAPK/Nrf2 pathway-mediated defense mechanisms in the marine copepod *Paracyclopina nana*. *Scientific Reports, 7*, 1-11. https://doi.org/10.1038/srep41323

Kaiser, D., Kowalski, N., & Waniek, J.J. (2017). Effects of biofouling on the sinking behavior of microplastics. *Environmental Research Letters*, *12*(12), 124003. https://doi.org/10.1088/1748-9326/aa8e8b

Kapp, K.J., & Yeatman, E. (2018). Microplastic hotspots in the snake and lower Columbia rivers: a

journey from the greater yellow stone ecosystem to the Pacific Ocean. *Environmental Pollution, 241*, 1082–1090. https://doi.org/10.1016/j.envpol.2018.06.033

Käppler, A., Fischer, D., Oberbeckmann, S., Schernewski, G., Labrenz, M., Eichhorn, K.J., & Voit, B. (2016). Analysis of environmental microplastics by vibrational microspectroscopy: FTIR, Raman or both? *Analytical and Bioanalytical Chemistry, 408*, 8377-8391. https://doi.org/10.1007/s00216-016-9956-3

Katija, K., Choy, C.A., Sherlock, R.E., Sherman, A.D., & Robison, B.H. (2017). From the surface to the seafloor: how giant larvaceans transport microplastics into the deep sea. *Science Advances, 3*(8), 1-6. https://doi.org/10.1126/sciadv.1700715

Kedzierski, M., Le Tilly, V., Bourseau, P., Bellegou, H., César, G., Sire, O., & Bruzaud, S. (2016). Microplastics elutriation from sandy sediments: A granulometric approach. *Marine Pollution Bulletin, 107*(1), 315–323. https://doi.org/10.1016/J.MARPOLBUL.2016.03.041

Keupers, I., & Willems, P. (2017). Development and testing of a fast conceptual river water quality model. *Water Research, 113,* 62–71. https://doi.org/10.1016/j.watres.2017.01.054

Klein, S., Dimzon, I.K., Eubeler, J., & Knepper, T.P. (2018). Analysis, occurrence, and degradation of microplastics in the aqueous environment. In M, Wagner, & S, Lambert (Eds.). *Freshwater microplastics* (1st ed., pp. 51-67). Cham, Switzerland: Springer

Klein, S., Worch, E., & Knepper, T.P. (2015). Occurrence and spatial distribution of microplastics in river shore sediments of the Rhine-Main Area in Germany. *Environmental Science & Technology, 49*(10), 6070-6076. https://doi.org/10.1021/acs.est.5b00492

Kolandhasamy, P., Su, L., Li, J., Qu, X., Jabeen, K., & Shi, H. (2018). Adherence of microplastics to soft tissue of mussels: a novel way to uptake microplastics beyond ingestion. *Science of the Total Environment, 610-611,* 635-640. https://doi.org/10.1016/j.scitotenv.2017.08.053

Kole, P.J., Löhr, A.J., Van Belleghem, F.G.A.J., & Ragas, A.M.J. (2017). Wear and tear of tyres: a stealthy source of microplastics in the environment. *International Journal of Environmental Research and Public Health, 14*(10), 1265. https://doi.org/10.3390/ijerph14101265

Kooi, M., Reisser, J., Slat, B., Ferrari, F.F., Schmid, M.S., Cunsolo, S., Brambini, R., Noble, K., Sirks, L.A., Linders, T.E.W., Schoeneich-Argent, R.I., & Koelmans, A.A. (2016). The effect of particle properties on the depth profile of buoyant plastics in the ocean. *Scientific Reports*, *6*, 1-10. https://doi.org/10.1038/srep33882

Kooi, M., Van Nes, E.H., Scheffer, M., & Koelmans, A.A. (2017). Ups and downs in the ocean: effects of biofouling on vertical transport of microplastics. *Environmental Science and Technology*, *51*(14), 7963–7971. https://doi.org/10.1021/acs.est.6b04702

Kowalski, N., Reichardt, A.M., & Waniek, J.J. (2016). Sinking rates of microplastics and potential implications of their alteration by physical, biological, and chemical factors. *Marine Pollution Bulletin*, *109*(1), 310–319. https://doi.org/10.1016/j.marpolbul.2016.05.064

Kumar, R., Sharma, P., Verma, A., Kumar Jha, P., Singh, P., Kumar Gupta, P., Chandra, R., Vara Prasad, P.V, An, L., Xu, L., & Zhu, L. (2021). Effect of physical characteristics and hydrodynamic conditions on transport and deposition of microplastics in riverine ecosystem. *Water*, *13*(19), 2710. https://doi.org/10.3390/w13192710

Lahens, L., Strady, E., Kieu-Le, T. C., Dris, R., Boukerma, K., Rinnert, E., Gasperi, J., & Tassin, B. (2018). Macroplastic and microplastic contamination assessment of a tropical river (Saigon River, Vietnam) transversed by a developing megacity. *Environmental Pollution*, *236*, 661-671. https://doi.org/10.1016/j.envpol.2018.02.005

Lavers, J.L., Oppel, S., & Bond, A.L. (2016). Factors influencing the detection of beach plastic debris. *Marine Environmental Research*, *119*, 245–251. https://doi.org/10.1016/j.marenvres.2016.06.009

Law, K.L., Morét-Ferguson, S.E., Goodwin, D.S., Zettler, E.R., Deforce, E., Kukulka, T., & Proskurowski, G. (2014). Distribution of surface plastic debris in the eastern Pacific Ocean from an 11-year data set. *Environmental Science & Technology*, *48*(9), 4732-4738. https://doi.org/10.1021/es4053076

Law, K.L., Morét-Ferguson, S.E., Maximenko, N.A., Proskurowski, G., Peacock, E.E., Hafner, J., & Reddy, J.M. (2010). Plastic accumulation in the North Atlantic subtropical gyre. *Science*, *329*(5996), 1185-1188. https://doi.org/10.1126/science.1192321

Leads, R.R., Weinstein, J.E., Kell, S.E., Overcash, J.M., Ertel, B.M., & Gray, A.D. (2023). Spatial and temporal variability of microplastic abundance in estuarine intertidal sediments: implications for sampling frequency. *Science of the Total Environment, 859,* 160308. https://doi.org/10.1016/j.scitotenv.2022.160308

Lebreton, L.C.M., Greer, S.D., & Borrero, J.C. (2012). Numerical modelling of floating debris in the world's oceans. *Marine Pollution Bulletin, 64*(3), 653-661. https://doi.org/10.1016/j.marpolbul.2011.10.027

Lebreton, L.C.M., Van Der Zwet, J., Damsteeg, J.W., Slat, B., Andrady, A., & Reisser, J. (2017). River plastic emissions to the world's oceans. *Nature Communications, 8,* 15611. https://doi.org/10.1038/ncomms15611

Lechner, A., Keckeis, H., Lumesberger-Loisl, F., Zens, B., Krusch, R., Tritthart, M., Glas, M., & Schludermann, E. (2014). The Danube so colourful: a potpourri of plastic litter outnumbers fish larvae in Europe's second largest river. *Environmental Pollution, 188,* 177-181. https://doi.org/10.1016/j.envpol.2014.02.006

Leslie, H.A., Brandsma, S.H., van Velzen, M.J.M., & Vethaak, A.D. (2017). Microplastics en route: field measurements in the Dutch river delta and Amsterdam canals, wastewater treatment plants, North Sea sediments and biota. *Environment International, 101,* 133-142. https://doi.org/10.1016/j.envint.2017.01.018

Li, J., Huang, W., Xu, Y., Jin, A., Zhang, D., & Zhang, C. (2020). Microplastics in sediment cores as indicators of temporal trends in microplastic pollution in Andong salt marsh, Hangzhou Bay, China. *Regional Studies in Marine Science, 35,* 101149. https://doi.org/10.1016/J.RSMA.2020.101149

Li, J., Qu, X., Su, L., Zhang, W., Yang, D., Kolandhasamy, P., Li, D., & Shi, H. (2016). Microplastics in mussels along the coastal waters of China. *Environmental Pollution, 214,* 177-184. https://doi.org/10.1016/j.envpol.2016.04.012

Li, X. Y., & Yuan, Y. A. (2002). Settling velocities and permeabilities of microbial aggregates. *Water Research, 36*(12), 3110-3120. https://doi.org/10.1016/s0043-1354(01)00541-3

Li, Y., Wang, X., Fu, W., Xia, X., Liu, C., Min, J., Zhang, W., Crittenden, J.C., & Reif, J.A. (2019).

Interactions between nano/micro plastics and suspended sediment in water: implications on aggregation and settling. *Water Research*, *161*, 486–495. https://doi.org/10.1016/j.watres.2019.06.018

Lin, L., Zuo, L.Z., Peng, J.P., Cai, L.Q., Fok, L., Yan, Y., Li, H.X., & Xu, X.R. (2018). Occurrence and distribution of microplastics in an urban river: a case study in the Pearl River along Guangzhou City, China. *Science of the Total Environment*, *644*, 375–381. https://doi.org/10.1016/j.scitotenv.2018.06.327

Liubartseva, S., Coppini, G., Lecci, R., & Creti, S. (2016). Regional approach to modeling the transport of floating plastic debris in the Adriatic Sea. *Marine Pollution Bulletin*, *103*(1-2), 115-127. https://doi.org/10.1016/j.marpolbul.2015.12.031

Löder, M.G.J., & Gerdts, G. (2015). Methodology used for the detection and identification of microplastics - a critical appraisal. In M, Bergmann, L, Gutow, & M, Klages (Eds.) *Marine anthropogenic litter*. (1st ed., pp. 201-227). Cham, Switzerland: Springer

Long, M., Moriceau, B., Gallinari, M., Lambert, C., Huvet, A., Raffray, J., & Soudant, P. (2015). Interactions between microplastics and phytoplankton aggregates: impact on their respective fates. *Marine Chemistry*, *175*, 39-46. https://doi.org/10.1016/j.marchem.2015.04.003

Long, M., Paul-Pont, I., Hégaret, H., Moriceau, B., Lambert, C., Huvet, A., & Soudant, P. (2017). Interactions between polystyrene microplastics and marine phytoplankton lead to species-specific hetero-aggregation. *Environmental Pollution*, *228*, 454-463. https://doi.org/10.1016/j.envpol.2017.05.047

Ma, Y., Huang, A., Cao, S., Sun, F., Wang, L., Guo, H., & Ji, R. (2016). Effects of nanoplastics and microplastics on toxicity, bioaccumulation, and environmental fate of phenanthrene in fresh water. *Environmental Pollution*, *219*, 166–173. https://doi.org/10.1016/j.envpol.2016.10.061

Mani, T., Hauk, A., Walter, U., & Burkhardt-Holm, P. (2015). Microplastics profile along the Rhine River. *Scientific Reports*, *5*, 17988. https://doi.org/10.1038/srep17988

Mao, L., Uyttendaele, G.P., Iroumé, A., & Lenzi, M.A. (2008). Field based analysis of sediment entrainment in two high gradient streams located in Alpine and Andine environments. *Geomorphology*, *93*(3-4), 368–383. https://doi.org/10.1016/J.GEOMORPH.2007.03.008

Mariano, S., Tacconi, S., Fidaleo, M., Rossi, M., & Dini, L. (2021). Micro and nanoplastics identification: classic methods and innovative detection techniques. *Frontiers in Toxicology*, *3*, 1–17. https://doi.org/10.3389/ftox.2021.636640

Masura, J., Baker, J., Foster, G., & Arthur, C. (2015). *Laboratory methods for the analysis of microplastics in the marine environment: recommendations for quantifying synthetic particles in waters and sediments.* Silver Spring, MD: NOAA Marine Debris Division (NOAA Technical Memorandum NOS-OR&R-48). http://dx.doi.org/10.25607/OBP-604

McNeish, R.E., Kim, L.H., Barrett, H.A., Mason, S.A., Kelly, J.J., & Hoellein, T.J. (2018). Microplastic in riverine fish is connected to species traits. *Scientific Reports*, *8*, 11639. https://doi.org/10.1038/s41598-018-29980-9

Menges, F. (2020). Spectragryph - optical spectroscopy software, Version 1.2.15, http://www.effemm2.de/spectragryph/

Millar, R.G. (1999). Grain and form resistance in gravel-bed rivers. *Journal of Hydraulic Research*, *37*(3), 303-312. https://doi.org/10.1080/00221686.1999.9628249

Millero, F.J. (1984). The conductivity-density-salinity-chlorinity relationships for estuarine waters, *Limnology and Oceanography*, *29*(6), 1317-1321. https://doi.org/10.4319/lo.1984.29.6.1317

Moore, C.J., Lattin, G.L., & Zellers, A.F. (2011). Quantity and type of plastic debris flowing from two urban rivers to coastal waters and beaches of Southern California. Journal of Integrated Coastal Zone Management, *11*(1), 65-73. https://doi.org/10.5894/rgci194

Mountford, G.L., Atkinson, P.M., Dash, J., Lankester, T., & Hubbard, S. (2017). Sensitivity of vegetation phenological parameters: from satellite sensors to spatial resolution and temporal compositing period. In G.P, Petropoulos, & P.K, Srivastava (Eds.). *Sensitivity analysis in earth observation modelling* (1st ed., pp. 75-90). Retrieved from https://doi.org/10.1016/B978-0-12-803011-0.00004-5

Mulligan, M., & Wainwright, J. (2004). Modelling and model building. In J, Wainwright, & M, Mulligan (Eds.). *Environmental modelling: finding simplicity in complexity* (1st ed., pp. 7-73). London, UK: Wiley

Näkki, P., Setälä, O., & Lehtiniemi, M. (2017). Bioturbation transports secondary microplastics to deeper layers in soft marine sediments of the northern Baltic Sea. *Marine Pollution Bulletin*, *119*(1), 255-261. https://doi.org/10.1016/j.marpolbul.2017.03.065

Napper, I.E., & Thompson, R.C. (2016). Release of synthetic microplastic plastic fibres from domestic washing machines: effects of fabric type and washing conditions. *Marine Pollution Bulletin*, *112*(1-2), 39-45. https://doi.org/10.1016/j.marpolbul.2016.09.025

Napper, I.E., Baroth, A., Barrett, A.C., Bhola, S., Chowdhury, G.W., Davies, B.F.R., Duncan, E.M., Kumar, S., Nelms, S.E., Hasan Niloy, M.N., Nishat, B., Maddalene, T., Thompson, R.C., & Koldewey, H. (2021). The abundance and characteristics of microplastics in surface water in the transboundary Ganges River. *Environmental Pollution*, *274*, 116348 https://doi.org/10.1016/J.ENVPOL.2020.116348

Nel, H.A., Dalu, T., & Wasserman, R.J. (2018). Sinks and sources: Assessing microplastic abundance in river sediment and deposit feeders in an Austral temperate urban river system. *Science of the Total Environment*, *612*, 950–956. https://doi.org/10.1016/j.scitotenv.2017.08.298

Nelms, S.E., Galloway, T.S., Godley, B.J., Jarvis, D.S., & Lindeque, P.K. (2018). Investigating microplastic trophic transfer in marine top predators. *Environmental Pollution*, *238*, 999-1007. https://doi.org/10.1016/j.envpol.2018.02.016

Nghiem, J.A., Fischer, W.W., Li, G.K., & Lamb, M.P. (2022). A mechanistic model for mud flocculation in freshwater rivers. *Journal of Geophysical Research: Earth Surface*, *127*(5), e2021JF006392. https://doi.org/10.1029/2021JF006392

Nguyen, T.H., Kieu-Le, T.C., Tang, F.H.M., & Maggi, F. (2022). Controlling factors of microplastic fibre settling through a water column. *Science of the Total Environment*, *838*, 156011. https://doi.org/10.1016/j.scitotenv.2022.156011

Nielsen, P. (1993). Turbulence effects on the settling of suspended particles. *Journal of Sedimentary Research*, *63*(5), 835–838. https://doi.org/10.1306/D4267C1C-2B26-11D7-8648000102C1865D

Nizzetto, L., Bussi, G., Futter, M.N., Butterfield, D., & Whitehead, P.G. (2016a). A theoretical assessment of microplastic transport in river catchments and their retention by soils and river sediments. *Environmental Science: Processes and Impacts*, *18*(8), 1050–1059. https://doi.org/10.1039/c6em00206d

Nizzetto, L., Futter, M., & Langaas, S. (2016b). Are agricultural soils dumps for microplastics of urban origin? *Environmental Science & Technology*, *50*(20), 10777-10779. https://doi.org/10.1021/acs.est.6b04140

Noren, F., & Naustvoll, F. (2010). Survey of microscopic anthropogenic particles in Skagerrak. Norway: Report commissioned by Klima-og Forurensningsdirektoratet

Nuelle, M.T., Dekiff, J.H., Remy, D., & Fries, E. (2014). A new analytical approach for monitoring microplastics in marine sediments. *Environmental Pollution*, *184*, 161–169. https://doi.org/10.1016/j.envpol.2013.07.027

Odum, B., Xu, C., Chen, Y., Yao, Y., & Zhou, Y. (2023). Experimental study on the effect of hydrodynamic conditions on flocculation and settling properties of fine-grain sediment. *International Journal of Sediment Research*, *In Press.* https://doi.org/10.1016/J.IJSRC.2023.08.001

Oliveira, M., Ribeiro, A., Hylland, K., & Guilhermino, L. (2013). Single and combined effects of microplastics and pyrene on juveniles (0+ group) of the common goby Pomatoschistus microps (Teleostei, Gobiidae). *Ecological Indicators*, *34*, 641-647. https://doi.org/10.1016/j.ecolind.2013.06.019

Ory, N. C., Sobral, P., Ferreira, J. L., & Thiel, M. (2017). Amberstripe scad *Decapterus muroadsi* (Carangidae) fish ingest blue microplastics resembling their copepod prey along the coast of Rapa Nui (Easter Island) in the South Pacific subtropical gyre. *Science of the Total Environment*, *586*, 430-437. https://doi.org/10.1016/j.scitotenv.2017.01.175

Özgüler, Ü., Demir, A., Can Kayadelen, G., & Kıdeys¸, A.E. (2022). Riverine microplastic loading to Mersin Bay, Turkey on the north-eastern Mediterranean. *Turkish Journal of Fisheries and Aquatic*

Sciences, *22*(SI), TRJFAS20253. https://doi.org/10.4194/TRJFAS20253

Patel, M.M., Goyal, B.R., Bhadada, S.V., Bhatt, J.S., & Amin, A.F. (2009). Getting into the brain. *CNS Drugs*, *23*, 35–58. https://doi.org/10.2165/0023210-200923010-00003

Peng, G., Xu, P., Zhu, B., Bai, M., & Li, D. (2018). Microplastics in freshwater river sediments in Shanghai, China: a case study of risk assessment in mega-cities. *Environmental Pollution*, *234*, 448-456. https://doi.org/10.1016/j.envpol.2017.11.034

PlasticsEurope (2021). *An analysis of European plastics production, demand and waste data*. PlasticsEurope.

Prata, J.C., da Costa, J.P., Duarte, A.C., & Rocha-Santos, T. (2019). Methods for sampling and detection of microplastics in water and sediment: a critical review. *TrAC Trends in Analytical Chemistry*, *110*, 150–159. https://doi.org/10.1016/j.trac.2018.10.029

Prego Meleiro, P., & García-Ruiz, C. (2016). Spectroscopic techniques for the forensic analysis of textile fibers. *Applied Spectroscopy Reviews*, *51*(4), 278–301. https://doi.org/10.1080/05704928.2015.1132720

Quinn, B., Murphy, F., & Ewins, C. (2016). Validation of density separation for the rapid recovery of microplastics from sediment. *Analytical Methods*, *9*, 1491-1498. http://doi.org/10.1039/c6ay02542k

Radzi, A.M., Sapuan, S.M., Huzaifah, M.R.M., Noor Azammi, A.M., Ilyas, R.A., & Nadlene, R. (2021). A review of the mechanical properties of roselle fiber-reinforced polymer hybrid composites. In S.M., Sapuan, R, Nadlene, A.M, Radzi, & R.A, Ilyas (Eds.). *Roselle: production, processing, products and biocomposites* (1st ed., pp. 259–269). https://doi.org/10.1016/B978-0-323-85213-5.00017-2

Reichert, J., Schellenberg, J., Schubert, P., & Wilke, T. (2018). Responses of reef building corals to microplastic exposure. *Environmental Pollution*, *237*, 955-960. https://doi.org/10.1016/j.envpol.2017.11.006

Ribeiro-Claro, P., Nolasco, M.M., & Araújo, C. (2017). Characterization of microplastics by Raman spectroscopy. *Comprehensive Analytical Chemistry, 75*, 119–151. http://doi.org/10.1016/bs.coac.2016.10.001

Richards, K. (1982). *Rivers: form and process in alluvial channels*. New Jersey, USA: The Blackburn Press

Rodrigues, M.O., Abrantes, N., Gonçalves, F.J.M., Nogueira, H., Marques, J.C., & Gonçalves, A.M.M. (2018). Spatial and temporal distribution of microplastics in water and sediments of a freshwater system (Antuã River, Portugal). *Science of the Total Environment, 633*, 1549–1559. https://doi.org/10.1016/j.scitotenv.2018.03.233

Rodríguez-Seijo, A., & Pereira, R. (2019). Microplastics in agricultural soils: are they a real environmental hazard? In J.C, Sanchez-Hernandez (Ed.). *Bioremediation of agricultural soils*. (1st ed., pp. 45-60). Florida, USA: CRC Press

Romeo, T., Pietro, B., Pedà, C., Consoli, P., Andaloro, F., & Fossi, M.C. (2015). First evidence of presence of plastic debris in stomach of large pelagic fish in the Mediterranean Sea. *Marine Pollution Bulletin, 95*(1), 358–361. https://doi.org/10.1016/j.marpolbul.2015.04.048

Ryan, P.G., Moore, C.J., van Franeker, J.A., & Moloney, C.L. (2009). Monitoring the abundance of plastic debris in the marine environment. *Philosophical Transactions of the Royal Society B, 364*(1526), 1999-2012. https://doi.org/10.1098/rstb.2008.0207

Shamskhany, A., & Karimpour, S. (2022). Entrainment and vertical mixing of aquatic microplastics in turbulent flow: The coupled role of particle size and density. *Marine Pollution Bulletin, 184*, 114160. https://doi.org/10.1016/J.MARPOLBUL.2022.114160

Shen, M., Zeng, Z., Song, B., Yi, H., Hu, T., Zhang, Y., Zeng, G., & Xiao, R. (2021). Neglected microplastics pollution in global COVID-19: disposable surgical masks. *Science of the Total Environment, 790*, 148130. https://doi.org/10.1016/J.SCITOTENV.2021.148130

Shen, X., Huo, H., Zhang, Y., Zhu, Y., Fettweis, M., Bi, Q., Lee, B. J., Maa, J.P.Y., & Chen, Q. (2023). Effects of organic matter on the aggregation of anthropogenic microplastic particles in turbulent environments. *Water Research, 232*, 119706.

https://doi.org/10.1016/J.WATRES.2023.119706

Shields, A. (1936). Anwendung der Ähnlichkeitsmechanik und der Turbulenzforschung auf die Geschiebebewegung. Berlin, Germany: Mitt. der Preuss. Versuchsanstalt für Wasserbau und Schiffbau.

Shim, W.J., Hong, S.H., & Eo, S. (2017). Identification methods in microplastic analysis: a review. *Analytical Methods, 9*(9), 1384-1391. http://doi.org/10.1039/c6ay02558g

Siegfried, M., Koelmans, A.A., Besseling, E., & Kroeze, C. (2017). Export of microplastics from land to sea. A modelling approach. *Water Research, 127*, 249-257. https://doi.org/10.1016/j.watres.2017.10.011

Silva-Cavalcanti, J.S., Silva, J.D.B., França, E.J. de, Araújo, M.C.B. de, & Gusmão, F. (2017). Microplastics ingestion by a common tropical freshwater fishing resource. *Environmental Pollution, 221*, 218-226. https://doi.org/10.1016/j.envpol.2016.11.068

Simon-Sánchez, L., Grelaud, M., Garcia-Orellana, J., & Ziveri, P. (2019). River Deltas as hotspots of microplastic accumulation: The case study of the Ebro River (NW Mediterranean). *Science of the Total Environment, 687*, 1186–1196. https://doi.org/10.1016/J.SCITOTENV.2019.06.168

Singh, N., Mondal, A., Bagri, A., Tiwari, E., Khandelwal, N., Monikh, F.A., & Darbha, G.K. (2021). Characteristics and spatial distribution of microplastics in the lower Ganga River water and sediment. *Marine Pollution Bulletin, 163*, 111960 https://doi.org/10.1016/J.MARPOLBUL.2020.111960

Song, Z., Yang, X., Chen, F., Zhao, F., Zhao, Y., Ruan, L., Wang, Y., & Yang, Y. (2019). Fate and transport of nanoplastics in complex natural aquifer media: effect of particle size and surface functionalization. *Science of the Total Environment, 669*, 120–128. https://doi.org/10.1016/J.SCITOTENV.2019.03.102.

Sterman, J.D. (2001). System dynamics modeling: tools for learning in a complex world. *California Management Review, 43*(4), 8–25. https://doi.org/10.2307/41166098

Stride, B., Abolfathi, S., Odara, M.G.N., Bending, G.D., & Pearson, J. (2023). Modeling microplastic and solute transport in vegetated flows. *Water Resources Research, 59*(5) e2023WR034653.

https://doi.org/10.1029/2023WR034653

Sun, X., Li, Q., Zhu, M., Liang, J., Zheng, S., & Zhao, Y. (2017). Ingestion of microplastics by natural zooplankton groups in the northern South China Sea. *Marine Pollution Bulletin*, *115*(1-2), 217-224. https://doi.org/10.1016/j.marpolbul.2016.12.004

Tagg, A.S., Sapp, M., Harrison, J.P., & Ojeda, J.J. (2015). Identification and quantification of microplastics in wastewater using focal plane array-based reflectance micro-FT-IR imaging. *Analytical Chemistry*, *87*(12), 6032−6040. https://doi.org/10.1021/acs.analchem.5b00495

Thiele, C.J., Hudson, M.D., & Russell, A.E. (2019). Evaluation of existing methods to extract microplastics from bivalve tissue: adapted KOH digestion protocol improves filtration at single-digit pore size. *Marine Pollution Bulletin, 142,* 384-393. https://doi.org/10.1016/j.marpolbul.2019.03.003

Thomas, J., Buzzini, P., Massonnet, G., Reedy, B., & Roux, C. (2005). Raman spectroscopy and the forensic analysis of black/grey and blue cotton fibres: Part 1. Investigation of the effects of varying laser wavelength. *Forensic Science International*, *152*(2-3), 189–197. https://doi.org/10.1016/j.forsciint.2004.08.009

Thompson, R.C. (2006). Plastic debris in the marine environment: consequences and solutions. In J. C, Krause, H, Nordheim, & S, Bräger (Eds.). *Marine Nature Conservation in Europe*. (1st ed., pp. 107-115). Stralsund, Germany: Federal Agency for Nature Conservation

Thompson, R.C., Olsen, Y., Mitchell, R.P., Davis, A., Rowland, S.J., John, A.W.G., McGonigle, D., & Russell, A.E. (2004). Lost at sea: where is all the plastic? *Science*, *304*(5672), 838–838. https://doi.org/10.1126/science.1094559

Tokatlı, C., & Varol, M. (2021). Impact of the COVID-19 lockdown period on surface water quality in the Meriç-Ergene River Basin, Northwest Turkey. *Environmental Research*, *197*, 111051. https://doi.org/10.1016/J.ENVRES.2021.111051

Tosetto, L., Brown, C., & Williamson, J.E. (2016). Microplastics on beaches: ingestion and behavioural consequences for beachhoppers. *Marine Biology*, *163*, 199. https://doi.org/10.1007/s00227-016-2973-0

Uddin, S., Fowler, S.W., Uddin, M.F., Behbehani, M., & Naji, A. (2021). A review of microplastic distribution in sediment profiles. *Marine Pollution Bulletin*, *163*, 111973. https://doi.org/10.1016/j.marpolbul.2021.111973

UNEP, 2021. *From pollution to solution: a global assessment of marine litter and plastic pollution*. Nairobi, Kenya: United Nations Environment Programme

Unice, K.M., Weeber, M.P., Abramson, M.M., Reid, R.C.D., van Gils, J.A.G., Markus, A.A., Vethaak, A.D., & Panko, J.M. (2019a). Characterizing export of land-based microplastics to the estuary - Part I: application of integrated geospatial microplastic transport models to assess tire and road wear particles in the Seine watershed. *Science of the Total Environment*, *646*, 1639-1649. https://doi.org/10.1016/j.scitotenv.2018.07.368

Unice, K.M., Weeber, M.P., Abramson, M.M., Reid, R.C.D., van Gils, J.A.G., Markus, A.A., Vethaak, A.D., & Panko, J.M. (2019b). Characterizing export of land-based microplastics to the estuary e Part II: sensitivity analysis of an integrated geospatial microplastic transport modeling assessment of tire and road wear particles. *Science of the Total Environment*, *646*, 1650-1659. https://doi.org/10.1016/j.scitotenv.2018.08.301

Uzun, P., Farazande, S., & Guven, B. (2022). Mathematical modeling of microplastic abundance, distribution, and transport in water environments: a review. *Chemosphere*, *288*(P2), 132517. https://doi.org/10.1016/j.chemosphere.2021.132517

Vardar, S., Onay, T.T., Demirel, B., & Kideys, A.E. (2021). Evaluation of microplastics removal efficiency at a wastewater treatment plant discharging to the Sea of Marmara. *Environmental Pollution*, *289*, 117862 https://doi.org/10.1016/j.envpol.2021.117862

Vermaire, J.C., Pomeroy, C., Herczegh, S.M., Haggart, O., & Murphy, M. (2017). Microplastic abundance and distribution in the open water and sediment of the Ottawa River, Canada, and its tributaries. *Facets*, *2*(1), 301-314. https://doi.org/10.1139/facets-2016-0070

Vianello, A., Boldrin, A., Guerriero, P., Moschino, V., Rella, R., Sturaro, A., & Da Ros, L. (2013). Microplastic particles in sediments of Lagoon of Venice, Italy: first observations on occurrence, spatial patterns and identification. *Estuarine, Coastal and Shelf Science*, *130*, 54-61. https://doi.org/10.1016/j.ecss.2013.03.022

von Moos, N., Burkhardt-Holm, P., & Köhler, A. (2012). Uptake and effects of microplastics on cells and tissue of the blue mussel Mytilus edulis L. after an experimental exposure. *Environmental Science & Technology*, *46*(20), 11327–11335. https://doi.org/10.1021/es302332w

Waldschläger, K., & Schüttrumpf, H. (2019a). Effects of particle properties on the settling and rise velocities of microplastics in freshwater under laboratory conditions. *Environmental Science and Technology*, *53*(4), 1958–1966. https://doi.org/10.1021/acs.est.8b06794

Waldschläger, K., & Schüttrumpf, H. (2019b). Erosion behavior of different microplastic particles in comparison to natural sediments. *Environmental Science and Technology*, *53*(22), 13219-13227. https://doi.org/10.1021/acs.est.9b05394

Wang, G., Lu, J., Li, W., Ning, J., Zhou, L., Tong, Y., Liu, Z., Zhou, H., & Xiayihazi, N. (2021a). Seasonal variation and risk assessment of microplastics in surface water of the Manas River Basin, China. *Ecotoxicology and Environmental Safety*, *208*, 111477. https://doi.org/10.1016/J.ECOENV.2020.111477

Wang, J., Tan, Z., Peng, J., Qiu, Q., & Li, M. (2016). The behaviors of microplastics in the marine environment. *Marine Environmental Research*, *113*, 7-17. https://doi.org/10.1016/j.marenvres.2015.10.014

Wang, W., Ndungu, A.W., Li, Z., & Wang, J. (2017). Microplastics pollution in inland freshwaters of China: a case study in urban surface waters of Wuhan, China. *Science of the Total Environment*, *575*, 1369–1374. https://doi.org/10.1016/j.scitotenv.2016.09.213

Wang, Z., Dou, M., Ren, P., Sun, B., Jia, R., & Zhou, Y. (2021b). Settling velocity of irregularly shaped microplastics under steady and dynamic flow conditions. *Environmental Science and Pollution Research*, *28*(44), 62116–62132. https://doi.org/10.1007/s11356-021-14654-3

Was-Gubala, J., & Machnowski, W. (2014). Application of Raman spectroscopy for differentiation among cotton and viscose fibers dyed with several dye classes. *Spectroscopy Letters*, *47*(7), 527–535. https://doi.org/10.1080/00387010.2013.820760

Watts, A.J.R., Lewis, C., Goodhead, R.M., Beckett, S.J., Moger, J., Tyler, C.R., & Galloway, T.S. (2014). Uptake and retention of microplastics by the shore crab *Carcinus maenas*. *Environmental Science & Technology*, *48*(15), 8823-8830. https://doi.org/10.1021/es501090e

Whitehead, P., Young, P., & Hornberger, G. (1979). A systems model of stream flow and water quality in the bedford-ouse river—1. stream flow modelling. *Water Research*, *13*(12), 1155-1169. https://doi.org/10.1016/0043-1354(79)90159-3

Whitehead, P.G., Bussi, G., Hughes, J.M.R., Castro-Castellon, A.T., Norling, M.D., Jeffers, E.S., Rampley, C.P.N., Read, D.S., & Horton, A.A. (2021). Modelling microplastics in the river Thames: sources, sinks and policy implications. *Water*, *13*(6), 861. https://doi.org/10.3390/w13060861

Wicaksono, E.A., Werorilangi, S., Galloway, T.S., & Tahir, A. (2021). Distribution and seasonal variation of microplastics in Tallo river, Makassar, Eastern Indonesia. *Toxics*, *9*(6), 1–13. https://doi.org/10.3390/toxics9060129

Wong, G., Löwemark, L., & Kunz, A. (2020). Microplastic pollution of the Tamsui River and its tributaries in northern Taiwan: spatial heterogeneity and correlation with precipitation. *Environmental Pollution*, *260*, 113935 https://doi.org/10.1016/J.ENVPOL.2020.113935

Woodall, L.C., Sanchez-Vidal, A., Canals, M., Paterson, G.L.J., Coppock, R., Sleight, V., Calafat, A., Rogers, A.D., Narayanaswamy, B.E., & Thompson, R.C. (2014). The deep sea is a major sink for microplastic debris. *Royal Society Open Science*, *1*(4), 140317. https://doi.org/10.1098/rsos.140317

Wu, P., Tang, Y., Dang, M., Wang, S., Jin, H., Liu, Y., Jing, H., Zheng, C., Yi, S., & Cai, Z. (2020). Spatial-temporal distribution of microplastics in surface water and sediments of Maozhou River within Guangdong-Hong Kong-Macao Greater Bay Area. *Science of the Total Environment*, *717*, 135187. https://doi.org/10.1016/j.scitotenv.2019.135187

Xiao, F., Li, X.Y., Lam, K.M., & Wang, D.S. (2012). Investigation of the hydrodynamic behavior of diatom aggregates using particle image velocimetry. *Journal of Environmental Sciences*, *24*(7), 1157-1164. https://doi.org/10.1016/S1001-0742(11)60960-1

Xing, L., Bolster, D., Liu, H., Sherman, T., Richter, D.H., Rocha-Brownell, K., & Ru, Z. (2022). Markovian models for microplastic transport in open-channel flows. *Water Resources Research*,

58(8), e2021WR031746. https://doi.org/10.1029/2021WR031746

Xu, Y., Chan, F. K. S., Johnson, M., Stanton, T., He, J., Jia, T., Wang, J., Wang, Z., Yao, Y., Yang, J., Liu, D., Xu, Y., & Yu, X. (2021). Microplastic pollution in Chinese urban rivers: the influence of urban factors. *Resources, Conservation and Recycling*, *173*, 105686. https://doi.org/10.1016/J.RESCONREC.2021.105686

Yan, M., Nie, H., Xu, K., He, Y., Hu, Y., Huang, Y., & Wang, J. (2019). Microplastic abundance, distribution and composition in the Pearl River along Guangzhou city and Pearl River estuary, China. *Chemosphere*, *217*, 879–886. https://doi.org/10.1016/j.chemosphere.2018.11.093

Yan, M., Wang, L., Dai, Y., Sun, H., & Liu, C. (2021). Behavior of microplastics in inland waters: aggregation, settlement, and transport. *Bulletin of Environmental Contamination and Toxicology*, *107*, 700–709. https://doi.org/10.1007/s00128-020-03087-2

Yonkos, L.T., Friedel, E.A., Perez-Reyes, A.C., Ghosal, S., & Arthur, C.D. (2014). Microplastics in four estuarine rivers in the Chesapeake Bay, USA. *Environmental Science & Technology*, *48*(24), 14195-14202. https://doi.org/10.1021/es5036317

Zeidan, B.A. (2017). Mathematical modeling of environmental problems. *Environmental Science and Engineering, Instrument, Modeling and Analysis*, *7*, 422–461.

Zhang, H. (2017). Transport of microplastics in coastal seas. *Estuarine, Coastal and Shelf Science*, *199*, 74-86. https://doi.org/10.1016/j.ecss.2017.09.032

Zhao, W., Huang, W., Yin, M., Huang, P., Ding, Y., Ni, X., Xia, H., Liu, H., Wang, G., Zheng, H., & Ca, M. (2020). Tributary inflows enhance the microplastic load in the estuary: a case from the Qiantang River. *Marine Pollution Bulletin*, *156*, 111152. https://doi.org/10.1016/j.marpolbul.2020.111152

Zitko, V., & Hanlon, M. (1991). Another source of pollution by plastics: skin cleansers with plastic scrubbers. *Marine Pollution Bulletin*, *22*(1), 41–42. https://doi.org/10.1016/0025-326X(91)90444-W

APPENDIX A: MICROPLASTIC ABUNDANCE DATA IN THE WATER AND SEDIMENT SAMPLES

Table A.1. The calculation of microplastic concentrations in the water samples.

Date	Site	The Number of Microplastics (items)				The Concentration of Microplastics (items L^{-1})			
		R1	Sample Volume (L)	R2	Sample Volume (L)	R1	R2	Mean	SD
May 20, 2019	S1	28	12.20	11	12.20	2.30	0.90	1.60	0.99
	S2	147	14.30	38	13.00	10.28	2.92	6.60	5.20
	S3	51	12.00	126	11.85	4.25	10.63	7.44	4.51
	S4	52	10.60	19	10.95	4.91	1.74	3.32	2.24
	S5	57	12.25	24	12.05	4.65	1.99	3.32	1.88
	S6	78	11.00	40	9.75	7.09	4.10	5.60	2.11
Sep 30, 2020	S1	52	13.05	36	12.05	3.98	2.99	3.49	0.71
	S2	47	12.80	57	13.40	3.67	4.25	3.96	0.41
	S3	207	12.95	238	12.50	15.98	19.04	17.51	2.16
	S4	32	11.05	29	11.55	2.90	2.51	2.70	0.27
	S5	77	12.70	43	13.00	6.06	3.31	4.69	1.95
	S6	154	11.80	59	11.75	13.05	5.02	9.04	5.68

Table A.2. The calculation of microplastic concentrations in the sediment samples.

Date	Site	The Number of Microplastics (items)						The Concentration of Microplastics (items kg^{-1})				
		R1	Sample Weight (g)	R2	Sample Weight (g)	R3	Sample Weight (g)	R1	R2	R3	Mean	SD
May 20, 2019	S1	4	80.57	3	62.49	4	54.15	49.64	48.01	73.87	57.18	14.48
	S2	1	66.35	4	81.67	6	54.58	15.07	48.97	109.92	57.99	48.06
	S3	2	65.98	7	60.60	3	70.66	30.31	115.50	42.45	62.76	46.08
	S4	2	82.80	4	78.18	5	83.69	24.15	51.17	59.74	45.02	18.57
	S5	7	69.66	24	64.89	18	63.93	100.49	369.85	281.58	250.64	137.32
	S6	8	75.06	11	69.80	5	64.72	106.58	157.59	77.25	113.81	40.66
Sep 30, 2020	S1	36	68.46	27	66.21	29	70.20	525.83	407.82	413.10	448.92	66.66
	S2	10	76.53	4	65.64	7	53.88	130.66	60.94	129.91	107.17	40.04
	S3	18	78.11	10	108.34	6	110.19	230.45	92.30	54.45	125.73	92.64
	S4	3	78.52	41	55.47	3	56.51	38.21	739.11	53.09	276.80	400.44
	S5	4	47.87	2	48.77	4	51.99	83.55	41.01	76.94	67.17	22.89
	S6	66	58.91	13	53.66	37	66.11	1120.35	242.25	559.67	640.76	444.63

APPENDIX B: DATA ON SHAPE, SIZE, COLOR, AND POLYMER DISTRIBUTION OF MICROPLASTICS

Table B.1. Microplastic shape distribution in the water samples in May 2019.

Site	Replicate	Fiber	Hard Fragment	Soft Fragment	Pellet	Foam	Other	Total
S1	R1	20	4	0	3	1	0	28
	R2	5	1	0	5	0	0	11
S2	R1	124	5	7	1	0	10	147
	R2	32	2	2	0	0	2	38
S3	R1	51	0	0	0	0	0	51
	R2	122	2	2	0	0	0	126
S4	R1	47	0	5	0	0	0	52
	R2	11	1	7	0	0	0	19
S5	R1	44	2	9	0	0	2	57
	R2	18	0	0	6	0	0	24
S6	R1	36	3	6	9	24	0	78
	R2	35	1	1	1	2	0	40

Table B.2. Microplastic shape distribution in the water samples in September 2020.

Site	Replicate	Fiber	Hard Fragment	Soft Fragment	Pellet	Total
S1	R1	50	2	0	0	52
	R2	28	7	1	0	36
S2	R1	41	4	1	1	47
	R2	49	3	5	0	57
S3	R1	203	3	0	1	207
	R2	235	2	1	0	238
S4	R1	31	1	0	0	32
	R2	27	2	0	0	29
S5	R1	64	4	8	1	76
	R2	37	4	2	0	43
S6	R1	143	11	0	0	154
	R2	50	4	5	0	59

Table B.3. Microplastic shape distribution in the sediment samples in May 2019.

Site	Replicate	Fiber	Hard Fragment	Soft Fragment	Other	Total
S1	R1	2	2	0	0	4
	R2	2	1	0	0	3
	R3	4	0	0	0	4
S2	R1	1	0	0	0	1
	R2	1	3	0	0	4
	R3	0	6	0	0	6
S3	R1	2	0	0	0	2
	R2	7	0	0	0	7
	R3	3	0	0	0	3
S4	R1	1	0	0	1	2
	R2	1	2	1	0	4
	R3	2	2	1	0	5
S5	R1	1	5	1	0	7
	R2	4	20	0	0	24
	R3	8	10	0	0	18
S6	R1	8	0	0	0	8
	R2	9	2	0	0	11
	R3	1	4	0	0	5

Table B.4. Microplastic shape distribution in the sediment samples in September 2020.

Site	Replicate	Fiber	Hard Fragment	Soft Fragment	Pellet	Total
S1	R1	26	9	0	1	36
	R2	17	9	0	1	27
	R3	22	5	2	0	29
S2	R1	7	2	1	0	10
	R2	0	3	1	0	4
	R3	2	5	0	0	7
S3	R1	16	2	0	0	18
	R2	9	1	0	0	10
	R3	5	1	0	0	6
S4	R1	2	1	0	0	3
	R2	31	1	4	5	41
	R3	0	0	3	0	3
S5	R1	1	1	2	0	4
	R2	2	0	0	0	2
	R3	3	0	1	0	4
S6	R1	66	0	0	0	66
	R2	13	0	0	0	13
	R3	27	6	3	1	37

Table B.5. Microplastic size distribution in the water samples in May 2019.

Site	Replicate	45-1000 µm	1000-2000 µm	2000-3000 µm	3000-5000 µm	>5000 µm	Total
S1	R1	12	18	9	5	4	48
	R2	5	1	2	1	2	11
S2	R1	83	43	12	14	13	165
	R2	25	11	2	0	0	38
S3	R1	6	13	13	13	17	62
	R2	24	53	24	24	12	137
S4	R1	16	18	13	8	3	58
	R2	17	6	2	2	0	27
S5	R1	34	23	7	6	6	76
	R2	8	9	5	5	3	30
S6	R1	26	35	9	10	3	83
	R2	25	18	5	1	0	49

Table B.6. Microplastic size distribution in the water samples in September 2020.

Site	Replicate	45-1000 µm	1000-2000 µm	2000-3000 µm	3000-5000 µm	>5000 µm	Total
S1	R1	23	21	11	11	3	69
	R2	10	17	8	1	2	38
S2	R1	6	17	14	11	2	50
	R2	13	24	12	2	8	59
S3	R1	56	90	39	24	4	213
	R2	55	102	54	21	8	240
S4	R1	2	14	7	9	2	34
	R2	3	10	10	8	1	32
S5	R1	24	32	17	6	2	81
	R2	7	14	13	8	7	49
S6	R1	45	58	20	25	6	154
	R2	24	19	12	7	4	66

Table B.7. Microplastic size distribution in the sediment samples in May 2019.

Site	Replicate	45-1000 µm	1000-2000 µm	2000-3000 µm	3000-5000 µm	>5000 µm	Total
S1	R1	6	1	0	2	0	9
	R2	3	1	1	0	1	6
	R3	6	1	0	0	0	7
S2	R1	1	5	0	1	0	7
	R2	2	4	1	0	0	7
	R3	6	1	1	1	0	9
S3	R1	2	1	1	0	0	4
	R2	5	4	3	0	1	13
	R3	4	0	1	0	0	5
S4	R1	1	1	0	1	0	3
	R2	1	2	1	1	0	5
	R3	1	3	1	0	0	5
S5	R1	7	2	0	1	1	11
	R2	22	6	0	1	0	29
	R3	14	6	1	0	0	21
S6	R1	7	3	0	0	1	11
	R2	5	2	2	2	3	14
	R3	5	3	1	0	0	9

Table B.8. Microplastic size distribution in the sediment samples in September 2020.

Site	Replicate	45-1000 µm	1000-2000 µm	2000-3000 µm	3000-5000 µm	>5000 µm	Total
S1	R1	16	21	4	0	0	41
	R2	12	12	8	0	0	32
	R3	17	13	2	1	1	34
S2	R1	6	4	0	1	1	12
	R2	2	2	0	0	0	4
	R3	6	1	1	0	0	8
S3	R1	10	5	4	0	0	19
	R2	3	7	1	0	0	11
	R3	3	4	0	0	0	7
S4	R1	2	4	0	0	0	6
	R2	23	11	7	3	0	44
	R3	0	0	2	0	2	4
S5	R1	0	2	0	2	1	5
	R2	2	1	1	0	0	4
	R3	1	3	1	0	0	5
S6	R1	54	14	1	0	0	69
	R2	9	5	0	1	0	15
	R3	24	10	3	1	1	39

Table B.9. Microplastic color distribution in water samples in May 2019.

Site	Replicate	Black	Blue	Red	White	Green	Brown	Orange	Pink	Transparent	Yellow	Total
S1	R1	0	17	2	5	0	0	4	0	0	0	28
	R2	3	2	1	2	0	3	0	0	0	0	11
S2	R1	68	43	14	15	3	0	2	2	0	0	147
	R2	17	12	2	4	0	3	0	0	0	0	38
S3	R1	36	1	13	1	0	0	0	0	0	0	51
	R2	52	52	11	2	1	7	1	0	0	0	126
S4	R1	32	5	6	2	1	4	0	1	1	0	52
	R2	3	7	3	2	0	0	1	0	1	2	19
S5	R1	21	16	4	3	4	5	0	0	4	0	57
	R2	11	2	5	6	0	0	0	0	0	0	24
S6	R1	17	15	7	33	1	0	0	0	5	0	78
	R2	23	7	6	3	0	0	0	0	1	0	40

Table B.10. Microplastic color distribution in water samples in September 2020.

Site	Replicate	Black	Blue	Red	White	Green	Brown	Orange	Pink	Transparent	Yellow	Purple	Grey	Total
S1	R1	31	17	2	0	0	2	0	0	0	0	0	0	52
	R2	18	13	1	1	0	2	0	0	0	0	0	1	36
S2	R1	28	10	7	0	0	1	0	0	1	0	0	0	47
	R2	27	11	14	0	0	1	0	1	0	1	0	2	57
S3	R1	110	46	38	0	2	0	0	2	0	2	7	0	207
	R2	126	61	37	0	3	2	0	0	0	1	8	0	238
S4	R1	19	4	8	0	0	1	0	0	0	0	0	0	32
	R2	15	7	7	0	0	0	0	0	0	0	0	0	29
S5	R1	28	26	12	5	0	1	3	1	0	1	0	0	77
	R2	31	7	4	0	0	0	0	1	0	0	0	0	43
S6	R1	75	38	25	0	6	0	8	0	0	1	1	0	154
	R2	38	9	7	2	1	0	0	1	0	0	0	1	59

Table B.11. Microplastic color distribution in sediment samples in May 2019.

Site	Replicate	Black	Blue	Red	White	Green	Brown	Transparent	Purple	Grey	Crystalline	Total
S1	R1	1	0	0	1	1	0	0	1	0	0	4
	R2	0	0	2	0	1	0	0	0	0	0	3
	R3	3	0	0	0	1	0	0	0	0	0	4
S2	R1	0	1	0	0	0	0	0	0	0	0	1
	R2	0	0	1	1	0	0	2	0	0	0	4
	R3	0	0	0	0	0	0	6	0	0	0	6
S3	R1	0	0	0	0	0	2	0	0	0	0	2
	R2	3	1	0	0	0	3	0	0	0	0	7
	R3	1	2	0	0	0	0	0	0	0	0	3
S4	R1	0	0	0	2	0	0	0	0	0	0	2
	R2	0	0	1	3	0	0	0	0	0	0	4
	R3	1	1	0	1	0	0	1	0	1	0	5
S5	R1	1	1	0	0	0	0	4	0	0	1	7
	R2	2	1	0	0	0	1	16	0	0	4	24
	R3	3	2	2	0	0	1	6	0	0	4	18
S6	R1	5	0	1	0	1	0	0	1	0	0	8
	R2	4	0	3	2	1	1	0	0	0	0	11
	R3	0	0	1	2	0	0	2	0	0	0	5

Table B.12. Microplastic color distribution in sediment samples in September 2020.

Site	Replicate	Black	Blue	Red	White	Green	Brown	Orange	Pink	Transparent	Yellow	Purple	Grey	Total
S1	R1	17	5	6	1	0	0	0	0	4	0	0	3	36
	R2	6	6	8	2	2	1	0	1	0	1	0	0	27
	R3	15	4	6	1	0	0	0	0	2	0	0	1	29
S2	R1	2	0	6	1	0	0	0	0	1	0	0	0	10
	R2	2	0	0	0	0	0	0	0	2	0	0	0	4
	R3	2	2	1	0	1	0	0	0	0	1	0	0	7
S3	R1	12	4	2	0	0	0	0	0	0	0	0	0	18
	R2	7	3	0	0	0	0	0	0	0	0	0	0	10
	R3	4	1	1	0	0	0	0	0	0	0	0	0	6
S4	R1	2	1	0	0	0	0	0	0	0	0	0	0	3
	R2	22	9	5	0	0	0	0	0	1	1	2	1	41
	R3	0	0	0	0	0	0	0	0	3	0	0	0	3
S5	R1	1	0	0	1	0	0	0	0	2	0	0	0	4
	R2	1	0	1	0	0	0	0	0	0	0	0	0	2
	R3	3	0	0	1	0	0	0	0	0	0	0	0	4
S6	R1	35	18	9	0	2	0	1	1	0	0	0	0	66
	R2	6	3	0	0	1	0	0	3	0	0	0	0	13
	R3	11	12	5	1	1	0	1	0	5	0	1	0	37

Table B.13. Polymer distribution in water and sediment samples.

Sample	Plastic							Plastic additive	Non-plastic		n/a	Total
	PS	PA	PET	PE	PP	PI	PSU/PA Composite	Mortoperm Blue	SiO_2	Cotton		
Water	21	29	31	21	5	2	0	1	1	2	36	149
Sediment	14	3	0	5	2	0	1	0	8	4	14	51
Total	35	32	31	26	7	2	1	1	9	6	50	200

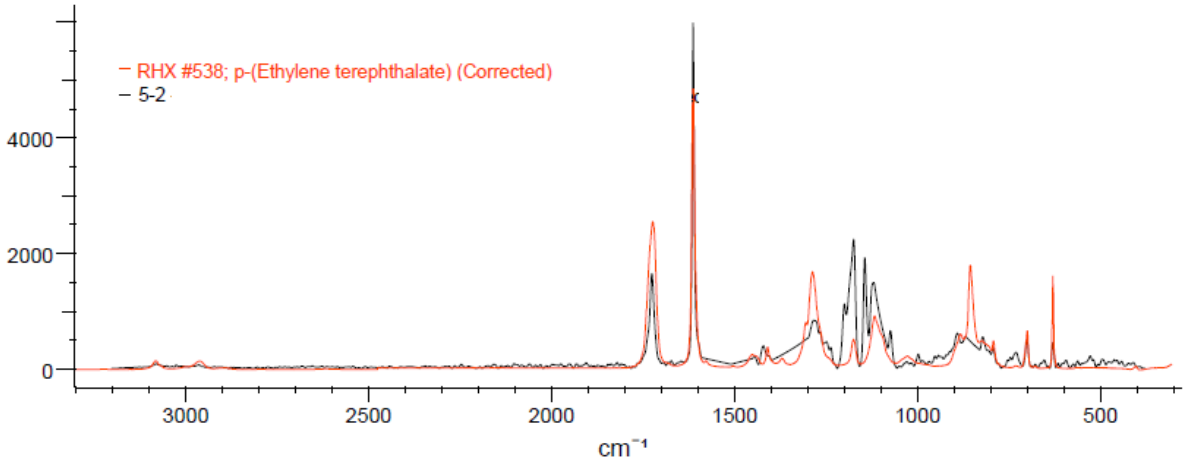

Figure B.1. Raman spectrum of PET particle in the water sample from Site 3.

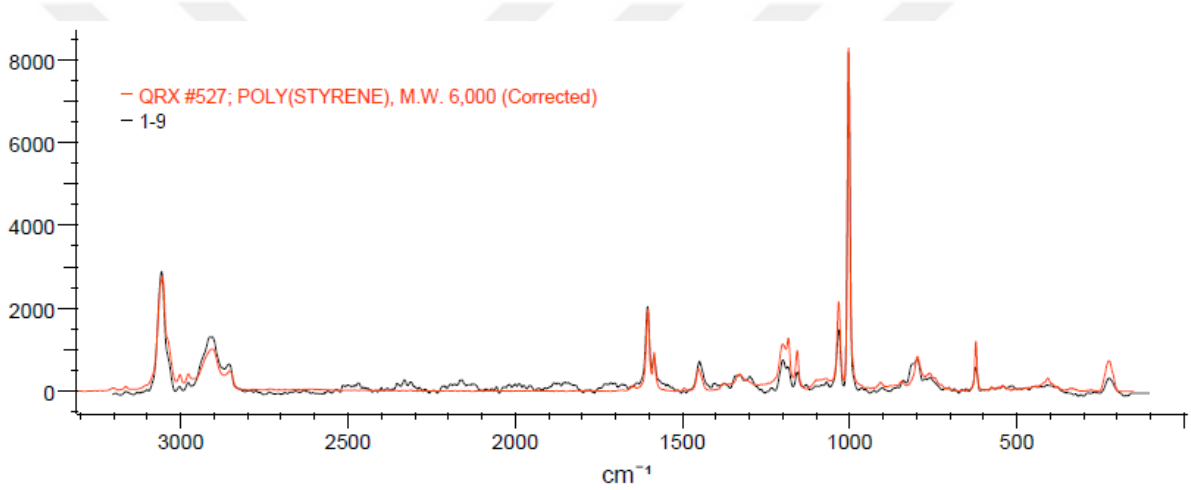

Figure B.2. Raman spectrum of PS particle in the water sample from Site 1.

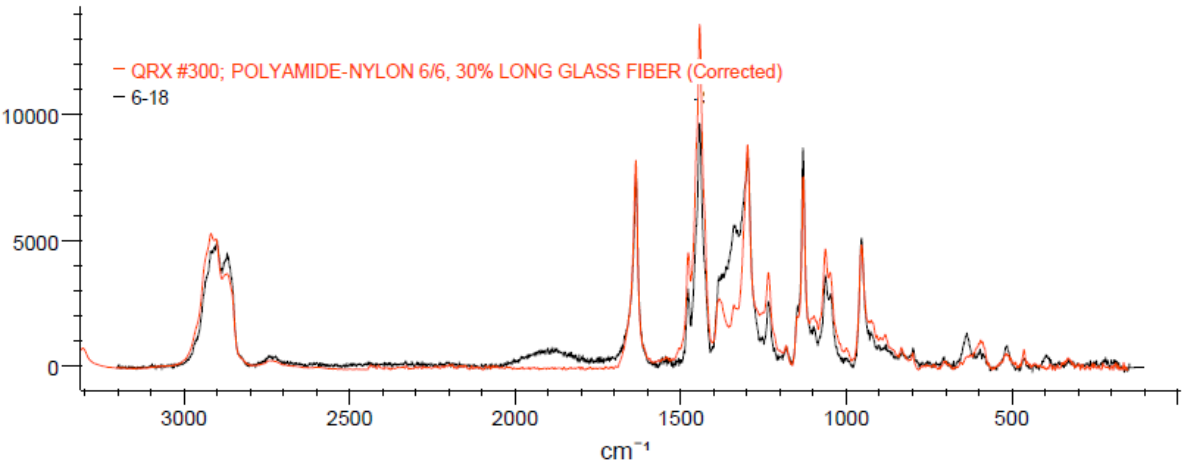

Figure B.3. Raman spectrum of PA particle in the water sample from Site 3.

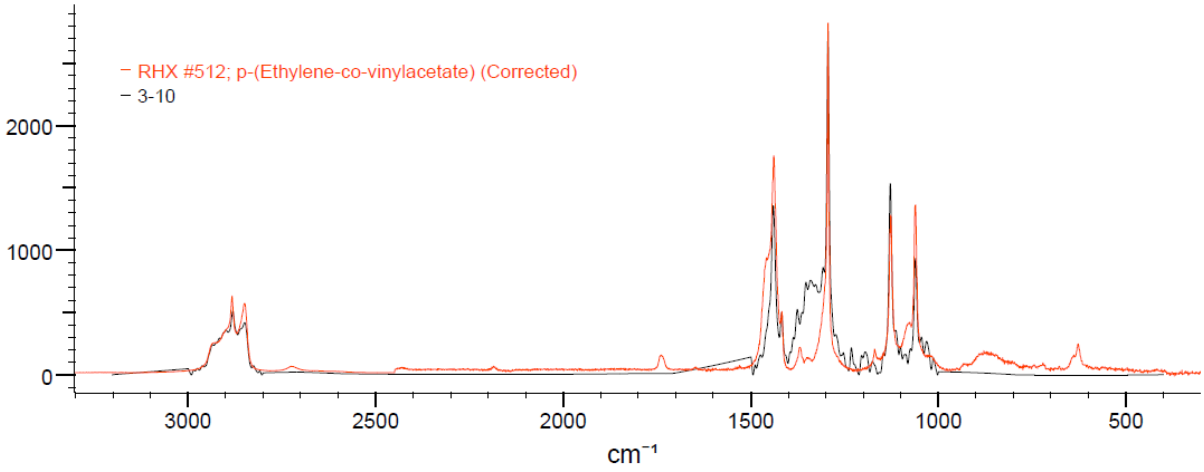

Figure B.4. Raman spectrum of poly(ethylene-co-vinylacetate) particle in the water sample from Site 2.

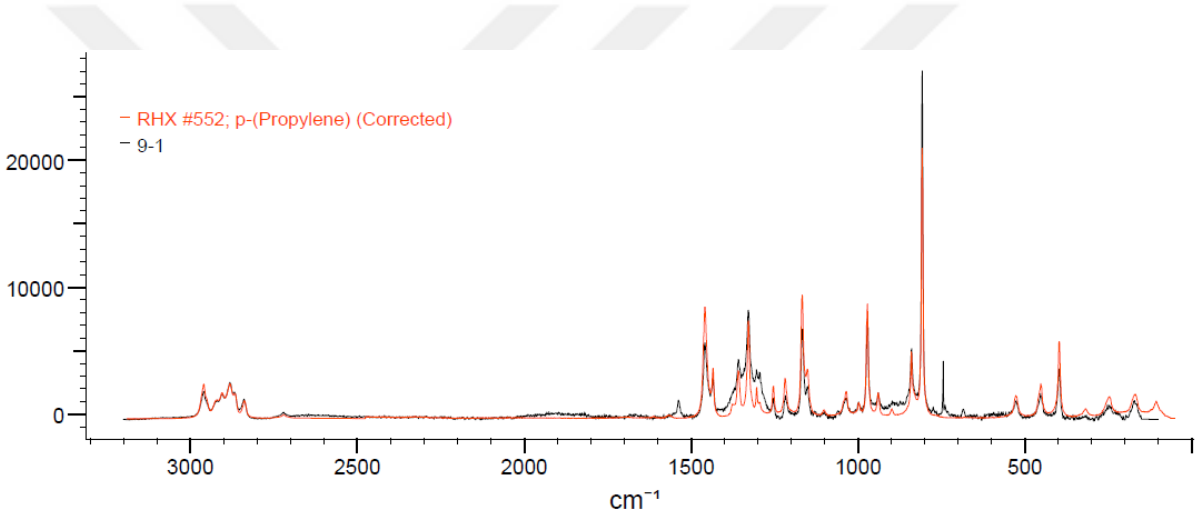

Figure B.5. Raman spectrum of PP particle in the water sample from Site 5.

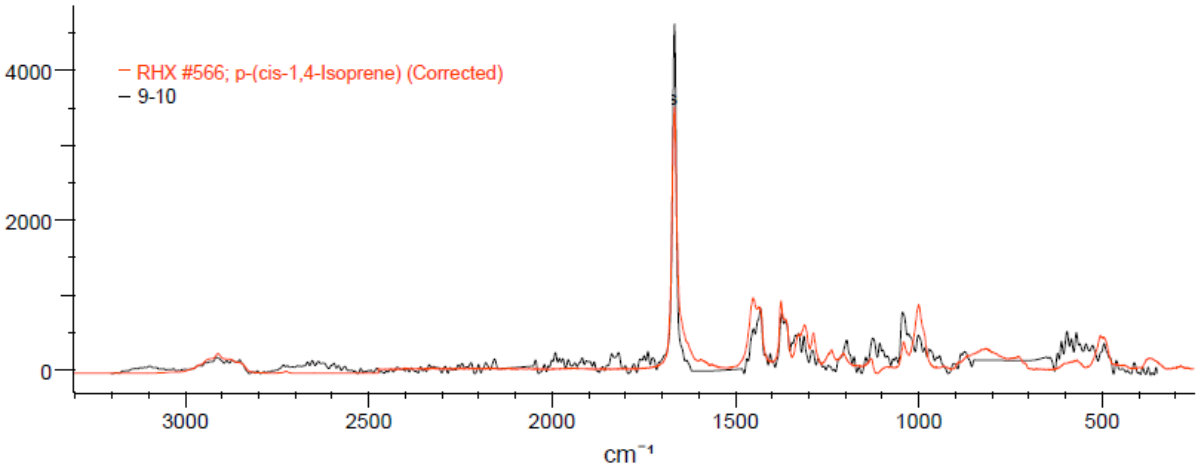

Figure B.6. Raman spectrum of PI particle in the water sample from Site 5.

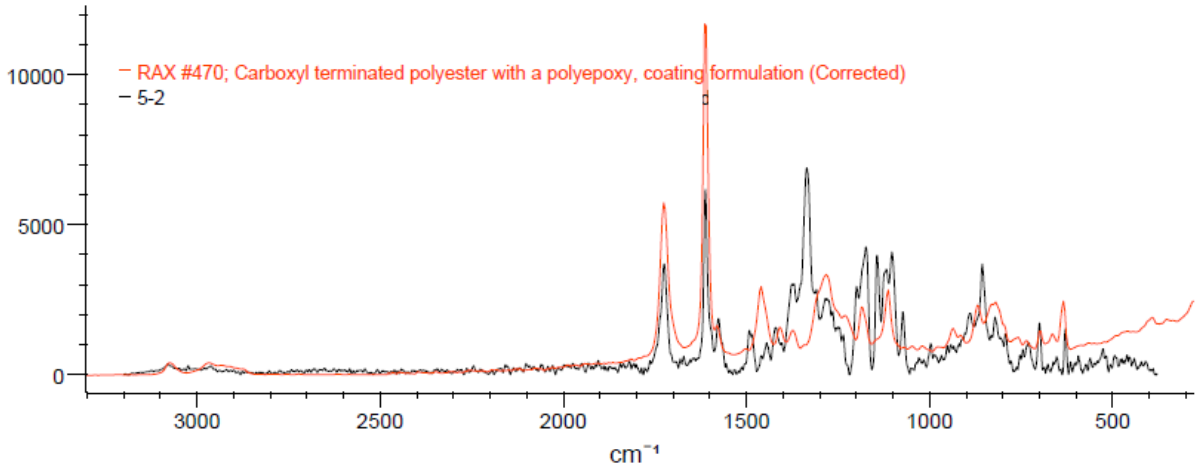

Figure B.7. Raman spectrum of carboxyl-terminated polyester with epoxy coating found in the water sample from Site 3.

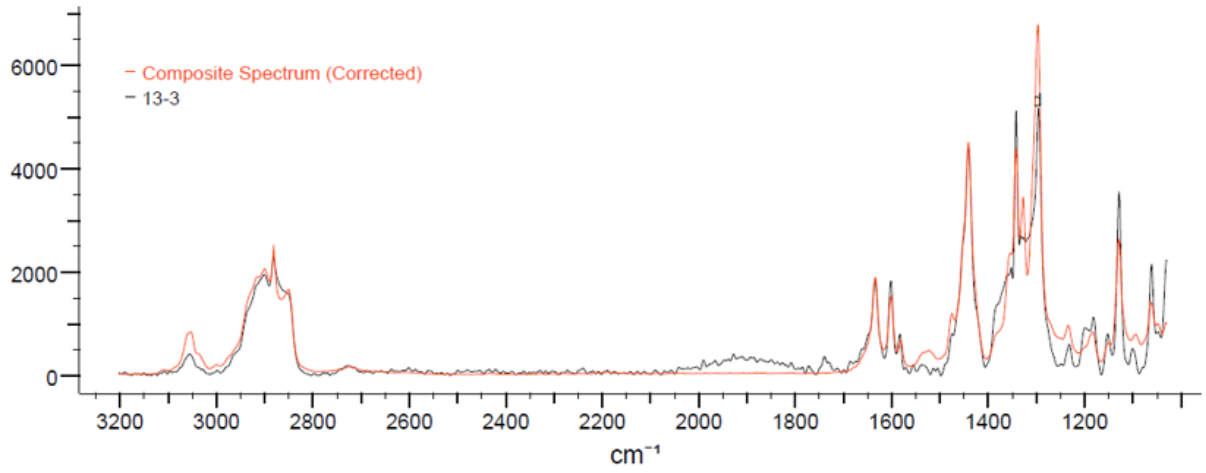

Figure B.8. Raman spectrum of a composite polymer (PSU/PA) found in the sediment sample from Site 1.

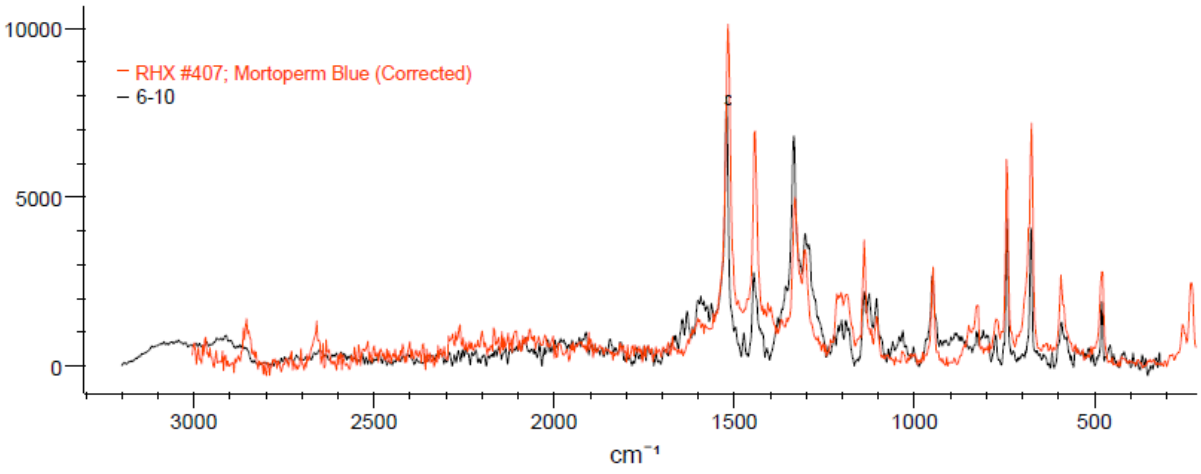

Figure B.9. Raman spectrum of a plastic colorant (Mortoperm blue) found in the water sample from Site 3.

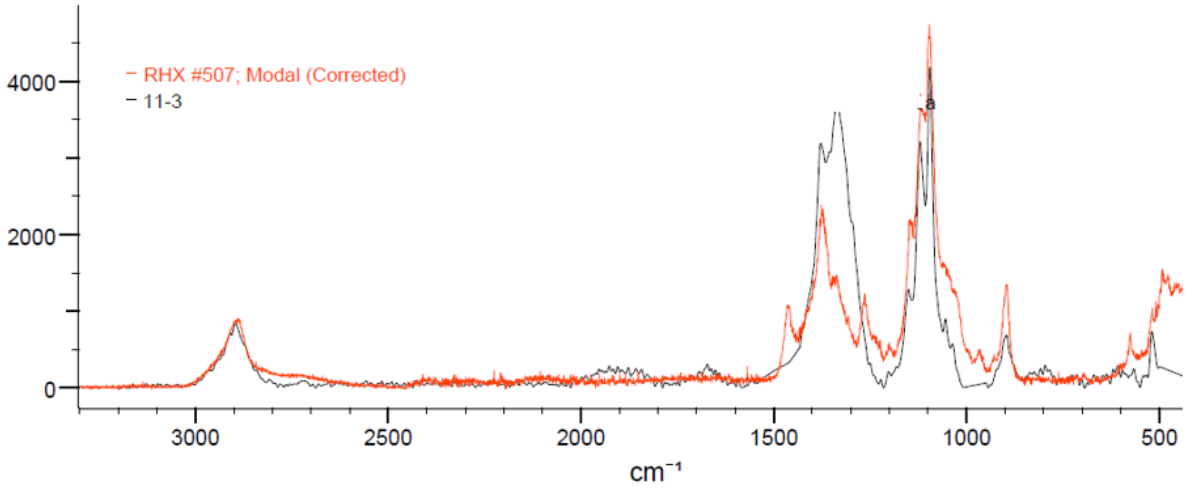

Figure B.10. Raman spectrum of modal particle in the water sample from Site 6.

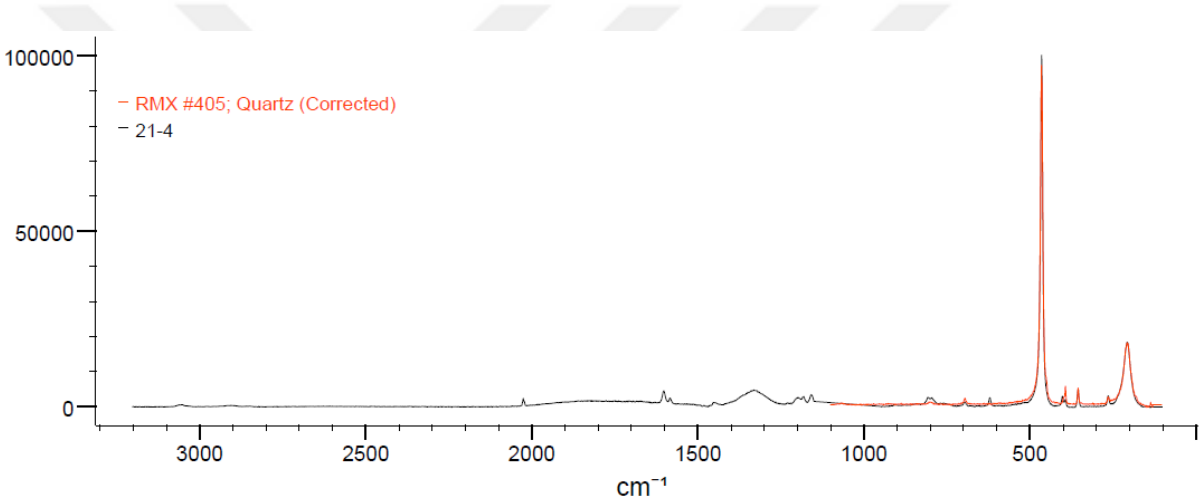

Figure B.11. Raman spectrum of quartz (SiO_2) particle in the sediment sample from Site 5.

APPENDIX C: SETTLING VELOCITIES OF MICROPLASTICS WITH DIFFERENT TYPE AND SHAPE

Table C.1. Calculation of the settling velocity of near-spherical polymers.

T (°C)	ρ_p (kg m^{-3})			ρ_w (kg m^{-3})	μ (m^2 s^{-1})	g (m s^{-2})	a (mm)	φ	D_n (m)	D_*		
	PS	PA	PET							PS	PA	PET
20	1050	1140	1390	998	1E-06	9.81	0.069	0.95	0.00007	0.14	0.39	1.08
20	1050	1140	1390	998	1E-06	9.81	0.371	0.95	0.00035	22.28	60.83	167.93
20	1050	1140	1390	998	1E-06	9.81	1.167	0.95	0.00111	693.31	1893.28	5226.52
20	1050	1140	1390	998	1E-06	9.81	1.895	0.95	0.00180	2968.55	8106.43	22378.32
20	1050	1140	1390	998	1E-06	9.81	1.927	0.95	0.00183	3121.49	8524.08	23531.25
20	1050	1140	1390	998	1E-06	9.81	3.565	0.95	0.00339	19764.95	53973.52	148997.33

Table C.1. (continued).

$log\omega_*$			ω_*			ω_s (m s^{-1})		
PS	PA	PET	PS	PA	PET	PS	PA	PET
-5.46	-4.57	-3.70	0.00	0.00	0.00	0.00	0.00	0.00
-1.36	-0.66	-0.01	0.04	0.22	0.98	0.00	0.01	0.02
0.83	1.36	1.86	6.71	23.13	72.68	0.02	0.03	0.07
1.59	2.06	2.50	38.91	115.45	313.13	0.03	0.05	0.11
1.61	2.08	2.52	41.18	121.58	328.13	0.03	0.06	0.11
2.45	2.84	3.19	278.65	686.88	1557.89	0.05	0.10	0.18

Table C.2. Calculation of the settling velocity of fragment polymers.

T (°C)	ρ_p (kg m^{-3})			ρ_w (kg m^{-3})	μ (m^2 s^{-1})	g (m s^{-2})	a (mm)	φ	D_n (m)	D_*		
	PS	PA	PET							PS	PA	PET
20	1050	1140	1390	998	1E-06	9.81	0.138	0.6	0.0001	0.29	0.79	2.18
20	1050	1140	1390	998	1E-06	9.81	0.265	0.6	0.0002	2.05	5.58	15.42
20	1050	1140	1390	998	1E-06	9.81	0.697	0.6	0.0004	37.21	101.62	280.53
20	1050	1140	1390	998	1E-06	9.81	1.131	0.6	0.0007	159.00	434.18	1198.59
20	1050	1140	1390	998	1E-06	9.81	2.858	0.6	0.0017	2565.59	7006.03	19340.58
20	1050	1140	1390	998	1E-06	9.81	3.234	0.6	0.0019	3717.24	10150.91	28022.24

Table C.2. (continued).

$log\omega_*$			ω_*			ω_s (m s^{-1})		
PS	PA	PET	PS	PA	PET	PS	PA	PET
-4.84	-3.97	-3.13	0.00	0.00	0.00	0.000	0.001	0.001
-3.18	-2.38	-1.62	0.00	0.00	0.02	0.001	0.002	0.005
-1.00	-0.33	0.30	0.10	0.47	2.01	0.004	0.009	0.020
-0.04	0.56	1.13	0.90	3.64	13.34	0.008	0.017	0.037
1.52	2.00	2.44	32.94	99.20	272.98	0.026	0.052	0.102
1.70	2.16	2.59	50.08	145.26	385.36	0.029	0.059	0.114

Table C.3. Calculation of the settling velocity of fiber polymers.

T (°C)	ρ_p (kg m^{-3})			ρ_w (kg m^{-3})	μ (m^2 s^{-1})	g (m s^{-2})	a (mm)	φ	D_n (m)	D_*		
	PS	PA	PET							PS	PA	PET
20	1050	1140	1390	998	1E-06	9.81	1.10	0.1	0.0001	0.68	1.85	5.11
20	1050	1140	1390	998	1E-06	9.81	2.25	0.1	0.0002	5.80	15.83	43.69
20	1050	1140	1390	998	1E-06	9.81	4.25	0.1	0.0004	39.06	106.66	294.44
20	1050	1140	1390	998	1E-06	9.81	5.00	0.1	0.0005	63.60	173.68	479.45

Table C.3. (continued).

$log\omega_*$			ω_*			ω_s (m s^{-1})		
PS	PA	PET	PS	PA	PET	PS	PA	PET
-4.10	-3.26	-2.45	0.00	0.00	0.00	3.45E-04	9.17E-04	2.39E-03
-2.35	-1.60	-0.89	0.00	0.02	0.13	1.31E-03	3.27E-03	7.94E-03
-0.96	-0.30	0.33	0.11	0.51	2.15	3.82E-03	8.91E-03	2.03E-02
-0.63	0.01	0.62	0.23	1.03	4.15	4.92E-03	1.13E-02	2.52E-02

APPENDIX D: MODELING MICROPLASTIC TRANSPORT IN GOLDSIM SOFTWARE

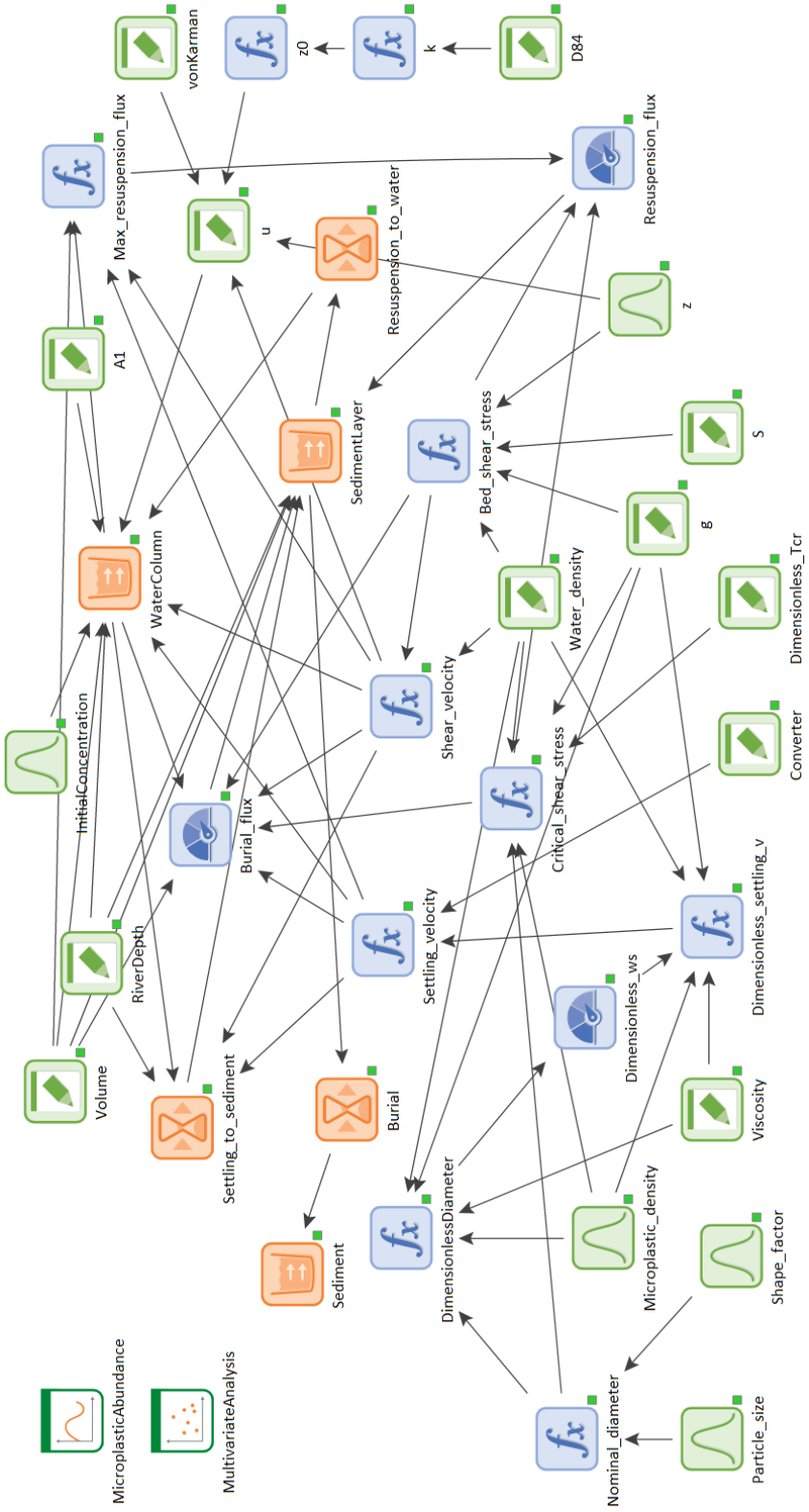

Figure D.1. Model layout in GoldSim.

As mentioned in Section 4.2, water samples were collected in duplicates, therefore initial concentrations (C_0) were entered to the model considering the range of microplastic concentrations in water for each each sampling site. Apart from this, the model was also run utilizing the mean values of C_0 to examine the effect of microplastic levels on the model results more clearly. The model results for the water column and sediment are given from Figure D.2 to D.5 for the years 2019 and 2020, respectively.

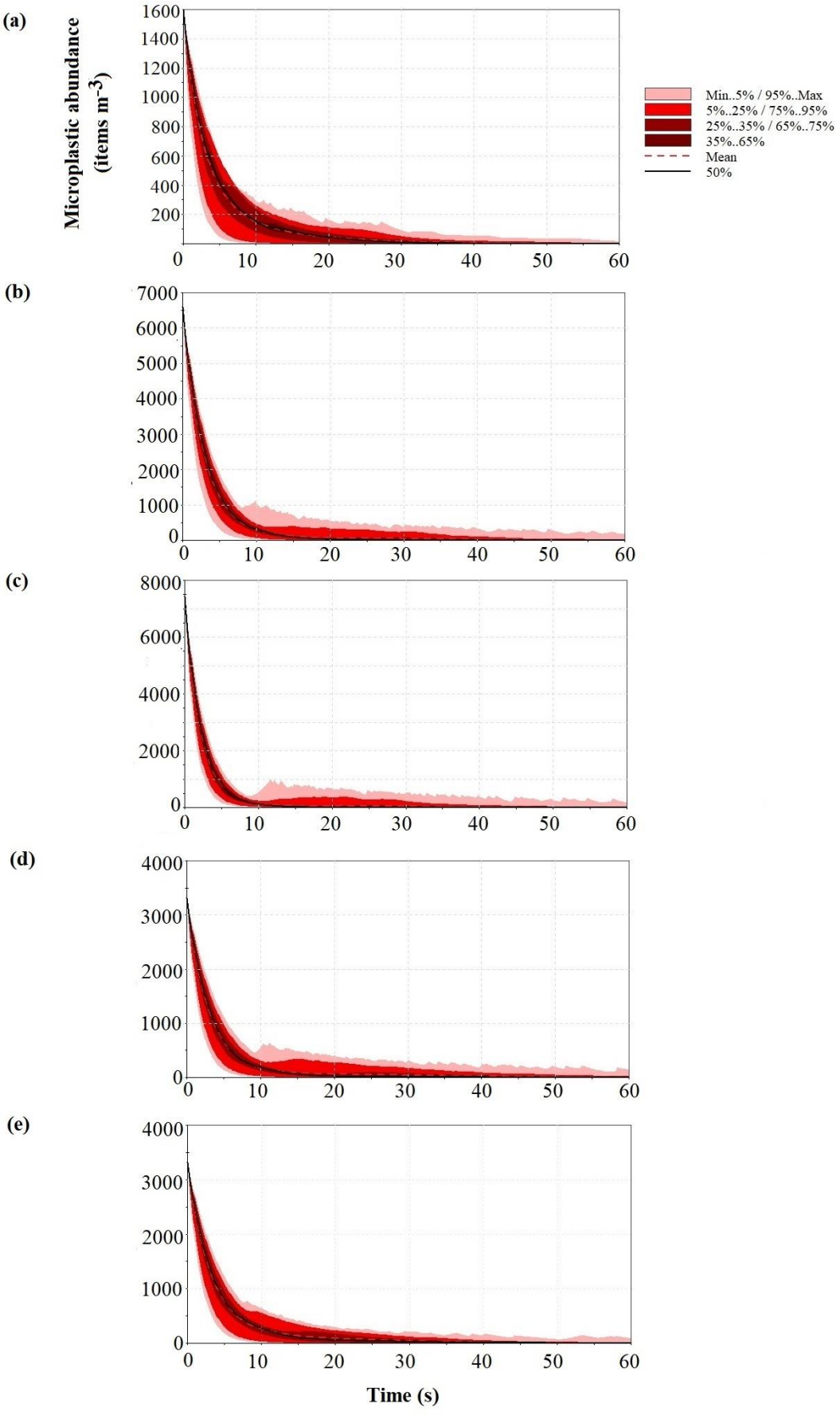

Figure D.2. Probable variation of microplastic concentration in water under turbulent flow conditions in (a) Site 1, (b) Site 2, (c) Site 3, (d) Site 4, and (e) Site 5 in 2019 (with mean C_0).

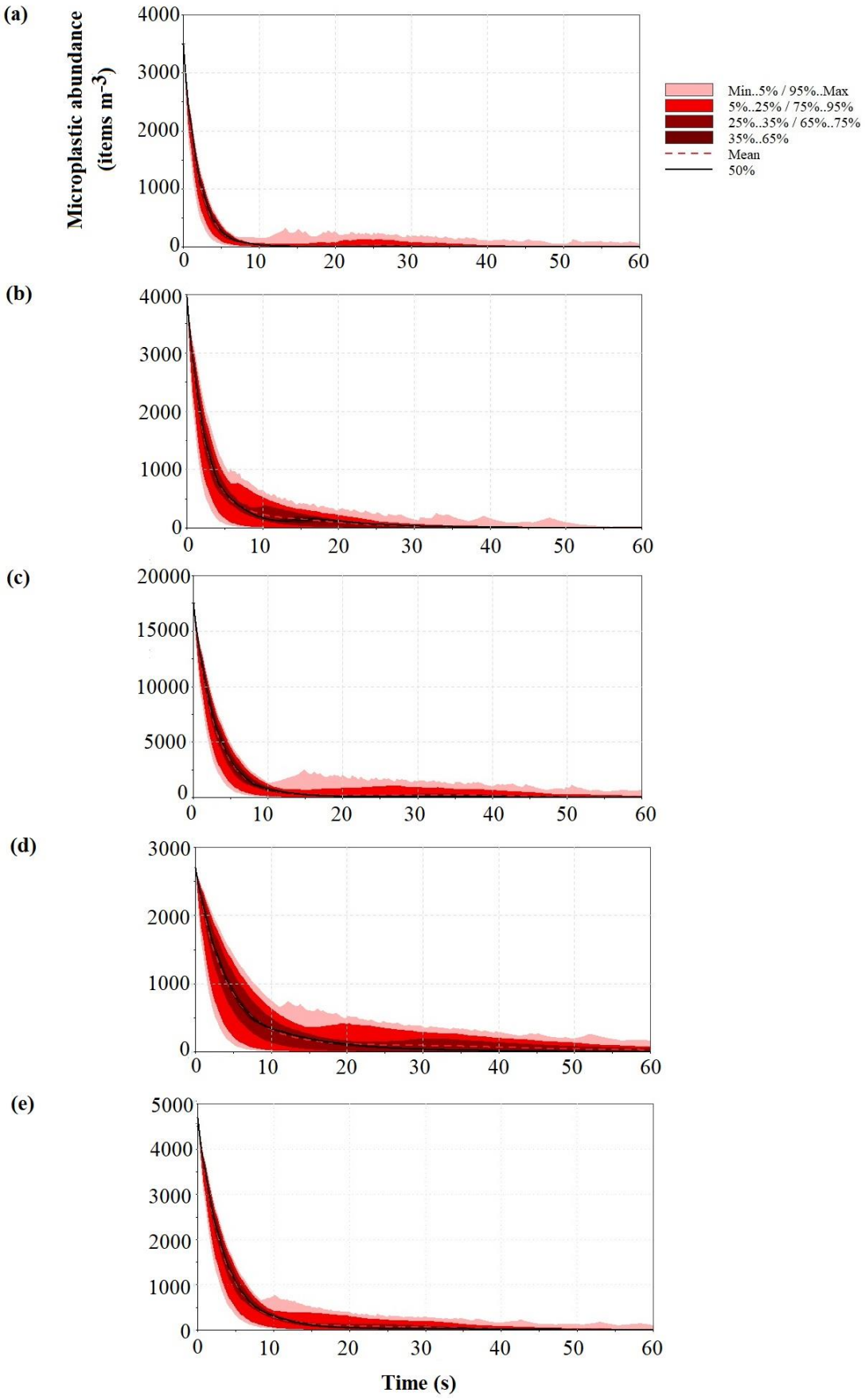

Figure D.3. Probable variation of microplastic concentration in water under turbulent flow conditions in (a) Site 1, (b) Site 2, (c) Site 3, (d) Site 4, and (e) Site 5 in 2020 (with mean C_0).

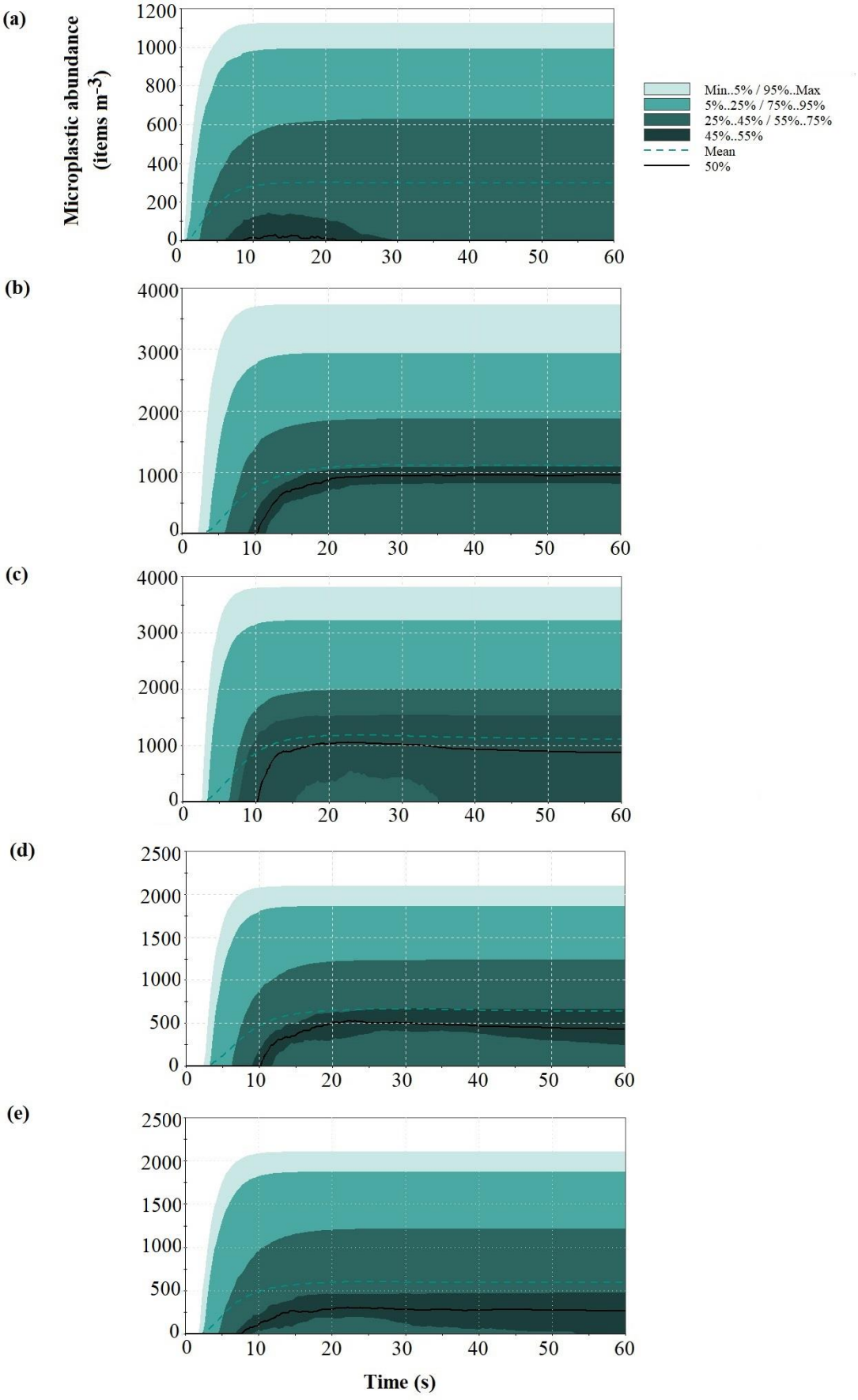

Figure D.4. Probable variation of microplastic concentration in sediment under turbulent flow conditions in (a) Site 1, (b) Site 2, (c) Site 3, (d) Site 4, and (e) Site 5 in 2019 (with mean C_0).

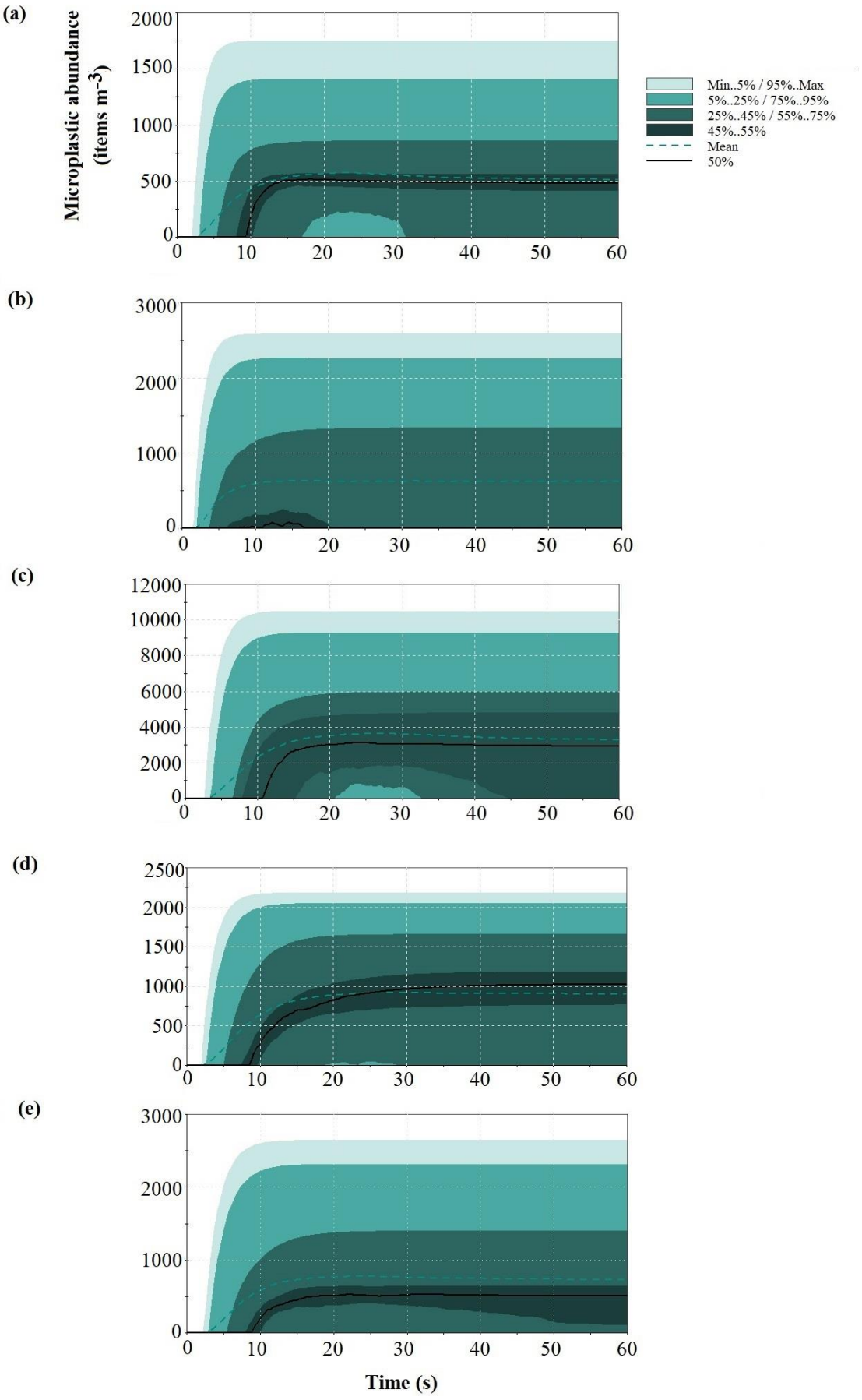

Figure D.5. Probable variation of microplastic concentration in sediment under turbulent flow conditions in (a) Site 1, (b) Site 2, (c) Site 3, (d) Site 4, and (e) Site 5 in 2020 (with mean C_0).

APPENDIX E: SCENARIO ANALYSIS

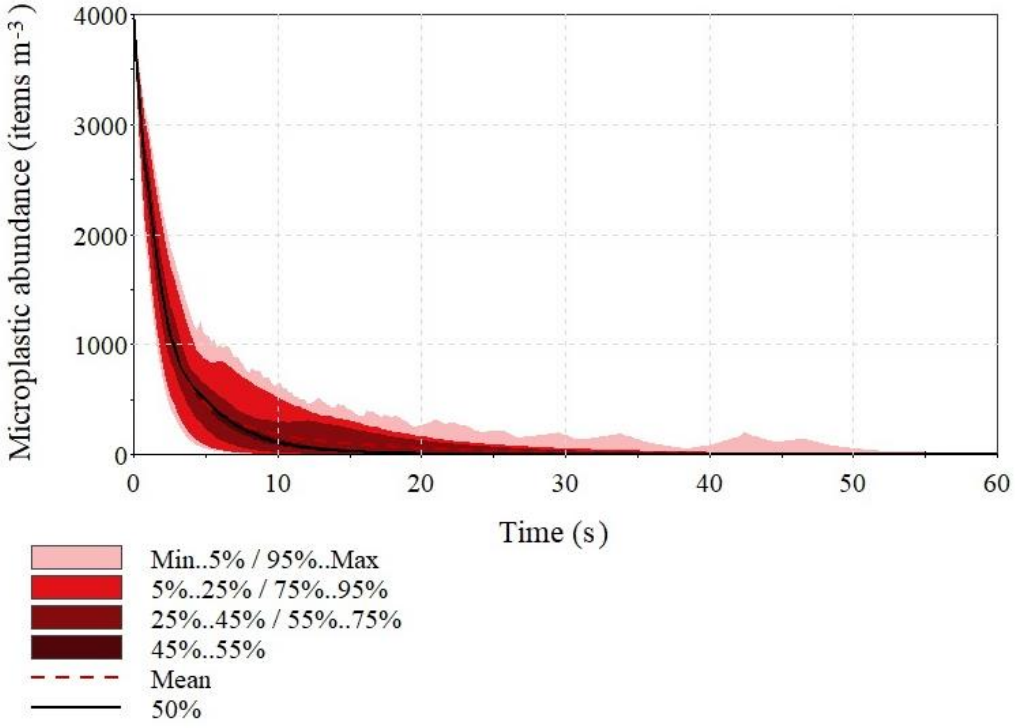

Figure E.1. Probable variation of concentration of near-spherical particles in water within Site 2.

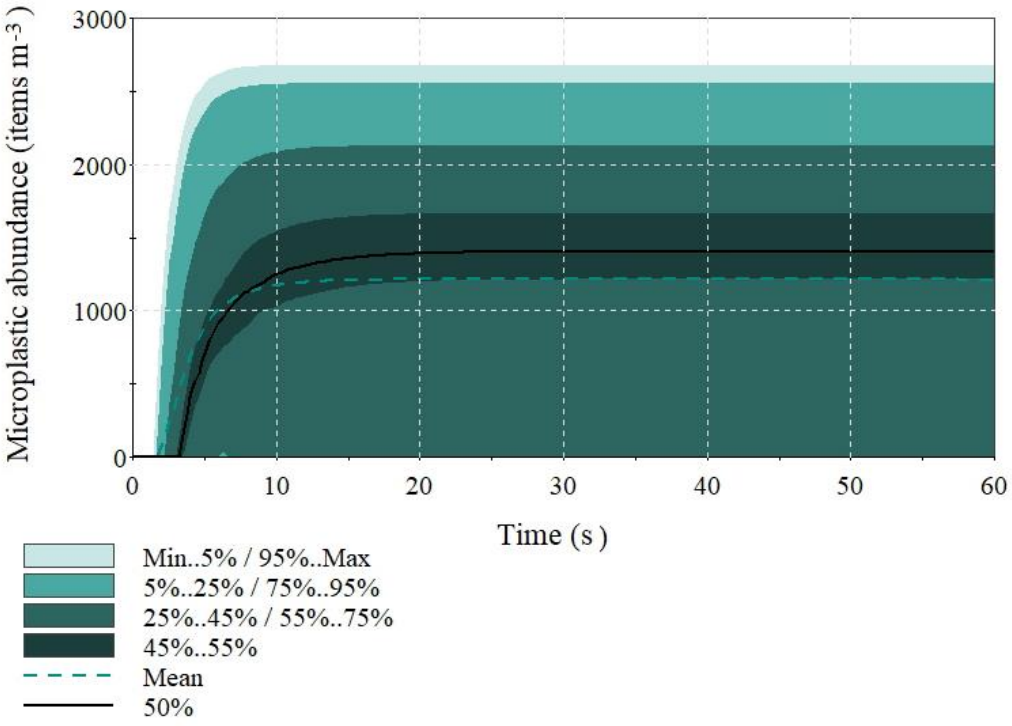

Figure E.2. Probable variation of concentration of near-spherical particles in sediment within Site 2.

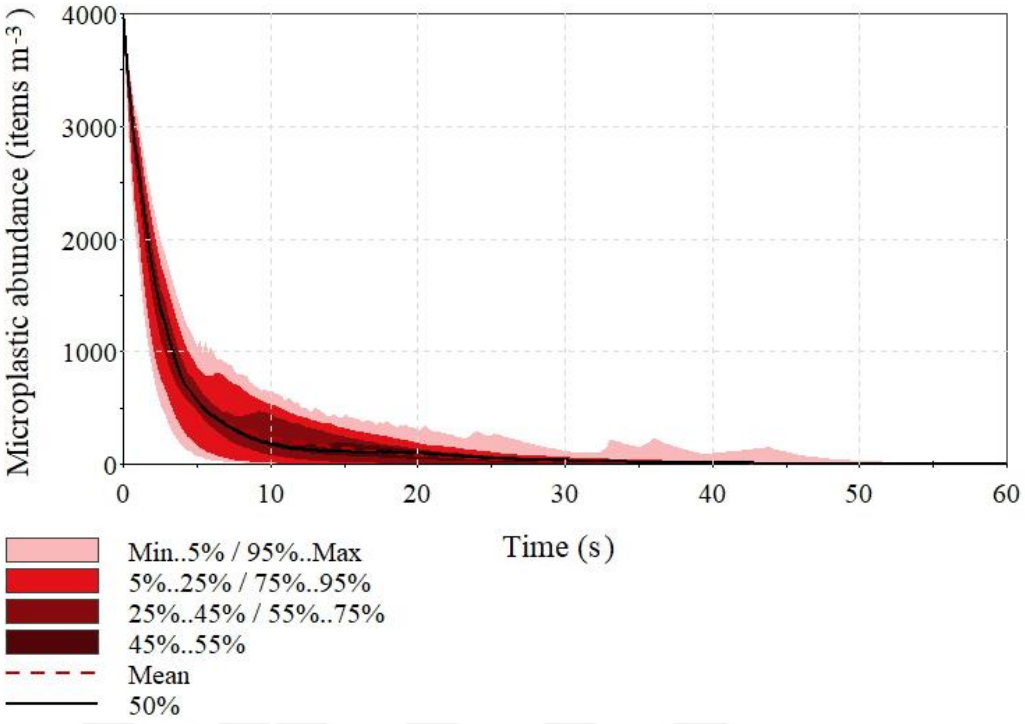

Figure E.3. Probable variation of concentration of fragments in water within Site 2.

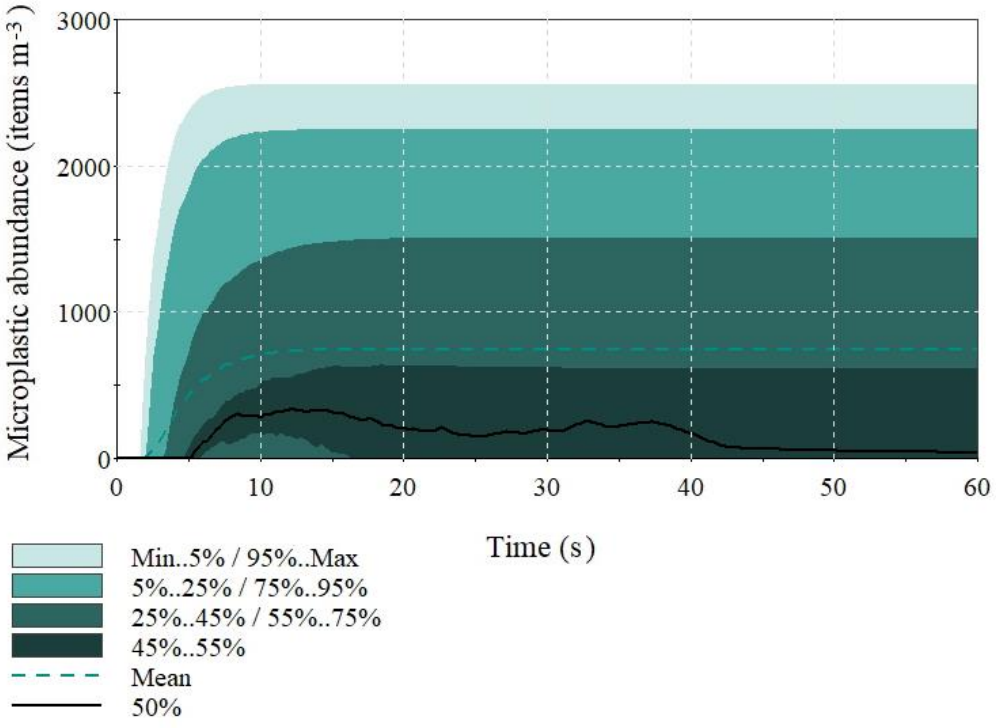

Figure E.4. Probable variation of concentration of fragments in sediment within Site 2.

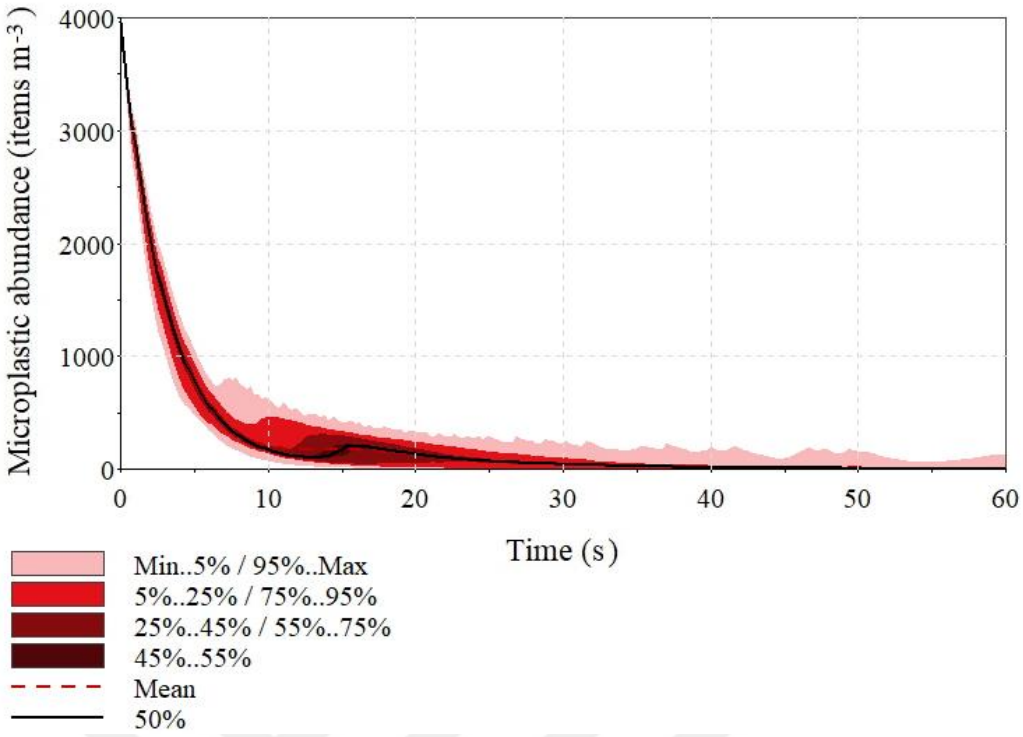

Figure E.5. Probable variation of concentration of fibers in water within Site 2.

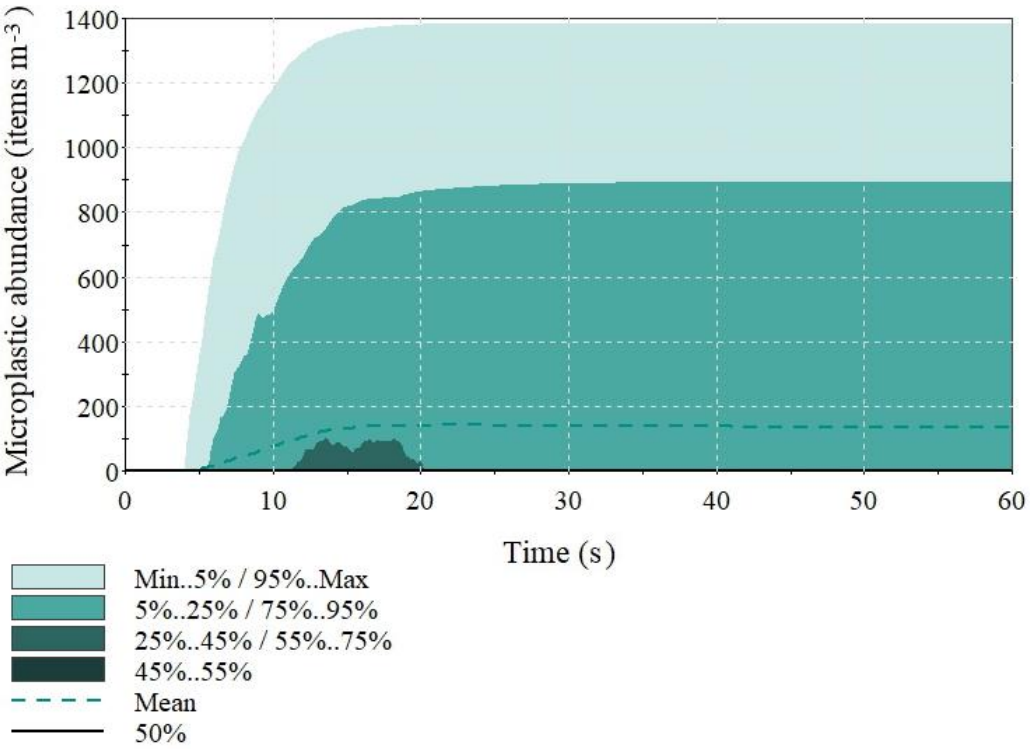

Figure E.6. Probable variation of concentration of fibers in sediment within Site 2.

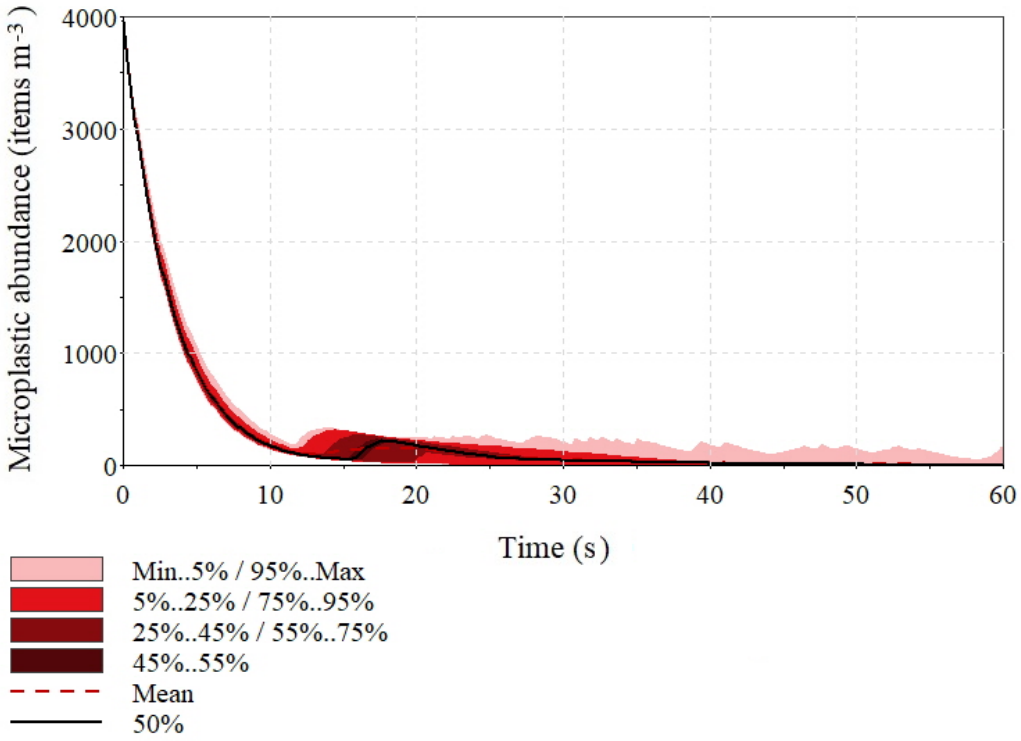

Figure E.7. Probable variation of concentration of 50 µm-particles in water within Site 2.

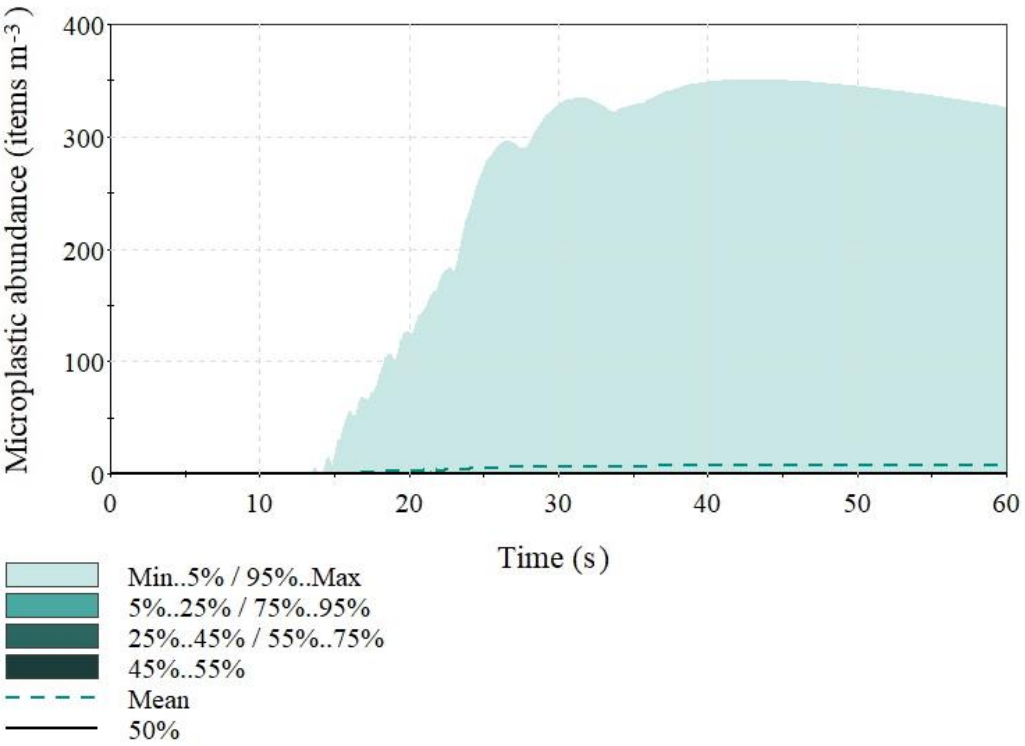

Figure E.8. Probable variation of concentration of 50 µm-particles in sediment within Site 2.

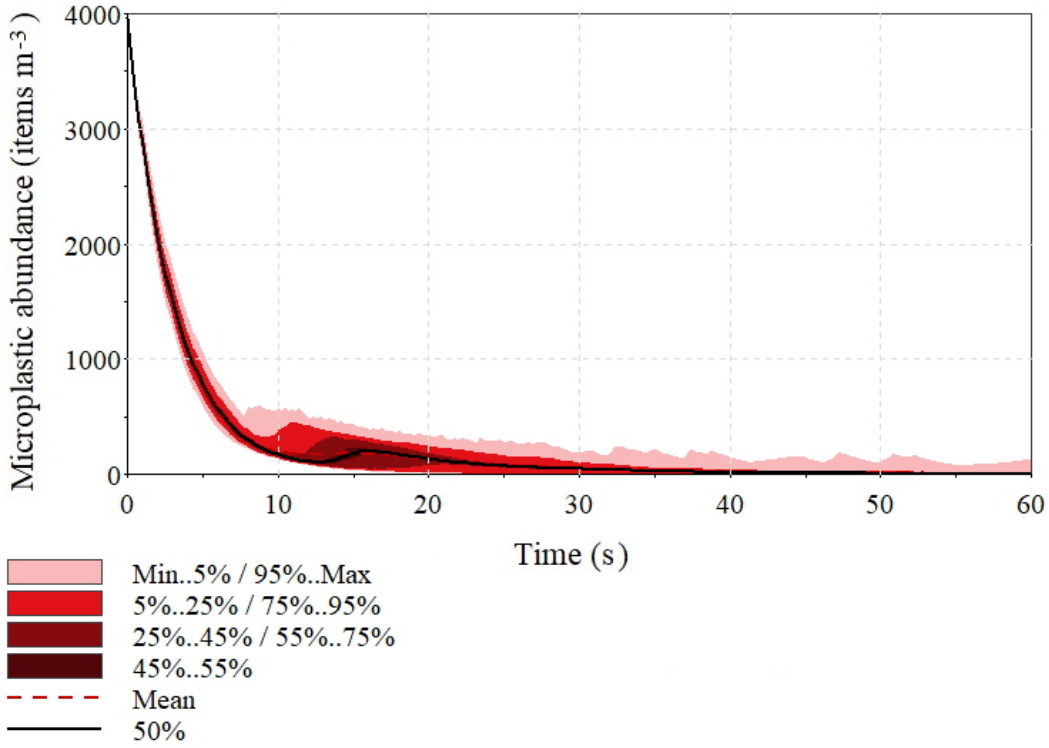

Figure E.9. Probable variation of concentration of 500 µm-particles in water within Site 2.

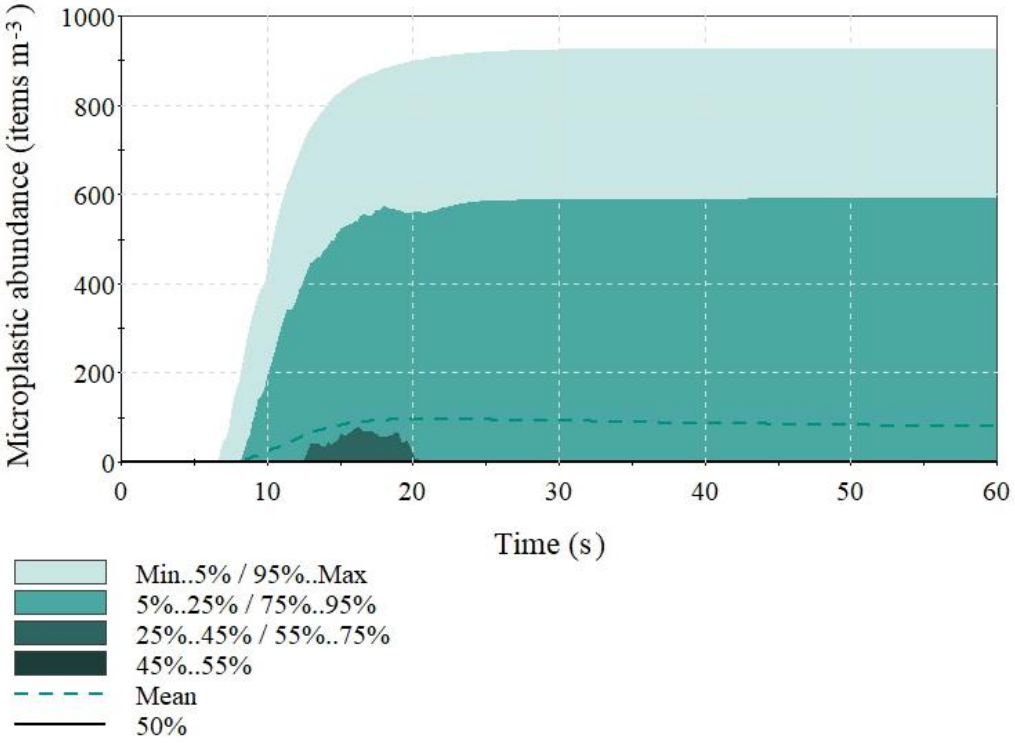

Figure E.10. Probable variation of concentration of 500 µm-particles in sediment within Site 2.

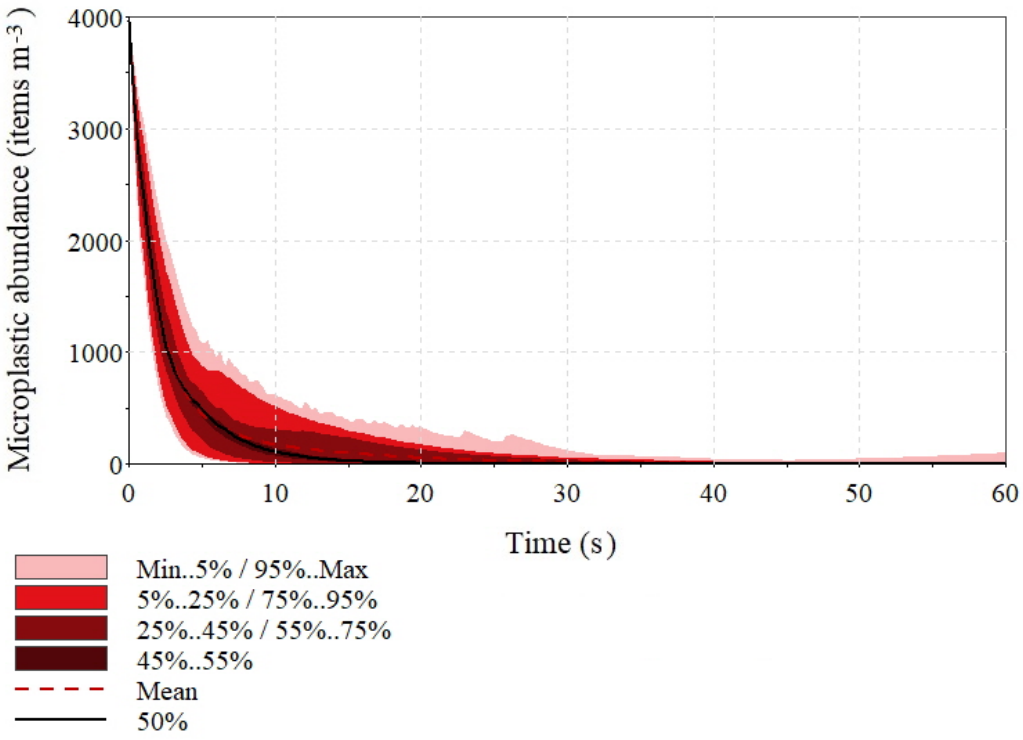

Figure E.11. Probable variation of concentration of 5000 µm-particles in water within Site 2.

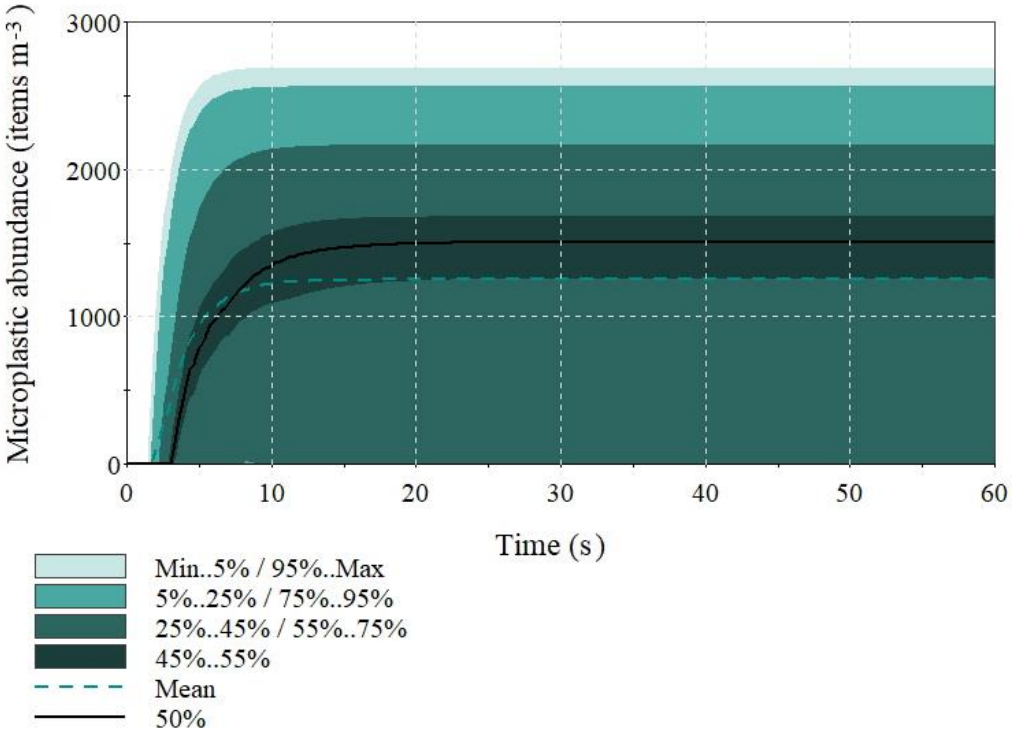

Figure E.12. Probable variation of concentration of 5000 µm-particles in sediment within Site 2.

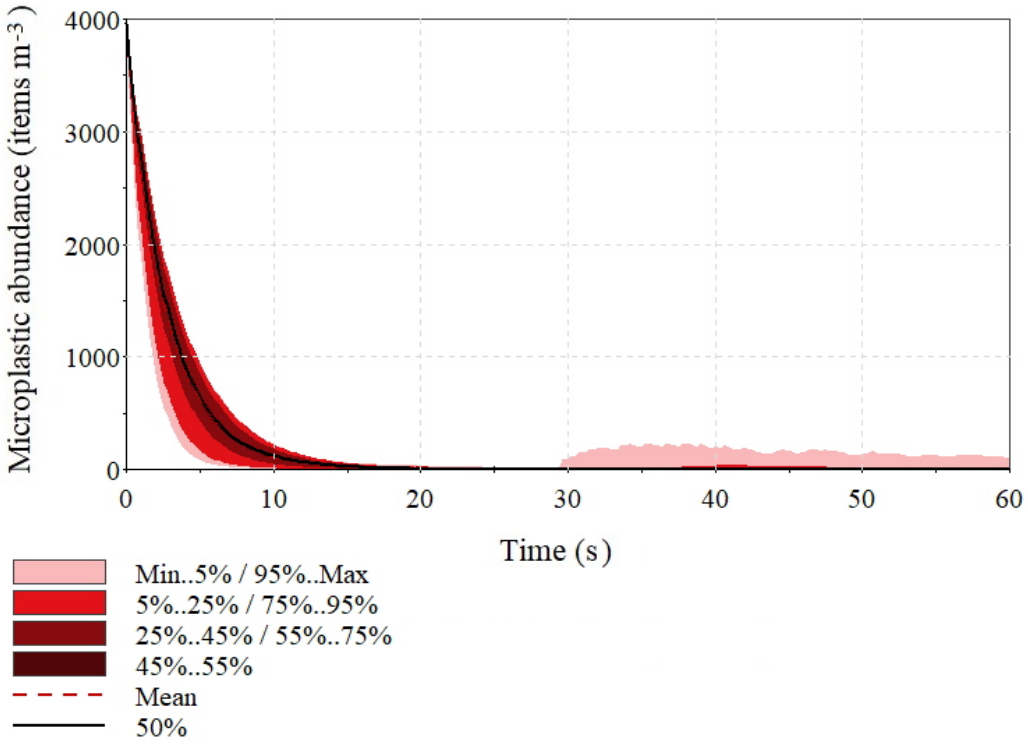

Figure E.13. Probable variation of microplastic concentration in water under 0.15 N m^{-2} bed shear stress.

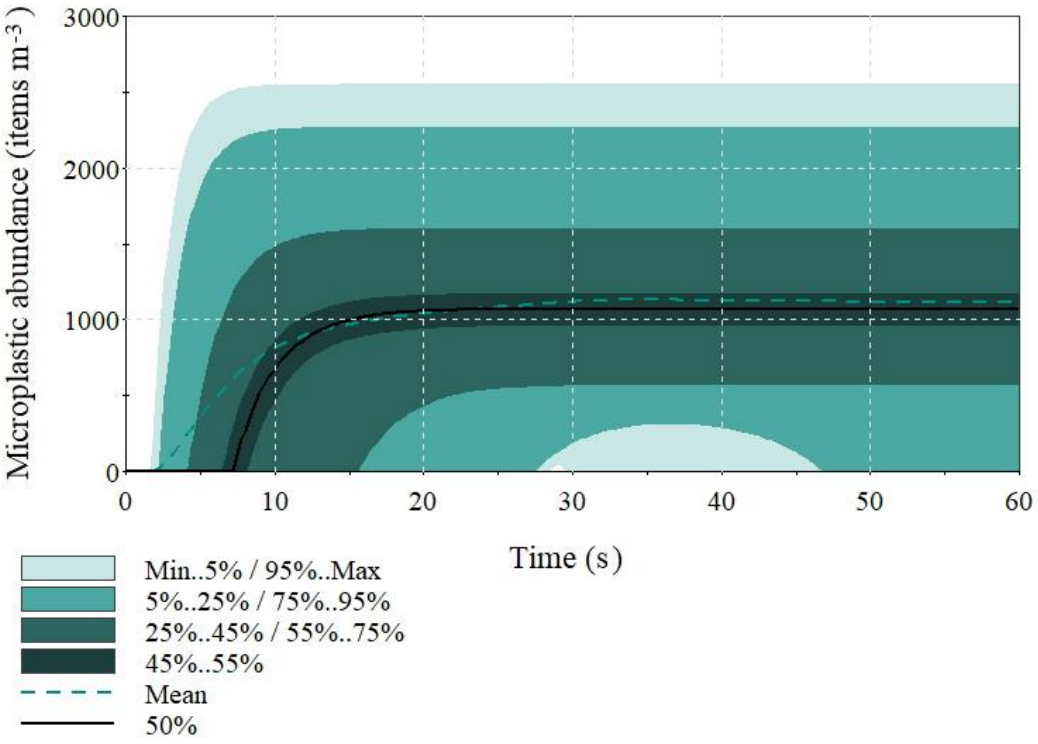

Figure E.14. Probable variation of microplastic concentration in sediment under 0.15 N m^{-2} bed shear stress.

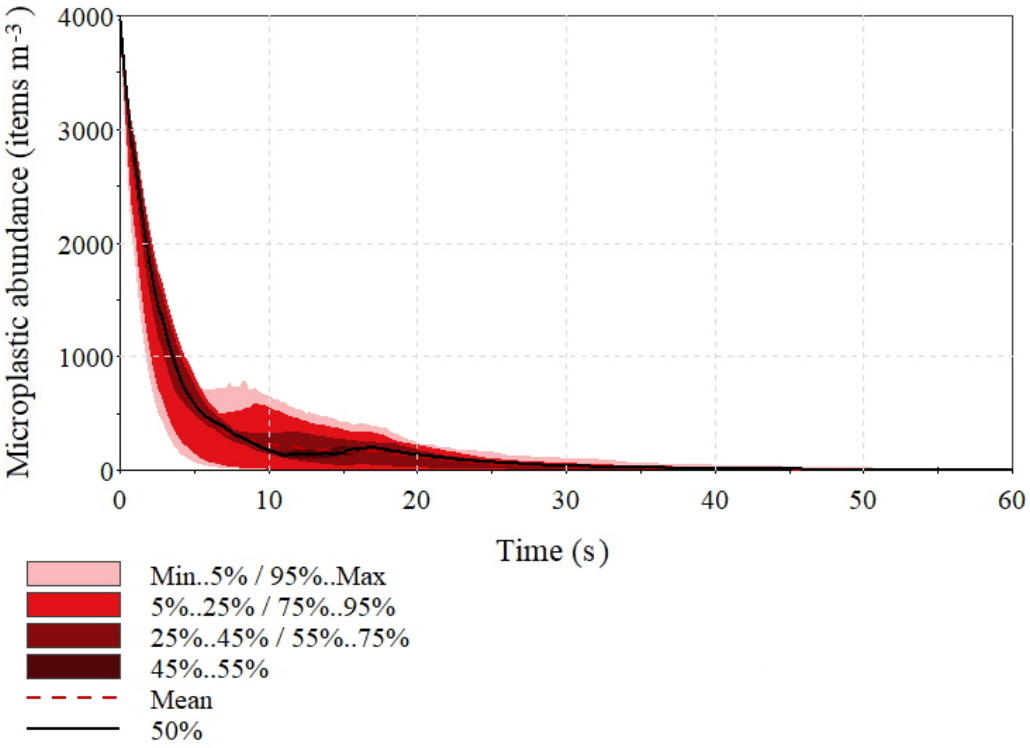

Figure E.15. Probable variation of microplastic concentration in water under 0.50 N m^{-2} bed shear stress.

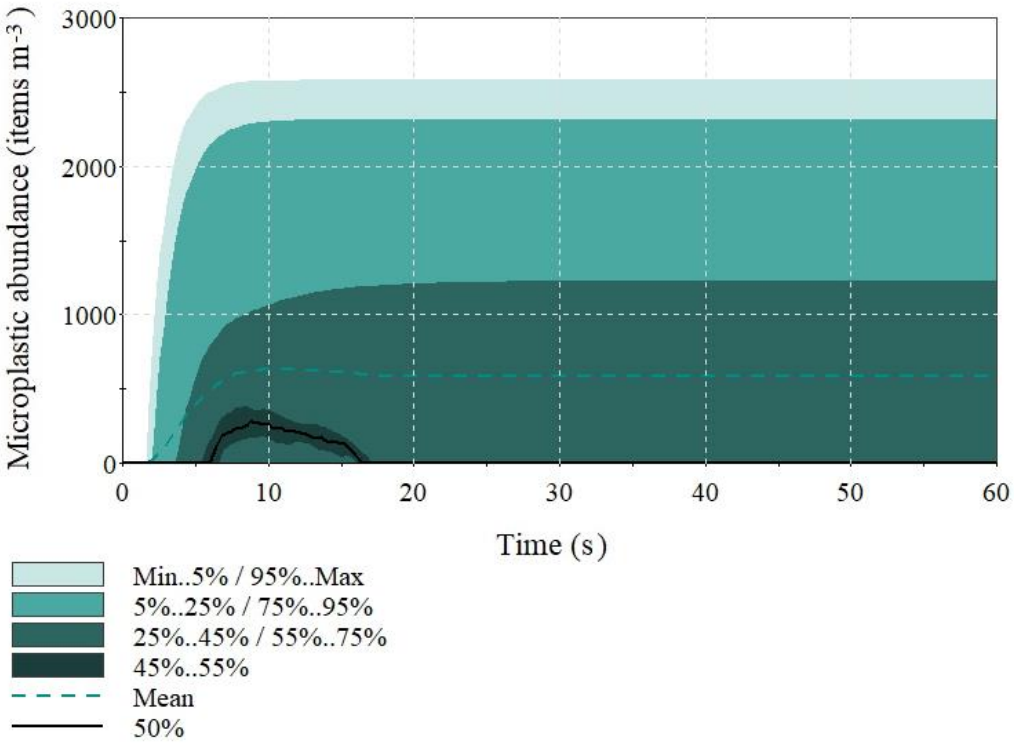

Figure E.16. Probable variation of microplastic concentration in sediment under 0.50 N m^{-2} bed shear stress.

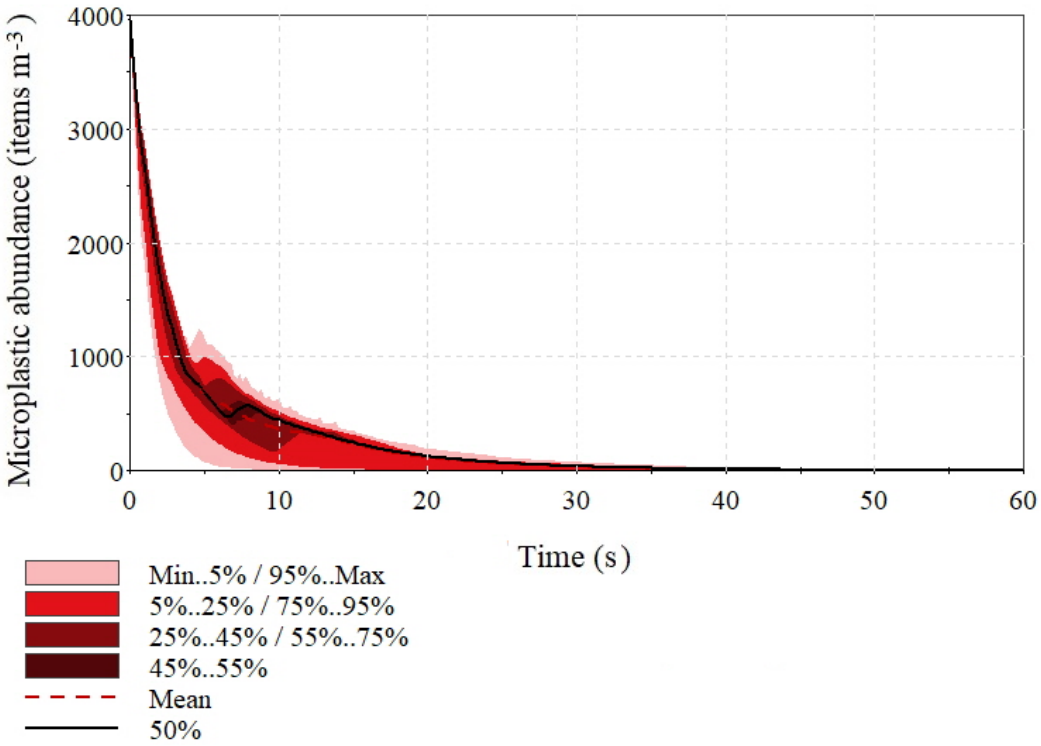

Figure E.17. Probable variation of microplastic concentration in water under 0.90 N m^{-2} bed shear stress.

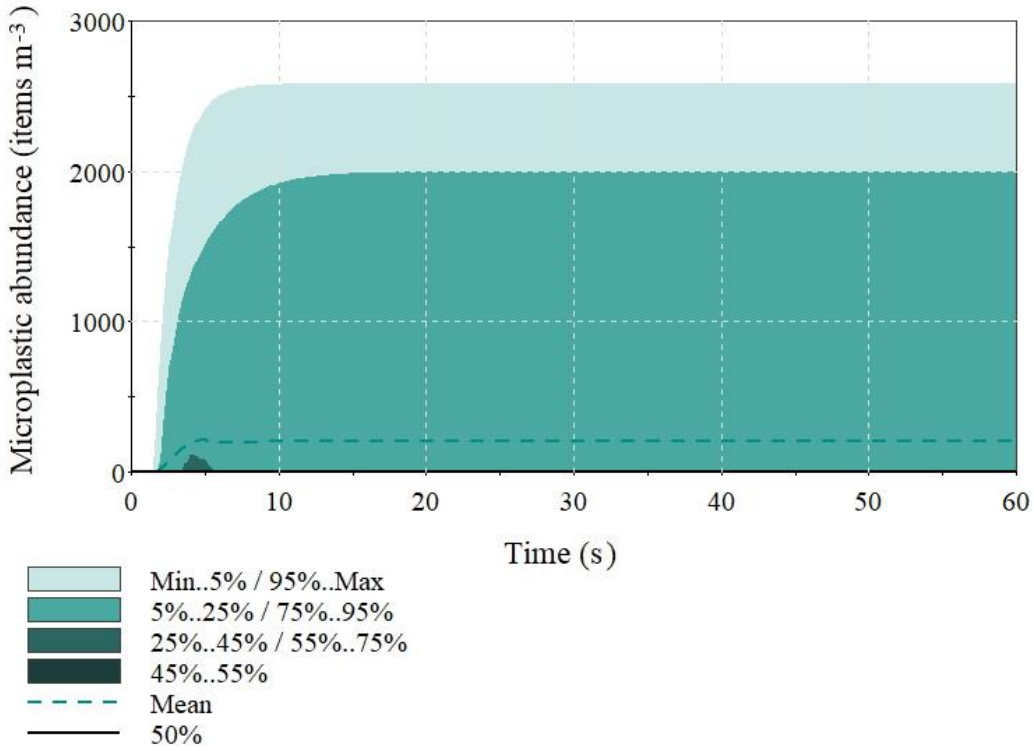

Figure E.18. Probable variation of microplastic concentration in sediment under 0.90 N m^{-2} bed shear stress.

APPENDIX F: SENSITIVITY ANALYSIS

Table F.1. Model response (microplastic concentration in water) to changes in input parameters.

D_{84}	Output	d	Output	μ	Output	τ_{cr}^*	Output	φ	Output	S	Output	C_o	Output	a	Output	ρ_p	Output	ρ_w	Output
0.00005	392.6	0.2	279.0	0.0000004	376.4	0.03	572.8	0.25	514.1	0.00005	501.4	800	206.9	0.0013	514.1	1103	509.5	995.0	411.7
0.00006	398.1	0.3	318.7	0.0000005	385.3	0.03	514.5	0.30	496.6	0.00006	471.5	960	248.3	0.0015	496.6	1127	506.5	995.8	412.8
0.00007	402.8	0.3	346.3	0.0000006	393.8	0.04	476.2	0.35	490.1	0.00007	445.6	1120	289.7	0.0018	490.1	1152	489.4	996.6	413.2
0.00008	406.9	0.3	368.8	0.0000007	401.2	0.04	449.2	0.40	469.9	0.00008	426.4	1280	331.1	0.0020	469.9	1176	466.7	997.4	414.4
0.00009	410.5	0.4	394.7	0.0000008	407.9	0.05	429.2	0.45	443.9	0.00009	419.4	1440	372.4	0.0023	443.9	1201	439.9	998.2	415.6
0.00010	413.8	0.4	413.8	0.0000009	413.8	0.06	413.8	0.50	413.8	0.00010	413.8	1600	413.8	0.0025	413.8	1225	413.8	999.0	416.7
0.00011	416.8	0.5	428.8	0.0000010	419.8	0.06	401.6	0.55	383.8	0.00011	410.7	1760	455.2	0.0028	383.8	1250	388.6	999.8	417.9
0.00012	419.6	0.5	439.2	0.0000011	424.9	0.07	391.7	0.60	354.1	0.00012	408.4	1920	496.6	0.0030	354.1	1274	364.1	1000.6	419.1
0.00013	422.1	0.5	446.9	0.0000012	429.4	0.07	383.9	0.65	326.2	0.00013	407.8	2080	538	0.0033	326.2	1299	343.7	1001.4	420.0
0.00014	424.5	0.6	451.6	0.0000013	434.1	0.08	383.9	0.70	309.7	0.00014	408.1	2240	579.4	0.0035	309.7	1323	332.0	1002.2	420.5
0.00015	426.7	0.6	454.7	0.0000013	438.0	0.08	383.9	0.75	294.4	0.00015	409.8	2400	620.7	0.0038	294.4	1348	320.9	1003.0	421.7

Table F.2. Input Variation (IV), Output Variation (OV), and Ratio of Variation (ROV) for the model results for water.

D_{84}		d		μ		$\tau_{cr}{}^{*}$		φ		S		C_o		a		ρ_p		ρ_w	
IV	**OV**	**IV**	**OV**	**IV**	**OV**	**IV**	**OV**	**IV**	**OV**	**IV**	**OV**	**IV**	**OV**	**IV**	**OV**	**IV**	**OV**	**IV**	**OV**
-50	-5.12	-50	-32.58	-50	-9.04	-50	38.42	-50	24.24	-50	21.17	-50	-50.00	-50	24.24	-10	23.13	-0.40	-1.20
-40	-3.79	-40	-22.98	-40	-6.89	-40	24.34	-40	20.01	-40	13.94	-40	-40.00	-40	20.01	-8	22.40	-0.32	-0.94
-30	-2.66	-30	-16.31	-30	-4.83	-30	15.08	-30	18.44	-30	7.68	-30	-29.99	-30	18.44	-6	18.27	-0.24	-0.84
-20	-1.67	-20	-10.87	-20	-3.04	-20	8.55	-20	13.56	-20	3.04	-20	-19.99	-20	13.56	-4	12.78	-0.16	-0.55
-10	-0.80	-10	-4.62	-10	-1.43	-10	3.72	-10	7.27	-10	1.35	-10	-10.00	-10	7.27	-2	6.31	-0.08	-0.26
0	0.00	0	0.00	0	0.00	0	0.00	0	0.00	0	0.00	0	0.00	0	0.00	0	0.00	0	0.00
10	0.72	10	3.62	10	1.45	10	-2.95	10	-7.25	10	-0.75	10	10.00	10	-7.25	2	-6.09	0.08	0.29
20	1.40	20	6.14	20	2.68	20	-5.34	20	-14.43	20	-1.30	20	20.01	20	-14.43	4	-12.01	0.16	0.58
30	2.01	30	8.00	30	3.77	30	-7.23	30	-21.17	30	-1.45	30	30.01	30	-21.17	6	-16.94	0.24	0.79
40	2.59	40	9.13	40	4.91	40	-7.23	40	-25.16	40	-1.38	40	40.02	40	-25.16	8	-19.77	0.32	0.91
50	3.12	50	9.88	50	5.85	50	-7.23	50	-28.85	50	-0.97	50	50.00	50	-28.85	10	-22.45	0.40	1.20

Table F.2. (continued).

ROV									
D_{84}	d	μ	$\tau_{cr}{}^{*}$	φ	S	C_o	a	ρ_p	ρ_w
0.10	0.65	0.18	-0.77	-0.48	-0.42	1.00	-0.48	-2.32	3.00
0.09	0.57	0.17	-0.61	-0.50	-0.35	1.00	-0.50	-2.80	2.92
0.09	0.54	0.16	-0.50	-0.61	-0.26	1.00	-0.61	-3.07	3.50
0.08	0.54	0.15	-0.43	-0.68	-0.15	1.00	-0.68	-3.20	3.45
0.08	0.46	0.14	-0.37	-0.73	-0.14	1.00	-0.73	-3.22	3.30
0.00	0.00	0.00	0.00	0.00	0.00	0.00	0.00	0.00	0.00
0.07	0.36	0.14	-0.29	-0.72	-0.07	1.00	-0.72	-2.98	3.60
0.07	0.31	0.13	-0.27	-0.72	-0.07	1.00	-0.72	-3.00	2.88
0.07	0.27	0.13	-0.24	-0.71	-0.05	1.00	-0.71	-2.80	3.96
0.06	0.23	0.12	-0.18	-0.63	-0.03	1.00	-0.63	-2.47	3.04
0.06	0.20	0.12	-0.14	-0.58	-0.02	1.00	-0.58	-2.24	3.00
0.07[a]	0.38[a]	0.13[a]	-0.35[a]	-0.58[a]	-0.14[a]	0.91[a]	-0.58[a]	-2.55[a]	2.97[a]

[a]Mean value.

Table F.3. Model response (microplastic concentration in sediment) to changes in input parameters.

D_{84}	Output	d	Output	μ	Output	$\tau_{cr}{}^{*}$	Output	φ	Output	S	Output	C_o	Output	a	Output	ρ_p	Output	ρ_w	Output
0.00005	271.7	0.2	515.8	0.0000004	372.8	0.03	64.2	0.25	0.0	0.00005	331.3	800	136.4	0.0013	0.0	1103	21.5	995.0	277.0
0.00006	272.0	0.3	454.0	0.0000005	349.7	0.03	141.1	0.30	24.1	0.00006	320.5	960	163.7	0.0015	24.1	1127	65.0	995.8	275.0
0.00007	272.2	0.3	406.6	0.0000006	327.6	0.04	191.2	0.35	81.7	0.00007	308.8	1120	190.9	0.0018	81.7	1152	115.3	996.6	273.9
0.00008	272.4	0.3	363.7	0.0000007	307.6	0.04	226.4	0.40	144.1	0.00008	297.0	1280	218.2	0.0020	144.1	1176	166.8	997.4	271.7
0.00009	272.6	0.4	314.3	0.0000008	289.5	0.05	252.5	0.45	207.5	0.00009	284.9	1440	245.5	0.0023	207.5	1201	221.1	998.2	269.4
0.00010	272.8	0.4	272.8	0.0000009	272.8	0.06	272.8	0.50	272.8	0.00010	272.8	1600	272.8	0.0025	272.8	1225	272.8	999.0	267.1
0.00011	272.9	0.5	235.5	0.0000010	256.3	0.06	288.9	0.55	335.7	0.00011	258.5	1760	300.1	0.0028	335.7	1250	322.3	999.8	264.9
0.00012	273.1	0.5	203.9	0.0000011	241.7	0.07	302.0	0.60	397.4	0.00012	244.5	1920	327.3	0.0030	397.4	1274	370.7	1000.6	262.6
0.00013	273.2	0.5	175.4	0.0000012	228.3	0.07	312.3	0.65	455.9	0.00013	229.1	2080	354.6	0.0033	455.9	1299	412.9	1001.4	260.8
0.00014	273.3	0.6	150.6	0.0000013	214.7	0.08	312.1	0.70	496.1	0.00014	213.2	2240	381.9	0.0035	496.1	1323	441.6	1002.2	259.6
0.00015	273.4	0.6	127.9	0.0000013	202.7	0.08	311.9	0.75	533.3	0.00015	196.1	2400	409.2	0.0038	533.3	1348	468.4	1003.0	257.3

Table F.4. Input Variation (IV), Output Variation (OV), and Ratio of Variation (ROV) for the model results for sediment.

D_{84}		d		μ		$\tau_{cr}{}^{*}$		φ		S		C_o		a		ρ_p		ρ_w	
IV	**OV**	**IV**	**OV**	**IV**	**OV**	**IV**	**OV**	**IV**	**OV**	**IV**	**OV**	**IV**	**OV**	**IV**	**OV**	**IV**	**OV**	**IV**	**OV**
-50	-0.40	-50	89.08	-50	36.66	-50	-76.45	-50	-100.00	-50	21.44	-50	-50.00	-50	-100.00	-10	-92.12	-0.40	3.71
-40	-0.29	-40	66.42	-40	28.19	-40	-48.28	-40	-91.17	-40	17.49	-40	-39.99	-40	-91.17	-8	-76.18	-0.32	2.96
-30	-0.22	-30	49.05	-30	20.09	-30	-29.91	-30	-70.06	-30	13.20	-30	-30.02	-30	-70.06	-6	-57.73	-0.24	2.55
-20	-0.15	-20	33.32	-20	12.76	-20	-17.01	-20	-47.18	-20	8.87	-20	-20.01	-20	-47.18	-4	-38.86	-0.16	1.72
-10	-0.07	-10	15.21	-10	6.12	-10	-7.44	-10	-23.94	-10	4.44	-10	-10.01	-10	-23.94	-2	-18.95	-0.08	0.86
0	0.00	0	0.00	0	0.00	0	0.00	0	0.00	0	0.00	0	0.00	0	0.00	0	0.00	0	0.00
10	0.04	10	-13.67	10	-6.05	10	5.90	10	23.06	10	-5.24	10	10.01	10	23.06	2	18.15	0.08	-0.82
20	0.11	20	-25.26	20	-11.40	20	10.70	20	45.67	20	-10.37	20	19.98	20	45.67	4	35.89	0.16	-1.68
30	0.15	30	-35.70	30	-16.31	30	14.48	30	67.12	30	-16.02	30	29.99	30	67.12	6	51.36	0.24	-2.36
40	0.18	40	-44.79	40	-21.30	40	14.41	40	81.85	40	-21.85	40	39.99	40	81.85	8	61.88	0.32	-2.81
50	0.22	50	-53.12	50	-25.70	50	14.33	50	95.49	50	-28.12	50	50.00	50	95.49	10	71.70	0.40	-3.67

Table F.4. (continued).

ROV									
D_{84}	d	μ	$\tau_{cr}{}^{*}$	φ	S	C_o	a	ρ_p	ρ_w
0.008	-1.78	-0.73	1.53	2.00	-0.43	1.00	2.00	9.25	-9.26
0.007	-1.66	-0.70	1.21	2.28	-0.44	1.00	2.28	9.52	-9.23
0.007	-1.63	-0.67	1.00	2.34	-0.44	1.00	2.33	9.69	-10.6
0.007	-1.67	-0.64	0.85	2.36	-0.44	1.00	2.36	9.71	-10.8
0.007	-1.52	-0.61	0.74	2.39	-0.44	1.00	2.39	9.67	-10.8
0.000	0.00	0.00	0.00	0.00	0.00	0.00	0.00	0.00	0.00
0.004	-1.37	-0.60	0.59	2.31	-0.52	1.00	2.31	8.89	-10.3
0.005	-1.26	-0.57	0.54	2.28	-0.52	1.00	2.29	8.97	-8.42
0.005	-1.19	-0.54	0.48	2.24	-0.53	1.00	2.24	8.5	-11.8
0.005	-1.12	-0.53	0.36	2.05	-0.55	1.00	2.05	7.73	-9.35
0.004	-1.06	-0.51	0.29	1.91	-0.56	1.00	1.91	7.14	-9.16
0.005[a]	-1.30[a]	-0.56[a]	0.69[a]	2.01[a]	-0.44[a]	0.91[a]	2.01[a]	8.10[a]	-9.05[a]

[a]Mean value.